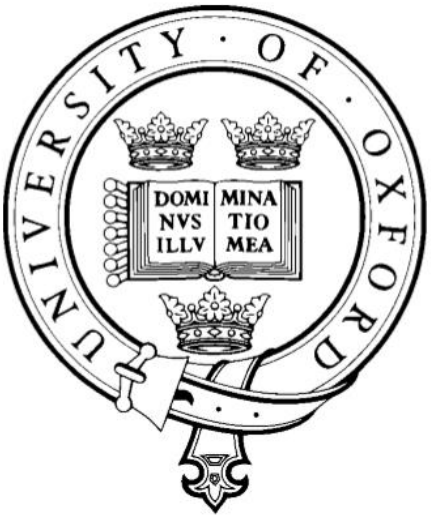
Development of Late-Stage

Difluoromethylation Strategies



Claudio Flavio Meyer

St Peter's College

University of Oxford

Supervised by

Professor Véronique Gouverneur, FRS

December 16, 2020

This thesis is submitted to the Board of the Faculty of Physical Sciences, in partial fulfilment of the requirements for the degree of Doctor of Philosophy at the University of Oxford

Declaration

I hereby declare that the work presented in this thesis was conducted under the supervision of Prof. Véronique Gouverneur FRS FRSC. All the work is my own, except where otherwise stated, and has not been submitted for any other degree at this or any other university.

Claudio Meyer

December 16, 2020

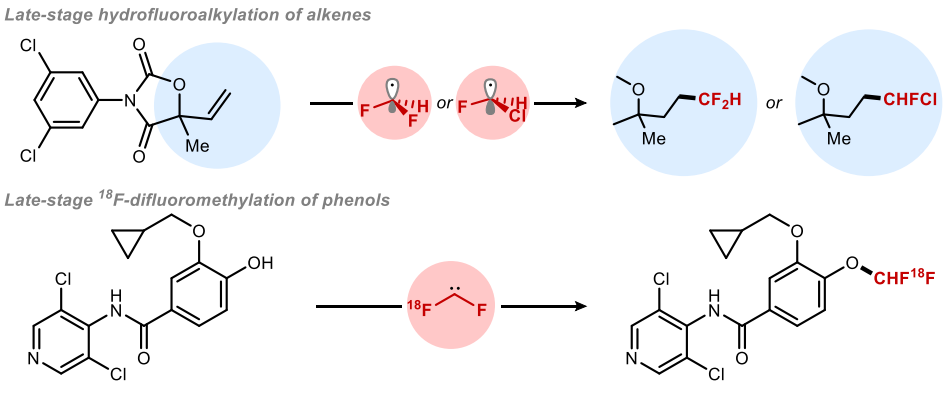
Dedication

This thesis is dedicated to my parents Hedy and Beat and my brother Raffaele, who always believed in me and supported me throughout all the milestones of my life.

Claudio Meyer - St Peter's College - DPhil Chemistry - Michaelmas Term 2020

Abstract: Development of Late-Stage Difluoromethylation Strategies

In the last decades, the introduction of the difluoromethyl group has attracted many interests in drug discovery. This thesis discusses the development of novel strategies for the late-stage introduction of the difluoromethyl group in the context of photochemistry and F-18 radiochemistry. The relevance of the difluoromethyl group and an introduction to the field of late-stage difluoromethylation is described in **Chapter 1**. In **Chapter 2**, a novel methodology for the photochemical late-stage hydrodifluoromethylation of alkenes with difluoroacetic acid is discussed. **Chapter 3** describes the expansion of this methodology to the hydrochlorofluoromethylation and hydrobromofluoromethylation of alkenes. Radiochemistry and its applications to positron emission tomography are introduced in **Chapter 4**. **Chapter 5** describes our recent efforts for the synthesis of an [^{18}F]difluorocarbene reagent for the ^{18}F-difluoromethylation of phenols, thiophenols and *N*-heterocycles. Experimental data for the work described in this thesis is given in **Chapter 6**.



Abbreviations

18-crown-6	1,4,7,10,13,16-Hexaoxacyclooctadecane
5-HT_6	5-Hydroxytryptamine subunit 6
9-BBN	9-Borabicyclo[3.3.1]nonan
Ac	Acetyl
ADME	Absorption, distribution, metabolism and elimination
AIBN	Azobis(isobutyronitril)
Alk	Alkyl
API	Active pharmaceutical ingredient
aq	Aqueous
Ar	Aryl
ATRA	Atom transfer radical addition
AUD	Alcohol use disorder
AY	Activity yield
BDE	Bond dissociation energy
BIOMe	1-Methoxy-1,2-benziodoxol-3-(1*H*)-one
Bn	Benzyl
Boc	*Tert*-butyloxycarbonyl
BPin	Boronic acid pinacol ester
Bu	Butyl
Bz	Benzoyl
Cbz	Carboxybenzyl group
CFTR	Cystic Fibrosis Transmembrane Conductance Regulator
CNS	Central Nervous system
Cys	Cysteine
DAST	*N*,*N*-Diethylaminosulfur trifluoride
dc	Decay corrected
DCE	1,2-Dichloroethane
DCM	Dichloromethane
Deoxo-Fluor®	*Bis*(2-methoxyethyl)aminosulfur trifluoride
DF	Difluoro
dF(CF_3)ppy	3,5-Difluoro-2-[5-(trifluoromethyl)-2-pyridinyl]benzene
DFC	Difluorocarbene
DFMS	Zinc difluoromethanesulfinate
diCy-18-crown-6	2,5,8,15,18,21-Hexaoxatricyclo[20.4.0.$0^{9.14}$]hexacosane
DMA	*N*,*N*-Dimethylacetamide
DMAP	4-Dimethylaminopyridine
DME	1,2-Dimethoxyethane
DMF	*N*,*N*-Dimethylformamide
DMP	Dess-Martin-Periodinane

DMPU	*N*,*N*'-Dimethylpropyleneurea
DMSO	Dimethylsulfoxide
dr	Diastereomeric ratio
dtbpy	4,4'-Di-*tert*-butyl-2,2'-dipyridyl
ee	Enantiomeric excess
EGFR	Epidermal growth factor receptor
E_{max}	Maximal positron energy
EoB	End of Bombardment
EoS	End of Synthesis
Et	Ethyl
EWG	Electron-withdrawing group
fac	Facial
FCH	Fluorocholine
FDG	2-Deoxy-2-fluoroglucose
FDOPA	6-Fluoro-L-3,4-dihydroxyphenylalanine
FET	*O*-Fluoroethyl-L-tyrosine
FMeNER	(*S*,*S*)-2-(alpha-(2-Fluoromethoxyphenoxy)benzyl)morpholine
Fmoc	Fluorenylmethoxycarbonyl
GC-MS	Gas chromatography mass spectroscopy
Glu	Glutamic acid
glyme	Ethylenglycoldimethylether
HAD	Hydrogen-atom donor
HAT	Hydrogen-atom transfer
HPLC	High-performance liquid chromatography
*i*Bu	*Iso*-butyl
impy	Imidazo[1,2-b]'pyridazine
*i*Pr	*Iso*-propyl
JAK1	Janus kinase 1
$K_{2.2.2.}$	4,7,13,16,21,24-Hexaoxa-1,10-diazabicyclo[8.8.8]hexacosane
K_ihB1	Human bradikynin B1
LC-MS	Liquid chromatography mass spectroscopy
LED	Light-emitting diode
Leu	Leucine
LG	Leaving group
LSF	Late-stage functionalisation
MA	Molar activity
MAGL	Monoacylglycerol lipase
Me	Methyl
mGluR2	Metabotropic glutamate receptor subtype 2
MTBE	Methyl *tert*-butyl ether
mTORC1/2	Mammalian target of rapamycin complex 1/2
MW	Microwave

N	Neutron
NMP	*N*-Methyl-2-pyrrolidinone
NMR	Nuclear magnetic resonance
NS3/4a protease	Non-structural 3/4a protease
ODC	Ornithin decarboxylase
ODS	Ozone-depleting substance
OTf	Trifluoromethanesulfonate
P	Proton
PAM	Positive allosteric modulator
PBP	Penicillin-binding proteins
PDE3/4	Phosphodiesterase 3/4
PET	Positron emission tomography
P-gp	P-glycoprotein
Ph	Phenyl
Phe	Phenylalanine
Phth	Phthalimide
PI3K	Phosphoinositide-3-kinase
PIDA	Phenyliodine(III) diacetate
PIFA	Phenyliodine(III) *bis*(trifluoroacetate)
PK-M2	Pyruvate kinase isozyme M2
ppm	Parts per million
ppy	2-Phenylpyridine
py	Pyridine
RCY	Radiochemical yield
R_{mean}	Mean positron range
rt	Room temperature
SAR	Structure activity relationship
Selectfluor™	1-Chloromethyl-4-fluoro-1,4-diazoniabicyclo[2.2.2]octane bis(tetrafluoroborate)
SET	Single-electron transfer
$t_{1/2}$	Half-life
TBAF	Tetrabutylammonium fluoride
TBS	*Tert*-butyldimethylsilyl
*t*Bu	*Tert*-butyl
TEMPO	2,2,6,6-Tetramethylpiperidinyloxyl
TFA	Trifluoroacetic acid
THF	Tetrahydrofuran
TMEDA	*N*,*N*,*N'*,*N'*-Tetramethylethylenediamine
TMS	Trimethylsilyl
USD	US dollar
UV	Ultraviolet
XtalFluor-E®	(Diethylamino)difluorosulfonium tetrafluoroborate
γ	High energy photon
ν	Neutrino

Acknowledgements

First of all, I would like to thank Véronique, for giving me the chance to pursue my DPhil studies in her research group. It was a very inspiring journey; I have enjoyed working with you a lot and I can proudly say I have learned a lot from you. You have been very supportive throughout these three years, helped me to work on my weaknesses and pushed me to become a better scientist. I will remember all our chats about science. I especially enjoyed discussing results and new ideas.

I would also like to thank my co-supervisor Ben Davis and his research group. I enjoyed the weekly group meetings, and coffee breaks and learned a lot from you. The Christmas trip to Paris last year was fantastic.

Furthermore, I would like to express my gratitude to Andrés. You have taught me very much over the years, which made me a better scientist and team worker. I will not forget the advises you have given me and I hope we will continue working together in the future. I would also like to thank Daniel. The time I have spent in your team in Beerse was fantastic. I will remember all the chats, coffees, and beers we had. Moreover, I would like to thank Antonio and Aldo for the guidance you provided me with, throughout my time in Toledo and Beerse. I would also like to thank Alejandro and Alberto for their help with my projects.

More generally, I would like to thank the whole Janssen Team in Toledo and Beerse. I will keep good memories from working at Janssen and I hope we keep in touch.

Next, I would like to thank Matt (Tredwell). I have learnt a lot from you about radiochemistry and automation. I especially enjoyed all the chats we had in your office. I am sure we will keep in touch.

I would like to thank Manuja for her continuous help and support with all organisational tasks. Many thanks also to Marie Skłodowska-Curie Actions for the funding throughout these three years.

I would also like to thank all the members of the VG group. It was a pleasure to work in this environment and I will keep you all in good memory. Special thanks to all the F11 crew: Rob, Kos, Jimmy, Sindy, Zijun, Matt and Khaled. It was awesome to work with you and I appreciate the much better taste of Music compared to F12! Thanks a lot Matt and Jimmy for always keeping the lab in order. I would like to thank the Cheminventory system for making chemistry fun. It's a pleasure to look for a chemical and find it in the correct place. Special thanks to all the friends that came to visit me in Oxford, Spain and/or Switzerland: Sindy, Tim, Tobi, Rob, Kos, Jimmy, Natan, Fabian, Wanja, Louisa, Raffaele, Tim (Berendsen) and Denise. Of course, many thanks to the FLUDD team: Tim, Tobi, Giulia and Sindy. We have had an awesome time in the two Janssen sites, and I enjoyed all of it. Many thanks to the SOMIL crew: Jeroen, Gianluca, Natan, Patrick, Rob, Adeline, Tobi, Zijun and Joe. The SOMIL crew will stay in my memory

as a group of freedom fighters, who oppose the regime and surveillance that Cheminventory has brought upon us. Many thanks also to Jeroen for the time in SOMIL and the countless dinners we enjoyed in Oxford and Cardiff. I would like to thank Sindy, Jeroen and Rob for proof-reading this thesis.

Thanks also to all the friends that regularly joined me in the pub: Sindy, Kos, Rob, Tim, Adeline, Francesco, Gianluca, Myrto, Sebastiano, Eddie, Alex, Ryan, Brian, Andrew, Colm and Natan.

I would also like to thank all my friends from Basel for their support: Daniel, David, Tom, Denise, Wanja, Louisa, Kristina, Fabian and Joscha. I appreciated the breaks from the stressful DPhil life.

I would of course like to thank all my family, especially my parents Hedy and Beat. It was only thanks to all your support that I could do this. Next, I would like to thank my brother Raffaele. You always supported me in whichever way you could. I am extremely grateful for that and I am very proud of you.

Last but not least, Sindy I would like to thank you for these last three years. You are an amazing co-worker, my best friend and partner. You made this time enjoyable and I would not have been able to make it without you. You kept me motivated but also reminded me that chemistry is not all that counts in life. It was amazing to travel with you to all these places (especially Marbella, Rotterdam and The Hague). I am so grateful to be able to submit this thesis at

the same time as you and I cannot wait for our next adventure in the United States.

Table of Contents

Chapter 1 – Introduction 1
1.1 Fluorine in Drug Discovery 2
1.1.1 Properties of the Difluoromethyl Group 3
1.1.2 The Difluoromethyl Group in Medicinal Chemistry 5
1.2 Traditional Synthesis of Difluoromethyl Compounds 6
1.2.1 Deoxyfluorination of Aldehydes 6
1.2.2 Cross-Coupling Strategies 7
1.2.3 Difluoromethylation of C(sp^3)-Centres 9
1.3 Radical Late-Stage Functionalisation of Biologically Relevant Molecules 11
1.3.1 Introduction to Photochemistry 11
1.3.2 Peculiarities of the Difluoromethyl Radical 12
1.3.3 Radical Late-Stage Difluoromethylation Reactions 14
1.3.4 Generation of the Difluoromethyl Radical and Application to Late-Stage Difluoromethylation 15
1.3.3 Metallaphotoredox Difluoromethylation of Aryl Bromides 17
1.3.4 Difluoromethylation of Alkenes 19
1.3.4 Late-Stage Cross-Coupling to Access the C(sp^3)-Difluoromethyl Group 22
1.4 Difluoromethylation of Heteroatoms 24
1.4.1 Introduction to Difluorocarbene 25
1.4.2 The Reactivity of Difluorocarbene 28
1.4.3 Control of Difluorocarbene Reactivity 29
1.5 Conclusion 30
1.6 References Chapter 1 31
Chapter 2 – Hydrodifluoromethylation of Alkenes with Difluoroacetic Acid 34
2.1 The C(sp^3)-linked Difluoromethyl Group 35
2.2 Synthetic Strategies Towards C(sp^3)-CF_2H Compounds 36
2.3 Aim of this Project 38
2.4 Optimisation of the Hydrodifluoromethylation of Unactivated Alkenes 40
2.5 Substrate Scope and Limitations of the Hydrodifluoromethylation of Alkenes 43
2.6 Scale-up Synthesis of (4,4-difluorobutyl)amine 47
2.6.1 Previous Syntheses of (4,4-difluorobutyl)amine 48
2.12.2 Synthesis of *N*-Boc-4,4-difluorobutyl-1-amine Using our Hydrodifluoromethylation Protocol 49

2.7 Mechanistic Experiments for the Hydrodifluoromethylation Protocol 52
2.8 Proposed Mechanism for the Hydrodifluoromethylation of Alkenes 56
2.9 Limitations 59
2.10 Conclusion 60
2.11 Outlook 61
2.12 References 62
Chapter 3 – Hydrochlorofluoro-methylation of Unactivated Alkenes with Chlorofluoroacetic Acid 64
3.1 Introduction to the Chlorofluoromethyl Group 65
3.1.1 The Chlorofluoromethyl Group in Medicinal Chemistry 65
3.1.2 Strategies to Access the Chlorofluoromethyl Group 68
3.1.3 Cross-Coupling Reactions with the Chlorofluoromethyl Group 70
3.1.4 The Chlorofluoromethyl Group as a Reactive Handle for F-18 Radiochemistry 72
3.2 Radical Halofluoromethylation Reactions 72
3.2.1 Previous Halofluoromethyl Radical Precursors 73
3.2.2 Bromodifluoromethylation Reactions 73
3.2.3 Chlorodifluoromethylation Reactions 76
3.3 This Work - Hydrochlorofluoromethylation of Unactivated Alkenes with Chlorofluoroacetic Acid 78
3.3.1 Synthesis of Starting Materials 80
3.3.2 Control Experiments and Optimisation 81
3.3.3 Substrate Scope for the Hydrochlorofluoromethylation of Alkenes 83
3.3.4 Limitations of the Hydrochlorofluoromethylation Protocol 85
3.3.5 Proposed Mechanism for the Hydrochlorofluoromethylation of Alkenes . 86
3.3.6 Further Applications of the Chlorofluoromethyl Radical 87
3.3.7 Application of Chlorofluoromethyl Alkanes 89
3.4 The Bromofluoromethyl Radical 91
3.4.1 Generation of the Bromofluoromethyl Radical from Bromofluoroacetic Acid 91
3.4.2 Generation of the Bromofluoromethyl Radical from Dibromofluoromethane 92
3.5 Conclusion 94
3.6 Outlook 94
3.7 References 95

Chapter 4 – Introduction to Positron Emission Tomography and F-18 Radiochemistry 97
4.1 Positron Emission Tomography 98
4.1.1 Introduction to Positron Emission Tomography 98
4.1.2 Radionuclides for Positron Emission Tomography 99
4.2 Concepts and Important Factors in F-18 Radiochemistry 101
4.2.1 Stoichiometry in F-18 Radiochemistry 101
4.2.2. Radiochemical Yield and Activity Yield 102
4.2.3 Molar Activity 103
4.2.4 Decay Correction 104
4.3 F-18 Radiochemistry 104
4.3.1 New Motifs in F-18 Radiochemistry 109
4.3.2. ^{18}F-Fluoroalkylation of Phenols 113
4.4 References 117
Chapter 5 – [^{18}F]Difluorocarbene Unlocks New Motifs for F-18 Radiochemistry 118
5.1 Introduction 119
5.1.1 Aim of this Project 119
5.1.2 Difluorocarbene in F-18 Radiochemistry 120
5.2 Generation of [^{18}F]Difluorocarbene and [^{18}F]Fluorocarbene 122
5.2.1 *In Situ* Fluorination of Halofluorocarbene 123
5.2.2 $PhSO_2CF_2H$ as a Difluorocarbene Reagent 124
5.2.3 Radiosynthesis of [^{18}F]4-*t*Bu-$PhSO_2CF_2H$ 129
5.2.4 Automated synthesis of [^{18}F]4-tBu$PhSO_2CF_2H$ 132
5.2.5 ^{18}F-Difluorocyclopropanation 134
5.2.6 ^{18}F-Difluoromethylation of (thio)phenols 135
5.2.7 ^{18}F-Difluoromethylation of *N*-heterocycles 141
5.2.8 ^{18}F-Difluoromethoxylation of an Aryl Boronic Acid 143
4.2.9 Competition experiments 143
5.2.10 ^{18}F-Difluoromethylation of Biologically Relevant Molecules 145
5.2.11 Proposed Mechanism for the ^{18}F-Difluoromethylation 149
5.3 Conclusion 150
5.4 Outlook 150
5.5 References 151
6. Supporting Information 153

6.1 General Information 153
6.2 Supporting information for Chapter 2 155
6.2.1 Synthesis of starting materials 155
6.2.2 Synthesis of Hydrodifluoromethylated Compounds 158
6.2.4 Mechanistic experiments 176
6.3 Supporting Information Chapter 3 179
6.3.1 Hydrochlorofluoromethylation of Alkenes 180
6.3.2 Chlorofluoromethylation of other substrates 189
6.3.4 Hydrobromofluoromethylation of Alkenes 192
6.4 Supporting Information Chapter 5 193
6.4.1 Mechanistic Experiments 193
6.4.2 Optimisation Data 193
6.4.3 Synthesis of F-19 Compounds 194
6.4.4 Synthesis of Reference Compounds 197
6.4.5 Radiochemistry: 208
6.4.6 Overlays of radiotraces 216
6.5 References 253

Chapter 1 – Introduction

1.1 Fluorine in Drug Discovery

Fluorine is amongst the scarcest elements found in natural products.[1] Contrastingly, due to the ubiquitous physicochemical properties of fluorine (χ = 4.0), organofluorine compounds account for 20-25% of drug structures.[2–8] It is generally accepted that the precise introduction of fluorine atoms into a drug candidate has prominent effects on its biological and chemical properties.[3,9] Due to its small size (Van der Waals radius (R) = 1.47 Å) and the relatively short C–F bond (C-F bond length ~ 1.35 Å), fluorine can often mimic C–H bond (R(H) = 1.20; C-H bond length ~ 1.09 Å,).[8,10] However, due to the much higher strength of a C-F bond (Bond Dissociation Energy (BDE) up to 130 kcal mol^{-1}) compared to a C-H bond (BDE(CH_4) = 103 kcal mol^{-1}), fluorine atoms are often introduced to improve overall biological function of drug candidates.[8,11] For example, fluorine incorporation can increase cellular membrane permeability, and generally elevate robustness towards cytochrome P-450 mediated metabolism.[12]

Fluoroalkyl groups recently emerged as bioisosteres of prevalent functional groups present in drug candidates. Bioisosteres are structurally different groups that are capable to mimic the physicochemical interactions of the original fragments.[7,13] For example, difluoromethylene groups can mimic carbonyls, whereby the fluorine atoms (hydrogen-bond acceptor) mimic the lone pairs of the carbonyl oxygen.[14] The incorporation of fluoroalkyl groups into novel biologically active compounds, such as pharmaceuticals and agrochemicals, has become a

common strategy in the pharmaceutical and agrochemical industry to improve on drug potency.

1.1.1 Properties of the Difluoromethyl Group

In the past decades, the field of fluorine chemistry has substantially evolved with the development of a plethora of methodologies allowing for the formation of carbon-fluorine bonds.[11] Specifically, tremendous efforts have been made to facilitate the introduction of trifluoromethyl (CF_3) or perfluoroalkyl ($C_nF_{(n+2)}$) groups into structurally complex molecules.[15–23] Nowadays, the incorporation of other fluorinated functional groups, such as the difluoromethyl (CF_2H) group, is actively pursued in synthetic organic chemistry.[24–26] As recently disclosed by Lippard and co-workers, the CF_2H group is a privileged motif, as its highly polarised C-H bond can participate in hydrogen-bonding interactions (Figure 1.1).[27] This feature has been demonstrated by the crystallisation of 2-nitro-1-difluoromethylbenzene (**1.1**), which crystallises in a similar dimer as 2-nitrophenol (**1.2**), whereby the CF_2H group of **1.1** engages in hydrogen bonding interactions with the neighbouring nitro group.



Figure 1.1. Hydrogen-bonding interactions of the difluoromethyl group by the example of difluoromethylarene **1.1** compared to phenol **1.2**.

The CF_2H group has subsequently been described as a metabolically stable lipophilic bioisostere of thiol, alcohol or amine functionalities, a highly desirable feature to medicinal chemists.[25–28]

The hydrogen-bonding properties of the CF_2H group have been described by its hydrogen-bond acidity [*A*].[26] This parameter can be quantified by ^1H NMR spectroscopy, whereby the chemical shift of the CF_2H-proton is measured in different solvents. The variation of the chemical shift directly correlates with the ability of the molecule to act as a hydrogen-bond donor. A comparative summary of the hydrogen-bonding properties of methylated and difluoromethylated compounds is described in Figure 1.2. It is evident that non-fluorinated molecules, such as toluene-derivatives and (thio)anisoles, are poor hydrogen-bond donors (**1.3** – **1.5**; $A \leq 0.011$).

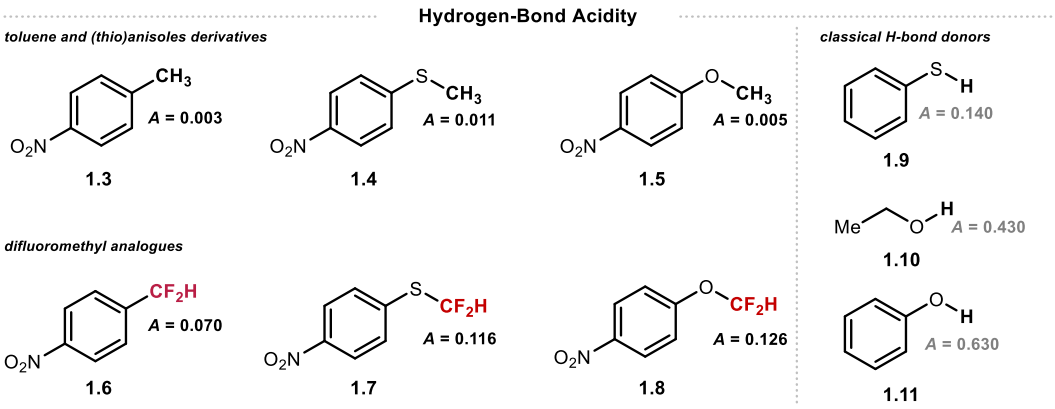


Figure 1.2. Hydrogen-bond acidity parameters of selected compounds.[26]

Difluoromethylbenzene (**1.6**; $A = 0.07$) and difluoromethyl (thio)ethers (**1.7** – **1.8**; $A \geq 0.116$) possess superior hydrogen-bond donor abilities. These values come within reach to the hydrogen-bond donating ability of thiophenol (**1.9**; $A = 0.140$),

clearly demonstrating the ability of CF_2H compounds to participate in hydrogen-bonding interactions. Nonetheless, the hydrogen-bonding properties of the CF_2H group are weaker than the one of ethanol (**1.10**; *A* = 0.430) and phenol (**1.11**; *A* = 0.630).

In addition to its prevalent hydrogen-bonding properties, the CF_2H group has unique lipophilicity properties. Difluoromethylbenzene is a moderate hydrogen-bond donor. It is however significantly less hydrophilic than phenol (ΔLogP = +0.94) and therefore, in terms of lipophilicity, closer to toluene (ΔLogP = –0.12).[26] Combined, these properties render the difluoromethyl group a potent lipophilic bioisostere of weak hydrogen-bond donors such as (thio)phenols.

1.1.2 The Difluoromethyl Group in Medicinal Chemistry

Due to the unique physicochemical properties associated with the CF_2H group, numerous novel drug candidates contain such a motif (**1.12** – **1.15**; Figure 1.3).[29–31] Wymann and co-workers recently disclosed a structure activity relationship (SAR) study of mammalian target of rapamycin complex 1/2 (mTORC1/2) selective inhibitors.[32] In binding assays the authors found that the CF_2H-containing compound PQR620 (**1.14**) achieved high degrees of mTOR selectivity over other structurally closely related kinases such as phosphoinositide-3-kinase (PI3K). Based on computational modelling studies, they suggested that the unique properties of the CF_2H group allow for hydrogen-bonding interactions with a neighbouring glutamate residue specific to mTOR (Glu2190).

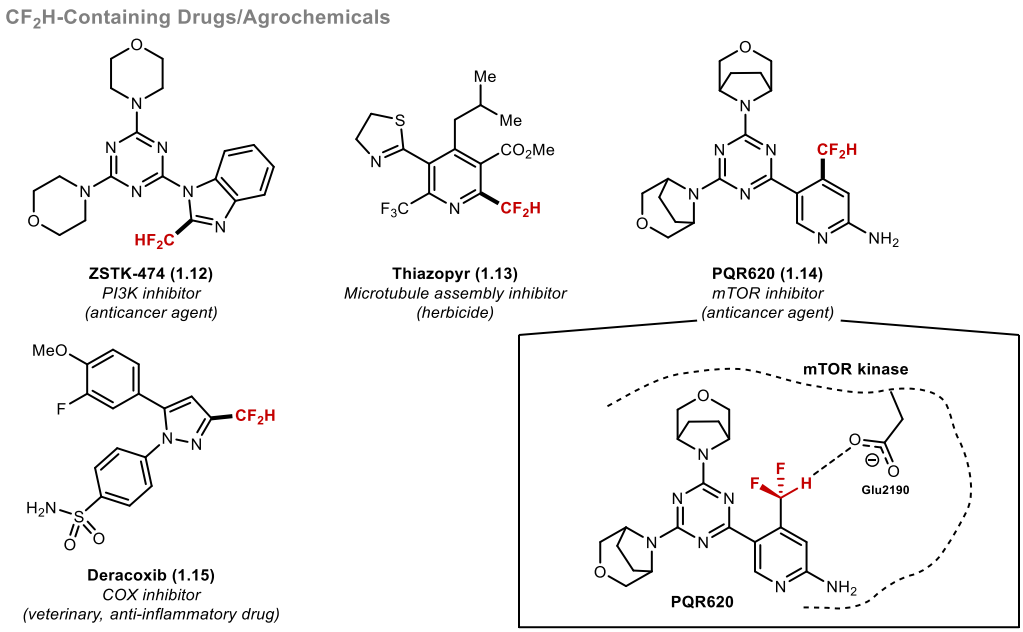


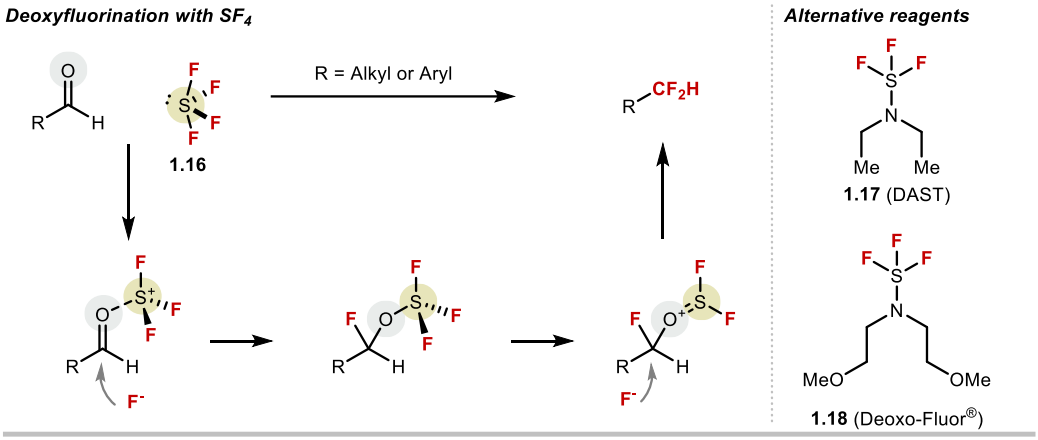
Figure 1.3. CF_2H-containing drug compounds and agrochemicals and hydrogen-bonding interaction between the CF_2H group of PQR620 (**1.14**) and a glutamate-2190 in the active site of mTOR kinase.

1.2 Traditional Synthesis of Difluoromethyl Compounds

1.2.1 Deoxyfluorination of Aldehydes

In the past decades, the most common method for the preparation of the CF_2H group relied on the deoxyfluorination of aldehydes (Scheme 1.1).[33] This transformation has been achieved with reagents such as the gaseous sulfur tetrafluoride (**1.16**; SF_4). More recently, safer and easier to handle sulfur trifluoride derivatives have been developed, such as *N*,*N*'-diethylaminosulfur trifluoride (**1.17**; DAST) and *bis*(2-methoxyethyl)aminosulfur trifluoride (**1.18**; Deoxo-Fluor®).[34] Although powerful, these deoxyfluorination methods have shown limitations in terms of scope, scalability, explosivity and toxicity.[35,36] A further limitation to this approach is the requirement for a pre-installed aldehyde function in the molecule, prior to deoxyfluorination. The selective

prefunctionalisation with an aldehyde function is often challenging due to their low stability.



Scheme 1.1. Synthesis of difluoromethyl compounds *via* deoxyfluorination.

1.2.2 Cross-Coupling Strategies

Based on the limitations of deoxyfluorination strategies, novel technologies allowing for the direct installation of a CF_2H group (difluoromethylation), employing readily available reactive handles are highly desirable.[24] Cross-coupling difluoromethylation is a strategy relying on the formation of a high valent transition metal-difluoromethyl (M-CF_2H) complex, that can undergo reductive elimination to afford the desired difluoromethyl compound. These M-CF_2H complexes can be accessed using a broad range of reagents (Figure 1.4). Nucleophilic reagents such as $TMSCF_2H$ (**1.19**), an analogue of the Ruppert-Prakash reagent, can be activated with nucleophiles such as fluoride, to undergo transmetallation.[37] One-electron processes, whereby the difluoromethyl radical adds to a metal centre with a free coordination site, have also been described. For example, bromodifluoromethane (**1.20**) has been used to generate the

difluoromethyl radical, which affords the desired M^{n+1}-CF_2H complex with transition metals such as nickel.[38] Electrophilic reagents such as difluoroiodomethane (**1.21**) undergo oxidative addition to afford the oxidised M^{n+2}-CF_2H complex with nickel catalysts.[39] Recently, the combination of difluorocarbene and a proton source has served as a CF_2H^+ surrogate. Ethyl bromodifluoroacetate (**1.22**) has been used as a difluorocarbene reagent, which in combination with a palladium catalyst, acts as a formal electrophilic coupling partner to access the M^{n+2}-CF_2H complex.[40]

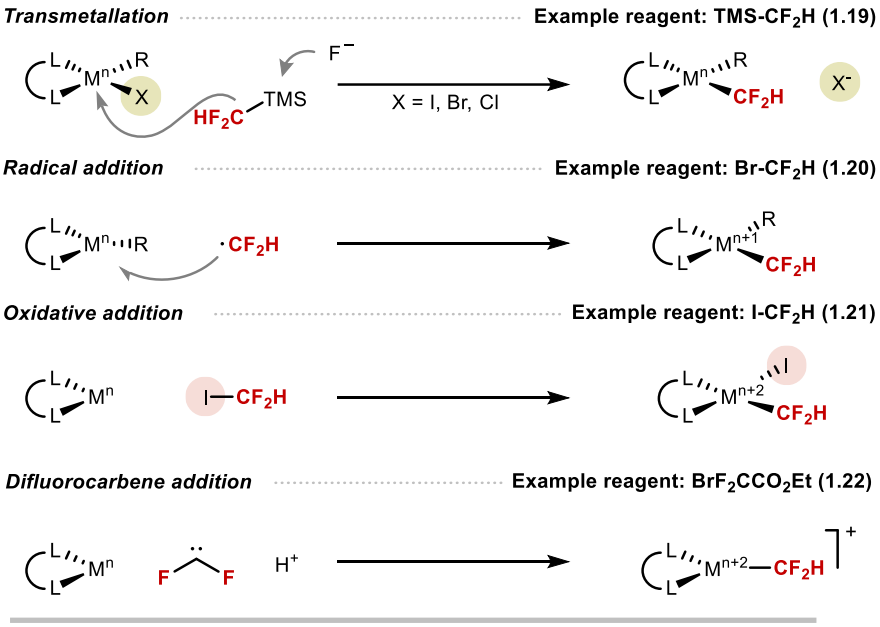


Figure 1.4. Access to M-CF_2H complexes with nucleophilic, electrophilic and radical difluoromethyl reagents or *via* difluorocarbene.

In 2012, Hartwig and co-workers reported the first direct copper-mediated difluoromethylation of aryl iodides.[37] Since then, numerous difluoromethylation strategies have been reported starting from a broad range of precursors, such as aryl (pseudo)halides,[37,38,40–42] aroyl chlorides,[43] aryl diazonium salts,[44] diaryl

iodonium triflates,[45] aryl Grignard reagents,[39] diaryl zinc reagents,[46] aryl zinc chlorides,[47] aryl boronates,[48] aryl boronic acids[49] and unfunctionalised arenes[50,51] (Figure 1.5).

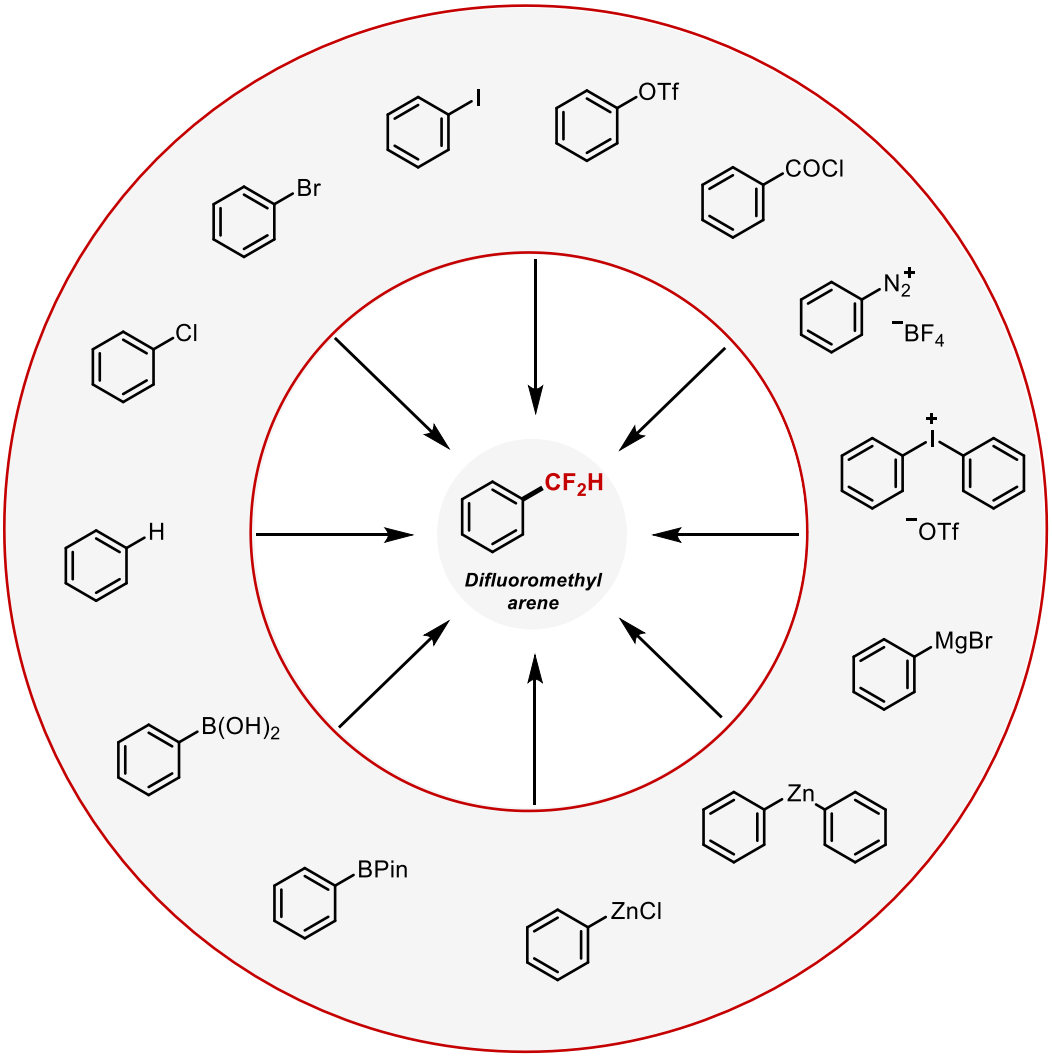


Figure 1.5. Cross-coupling difluoromethylation to access difluoromethylarenes.

1.2.3 Difluoromethylation of C(sp^3)-Centres

The above-mentioned cross-coupling protocols are efficient for the difluoromethylation of C(sp^2)-centres. However, with an increasing demand from the pharmaceutical sector for C(sp^3)-enriched building blocks, reactions to afford

C(sp^3)-CF_2H compounds are becoming highly sought-after transformations.[52] Other than *via* deoxyfluorination, the C(sp^3)-CF_2H motif can be accessed by direct difluoromethylation (Figure 1.6). Nucleophilic difluoromethylation of C(sp^3)-electrophiles has been addressed with reagents such as $TMSCF_2H$ (**1.19**).[53–55] In contrast, electrophilic difluoromethylation of carbon-based nucleophiles such as malonates can be achieved with the lithium-based activation of fluoroform (**1.23**).[56] This reaction is thermodynamically driven by the formation of the very strong lithium-fluoride bond (ΔHf_{298} = 577 kJ mol^{-1}).

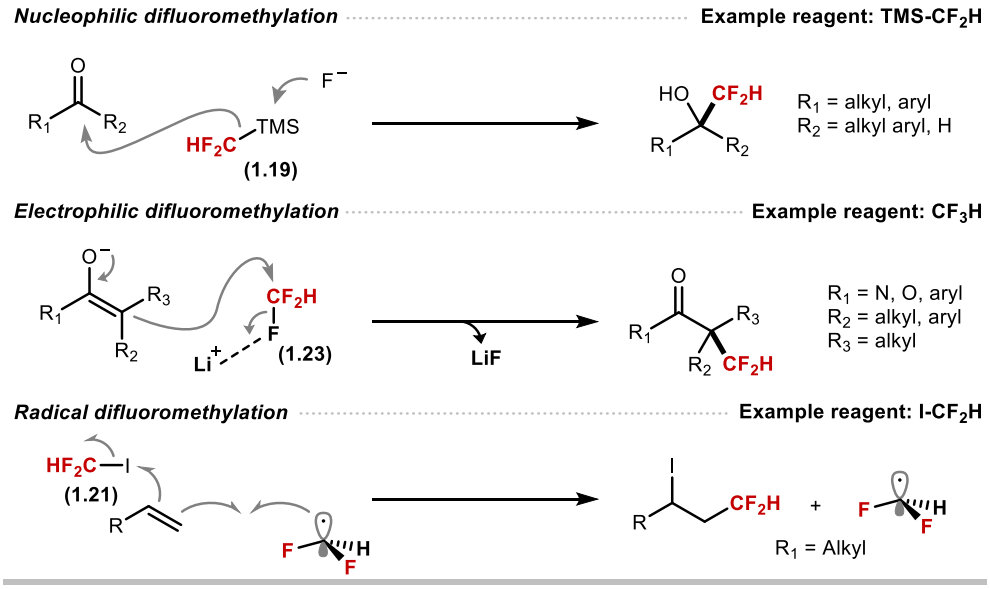


Figure 1.6. Access to the C(sp^3)-CF_2H motif *via* nucleophilic, electrophilic and radical difluoromethylation.

Another strategy to access the C(sp^3)-CF_2H motif relies on the addition of the CF_2H radical to an alkene. For example, difluoroiodomethane (**1.21**) has been used for the atom-transfer radical addition (ATRA) to unactivated alkenes, affording net iododifluoromethylated products.[57] The following section will focus on the

formation of the CF_2H radical and methodologies that harness the reactivity of this intermediate.

1.3 Radical Late-Stage Functionalisation of Biologically Relevant Molecules

Recently, the synthetic organic chemistry community witnessed a growing demand from the pharmaceutical sector for the development of methodologies, that would: 1) allow the derivatisation of native handles, and 2) tolerate all other functional groups present in active pharmaceutical ingredients (APIs). These methods would find application in the rapid generation of a library of analogue compounds for biological testing. Such methods are commonly referred to as late-stage functionalisation (LSF) methods.[58–61] Due to the excellent functional group tolerance observed in one-electron processes, many novel LSF methods rely on radical reactions.

1.3.1 Introduction to Photochemistry

Within the field of radical chemistry, the excitation of molecules by irradiation with light (photochemistry) has emerged as a powerful traceless energy source.[62–64] Upon irradiation of a molecule with a photon, an electron of the singlet ground state (S_0) is promoted to a singlet excited state (S_x) of higher energy (Figure 1.7). The excited molecule can then release this energy *via* different thermal or radiative pathways. Vibrational relaxation and internal conversion are non-radiative pathways, whereby the molecule undergoes relaxation to a less

energetic vibrational mode or to an energetically lower state. If the electron is in the first singlet excited state (S_1), the molecule can release its energy by emission of a photon *via* fluorescence. Another possible pathway is intersystem crossing, whereby the excited electron relaxes with spin inversion to a long-lived triplet excited state, lower in energy (e.g. S_1 to T_1). The electron can then relax from this triplet state to the singlet ground state *via* emission of a photon; a process called phosphorescence (T_1 to S_0).

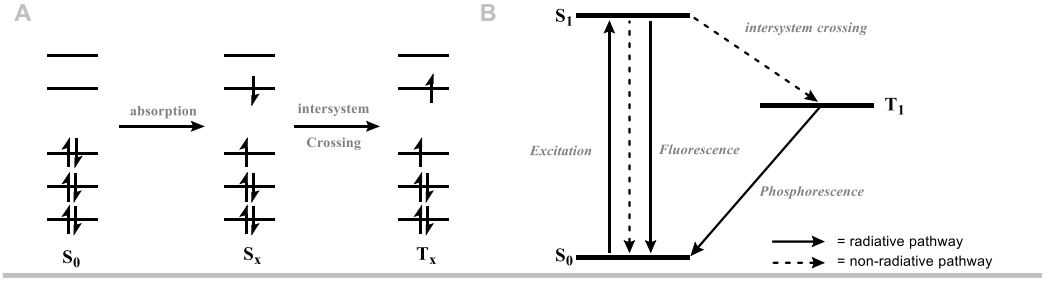


Figure 1.7 a) Simplified molecular orbital diagram; b) Simplified Jablonski-diagram.

1.3.2 Peculiarities of the Difluoromethyl Radical

The impact of α-halogen substitution on radical stability and geometry has been discussed in various reports.[65,66] Calculations by Marshall and co-workers revealed the geometries of a range of fluorinated and chlorinated radicals (Figure 1.8a).[67] It becomes evident that fluorine substitution leads to increased pyramidal character of the radical. Whilst the methyl radical is planar (sum of interbond angles (Σθ) = 360°), the fluoromethyl radical is only slightly pyramidal (Σθ = 352°). The difluoromethyl radical (Σθ = 339°) has a more pronounced pyramidal character, and the trifluoromethyl radical is nearly tetrahedral (Σθ = 334°).

The introduction of fluorine atoms can have a beneficial effect on radical stability. Various calculations as well as experimental work revealed that the stability of fluorinated methyl radicals decreases in the order CH_2F ~ CF_2H > CF_3.[68]

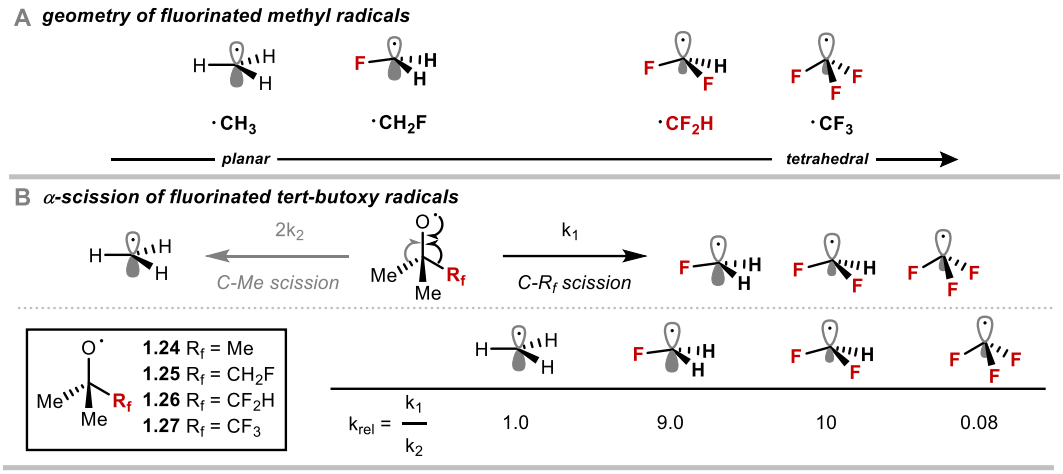


Figure 1.8. Stability and geometry of fluorinated radicals.

For example, Jiang, Li and co-workers reported kinetic data on the α-bond scission of fluorinated *tert*-butoxy radicals (**1.24** – **1.27**; Figure 1.8b).[69] Notably, the scission of the C-CF_2H (k_{rel} = 10) or C-CH_2F (k_{rel} = 9.0) bonds occurs at significantly higher rates than the scission of C-CH_3 bond (k_{rel} = 1.0). The C-CF_3 bond (k_{rel} = 0.08), however, is cleaved at a much lower rate than the C-CH_3, C-CH_2F or C-CF_2H bonds.

Furthermore, α-fluorine substitution has an influence on the nucleophilicity of the radical. Due to the p-donating effect of fluorine, the difluoromethyl radical is more nucleophilic than the methyl radical. In contrast, the high inductive effect of fluorine ($\chi_{(F)}$ = 4.0, Pauling scale) renders the trifluoromethyl radical (sum of electronegativities (Σχ) = 12.0) more electrophilic than the methyl radical (Σχ = 6.6).[68]

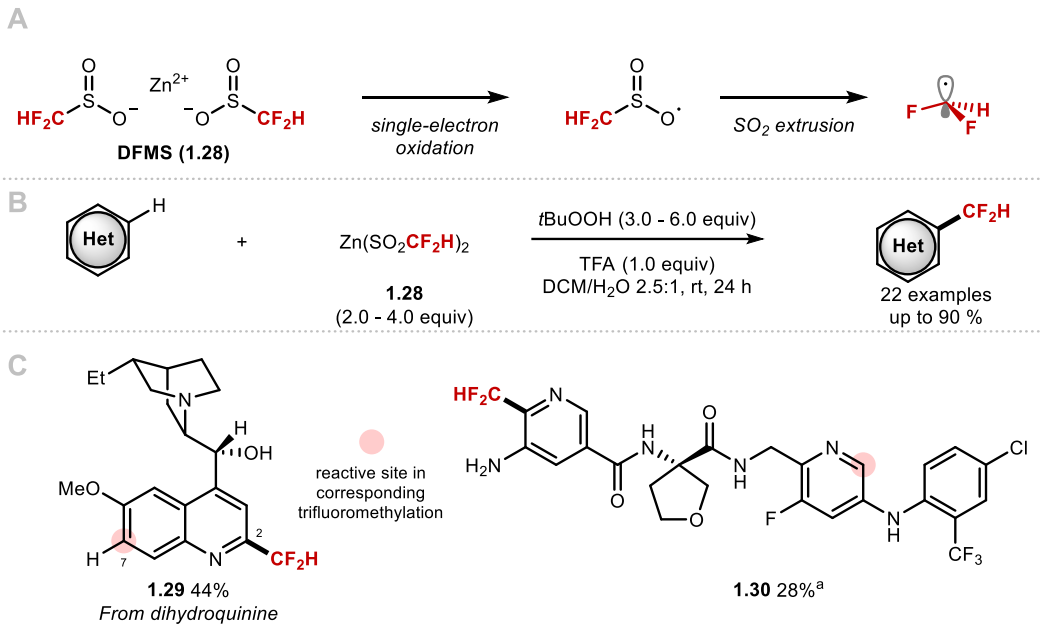
1.3.3 Radical Late-Stage Difluoromethylation Reactions

To date, the field of radical late-stage difluoromethylation is still in its infancy. However, since a pioneering example of Chen and co-workers, demonstrating that difluoroiodomethane (**1.21**) is an efficient difluoromethyl radical precursor,[57] methodologies harnessing the reactivity of this radical experienced an upsurge in recent years. To date, the difluoromethyl radical can be generated from an extensive repertoire of reagents, fine-tuned to fit specific reaction requirements. This section provides an overview of mechanistically different strategies for the late-stage introduction of the difluoromethyl group on C(sp^3) and C(sp^2) carbons.

The difluoromethyl radical has been shown to react in Minisci-type C-H functionalisations of heteroarenes. Due to the nucleophilic character of the CF_2H radical, it preferentially reacts with electron-deficient heteroarenes.[70] In contrast, electron-rich benzene derivatives are much less reactive towards this radical.[71] Furthermore, the difluoromethyl radical readily adds to alkenes and alkynes for vicinal difunctionalisation or hydrofunctionalisation reactions. Due to the high reactivity of radicals towards alkenes, these reactions show less electronic bias. Thus, the addition of the difluoromethyl radical to electron-deficient alkenes, unactivated alkenes and electron-rich alkenes has been reported.[72,73] Other than addition to unsaturated systems, transition metal catalysts readily capture the difluoromethyl radical to afford M^{n+1}-CF_2H complexes.[38]

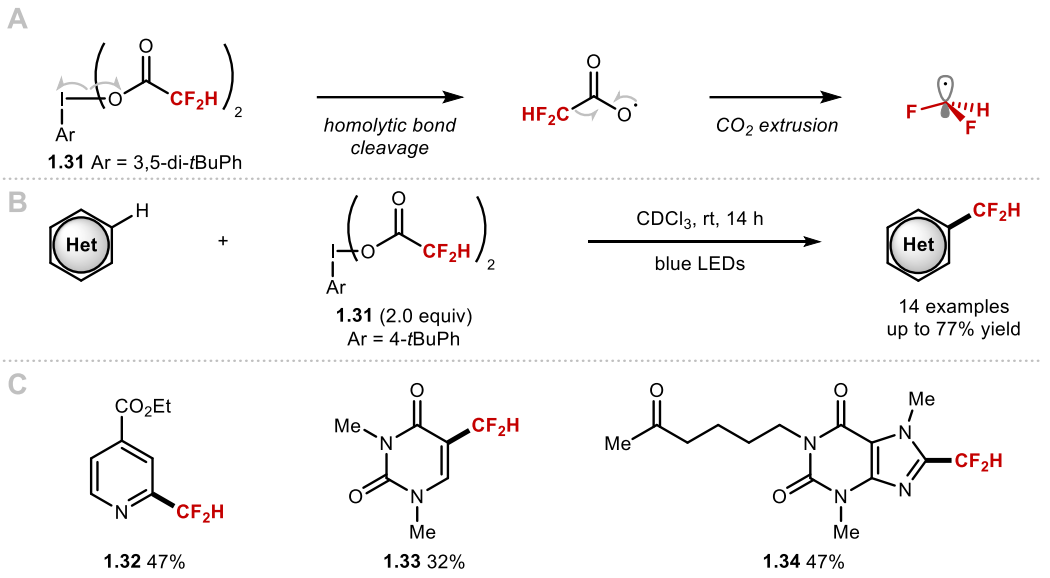
1.3.4 Generation of the Difluoromethyl Radical and Application to Late-Stage Difluoromethylation

Zinc difluoromethane sulfinate (**1.28**, DFMS), a reagent developed by Baran and co-workers in 2012, is readily activated by single-electron oxidation (Scheme 1.2).[70] This event affords a difluoromethanesulfonyl radical, that can undergo sulfur dioxide extrusion to form the difluoromethyl radical. Since the activation of DFMS (**1.28**) is performed under oxidising conditions, this reagent is well suited for Minisci-type reactions, traditionally performed in presence of strong oxidants such as peroxides or persulfates. In their report, Baran and co-workers disclosed several examples of LSF of biologically relevant molecules. For example, dihydroquinine undergoes selective C-2 difluoromethylation (**1.29**); in contrast, the corresponding trifluoromethylation employing trifluoromethanesulfinate occurs selectively at the C-7 position. This result is consistent with the more nucleophilic character of the difluoromethyl radical, compared to the trifluoromethyl radical. A later publication by Kuttruff and co-workers showed that the addition of iron salts can be beneficial for late-stage difluoromethylation with DFMS.[74] With their updated reaction conditions, the authors were able to selectively access **1.30** in low yields. The corresponding trifluoromethylation reaction afforded a mixture of products, reacting at the more electron-rich pyridine.



Scheme 1.2. Oxidative activation of zinc difluoromethanesulfinate allows for the Minisci-type difluoromethylation of heteroarenes. [a]Difluoromethylpyridine **1.30** was reported in a separate publication.[74]

In 2017, Maruoka and co-workers reported the direct activation of a hypervalent iodine reagent (**1.31**) under blue light irradiation (λ = 400 nm; Scheme 1.3).[75] Irradiation of the reagent with this wavelength could induce the homolytic iodine-oxygen bond cleavage to release iodobenzene and the chlorodifluoroacetyl radical. The latter can undergo decarboxylation to form the desired difluoromethyl radical. The authors have used this reagent for a late-stage Minisci-type difluoromethylation of heteroarenes. Simple 2-difluoromethylpyridines (**1.32**) and difluoromethyl-analogues of biologically relevant molecules (**1.33** – **1.34**) were accessed with this method in moderate yields.



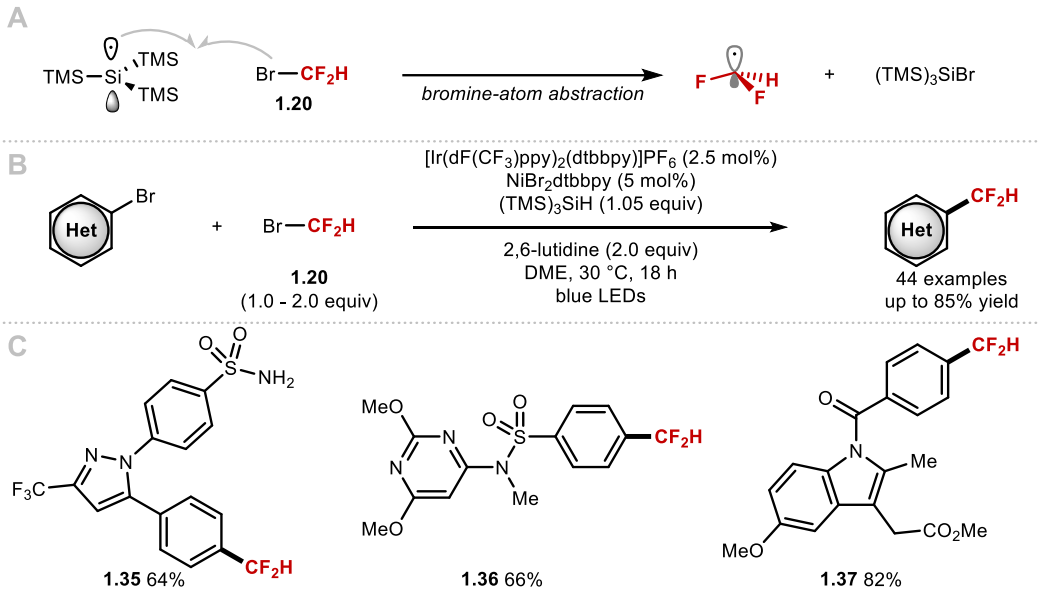
Scheme 1.3. A) Visible light activation of hypervalent iodine reagent **1.31**; B) Minisci-type difluoromethylation of heteroarenes; C) Examples of difluoromethylated heteroarenes.

1.3.3 Metallaphotoredox Difluoromethylation of Aryl Bromides

The regioselectivity of radical C-H functionalisations, such as the Minisci reaction, relies on the innate selectivity of both the radical and the targeted heteroarene. For substrates that contain several reactive sites, low regioselectivity is observed. When exploring the SAR of an API, it is often desirable to selectively modify the compound structure at a specific position. This can be achieved using precursors that are prefunctionalised with a reactive handle such as a halide or a boronate. These handles have been extensively employed in traditional cross-coupling reactions. However, the harsh reaction conditions (e.g. high temperature) often limit this approach in terms of LSF.

Recently, MacMillan and co-workers merged the field of traditional metal-catalysed cross-coupling with photoredox catalysis (metallaphotoredox catalysis).[76] In contrast to traditional cross-coupling reactions relying solely on

two-electron processes (e.g. Ullman, Suzuki, Negishi, Sonogashira, Buchwald-Hartwig, Kumada, Heck, Stille and Hiyama coupling), this new field harnesses the high reactivity of radicals in a combination of two-electron and single-electron processes under mild reaction conditions (at room temperature, using light as energy source).

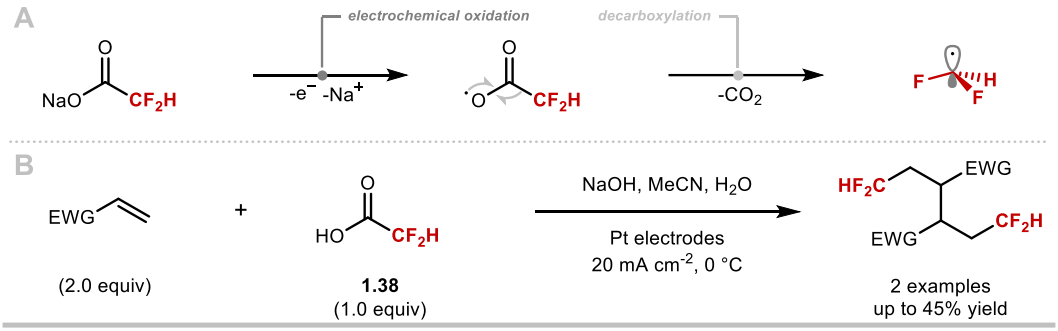


Scheme 1.4. Bromine-atom abstraction from bromodifluoromethane (**1.20**) by a silyl radical for the metallaphotoredox difluoromethylation of aryl bromides.

MacMillan and co-workers applied this metallaphotoredox strategy for the late-stage difluoromethylation of aryl bromides (Scheme 1.4).[38] In this report, bromodifluoromethane (**1.20**) is activated by bromine-atom abstraction from a silyl radical. In combination with a nickel salt, the coupling of the difluoromethyl radical with a broad range of structurally complex aryl bromides afford the desired difluoromethylarenes in high yields. The mild reaction conditions employed in this protocol allowed for the late-stage difluoromethylation of a range of drug compounds (**1.35** – **1.37**).

1.3.4 Difluoromethylation of Alkenes

The addition of the difluoromethyl radical to alkenes has been addressed in numerous reports. A seminal study, describing the difluoromethylation-dimerisation of electron-deficient alkenes, was disclosed in 1992 by Uneyama and co-workers (Scheme 1.5).[77]

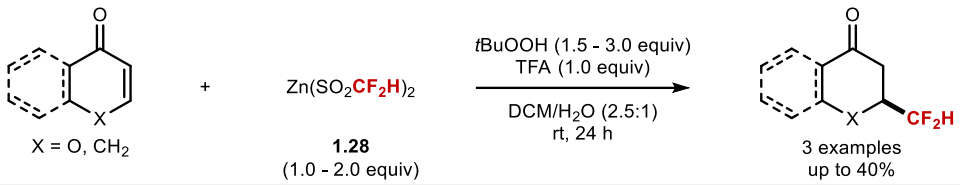


Scheme 1.5. a) Electrochemical oxidation of difluoroacetic acid; b) Difluoromethylation-dimerisation from difluoroacetic acid (**1.38**) by Uneyama and co-workers.

Electrochemical single-electron oxidation of difluoroacetic acid (**1.38**) afforded the difluoromethyl radical after extrusion of carbon dioxide. The difluoromethyl radical was reacted with electron-deficient alkenes and the resulting radicals dimerised.

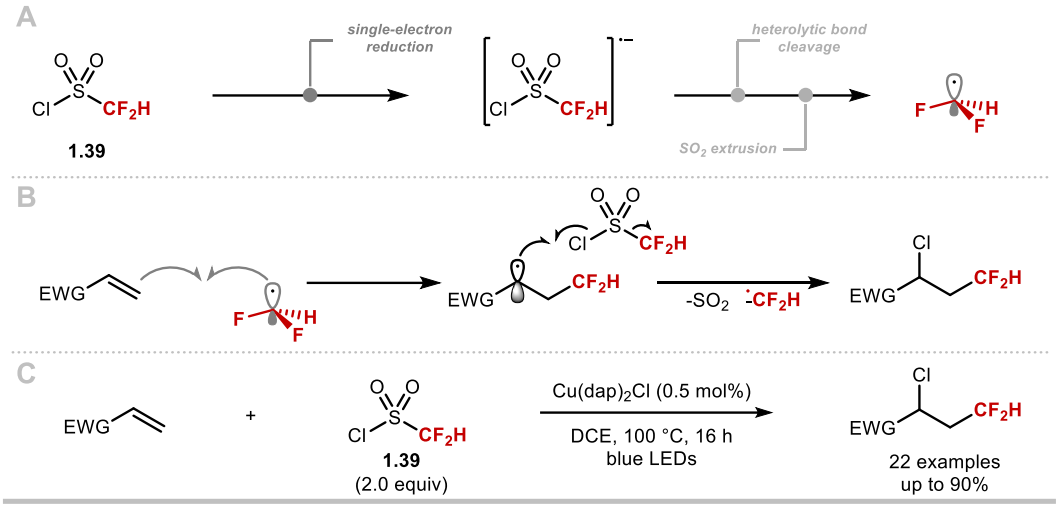
Only twenty years later, Baran and co-workers disclosed the C-H difluoromethylation of heteroarenes employing zinc difluoromethanesulfinate (DFMS, **1.28**) as a difluoromethylation reagent (see Scheme 1.2 for activation mode). This study focused on Minisci-type C-H difluoromethylation of heteroarenes. In addition, they reported that electron-deficient alkenes undergo hydrodifluoromethylation under identical reaction conditions, albeit in low yields

(Scheme 1.6).[70] The examples reported are limited to three cyclic internal alkenes.



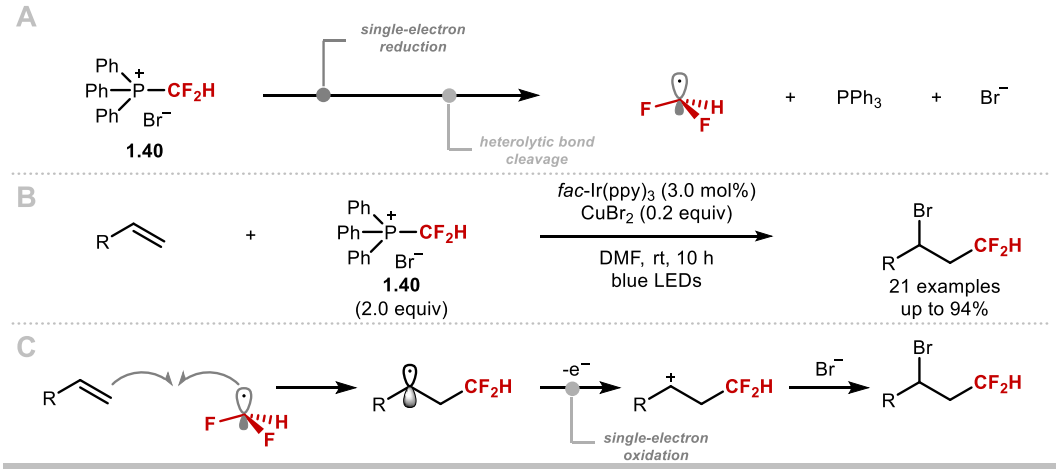
Scheme 1.6. Hydrodifluoromethylation of alkenes with zinc difluoromethane sulfinate (**1.28**). The activation of zinc difluoromethanesulfinate is described in Scheme 1.2.

More recently, numerous reports focused on the vicinal difunctionalisation of alkenes.[72,78–80] Dolbier and co-workers developed various difluoromethylation protocols employing difluoromethanesulfonyl chloride as radical precursor (**1.39**; Scheme 1.7).[78–80] This reagent is readily activated by single-electron reduction events. Single-electron reduction of difluoromethanesulfonyl chloride (**1.39**) affords the corresponding radical anion. Heterolytic bond cleavage of the sulfur-chlorine bond and extrusion of sulfur dioxide releases the difluoromethyl radical. Whilst this reagent has not yet found application to late-stage functionalisation, it has been used for ATRA reactions, and difluoromethylation-cyclisations, that allowed the preparation of a broad range of difluoromethyl-containing building blocks.



Scheme 1.7. a) Activation of difluoromethanesulfonyl chloride; b) Simplified mechanism for the atom transfer radical addition; c) Chlorodifluoromethylation of electron-deficient alkenes with difluoromethanesulfonyl chloride.

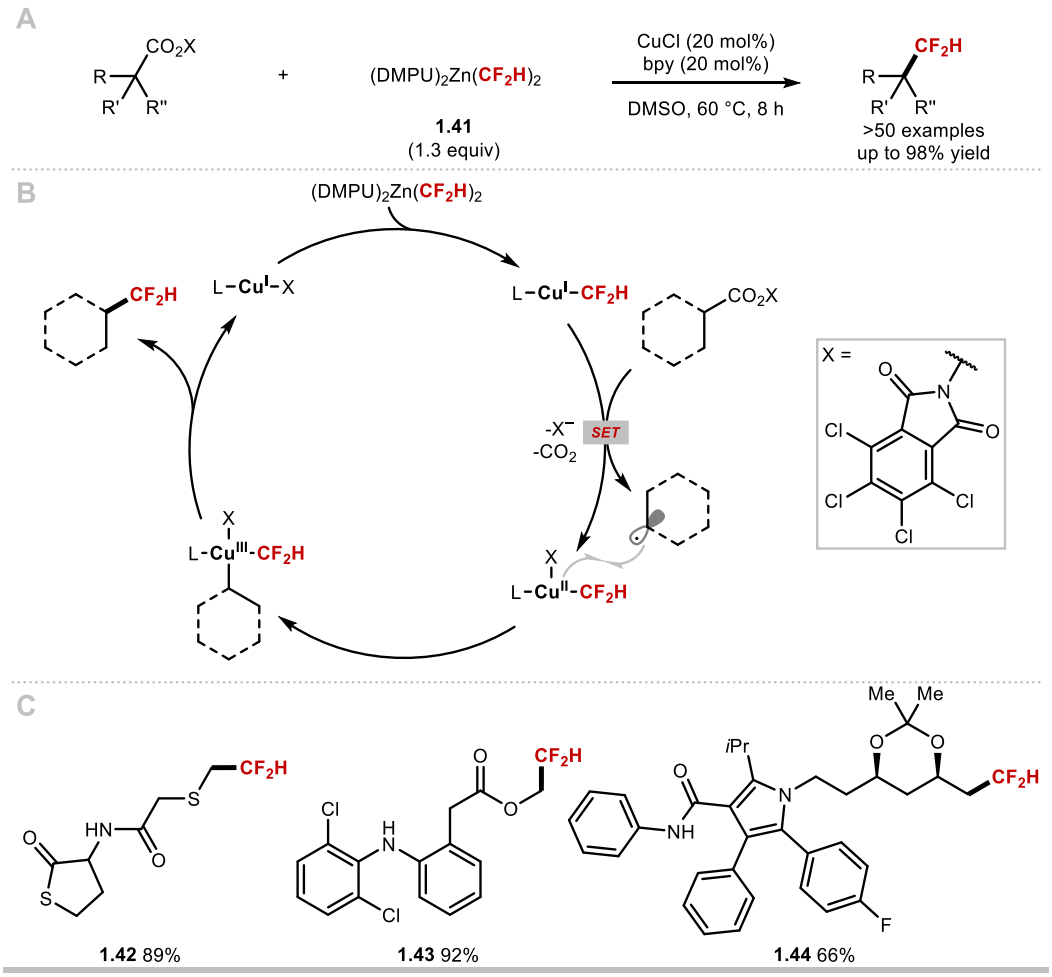
In 2016, Qing and co-workers reported a complementary approach for the bromodifluoromethylation of unactivated alkenes employing (difluoromethyl)triphenylphosphonium bromide (**1.40**, Scheme 1.8).[72] The (difluoromethyl)triphenylphosphonium reagent **1.40** is readily activated by single-electron reduction from an iridium-based photocatalyst. Mechanistically, this reaction is distinct to the report of Dolbier (Scheme 1.7), since the carbon-centred radical intermediate does not undergo halogen-atom abstraction but rather undergoes single-electron oxidation. This process yields a carbocation, which readily reacts with bromide. This reaction pathway was later explored for alternative vicinal difluoromethylation reactions. Qing and Akita disclosed intermolecular examples of oxydifluoromethylation,[81,82] and Zhang disclosed a difluoromethylation-cyclisation with oxygen-based nucleophiles.[83]



Scheme 1.8. a) Activation of (difluoromethyl)triphenylphosphonium bromide; b) Late-stage bromodifluoromethylation of unactivated alkenes; c) Proposed mechanism for the bromodifluoromethylation.

1.3.4 Late-Stage Cross-Coupling to Access the C(sp^3)-Difluoromethyl Group

Recently, a complementary approach for the late stage assembly of the C(sp^3)-CF_2H bond has been investigated by Liu and co-workers.[84] Instead of relying on the generation of the difluoromethyl radical, they investigated the cross-coupling of alkyl radicals with a Cu-CF_2H complex. Building up on pioneering work by Burton, Hartgraves[85] and Mikami[86] for copper-catalysed C(sp^3)-difluoromethylation, Liu and co-workers disclosed in 2019 the decarboxylative difluoromethylation of aliphatic redox-active esters with $(DMPU)_2Zn(CF_2H)_2$ (**1.41**; Scheme 1.9A).



Scheme 1.9. A) Late-stage decarboxylative difluoromethylation; b) Proposed mechanism for the difluoromethylation of redox-active esters; c) Examples of late-stage C(sp^3)-difluoromethylation.

It is known that this difluoromethyl-zinc reagent readily undergoes transmetallation to copper(I) to afford a copper(I)-difluoromethyl complex.[85,86] The authors suggest that this species is a suitable reductant for the activation of the phthalimide ester to generate the desired alkyl radical after decarboxylation (Scheme 1.9B). Recombination of this radical with the new copper(II)-difluoromethyl complex affords the alkyl-copper(III)-difluoromethyl complex. At this stage, a reductive elimination process affords the difluoromethylalkane and the regenerated copper(I) salt. The mild reaction conditions allowed for the late-

stage difluoromethylation of a broad range of drug compounds (**1.42** – **1.44**) (Scheme 1.9C). Later, Liu and co-workers expanded this approach to alkyl radicals generated from other precursors such as benzylic C-H bonds and alkyl pyridinium salts.[87,88] Both these methods employ the same zinc reagent and rely on a similar mechanism as described in Scheme 1.9B.

1.4 Difluoromethylation of Heteroatoms

Besides C-CF_2H building blocks, the synthesis of heteroatom-difluoromethyl (X-CF_2H) fragments is a field with high relevance to medicinal chemistry. Recently, a report from Pfizer discussed the effect of fluorination of aryl ethers in a set of lead-like drug structures on their absorption, distribution, metabolism and elimination (ADME) properties.[89] The authors found that most aryl difluoromethyl ethers exhibit lower lipophilicity ($\Delta_{logD} > 0.5$) compared to the corresponding aryl trifluoromethyl ethers. Furthermore, a number of aryl difluoromethyl ethers are metabolically more stable than the corresponding aryl trifluoromethyl ethers. Structural analysis of a range of compounds showed that whilst aryl methyl ethers preferentially adapt a coplanar structure, aryl trifluoromethyl ethers preferentially adopt an orthogonal structure (Figure 1.9). In contrast, aryl difluoromethyl ethers have no prevalence to either conformation. Thus, difluoromethyl ethers are more prone to adapt a desired configuration upon binding to a target protein.

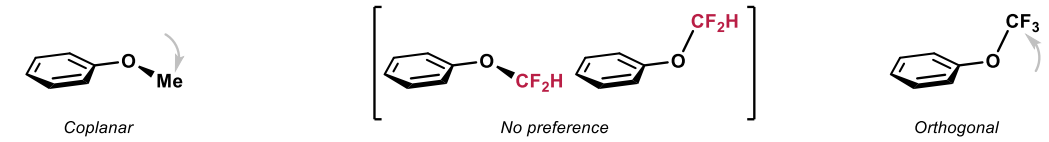
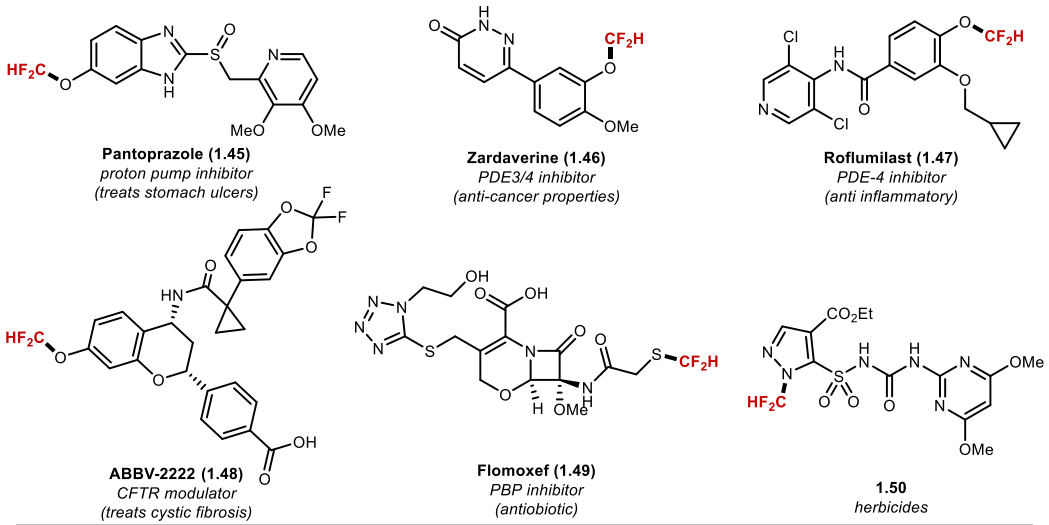


Figure 1.9. Conformational analysis of fluorinated aryl methyl ethers.

Drug compounds such as pantoprazole (**1.45**), zardaverine (**1.46**), roflumilast (**1.47**), and ABBV-2222 (**1.48**) all contain a difluoromethyl ether.[90] The antibiotic flomoxef (**1.49**) contains a C(sp^3)-linked difluoromethyl thioether. Furthermore, *N*-difluoromethyl-containing nitrogen heterocycles, such as *N*-difluoromethyl pyrazole **1.50**, have been investigated as herbicides.



Scheme 1.10. Biologically relevant molecules containing a XCF_2H moiety.

1.4.1 Introduction to Difluorocarbene

Difluorocarbene (DFC) is a common reactive intermediate for the synthesis of difluoromethyl (CF_2H) or difluoromethylene (CF_2) compounds. The geometries of singlet and triplet difluorocarbene are similar to that of methylene (Figure 1.10).[68,91]

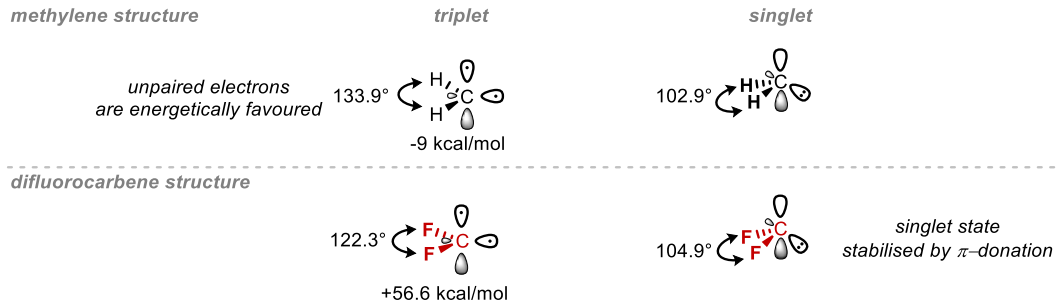


Figure 1.10. Structure of singlet and triplet methylene and difluorocarbene. [a]Energy difference to corresponding singlet carbene (deliberately set to 0 kcal/mol).

The F-C-F bond angle in singlet DFC is only marginally higher (104.9°) than that of methylene (102.9°). In the triplet state, the F-C-F bond angle is lower (122.3°) than that of methylene (133.9°). However, in contrast to many carbenes for which the triplet state is more stable than the singlet state (9 kcal mol^{-1} for methylene), DFC is more stable in its singlet state (energy difference of 56.6 kcal/mol). This can be attributed to the stabilisation of the singlet state by backbonding interactions of the fluorine lone pairs.

Difluorocarbene has been generated from various reagents *via* different activation modes. An overview of the most common difluorocarbene reagents is given in Figure 1.11.[73,92–100]

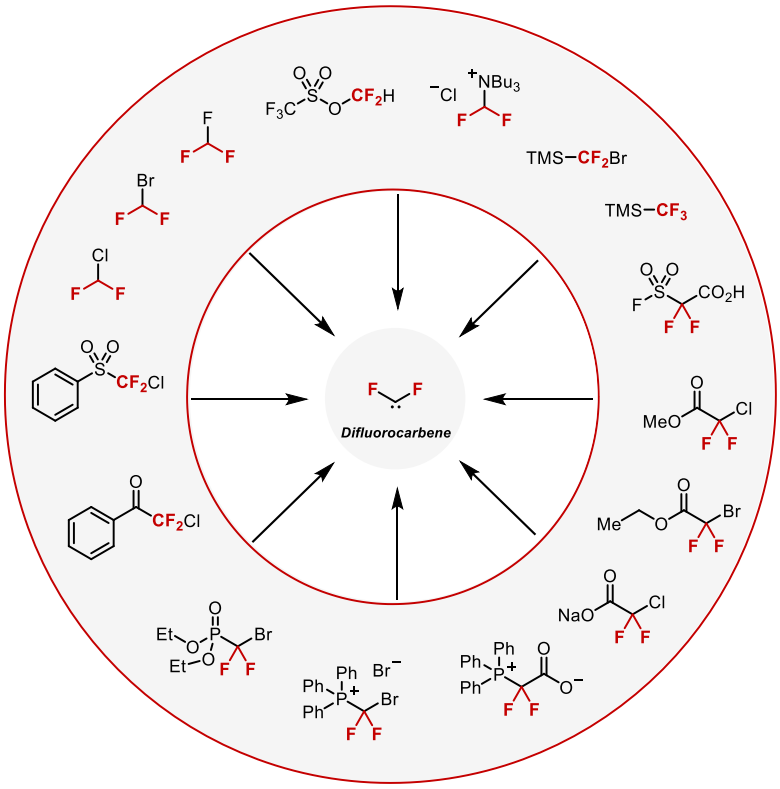
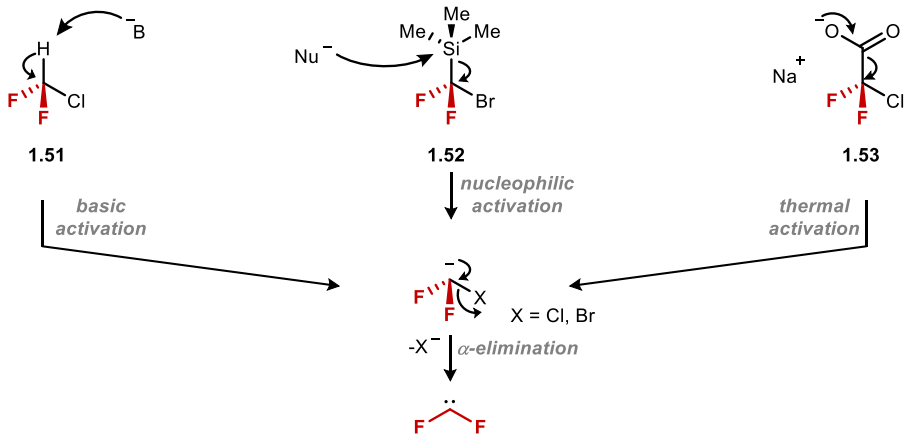


Figure 1.11. Relevant difluorocarbene precursors.

Most of these reagents follow similar activation modes (Scheme 1.11): Chlorodifluoromethane (**1.51**), a classical difluorocarbene precursor, is activated *via* deprotonation.[48] The anionic intermediate readily undergoes α-elimination to release difluorocarbene and chloride. Bromodifluoromethyl trimethylsilane (**1.52**), a reagent recently shown to be a versatile difluorocarbene precursor, is activated by nucleophilic attack on the silyl group to release a bromodifluoromethyl anion, which can in turn release bromide and difluorocarbene.[94] In contrast, sodium chlorodifluoroacetate (**1.53**) can release DFC by thermal activation without the need of initiators.[97] Decarboxylation occurs at temperatures as low as 50 °C to release the chlorodifluoromethyl anion that undergoes *α*-elimination.



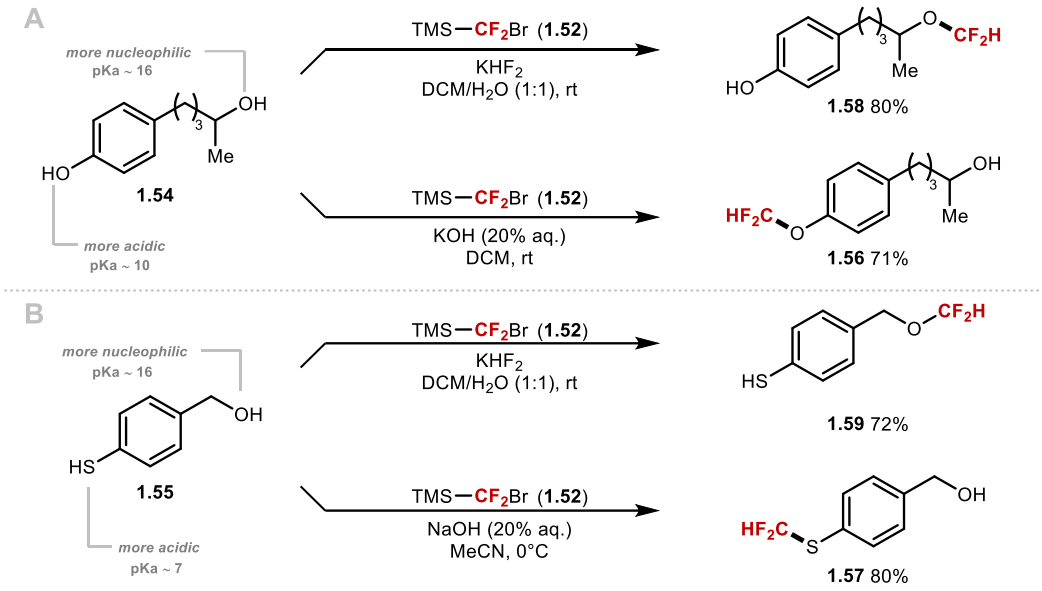
Scheme 1.11. Classical difluorocarbene reagents (**1.51** – **1.53**) and their activation modes. B = base (e.g. hydroxide); Nu = nucleophile (e.g. fluoride).

1.4.2 The Reactivity of Difluorocarbene

The common strategies for the synthesis of the X-CF_2H (X = O, N, S) motif mostly harness the reactivity of difluorocarbene. As an electrophilic singlet carbene, difluorocarbene readily reacts under mild reaction conditions with anionic species such as phenolates, thiophenolates and deprotonated *N*-heterocycles.[97,101,102] With uncharged nucleophiles such as alcohols, difluorocarbene readily undergoes an insertion reaction into the O-H bond.[103] Triplet carbenes generally undergo stepwise cyclopropanation reactions with alkenes.[104] In contrast, singlet carbenes, such as difluorocarbene in its ground state, undergo instead concerted cyclopropanation reactions. Therefore, the difluorocyclopropanation of alkenes is stereospecific; *E*-1,2-disubstituted alkenes afford *cis*-difluorocyclopropanes and *Z*-1,2-disubstituted alkenes afford *trans*-difluorocyclopropanes.[95,102]

1.4.3 Control of Difluorocarbene Reactivity

Carbenes are highly reactive intermediates and therefore difluorocarbene-based reactions often lack selectivity for substrates containing several reactive functional groups. Recently, Hu and co-workers disclosed the synthesis and application of $TMSCF_2Br$ (**1.52**).[101] The activation of this reagent relies on nucleophilic attack on its silyl group (see Scheme 1.12). Depending on the reaction conditions, the authors were able to steer the reactivity and achieve excellent selectivities. Under alkaline conditions, phenols ($pKa_{aq.} \approx 10$) and thiophenols ($pKa_{aq.} \approx 7$) readily deprotonate to form phenoxides or thiophenolates. In contrast, alcohols ($pKa_{aq.} \approx 16$) are less acidic and therefore less prone to deprotonation. The authors reacted phenol-containing alcohol **1.54** and thiophenol-containing alcohol **1.55** under basic conditions (aqueous potassium hydroxide or sodium hydroxide) with the difluorocarbene reagent $TMSCF_2Br$ (**1.52**). Under these conditions, the alcohol functionality was not reactive and difluoromethylation occurred selectively at the phenol and thiophenol to afford the difluoromethoxyarene **1.56** and the difluoromethylsulfide **1.57**. Given the higher nucleophilicity of aliphatic alcohols compared to phenols and thiophenols, alcohols react more readily under neutral or mildly acidic conditions. Therefore, when difluorocarbene was generated with potassium bifluoride (a weak acid), alcohols **1.54** and **1.55** underwent selective difluoromethylation and outcompete phenols and thiophenols to yield difluoromethylether **1.58** and difluoromethylether **1.59** in high yields.



Scheme 1.12. a) Divergent difluoromethylation of alcohol **1.54**; b) Divergent difluoromethylation of alcohol **1.55**.

1.5 Conclusion

Owing to the ubiquity of the CF_2H group, the work presented herein describes the development of novel methodologies for the late-stage introduction of the difluoromethyl group into complex biologically active molecules. The first section depicts our efforts leading to the development of a hydrodifluoromethylation reaction of unactivated alkenes with difluoroacetic acid. This reaction was expanded to the generation of halofluoromethyl radicals, such as the chlorofluoromethyl radical and the bromofluoromethyl radical. These radicals remain underexplored in the context of method development.

The second section discusses the generation of fluorine-18 labelled difluorocarbene for the preparation of $[^{18}F]XCF_2H$ motifs. Specifically, the synthesis of an F-18 labelled difluorocarbene reagent and the applications of this reagent towards the preparation of novel ^{18}F-difluoromethyl-analogues of highly relevant PET tracers are investigated.

1.6 References Chapter 1

[1] D. O'Hagan, D. B. Harper, *J. Fluor. Chem.* **1999**, *100*, 127–133.
[2] G. K. Surya Prakash, F. Wang, *Chim. Oggi/Chemistry Today* **2012**, *30*, 30–36.
[3] S. Purser, P. R. Moore, S. Swallow, V. Gouverneur, *Chem. Soc. Rev.* **2008**, *37*, 320–330.
[4] C. Isanbor, D. O'Hagan, *J. Fluor. Chem.* **2006**, *127*, 303–319.
[5] P. Shah, A. D. Westwell, *J. Enzyme Inhib. Med. Chem.* **2007**, *22*, 527–540.
[6] W. K. Hagmann, *J. Med. Chem.* **2008**, *51*, 4359–4369.
[7] N. A. Meanwell, *J. Med. Chem.* **2011**, *54*, 2529–2591.
[8] D. O'hagan, *Chem. Soc. Rev.* **2008**, *37*, 308–319.
[9] E. P. Gillis, K. J. Eastman, M. D. Hill, D. J. Donnelly, N. A. Meanwell, *J. Med. Chem.* **2015**, *58*, 8315–8359.
[10] A. Bondi, *J. Phys. Chem.* **1964**, *68*, 441–451.
[11] R. Szpera, D. F. J. Moseley, L. B. Smith, A. J. Sterling, V. Gouverneur, *Angew. Chemie - Int. Ed.* **2019**, *58*, 14824–14848.
[12] K. Müller, C. Faeh, F. Diederich, *Science (80-.).* **2007**, *317*, 1881–1886.
[13] T. S. Elliott, A. Slowey, Y. Ye, S. J. Conway, *Medchemcomm* **2012**, *3*, 735–751.
[14] B. Yang, X. H. Xu, F. L. Qing, *Org. Lett.* **2016**, *18*, 5956–5959.
[15] J. Charpentier, N. Früh, A. Togni, *Chem. Rev.* **2015**, *115*, 650–682.
[16] S. Barata-Vallejo, B. Lantano, A. Postigo, *Chem. - A Eur. J.* **2014**, *20*, 16806–16829.
[17] J. A. Ma, D. Cahard, *J. Fluor. Chem.* **2007**, *128*, 975–996.
[18] C. Zhang, *Org. Biomol. Chem.* **2014**, *12*, 6580–6589.
[19] X. Pan, H. Xia, J. Wu, *Org. Chem. Front.* **2016**, *3*, 1163–1185.
[20] S. Barata-Vallejo, S. M. Bonesi, A. Postigo, *RSC Adv.* **2015**, *5*, 62498–62518.
[21] N. V. Kirij, A. A. Filatov, G. Y. Khrapach, Y. L. Yagupolskii, *Chem. Commun.* **2017**, *53*, 2146–2149.
[22] G. K. S. Prakash, A. K. Yudin, *Chem. Rev.* **1997**, *97*, 757–786.
[23] J. A. Ma, D. Cahard, *Chem. Rev.* **2004**, *104*, 6119–6146.
[24] D. E. Yerien, S. Barata-Vallejo, A. Postigo, *Chem. - A Eur. J.* **2017**, *23*, 14676–14701.
[25] J. A. Erickson, J. I. McLoughlin, *J. Org. Chem.* **1995**, *60*, 1626–1631.
[26] Y. Zafrani, D. Yeffet, G. Sod-Moriah, A. Berliner, D. Amir, D. Marciano, E. Gershonov, S. Saphier, *J. Med. Chem.* **2017**, *60*, 797–804.
[27] C. D. Sessler, M. Rahm, S. Becker, J. M. Goldberg, F. Wang, S. J. Lippard, *J. Am. Chem. Soc.* **2017**, *139*, 9325–9332.
[28] N. Malquin, K. Rahgoshay, N. Lensen, G. Chaume, E. Miclet, T. Brigaud, *Chem. Commun.* **2019**, *55*, 12487–12490.
[29] S. I. Yaguchi, Y. Fukui, I. Koshimizu, H. Yoshimi, T. Matsuno, H. Gouda, S. Hirono, K. Yamazaki, T. Yamori, *J. Natl. Cancer Inst.* **2006**, *98*, 545–556.
[30] D. W. Cudney, S. B. Orloff, D. A. Demason, *Weed Technol.* **1993**, *7*, 860–864.
[31] D. Millis, J. Weigel, T. Moyers, F. Buonomo, D. Kressin, *Vet. Ther.* **2002**, *3*, 453–464.
[32] D. Rageot, T. Bohnacker, A. Melone, J. B. Langlois, C. Borsari, P. Hillmann, A. M. Sele, F. Beaufils, M. Zvelebil, P. Hebeisen, W. Löscher, J. Burke, D. Fabbro, M. P. Wymann, *J. Med. Chem.* **2018**, *61*, 10084–10105.
[33] W. L. Hu, X. G. Hu, L. Hunter, *Synth.* **2017**, *49*, 4917–4930.
[34] J. R. McCarthy, M. E. LeTourneau, N. P. Peet, M. Inbasekaran, *J. Am. Chem. Soc.* **1985**, *107*, 735–737.
[35] R. Szpera, N. Kovalenko, K. Natarajan, N. Paillard, B. Linclau, *Beilstein J. Org. Chem.* **2017**, *13*, 2883–2887.
[36] P. A. Messina, K. C. Mange, W. J. Middleton, *J. Fluor. Chem.* **1989**, *42*, 137–143.
[37] P. S. Fier, J. F. Hartwig, *J. Am. Chem. Soc.* **2012**, *134*, 5524–5527.
[38] V. Bacauanu, S. Cardinal, M. Yamauchi, M. Kondo, D. F. Fernández, R. Remy, D. W. C. MacMillan, *Angew. Chemie - Int. Ed.* **2018**, *57*, 12543–12548.

[39] H. Motohashi, K. Mikami, *Org. Lett.* **2018**, *20*, 5340–5343.
[40] T. Xia, L. He, Y. A. Liu, J. F. Hartwig, X. Liao, *Org. Lett.* **2017**, *19*, 2610–2613.
[41] J. R. Bour, S. K. Kariofillis, M. S. Sanford, *Organometallics* **2017**, *36*, 1220–1223.
[42] L. Xu, D. A. Vicic, *J. Am. Chem. Soc.* **2016**, *138*, 2536–2539.
[43] F. Pan, G. B. Boursalian, T. Ritter, *Angew. Chemie - Int. Ed.* **2018**, *57*, 16871–16876.
[44] C. Matheis, K. Jouvin, L. J. Goossen, *Org. Lett.* **2014**, *16*, 5984–5987.
[45] Y. Gu, D. Chang, X. Leng, Y. Gu, Q. Shen, *Organometallics* **2015**, *34*, 3065–3071.
[46] W. Miao, Y. Zhao, C. Ni, B. Gao, W. Zhang, J. Hu, *J. Am. Chem. Soc.* **2018**, *140*, 880–883.
[47] C. Bi, G. Che, D. Bao, W. Qiao, L. Sun, M. R. Collins, O. O. Fadeyi, G. M. Gallego, J. J. Mousseau, P. Nuhant, P. S. Baran, *Science (80-.).* **2018**, *80*, 75–80.
[48] Z. Feng, Q. Q. Min, X. P. Fu, L. An, X. Zhang, *Nat. Chem.* **2017**, *9*, 918–923.
[49] X. P. Fu, X. S. Xue, X. Y. Zhang, Y. L. Xiao, S. Zhang, Y. L. Guo, X. Leng, K. N. Houk, X. Zhang, *Nat. Chem.* **2019**, *11*, 948–956.
[50] S. Q. Zhu, Y. L. Liu, H. Li, X. H. Xu, F. L. Qing, *J. Am. Chem. Soc.* **2018**, *140*, 11613–11617.
[51] H. Zhao, S. Herbert, T. Kinzel, W. Zhang, Q. Shen, *J. Org. Chem.* **2020**, *85*, 3596–3604.
[52] F. Lovering, J. Bikker, C. Humblet, *J. Med. Chem.* **2009**, *52*, 6752–6756.
[53] D. Chen, C. Ni, Y. Zhao, X. Cai, X. Li, P. Xiao, J. Hu, *Angew. Chemie - Int. Ed.* **2016**, *55*, 12632–12636.
[54] Y. Zhao, W. Huang, J. Zheng, J. Hu, *Org. Lett.* **2011**, *13*, 5342–5345.
[55] G. F. Du, Y. Wang, C. Z. Gu, B. Dai, L. He, *RSC Adv.* **2015**, *5*, 35421–35424.
[56] T. Iida, R. Hashimoto, K. Aikawa, S. Ito, K. Mikami, *Angew. Chemie - Int. Ed.* **2012**, *51*, 9535–9538.
[57] P. Cao, J. X. Duan, Q. Y. Chen, *J. Chem. Soc. Chem. Commun.* **1994**, *204*, 737–738.
[58] T. Cernak, K. D. Dykstra, S. Tyagarajan, P. Vachal, S. W. Krska, *Chem. Soc. Rev.* **2016**, *45*, 546–576.
[59] J. Börgel, T. Ritter, *Chem* **2020**, *6*, 1877–1887.
[60] M. Moir, J. J. Danon, T. A. Reekie, M. Kassiou, *Expert Opin. Drug Discov.* **2019**, *14*, 1137–1149.
[61] D. A. DiRocco, K. Dykstra, S. Krska, P. Vachal, D. V. Conway, M. Tudge, *Angew. Chemie - Int. Ed.* **2014**, *53*, 4802–4806.
[62] G. E. M. Crisenza, P. Melchiorre, *Nat. Commun.* **2020**, *11*, 8–11.
[63] W. Liu, C. J. Li, *Recent Synthetic Applications of Catalyst-Free Photochemistry*, **2017**.
[64] D. Ravelli, D. Dondi, M. Fagnoni, A. Albini, *Chem. Soc. Rev.* **2009**, *38*, 1999–2011.
[65] S. El-Taher, *Int. J. Quantum Chem.* **2005**, *102*, 178–188.
[66] B. Wang, H. Hou, Y. Gu, *J. Phys. Chem. A* **1999**, *103*, 5075–5079.
[67] M. Schwartz, L. R. Peebles, R. J. Berry, P. Marshall, *J. Chem. Phys.* **2003**, *118*, 557–564.
[68] C. Ni, J. Hu, *Chem. Soc. Rev.* **2016**, *45*, 5441–5454.
[69] X. K. Jiang, X. Y. Li, K. Y. Wang, *J. Org. Chem.* **1989**, *54*, 5648–5650.
[70] Y. Fujiwara, J. A. Dixon, R. A. Rodriguez, R. D. Baxter, D. D. Dixon, M. R. Collins, D. G. Blackmond, P. S. Baran, *J. Am. Chem. Soc.* **2012**, *134*, 1494–1497.
[71] R. C. McAtee, J. W. Beatty, C. C. McAtee, C. R. J. Stephenson, *Org. Lett.* **2018**, *20*, 3491–3495.
[72] Q. Y. Lin, Y. Ran, X. H. Xu, F. L. Qing, *Org. Lett.* **2016**, *18*, 2419–2422.
[73] Q. Y. Lin, X. H. Xu, K. Zhang, F. L. Qing, *Angew. Chemie - Int. Ed.* **2016**, *55*, 1479–1483.
[74] C. A. Kuttruff, M. Haile, J. Kraml, C. S. Tautermann, *ChemMedChem* **2018**, *13*, 983–987.
[75] R. Sakamoto, H. Kashiwagi, K. Maruoka, *Org. Lett.* **2017**, *19*, 5126–5129.
[76] J. Twilton, C. C. Le, P. Zhang, M. H. Shaw, R. W. Evans, D. W. C. MacMillan, *Nat. Rev. Chem.* **2017**, *1*, DOI 10.1038/s41570-017-0052.
[77] K. Uneyama, H. Nanbu, *J. Org. Chem.* **1988**, *53*, 4598–4599.
[78] C. S. Thomoson, X. J. Tang, W. R. Dolbier, *J. Org. Chem.* **2015**, *80*, 1264–1268.
[79] X. J. Tang, C. S. Thomoson, W. R. Dolbier, *Org. Lett.* **2014**, *16*, 4594–4597.
[80] X. J. Tang, W. R. Dolbier, *Angew. Chemie - Int. Ed.* **2015**, *54*, 4246–4249.
[81] Y. Ran, Q. Y. Lin, X. H. Xu, F. L. Qing, *J. Org. Chem.* **2016**, *81*, 7001–7007.
[82] Y. Arai, R. Tomita, G. Ando, T. Koike, M. Akita, *Chem. - A Eur. J.* **2016**, *22*, 1262–1265.

[83] S. Zhang, L. Li, J. Zhang, J. Zhang, M. Xue, K. Xu, *Chem. Sci.* **2019**, *10*, 3181–3185.
[84] X. Zeng, W. Yan, S. B. Zacate, T. H. Chao, X. Sun, Z. Cao, K. G. E. Bradford, M. Paeth, S. B. Tyndall, K. Yang, T. C. Kuo, M. J. Cheng, W. Liu, *J. Am. Chem. Soc.* **2019**, *141*, 11398–11403.
[85] D. J. Burton, G. A. Hartgraves, *J. Fluor. Chem.* **2007**, *128*, 1198–1215.
[86] Y. Endo, K. Ishii, K. Mikami, *Tetrahedron* **2019**, *75*, 4099–4103.
[87] X. Zeng, W. Yan, S. B. Zacate, A. Cai, Y. Wang, D. Yang, K. Yang, W. Liu, *Angew. Chemie - Int. Ed.* **2020**, *59*, 16398–16403.
[88] X. Zeng, W. Yan, M. Paeth, S. B. Zacate, P. H. Hong, Y. Wang, D. Yang, K. Yang, T. Yan, C. Song, Z. Cao, M. J. Cheng, W. Liu, *J. Am. Chem. Soc.* **2020**, *141*, 19941–19949.
[89] L. Xing, D. C. Blakemore, A. Narayanan, R. Unwalla, F. Lovering, R. A. Denny, H. Zhou, M. E. Bunnage, *ChemMedChem* **2015**, *10*, 715–726.
[90] B. Gutmann, P. Hanselmann, M. Bersier, D. Roberge, C. O. Kappe, *J. Flow Chem.* **2017**, *7*, 46–51.
[91] D. L. S. Brahms, W. P. Dailey, *Chem. Rev.* **1996**, *96*, 1585–1632.
[92] P. S. Fier, J. F. Hartwig, *Angew. Chemie - Int. Ed.* **2013**, *52*, 2092–2095.
[93] E. Nawrot, A. Joñczyk, *J. Org. Chem.* **2007**, *72*, 10258–10260.
[94] Q. Xie, Z. Zhu, L. Li, C. Ni, J. Hu, *Angew. Chemie - Int. Ed.* **2019**, *58*, 6405–6410.
[95] A. García-Domínguez, T. H. West, J. J. Primozic, K. M. Grant, C. P. Johnston, G. G. Cumming, A. G. Leach, G. C. Lloyd-Jones, *J. Am. Chem. Soc.* **2020**, *142*, 14649–14663.
[96] M. Huiban, M. Tredwell, S. Mizuta, Z. Wan, X. Zhang, T. L. Collier, V. Gouverneur, J. Passchier, *Nat. Chem.* **2013**, *5*, 941–944.
[97] V. P. Mehta, M. F. Greaney, *Org. Lett.* **2013**, *15*, 5036–5039.
[98] C. S. Thomoson, W. R. Dolbier, *J. Org. Chem.* **2013**, *78*, 8904–8908.
[99] J. Zheng, Y. Li, L. Zhang, J. Hu, G. J. Meuzelaar, H. J. Federsel, *Chem. Commun.* **2007**, 5149–5151.
[100] Y. Zafrani, G. Sod-Moriah, Y. Segall, *Tetrahedron* **2009**, *65*, 5278–5283.
[101] Q. Xie, C. Ni, R. Zhang, L. Li, J. Rong, J. Hu, *Angew. Chemie - Int. Ed.* **2017**, *56*, 3206–3210.
[102] L. Li, F. Wang, C. Ni, J. Hu, *Angew. Chemie - Int. Ed.* **2013**, *52*, 12390–12394.
[103] R. Zhang, C. Ni, Q. Xie, J. Hu, *Tetrahedron* **2020**, *76*, 1–6.
[104] A. M. del Hoyo, A. G. Herraiz, M. G. Suero, *Angew. Chemie - Int. Ed.* **2017**, *56*, 1610–1613.

Chapter 2 – Hydrodifluoromethylation of Alkenes with Difluoroacetic Acid

The work discussed in this chapter was published in *Angewandte Chemie International Edition*.

Claudio F. Meyer, Sandrine M. Hell, Antonio Misale, Andrés A. Trabanco, Véronique Gouverneur, *Angew. Chem. Int. Ed.* **2019**, *58*, 8828–8833.

Author contributions: The project was conceived by Claudio Meyer, Sandrine Hell, Antonio Misale, Andrés A. Trabanco and Véronique Gouverneur. Reaction optimisation and mechanistic investigations were performed by Claudio Meyer. Substrate synthesis was performed by Claudio Meyer with help of Sandrine Hell. Scale-up experiments were performed by Claudio Meyer with help of Alejandro Diéguez-Vázquez.

2.1 The C(sp^3)-linked Difluoromethyl Group

With the recent fast-growing interest in the difluoromethyl group for drug discovery, numerous methodologies to install this group have been reported.

The C(sp^3)-CF_2H motif has been investigated in many SAR studies and can be found in various marketed drugs or drug candidates in clinical trials (Figure 2.1). The most prominent examples are the anti-viral drugs Voxilaprevir (**2.1**) and Glecaprevir (**2.2**). These structurally related non-structural protein 3/4a (NS3/4a) protease inhibitors both contain an unnatural difluoromethylcyclopropyl amino acid.[1]

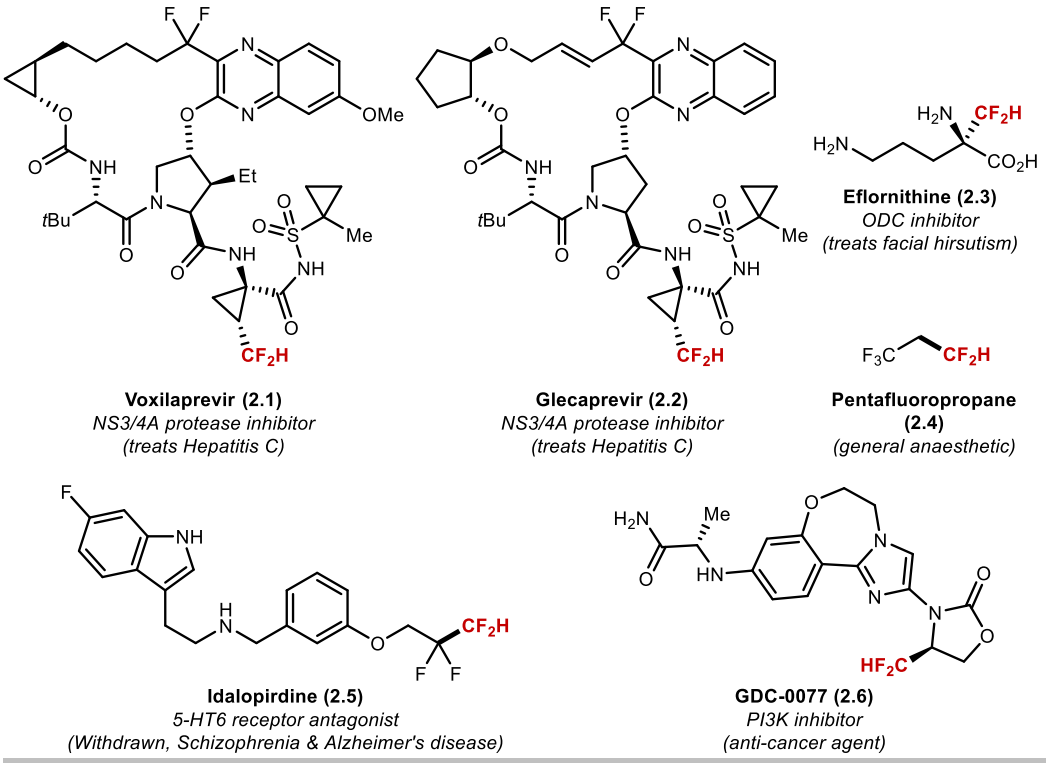


Figure 2.2. Biologically active compounds bearing a C(sp^3)-CF_2H group.

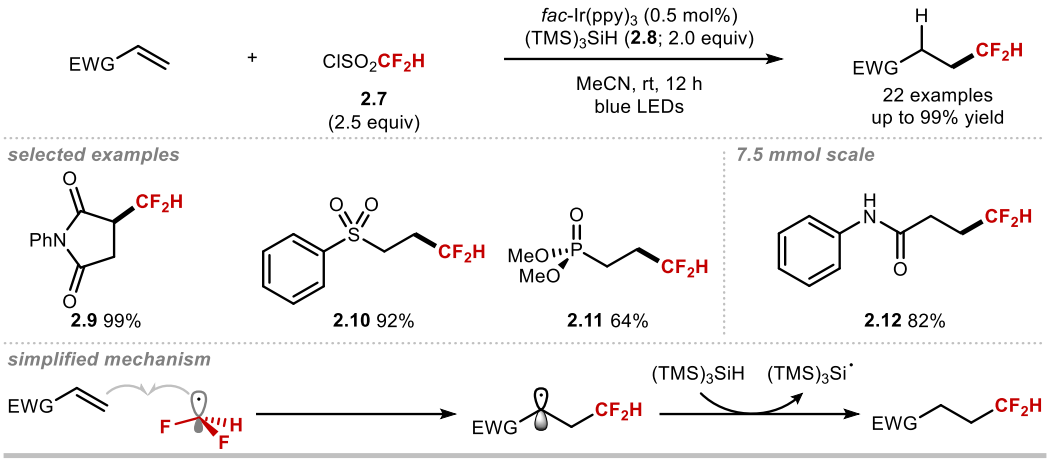
Other examples of C(sp^3)-CF_2H containing drugs or drug candidates are Eflornithine (**2.3**), an ornithine decarboxylase (ODC) inhibitor,[2] pentafluoropropane (**2.4**), a general anaesthetic,[3] Idalopirdine (**2.5**), a 5-

hydroxytryptamine subunit 6 (5-HT_6) receptor antagonist,[4] and GDC-0077 (**2.6**), a phosphoinositide 3-kinase (PI3K) inhibitor.[5]

An overview of strategies to access the C(sp^3)-CF_2H motif is summarized in Chapter 1. The typical strategies to access this motif include classical deoxyfluorination, and more recently nucleophilic, electrophilic, and radical difluoromethylation.

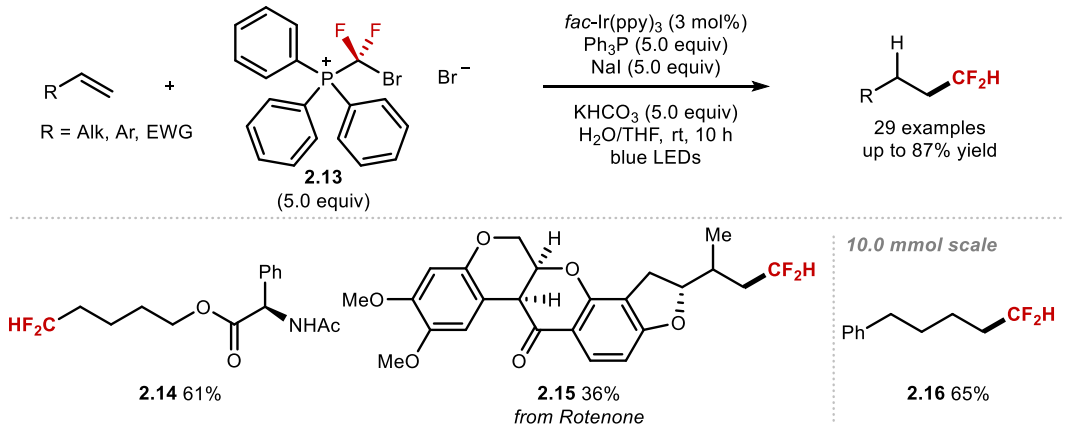
2.2 Synthetic Strategies Towards C(sp^3)-CF_2H Compounds

In contrast to the well explored field of vicinal difluoromethylation (Section 1.3.4), the field of hydrodifluoromethylation remains underexplored. In 2015, Dolbier and co-workers reported a general method for the hydrodifluoromethylation of electron-deficient alkenes (Scheme 2.1).[6] In this transformation, difluoromethanesulfonyl chloride (**2.7**) is used to generate the difluoromethyl radical, which undergoes Giese-addition to the alkene affording an electrophilic carbon-centred radical intermediate. This radical intermediate can undergo hydrogen-atom abstraction from tris(trimethylsilyl)silane (**2.8**). Due to a polarity match between the hydridic silane **2.8** and the electrophilic carbon-centred radical intermediate, this hydrogen-atom transfer (HAT) is preferred over unfavourable reactions, such as difluoromethylation-dimerisation or atom transfer radical addition (ATRA).[7–9] However, the requirement for a polarity matched HAT, limits the scope of this method to electron-deficient alkenes. A selection of products accessible through this strategy are shown in scheme 2.7 (**2.9** – **2.11**). Notably, the authors also demonstrated the scalability of their method with the gram scale synthesis of **2.12**.



Scheme 2.1. Hydrodifluoromethylation of electron-deficient alkenes with difluoromethanesulfonyl chloride (**2.7**).

In 2016, Qing and co-workers developed the first general hydrodifluoromethylation of unactivated alkenes (Scheme 2.2).[10] The use of excess (bromodifluoromethyl)triphenylphosphonium bromide (**2.13**) in combination with excess triphenylphosphine as well as the photocatalyst *fac*-Ir(ppy)$_3$ allowed for net hydrodifluoromethylation of a wide range of alkenes. The method displayed a broad scope of functional groups and was applied to the late-stage functionalisation of complex biologically active molecules to afford derivatives of phenylalanine (**2.14**) and Rotenone (**2.15**). The reaction is scalable as demonstrated by the synthesis of difluoromethylalkane **2.16** (10 mmol scale). However, the use of non-commercial reagent **2.13** in high excess, as well as the requirement for a glovebox to achieve high yields, limits the practicality of this protocol.



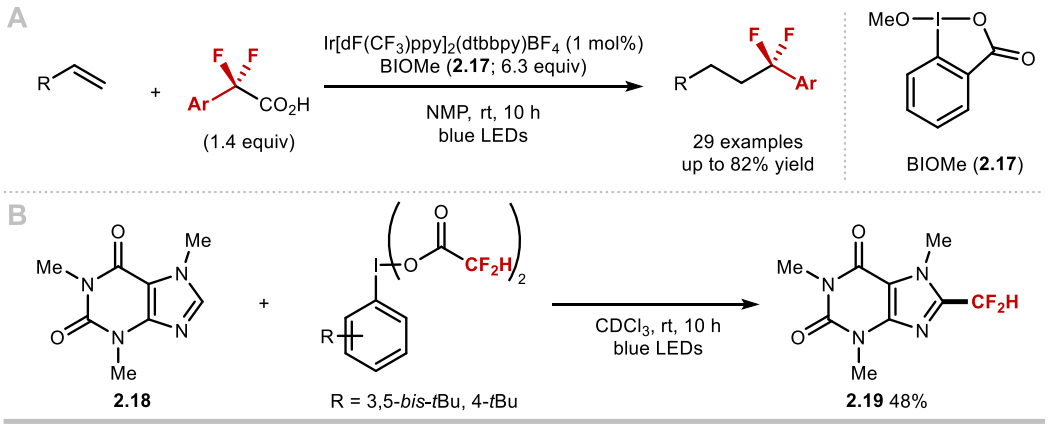
Scheme 2.2. Photocatalytic hydrodifluoromethylation of unactivated alkenes with (bromodifluoromethyl)triphenylphosphonium bromide (**2.13**).

The recent progress in late-stage difluoromethylation of alkenes, highlights the extensive functional group tolerance of radical reactions. However, despite these clear benefits, the procedures reported for alkene difluoromethylation are mostly limited to vicinal difunctionalisation with only a few examples of hydrodifluoromethylation. In addition, the examples showcased are limited to electron-deficient alkenes[6] or require a complex procedure with a non-commercial CF_2H source in combination with an excess of other reagents[10]. We therefore felt it was timely, to develop an operationally simple protocol for the hydrodifluoromethylation of alkenes. If successful, such a technology could proof invaluable and drastically reduce the number of required steps for the synthesis of C(sp^3)-CF_2H building blocks.

2.3 Aim of this Project

The development of a novel protocol for the hydrodifluoromethylation of unactivated alkenes that would not only allow for a broad substrate scope but would also be amenable to scale-up could overcome the current limitations

associated with difluoromethylation of alkenes. To achieve this, such a reaction would need to fulfil two criteria: 1) the reagents would need to be commercially available and inexpensive; and 2) the reaction would need to be operationally simple (ideally insensitive to air and water). Therefore, different ways to generate the difluoromethyl radical under mild conditions were examined. Qing and co-workers recently showed, that difluoroarylacetic acids can undergo decarboxylation in the presence of a hypervalent iodine reagent (**2.17**) and a photocatalyst to generate aryldifluoromethyl radicals (Scheme 2.3A).[11] These radicals were added to unactivated alkenes that underwent hydroaryldifluoromethylation. By performing deuteration experiments, the authors demonstrated that the solvent acts as hydrogen-atom donor (HAD) in this transformation.



Scheme 2.3. Hypervalent iodine reagents for the generation of CF_2R radicals (R = Ar, H). Ar = (hetero)aryl. A) Hydroaryldifluoromethylation of unactivated alkenes. B) C-H difluoromethylation of heteroarenes.

Furthermore, a recent publication by Maruoka and co-workers demonstrated that hypervalent iodine reagents containing difluoroacetoxy ligands can undergo homolytic iodine-oxygen bond cleavage, followed by decarboxylation of the difluoroacetoxy group to render the difluoromethyl radical (Scheme 2.3B).[12] The

difluoromethyl radical was added to heteroaryl substrates such as caffeine (**2.18**) affording the C-H difluoromethylated product **2.19** in good yield in the absence of photocatalysts.

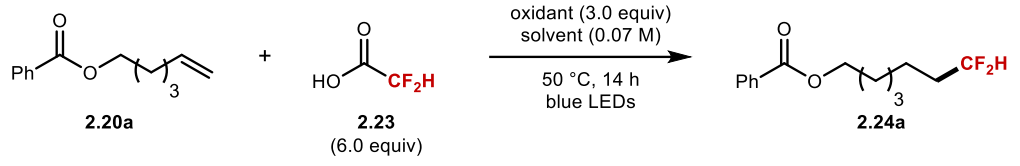
Based on these reports, we reasoned that combining alkenes with a hypervalent iodine reagent and difluoroacetic acid in a suitable solvent (as HAD) could allow for the hydrodifluoromethylation of alkenes. The utilisation of a suitable HAD could allow for selectivity in the case of substrates containing activated heteroarene C-H bonds.

2.4 Optimisation of the Hydrodifluoromethylation of Unactivated Alkenes

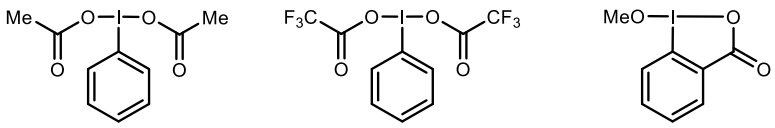
We started our optimisation by employing a model alkene substrate (**2.20a**) with different hypervalent iodine oxidants (**2.17**, **2.21 – 2.22**) and difluoroacetic acid (**2.23**) in tetrahydrofuran (THF) under blue LED (λ_{max} = 450 nm) irradiation. The reaction was performed under ambient atmosphere in non-dried solvents. After overnight reaction (14 h), *α*,*α*,*α*-trifluorotoluene was added as an internal standard. The mixtures were then analysed by quantitative ^{19}F NMR spectroscopy. The desired product **2.24a** displays a characteristic doublet of triplets ($\delta_{(ppm)}$ −116 (dt, $^{2}J_{H\text{-}F}$ = 57 Hz, $^{3}J_{H\text{-}F}$ = 17 Hz)), coupling to both the CF_2H hydrogen and the neighbouring methylene hydrogens. We observed that the conversion towards the desired product varied drastically depending on the nature of the hypervalent iodine oxidant. Whilst phenyliodine(III) diacetate (PIDA; **2.21**) resulted in high conversion towards the desired product (59%, Table 2.1, entry 1), its

polyfluorinated analogue **2.22** (PIFA) was much less reactive under analogous conditions (4%, entry 2). The corresponding hydrotrifluoromethylated compound was not formed under these conditions.

Table 2.1. Optimisation of the hydrodifluoromethylation of alkenes with difluoroacetic acid (**2.23**).[a]



oxidants



entry	solvent	oxidant	yield [%]
1	THF	**2.21**	59
2	THF	**2.22**	4[b]
3	THF	**2.17**	27
4	NMP	**2.21**	41
5	MTBE	**2.21**	41
6	MeCN	**2.21**	12
7	DMF	**2.21**	51
8	DMA	**2.21**	40
9	MeOH	**2.21**	2
10[c]	THF	**2.21**	60
11[d]	**THF**	**2.21**	**77**
12[e]	THF	**2.21**	21

[a]Reaction conditions: **2.20a** (0.1 mmol), oxidant (**2.17**, **2.21** – **2.22**) (0.3 mmol), **2.23** (0.6 mmol), solvent (1.5 mL), blue LED irradiation (λ_{max} = 450 nm) for 14 h at 50 °C. The yield was determined by quantitative ^{19}F NMR spectroscopy using α,α,α-trifluorotoluene as an internal standard. [b]Hydrotrifluoromethylation not observed. [c]THF (0.1 M). [d]A second portion of **2.21** (0.3 mmol) was added after 6 h. [e]Reaction in the absence of light. THF = tetrahydrofuran. NMP = *N*-methyl-2-pyrrolidone. MTBE = methyl *tert*-butyl ether. DMF = *N*,*N*-dimethylformamide. DMA = *N*,*N*-dimethylacetamide.

A third reagent, 1-methoxy-1,2-benziodoxol-3-(1H)-one (BIOMe; **2.17**) was also successful, yielding the desired hydrodifluoromethylated product, albeit in lower yield (27%, entry 3). Due to the high yield and low cost of PIDA (**2.21**; 220 USD kg^{-1}, 70 USD mol^{-1}) we continued the optimisation with this oxidant.

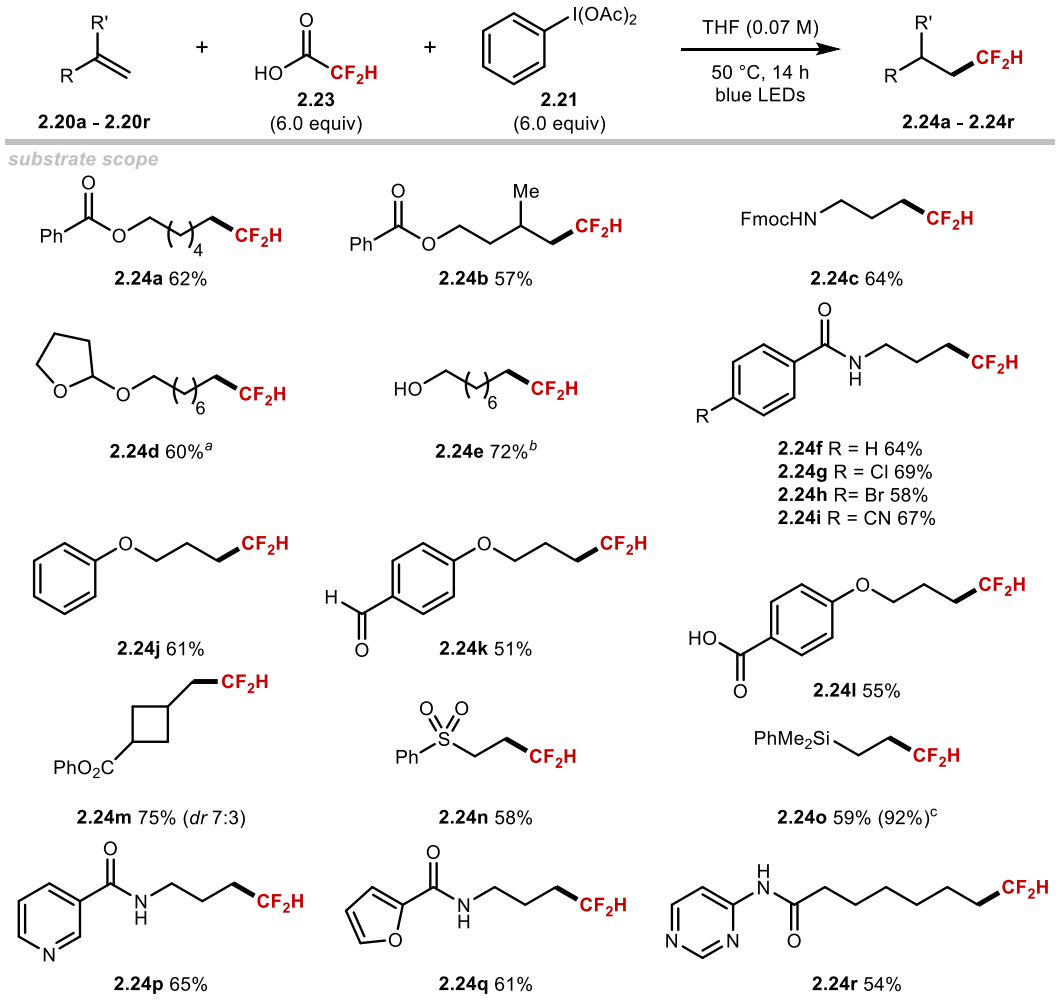
The nature of the hydrogen-atom donor could play a crucial role in this transformation and therefore the effect of the solvent was investigated; THF and other solvents have been shown to act as hydrogen-atom donors in similar transformations.[10,11,13] Interestingly, several solvents were suitable for this transformation, although all of them led to lower yields than THF. *N*-Methylpyrrolidinone (NMP), the preferred solvent from Qing's work[11] as well as methyl *tert*-butyl ether (MTBE) gave modest yields (41%, entries 4-5). Acetonitrile (MeCN) was low yielding (12%, entry 6), but when *N*,*N*-dimethylformamide (DMF) was used the desired product was obtained in similar yields to THF (51%, entry 7). The reaction does not proceed in protic solvents such as methanol (2%, entry 9). Notably, methanol was an effective H-atom donor for the hydrotrifluoromethylation of unactivated alkenes recently reported by Gouverneur and co-workers.[13] The incompatibility in this case could stem from deactivation of the hypervalent iodine reagent. Methanol is known to undergo nucleophilic attack on Iodine(III) compounds.[14] When the reaction was performed in higher concentration (0.1 M instead of 0.07 M), the yield was similar (60%, entry 10). When PIDA (**2.21**) was added portion wise and reintroduced after 6 h of reaction time, the yield was increased to 77% (entry 11). Control reactions

showed that the reaction proceeded in absence of light, albeit with lower efficiency (21%, entry 12).[12,14]

2.5 Substrate Scope and Limitations of the Hydrodifluoromethylation of Alkenes

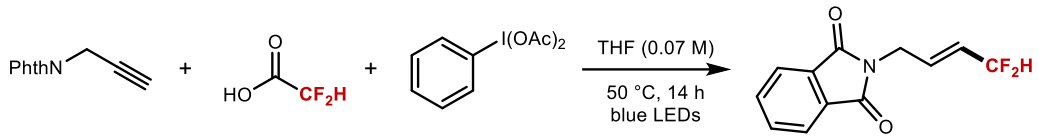
With the optimised conditions in hand, we turned our focus to the scope of this transformation. A broad range of alkenes (**2.20a** – **2.20r**) containing various functional groups were successfully hydrodifluoromethylated to afford products **2.24a** – **2.24r** (Scheme 2.4). Esters, Fmoc protected amines, alcohols, amides, aryl halides and nitriles were tolerated. In all cases, these functional groups had little effect on the reaction outcome (**2.24a** – **2.24i**). Allyl ethers containing potentially reactive functional groups such as aldehydes and benzoic acid were hydrodifluoromethylated in moderate yields (**2.24j** – **2.24l**). Such functional groups would require protecting groups in traditional deoxyfluorination reactions, as they are generally not tolerated if not protected. It was interesting to observe that the benzoic acid in **2.20l** was tolerated and did not undergo competitive decarboxylation. Geminal disubstituted alkenes such as **2.20b** and methylene cyclobutane **2.20m** were efficiently hydrodifluoromethylated and yielded the desired products **2.24b** and **2.24m** in good yields. The functionalisation of cyclobutanes is of special relevance due to their high prevalence in medicinal chemistry. Phenyl vinyl sulfone (**2.20n**), a representative electron-deficient alkene was hydrodifluoromethylated in moderate yield to afford *γ*,*γ*,-difluoropropylsulfone **2.24n**. A vinyl silane (**2.20o**) underwent the desired

transformation in moderate yield. According to quantitative ^{19}F NMR spectroscopy the yield of this product was significantly higher (92%). The moderate yield of isolated product is attributed to the volatility of the compound. We next turned our attention to substrates having heteroaromatic backbones. The difluoromethyl radical is reactive towards a range of heteroarenes *via* Minisci- reaction. In this case, alkenes containing pyridyl, pyrimidyl and furyl moieties underwent the desired transformation and no competitive Minisci-type C-H difluoromethylation was observed (**2.24p** – **2.24r**). This could be explained by the higher reactivity of olefins compared to heteroarenes. The radical addition to heteroarenes breaks the aromaticity of the system, a scenario not applicable to the radical addition to alkenes. The absence of C-H difluoromethylation was confirmed by quantitative ^{19}F NMR spectroscopy (heteroaromatic difluoromethyl groups show a characteristic doublet ($\delta_{(ppm)}$ −110 (d, $^{2}J_{H\text{-}F}$ = 52 Hz))).



Scheme 2.4. Substrate scope of the hydrodifluoromethylation of unactivated alkenes with difluoroacetic acid. Reaction conditions: **2.20a** – **2.20r** (0.3 mmol), phenyliodine(III) diacetate (**2.21**) (2 x 0.9 mmol), **2.23** (1.8 mmol), THF (4.5 mL), blue LED irradiation (λ_{max} = 450 nm) for 14 h at 50 °C. After this time, the mixture was concentrated and the product isolated *via* silica gel column chromatography. [a]Starting from 7-octen-1-ol (**2.20d**). [b]Starting from 7-octen-1-ol (**2.20d**). After 14 h, a workup using aqueous HCl (1 M) was performed. Purification *via* flash column chromatography yielded **2.24e**. [c]The yield in brackets is calculated from quantitative ^{19}F NMR spectroscopy of the crude reaction mixture using *α*,*α*,*α*-trifluorotoluene as an internal standard.

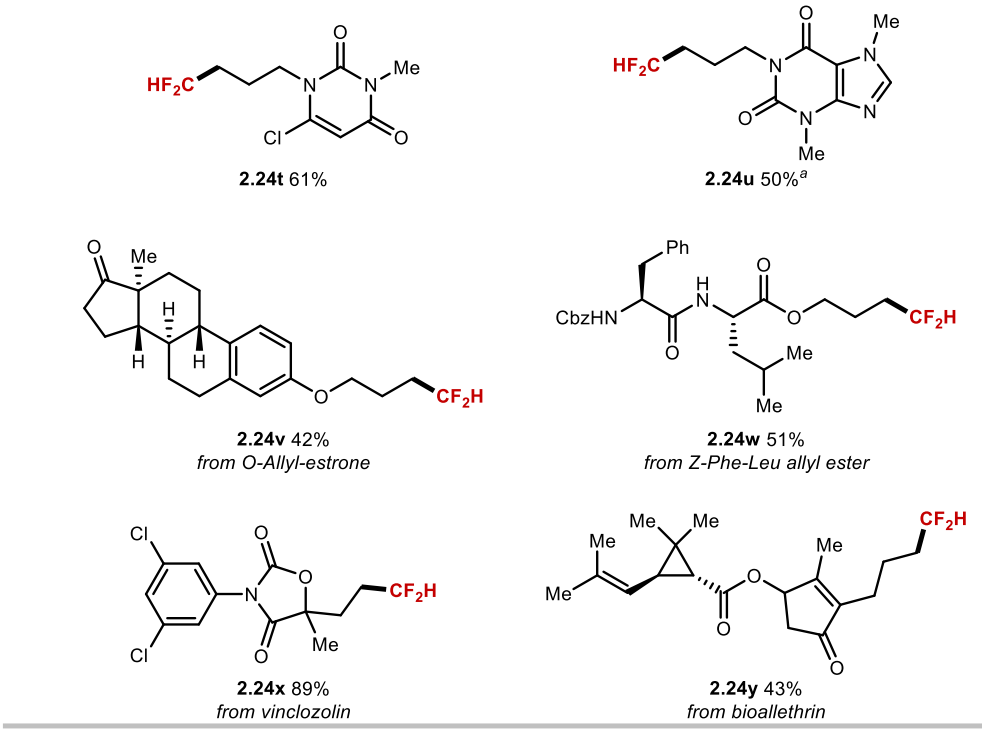
In the case of a terminal alkyne, the reaction proceeded in low yields to give the desired difluoromethyl-containing alkene **2.24s** as a mixture of *cis* and *trans* isomers (42%, E/Z = 85/15, determined by quantitative ^{19}F NMR spectroscopy of the crude reaction mixture, Scheme 2.5). Due to the low yield observed for this product, only the major isomer (*E*-isomer) was isolated.



2.20s | **2.23** (6.0 equiv) | **2.21** (6.0 equiv) | **2.24s** 32% (42% (E/Z 85/15))[a]

Scheme 2.5. Representative hydrodifluoromethylation of alkyne **2.20s** with difluoroacetic acid. Reaction conditions: **2.20s** (0.3 mmol), oxidant (**2.21**) (2 x 0.9 mmol), **2.23** (1.8 mmol), THF (4.5 mL), blue LED irradiation (λ_{max} = 450 nm) for 14 h at 50 °C. After this time, the mixture was concentrated, and the major isomer was isolated *via* silica gel column chromatography. [a]Yield and E/Z ratio determined by quantitative ^{19}F NMR analysis of the crude reaction mixture using *α*,*α*,*α*-trifluorotoluene as an internal standard.

Given the high functional group tolerance of our transformation, we investigated whether this method could be utilised for late-stage functionalisation (Scheme 2.6). Therefore, we tested the reaction on alkene-containing biologically relevant substrates (**2.20t** – **2.20y**). Uracil and theobromine derivatives underwent the desired transformation in moderate yield (**2.24t** – **2.24u**). In the quantitative ^{19}F NMR spectrum of the crude reaction mixture of *N*-allyl theobromine (**2.20u**), traces of C_8-H difluoromethylated product were observed in ($\delta_{(ppm)}$ −110 (d, $^2J_{H\text{-}F}$ = 52 Hz)). Upon purification by silica gel chromatography, the compound **2.24u** was isolated analytically pure (as proven by ^1H, ^{19}F or ^{13}C NMR spectroscopy). Furthermore, an estrone derivative and a dipeptide were hydrodifluoromethylated in low yields (**2.24v** – **2.24w**). The late-stage site-selective functionalisation of peptides is of high relevance to medicinal chemists since numerous drug compounds are based on a peptide structure (e.g. Figure 2.1; Glecaprevir and Voxilaprevir).



Scheme 2.6. Substrate scope of the late-stage hydrodifluoromethylation of unactivated alkenes with difluoroacetic acid. Reaction conditions: **2.20t** – **2.20y** (0.3 mmol), oxidant (**2.21**) (2 x 0.9 mmol), **2.23** (1.8 mmol), THF (4.5 mL), blue LED irradiation (λ_{max} = 450 nm) for 14 h at 50 °C. After this time, the mixture was concentrated and the product isolated *via* flash column chromatography. [a]Traces of C_8-H difluoromethylated product observed in quantitative ^{19}F NMR analysis of the crude reaction mixture using *α*,*α*,*α*-trifluorotoluene as an internal standard.

Finally, Vinclozolin (**2.20x**), a compound with fungicidal properties, and bioallethrin (**2.20y**), which is used to treat ectoparasitic infestations, underwent the desired transformation in moderate to excellent yields. In the case of bioallethrin, the reaction proceeded with complete regioselectivity and the vinyl cyclopropane as well as the *α*,*β*-unsaturated ketone were tolerated and remained intact.

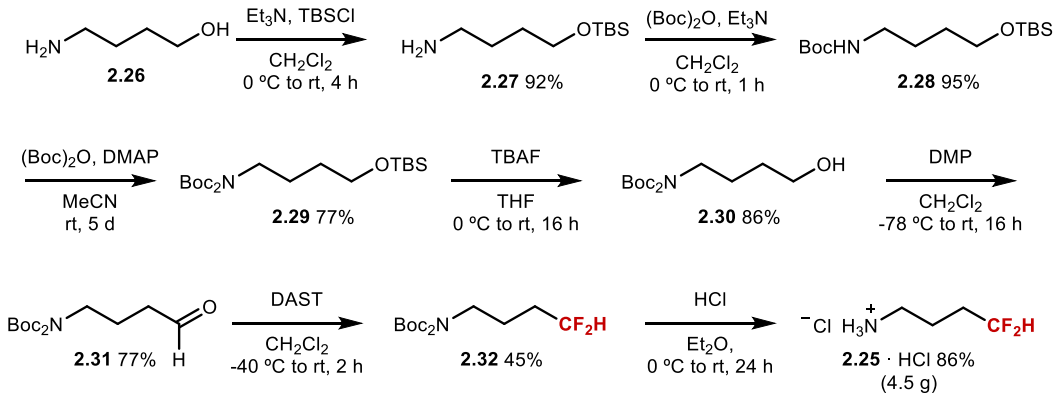
2.6 Scale-up Synthesis of (4,4-difluorobutyl)amine

Given the inexpensive nature of the reagents used in this protocol, we questioned whether our procedure could be amenable to scale-up. We therefore investigated

the large-scale synthesis of (4,4-difluorobutyl)amine (**2.25**), since this compound is of significant interest to the pharmaceutical industry.

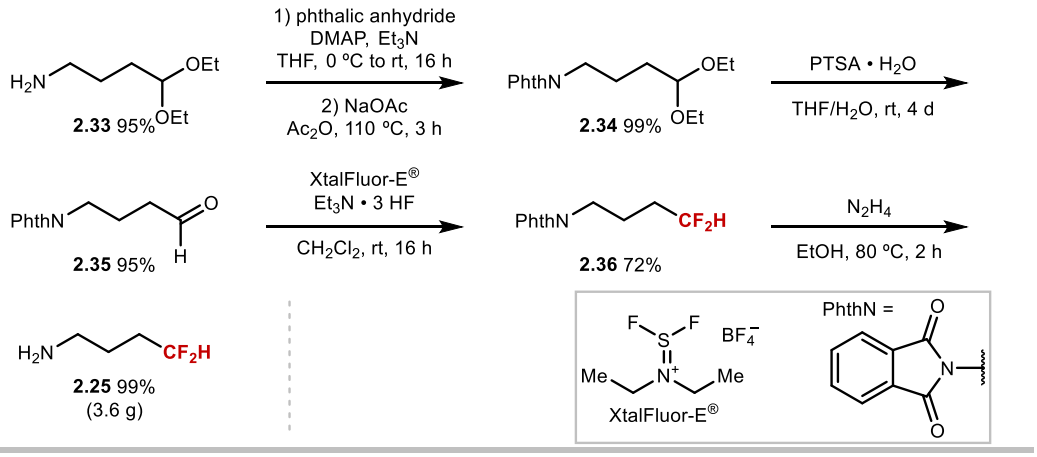
2.6.1 Previous Syntheses of (4,4-difluorobutyl)amine

The first synthesis of 4,4-difluorobutan-1-amine hydrochloride (**2.25** · HCl) was disclosed in 2008 as part of a medicinal chemistry program by AstraZeneca (Scheme 2.7).[15] The existing route's extensive use of protecting group chemistry resulted in a seven-step linear sequence to access this unprotected building block. The reaction sequence was started on a 20 g scale using 4-amino-1-butanol (**2.26**) as the starting material. The fluorine atoms were introduced upon deoxyfluorination with diethylaminosulfur trifluoride (DAST) at low temperature (-40 ˚C; 45% yield). The overall yield over seven steps was 17% and required a total of five silica gel chromatography purifications which allowed the isolation of 4.5 g of 4,4-difluorobutan-1-amine hydrochloride (**2.25** · HCl). Due to the low overall yield, the amount of silica purifications and the several steps requiring low temperatures or long reaction times, this synthesis is suboptimal for multigram preparation of 4,4-difluorobutan-1-amine.



Scheme 2.7. Synthesis of 4,4-difluorobutan-1-amine hydrochloride (**2.25** · HCl).

In 2013, scientists from Janssen improved the synthesis of 4,4-difluorobutan-1-amine (**2.25**) and developed a five-step synthesis with only one purification by silica gel chromatography (Scheme 2.8).[16] The success of this sequence lies within the use of an advanced starting material which features a protected aldehyde. The synthesis started with 12 g of 4,4-diethoxybutan-1-amine (**2.33**) to afford 4,4-difluorobutan-1-amine (**2.25**) in 67% yield (over 5 steps). The fluorine atoms were introduced *via* deoxyfluorination. The use of a phthalimide protecting group and a different deoxyfluorination reagent (XtalFluor-E®) however, significantly increased the yield of this step (72%).



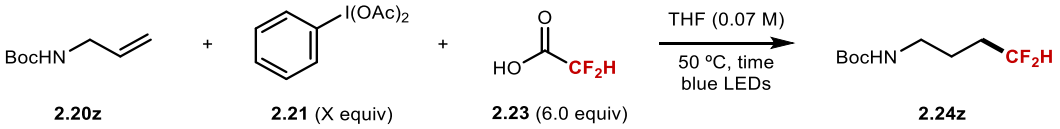
Scheme 2.8. Improved synthesis of 4,4-difluorobutan-1-amine (**2.25**).

2.12.2 Synthesis of *N*-Boc-4,4-difluorobutyl-1-amine Using our Hydrodifluoromethylation Protocol

Considering the lengthy synthesis of 4,4-difluorobutan-1-amine (Scheme 2.7 and 2.8), the herein reported hydrodifluoromethylation protocol was invastigated for the synthesis of a difluorobutylamine derivative. Since the hydrodifluoromethylation protocol is not applicable to unprotected amines, the reaction was performed on a carbamate protected precursor (*N*-Boc-allylamine,

2.20z). This precursor was chosen because it is commercial and inexpensive, and because AstraZeneca's sequence showed that Boc-deprotection was tolerated for such compounds (Scheme 2.7). Due to safety concerns, the excess of oxidant needed to be lowered for a large-scale reaction. Therefore, the influence of a sequential addition of oxidant in equimolar batches, was investigated on a one-gram scale. *N*-boc allylamine (**2.20z**) was reacted with difluoroacetic acid (**2.23**) in THF and the hypervalent iodine oxidant **2.21** was added in batches (1.0 equivalent each) every two hours. The consumption of alkene was monitored by GC-MS (Table 2.2). After 6 hours and overall addition of 3.0 equivalents of **2.21**, more than 95% of starting material was consumed.

Table 2.2 Optimisation of the hydrodifluoromethylation on one g scale.



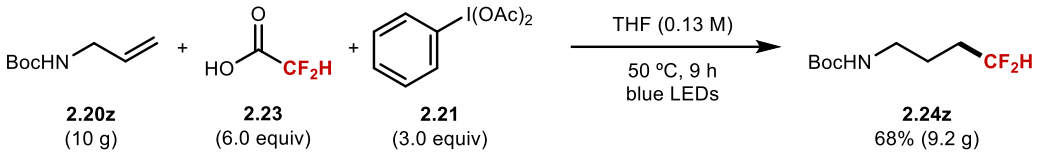
2.20z **2.21** (X equiv) **2.23** (6.0 equiv) **2.24z**

entry	equiv of 2.21 (X)[a]	time	conversion[b]
1	1.0	2 h	58%
2	2.0	4 h	89%
3	3.0	6 h	>95%

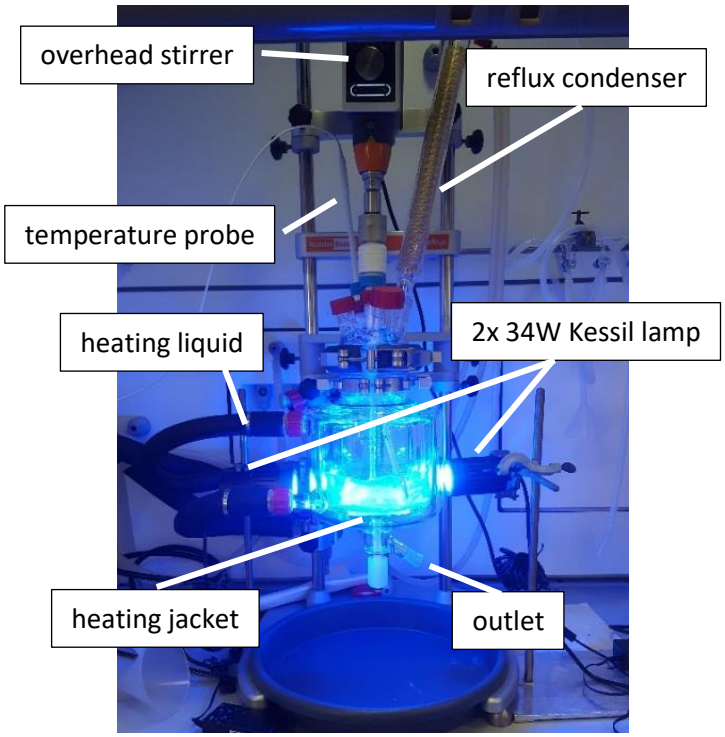
a) added in batches of 1.0 equivalents every 2 h. b) Conversion determined by GC-MS.

These updated conditions were applied to perform the hydrodifluoromethylation reaction on a decagram scale. The concentration was increased (from 0.07 M to 0.13 M) to reduce the amount of solvent. This allowed for the reaction to be performed in a two-litre reactor, equipped with a water heating jacket, mechanical overhead stirrer, nitrogen inlet, reflux condenser and internal temperature control (Scheme 2.9). Two blue LED lights (Kessil, 34 W) were used as light source. The

new optimised conditions (Table 2.2, entry 3) were used, and the progress of the reaction was monitored by GC-MS.



2.20z (10 g) + **2.23** (6.0 equiv) + **2.21** (3.0 equiv) → **2.24z** 68% (9.2 g)



Scheme 2.9. Large-scale hydrodifluoromethylation of *N*-Boc allylamine (**2.20z**). Reaction performed with help of Dr. Alejandro Diéguez-Vázquez.

The reaction scaled efficiently and the alkene starting material was fully consumed after nine hours reaction time (as determined by GC-MS). Excess oxidant was quenched with a concentrated aqueous solution of sodium bisulfite. After workup and silica gel chromatography, the desired hydrodifluoromethylated product **2.24z** (9.2 g, 68%) was isolated analytically pure (> 99% by ^{1}H NMR spectroscopy). Calorimetric data collected from the temperature control unit revealed that the addition of the hypervalent iodine oxidant **2.21** was endothermic (a temperature

drop from 50 °C to 48 °C was observed upon addition of the oxidant) and therefore does not impose an immediate safety hazard.

The same conditions were applied to the scale-up synthesis of a 3-difluoroethyl azetidine (**2.24aa**). 3-Difluoroethyl azetidines have previously been investigated as a potential bioisosteric replacement of the propyl group in the Janus kinase 1 (JAK1) selective inhibitor PF-04965842 (Figure 2.2; **2.37**, **2.38**).[17]

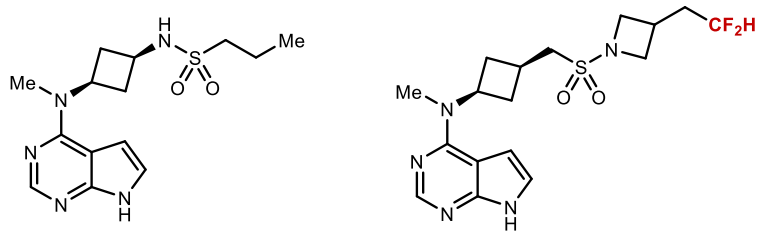
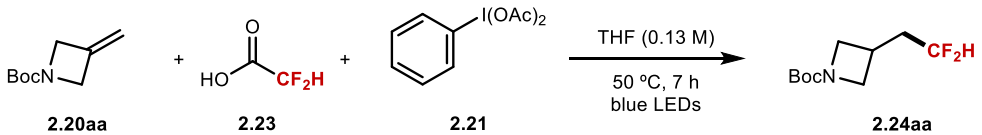


Figure 2.2. PF-04965842 and difluoroethyl azetidine analogue.

N-Boc-3-methyleneazetidine (**2.20aa**) was chosen as a starting material for the decagram synthesis of *N*-Boc-3-difluoroethylazetidine (**2.24aa**; Scheme 2.10). The reaction afforded 67% (8.9 g) of the desired azetidine **2.24aa** after seven hours reaction time (consumption of starting material was monitored by GC-MS).

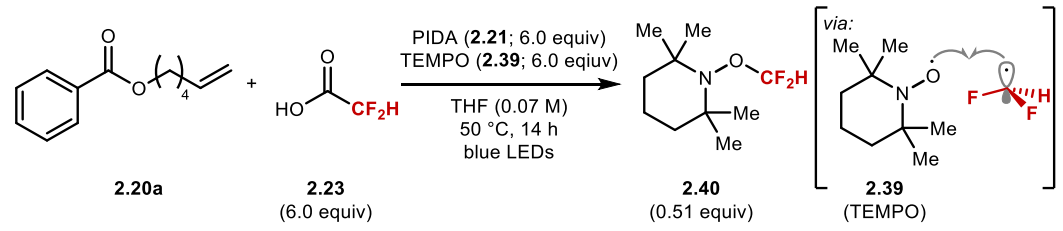


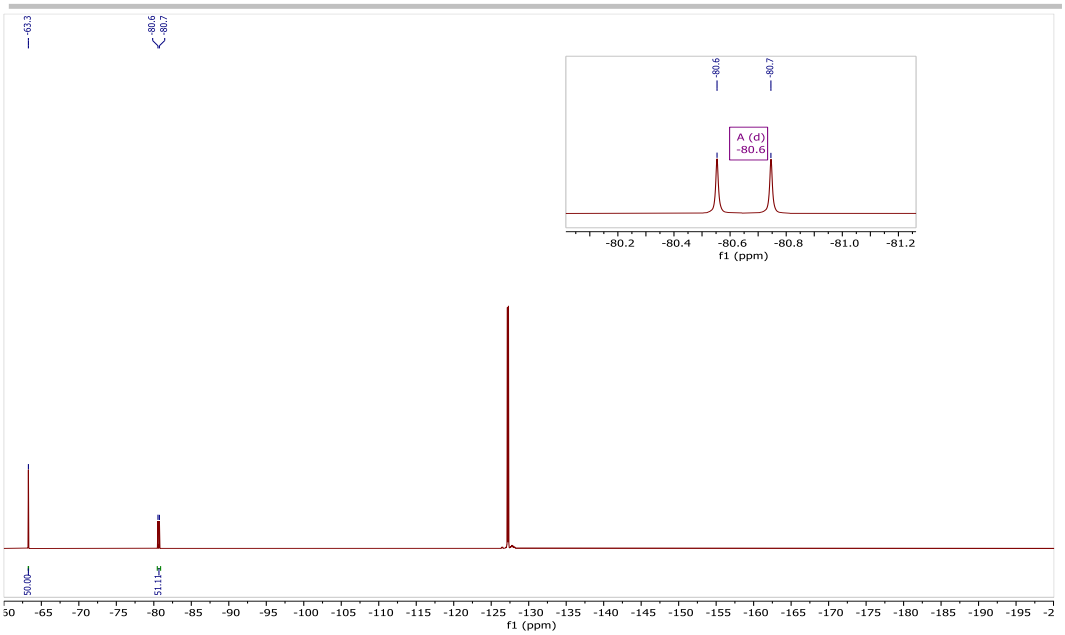
Scheme 2.10. Scale-up synthesis of azetidine building block **2.24aa**.

2.7 Mechanistic Experiments for the Hydrodifluoromethylation Protocol

Several control experiments were performed to elucidate the mechanism of this hydrodifluoromethylation procedure. In order to probe for a mechanism involving

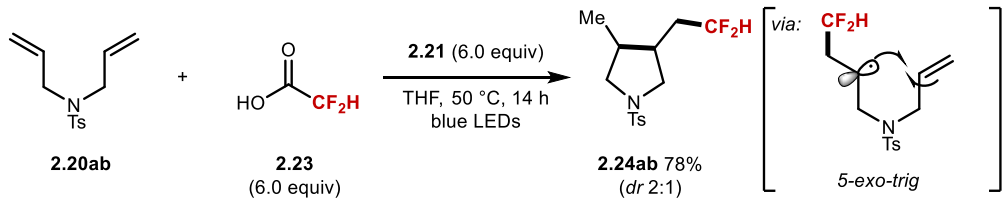
radical species, we performed an experiment in presence of the radical scavenger (2,2,6,6-tetramethylpiperidin-1-yl)oxyl (TEMPO, **2.39**; Scheme 2.11). When TEMPO (6.0 equiv) was added to the standard reaction conditions for the hydrodifluoromethylation of **2.20a**, the desired product **2.24a** was not formed; this was determined by quantitative ^{19}F NMR spectroscopy using *α*,*α*,*α*-trifluorotoluene as an internal standard. A new doublet was observed in the ^{19}F NMR spectrum ($\delta_{(ppm)}$ –80 ppm (d, $^{2}J_{H\text{-}F}$ = 72 Hz)), characteristic for OCF_2H compounds. We assigned this peak to the difluoromethyl adduct of TEMPO (**2.40**).[10] The formation of this product could be rationalised by radical-radical recombination between TEMPO (**2.39**) and the difluoromethyl radical. This result suggests that most likely the reaction proceeds *via* a radical mechanism.





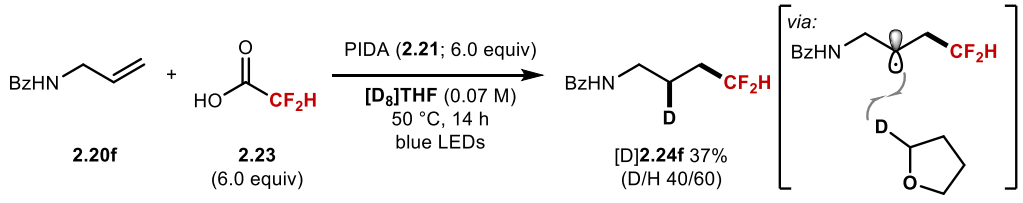
Scheme 2.11. Hydrodifluoromethylation of **2.20a** in presence of TEMPO (**2.39**). Yield determined by quantitative ^{19}F NMR spectroscopy using *α*,*α*,*α*-trifluorotoluene as an internal standard.

When the hydrodifluoromethylation reaction was performed on *N*-tosyl-diallylamine (**2.20ab**), a substrate that is known to undergo 5-*exo*-*trig* cyclisation upon radical addition, the reaction afforded difluoromethyl pyrrolidine **2.24ab** (Scheme 2.12). This result suggests that the reaction proceeds *via* a radical mechanism and that a long-lived carbon-centred radical intermediate is formed (the rate constant for radical 5-*exo*-*trig* cyclisation is approximately 2.3×10^5 s^{-1} at 298 K).[18] This radical intermediate could then undergo *5-exo-trig* cyclisation to afford product **2.24ab**. The reaction proceeded with moderate diastereoselectivity (2:1) and the diastereomers could not be separated by silica gel column chromatography.



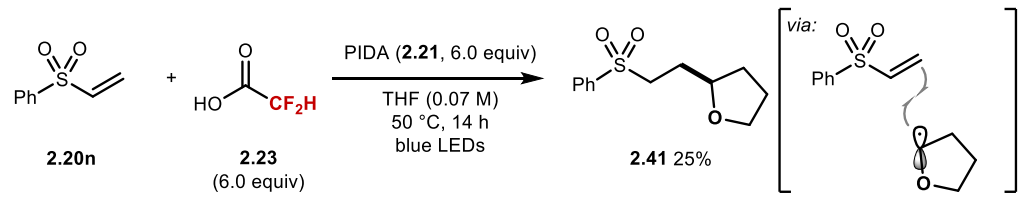
Scheme 2.12. Reaction of *N*,*N*-diallylsulfonamide **2.20ab**. Right: expected carbon-centred radical intermediate.

With deuterated [D_8]THF, the yield of the hydrodifluoromethylated product **2.24f** decreased (37% vs 64%), and deuterium incorporation was observed (40% deuterated, Scheme 2.13). This result indicates that the solvent acts as an H-atom donor in this procedure.



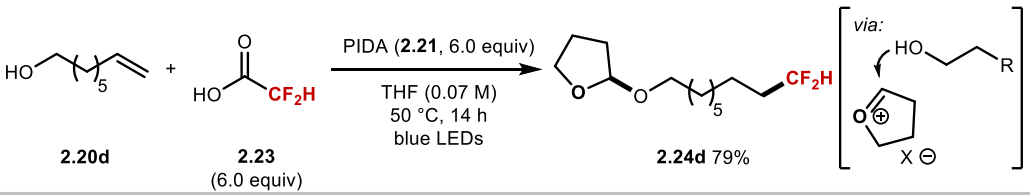
Scheme 2.13. Deuteration experiment on **2.20f**. The degree of deuterium incorporation was assessed by integration of the ^{1}H NMR spectrum of the isolated product.

In the reaction of phenyl vinyl sulfone, a side product was isolated alongside the desired hydrodifluoromethylated product (**2.24n**) (Scheme 2.14). Characterisation of this product by ^{1}H, ^{19}F and ^{13}C NMR spectroscopy revealed the structure of a THF addition product (**2.41**). This is likely due to the *in-situ* formation of the THF *α*-radical, which undergoes Giese addition the electron-deficient alkene **2.20n**. This competing Giese-reaction was unique to the hydrodifluoromethylation reaction of phenyl vinyl sulfone; the high nucleophilicity of the THF α-radical, matches best with electron-deficient alkenes. We have not observed analogous adducts with any other substrate (unactivated alkenes).



Scheme 2.14. THF radical addition to phenyl vinyl sulfone (**2.20n**).

When a terminal alcohol was present in the substrate and no workup was performed, a THF adduct to the alcohol was isolated by silica gel chromatography (Scheme 2.15). This adduct likely stems from nucleophilic attack of the alcohol to a THF oxonium ion. This ion could be obtained *via* single-electron oxidation of the THF *α*-radical.



Scheme 2.15. THF oxonium ion can be trapped by alcohols.

2.8 Proposed Mechanism for the Hydrodifluoromethylation of Alkenes

Based on these mechanistic experiments, we propose the following reaction mechanism (Figure 2.3). Initial exchange of difluoroacetic acid with the acetate ligands of PIDA (**2.21**) affords a difluoroacetoxy hypervalent iodine complex (**2.42**). Upon visible light irradiation, this complex undergoes homolytic iodine-oxygen bond cleavage to release a difluoroacetoxy radical (**A**). This radical then undergoes decarboxylation to afford difluoromethyl radical (**B**). Notably, significant gas evolution occurs under the standard reaction conditions. This observation is in accordance with the release of carbon dioxide. Addition of the difluoromethyl radical (**B**) to an unactivated alkene affords a carbon-centred radical intermediate (**C**). Hydrogen atom abstraction from the solvent affords the desired product **2.24** alongside a THF α-radical (**D**). Oxidation of this radical *via* single-electron oxidation from hypervalent iodine complex **2.42** could close the radical chain propagation cycle by affording the difluoroacetoxy radical **B** alongside iodobenzene, difluoroacetate and the THF oxonium ion **E**.

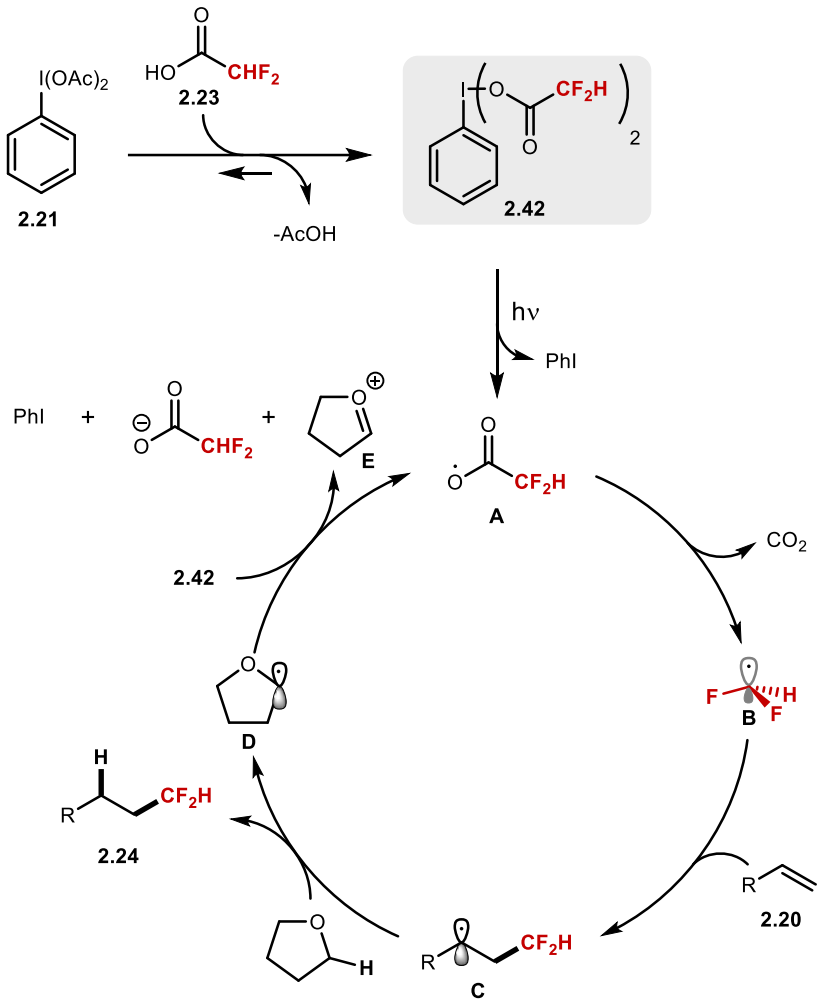


Figure 2.3. Proposed initiation, radical chain propagation mechanism for the hydrodifluoromethylation of alkenes.

A further mechanistic experiment to probe for the proposed chain propagation mechanism was performed (Figure 2.4). The consumption of difluoroacetic acid (**2.23**) in the hydrodifluoromethylation of **2.20f** was compared in presence and absence of the radical scavenger TEMPO (**2.39**). In Scheme 2.11, we have shown that the presence of TEMPO inhibits the hydrodifluoromethylation reaction. TEMPO recombines with the difluoromethyl radical generated *in situ* to afford difluoromethyl hydroxylamine **2.40**. According to the proposed mechanism, the presence of TEMPO should therefore inhibit the chain propagation. Thus,

comparing the consumption of difluoroacetic acid (**2.23**) in presence and absence of TEMPO could reveal valuable information about the reaction mechanism.

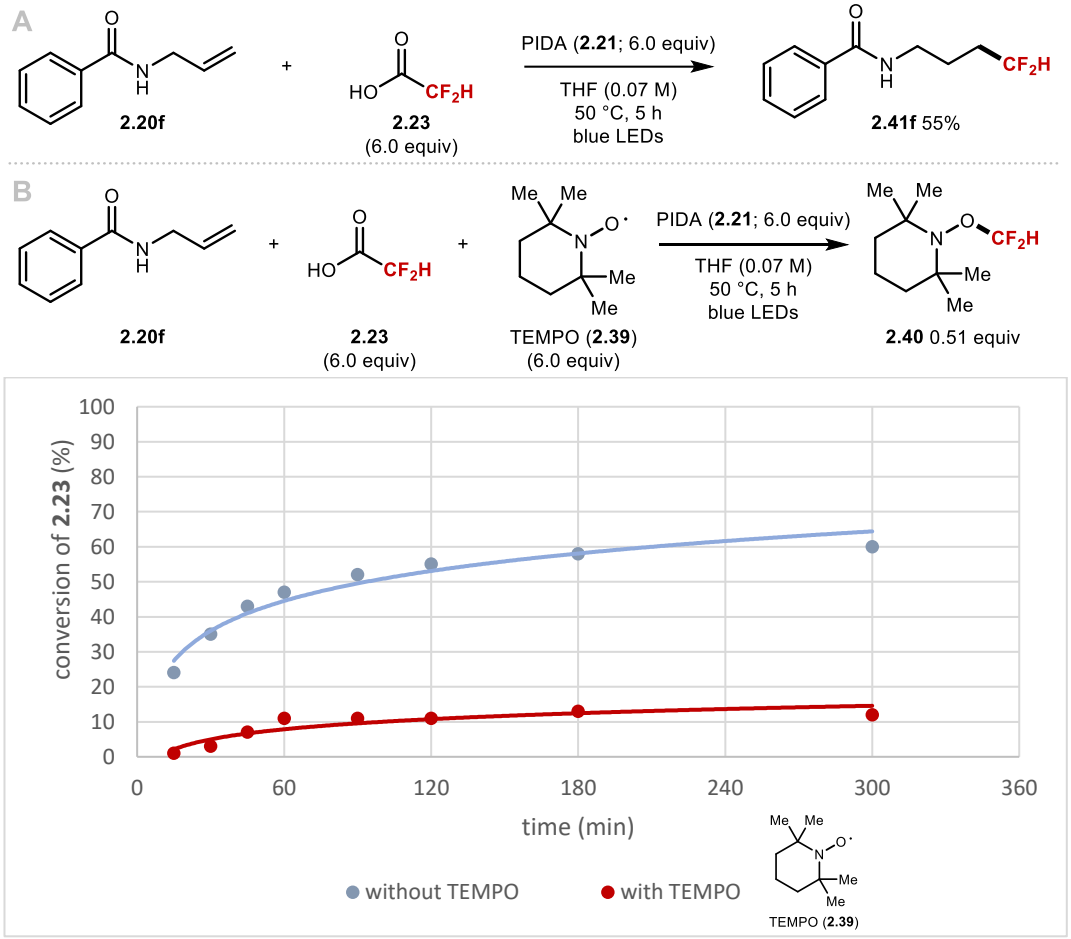


Figure 2.4. Consumption of difluoroacetic acid (**2.23**) in presence (red) and absence (blue) of TEMPO (**2.39**).

We observed significantly higher consumption of difluoroacetic acid (**2.23**) in absence of TEMPO (**2.39**) compared to the reaction performed in presence of TEMPO. In presence of TEMPO, the only factor leading to consumption of **2.23** is the initiation pathway. The higher consumption of **2.23** in absence of TEMPO means that under these conditions, an additional consumption pathway must be operative. This was attributed to the radical chain propagation as suggested in

Figure 2.3. The outcome of the reactions presented in Figure 2.4 advocates in favour of the proposed radical chain propagation mechanism.

2.9 Limitations

Limitations of this hydrodifluoromethylation strategy include the lack of tolerance towards amines and thiols, both of which proved incompatible under our standard reaction conditions. A reason for this incompatibility could be deactivation of the iodine(III) reagent by nucleophilic addition of the amine or thiol.

When applying the hydrodifluoromethylation conditions to styrene derivatives, the reaction resulted in a mixture of fluorinated products, likely due to an inefficient hydrogen-atom transfer step. The addition of the difluoromethyl radical to styrenes affords a benzylic radical intermediate. Benzylic radicals (BDE($PhCH_2$-H) = 352 kJ mol^{-1})[19] are more stable than the THF α-radical (α-C-H BDE(THF) = 385 kJ mol^{-1})[20] and therefore, the hydrogen-atom transfer from THF to a benzylic radical intermediate is thermodynamically unfavoured. In contrast, benzylic radicals require a protic hydrogen-atom donor with a weaker bond dissociation energy, such as thiophenol derivatives (BDE(PhS-H) = 330 kJ mol^{-1}).[21–23]

Electron-rich alkenes such as enols and enamides are also not suitable for this hydrodifluoromethylation protocol. Again, this could be explained by an inefficient hydrogen-atom transfer event: upon difluoromethyl radical addition to electron-rich alkenes, nucleophilic radical intermediates are formed. Kinetic factors (polarity mismatch) in the hydrogen-atom transfer step could account for the

incompatibility of electron-rich alkenes to this hydrodifluoromethylation protocol: hydrogen-atom transfer with a hydridic H-atom donor, such as THF, to a nucleophilic radical is kinetically unfavoured.[24]

Electron-deficient alkenes such as α,β-unsaturated ketones or α,β-unsaturated esters and cyclic internal alkenes were low yielding (<25%). This could be attributed to competitive THF radical addition to electron as observed in the case of phenyl vinyl sulfone (**2.20n**).

Benzoic acid **2.20l** was tolerated under our reaction conditions but unprotected aliphatic carboxylic acids such as amino acids proofed incompatible. This could be explained by competitive iodine(III)-mediated radical decarboxylation of aliphatic carboxylic acids. In contrast, the low stability of aryl radicals, formed upon radical decarboxylation of benzoic acids, could account for the tolerance of benzoic acids in this protocol.

2.10 Conclusion

In conclusion, we developed a new procedure for the hydrodifluoromethylation of alkenes. The reaction is performed with readily available unactivated alkenes and commercial, inexpensive reagents. The combination of phenyliodine(III) diacetate and difluoroacetic acid serves as a privileged source of the difluoromethyl radical. The reaction is best performed in tetrahydrofuran, as it was found to act as both solvent and hydrogen-atom donor in this transformation.

The new hydrodifluoromethylation protocol was applied to the synthesis of a broad range of difluoromethylalkanes. Various functional groups are tolerated

under the optimised reaction conditions allowing for the late-stage hydrodifluoromethylation of biologically relevant molecules. The use of inexpensive reagents makes this procedure an attractive strategy for the preparation of C(sp^3)-CF_2H building blocks. We have demonstrated the decagram scale synthesis of two building blocks of interest to our industrial collaborators.

Mechanistic experiments corroborate with the formation of the difluoromethyl radical *via* radical-mediated decarboxylation of difluoroacetic acid. Considering the simplicity of this procedure and the relevance of the CF_2H group, we believe that this method will find applications in the pharmaceutical and agrochemical industry.

2.11 Outlook

The Markovnikov hydrodifluoromethylation of alkenes remains largely unknown.[25] Future developments in the field of hydrodifluoromethylation should focus on developing novel methods with complementary regioselectivity, allowing for the preparation of Markovnikov hydrodifluoromethylated products. Furthermore, the field of asymmetric difluoromethylation is still in its infancy. Known procedures include a catalytic enantioselective vicinal aminodifluoromethylation to access difluoroethylpyrrolidines and the copper catalysed enantioselective difluoromethylation of benzylidene Meldrum acids.[26,27] However, both these methods lack in scope and generality. Due to the high relevance of chiral difluoromethyl-containing compounds to the pharmaceutical industry, further developments in this area would be of high interest.

Furthermore, the expansion of hydrodifluoromethylation protocols to other dihalomethyl radicals remains underexplored. For example, the synthetic applications of the chlorofluoromethyl radical and the bromofluoromethyl radical have not been investigated. This challenge is addressed in Chapter 3.

2.12 References

[1] J. G. Taylor, S. Zipfel, K. Ramey, R. Vivian, A. Schrier, K. K. Karki, A. Katana, D. Kato, T. Kobayashi, R. Martinez, M. Sangi, D. Siegel, C. V. Tran, Z. Y. Yang, J. Zablocki, C. Y. Yang, Y. Wang, K. Wang, K. Chan, O. Barauskas, G. Cheng, D. Jin, B. E. Schultz, T. Appleby, A. G. Villaseñor, J. O. Link, *Bioorganic Med. Chem. Lett.* **2019**, *29*, 2428–2436.

[2] B. Gutmann, P. Hanselmann, M. Bersier, D. Roberge, C. O. Kappe, *J. Flow Chem.* **2017**, *7*, 46–51.

[3] T. H. S. Burns, J. M. Hall, A. Bracken, G. Gouldstone, *Anaesthesia* **1974**, *29*, 435–444.

[4] M. Dudek, M. Marcinkowska, A. Bucki, A. Olczyk, M. Kołaczkowski, *Metab. Brain Dis.* **2015**, *30*, 1487–1494.

[5] C. Han, S. M. Kelly, T. Cravillion, S. J. Savage, T. Nguyen, F. Gosselin, *Tetrahedron* **2019**, *75*, 4351–4357.

[6] X. J. Tang, Z. Zhang, W. R. Dolbier, *Chem. - A Eur. J.* **2015**, *21*, 18961–18965.

[7] K. Uneyama, H. Nanbu, *J. Org. Chem.* **1988**, *53*, 4598–4599.

[8] X. J. Tang, W. R. Dolbier, *Angew. Chemie - Int. Ed.* **2015**, *54*, 4246–4249.

[9] C. S. Thomoson, X. J. Tang, W. R. Dolbier, *J. Org. Chem.* **2015**, *80*, 1264–1268.

[10] Q. Y. Lin, X. H. Xu, K. Zhang, F. L. Qing, *Angew. Chemie - Int. Ed.* **2016**, *55*, 1479–1483.

[11] B. Yang, X. H. Xu, F. L. Qing, *Org. Lett.* **2016**, *18*, 5956–5959.

[12] R. Sakamoto, H. Kashiwagi, K. Maruoka, *Org. Lett.* **2017**, *19*, 5126–5129.

[13] S. Mizuta, S. Verhoog, K. M. Engle, T. Khotavivattana, M. O'Duill, K. Wheelhouse, G. Rassias, M. Médebielle, V. Gouverneur, *J. Am. Chem. Soc.* **2013**, *135*, 2505–2508.

[14] R. Moriarty, O. Prakash, in *Org. React. Vol. 54*, John Wiley & Sons, Inc, Chicago, **1999**, pp. 273–337.

[15] A. Bjore, J. Bostrom, O. Davidsson, H. Emtenas, U. Gran, T. Iliefski, J. Kajanus, R. Olsson, L. Sandberg, G. Strandlund, J. Sundell, Z.-Q. Yuan, *WO2013/186335: 1,3-Dihydro-2H-Benzimidazol-2-One Derivatives Substituted with Heterocycles as Respiratory Syncytial Virus Antiviral Agents*, **2008**, US 9,845,321 B2.

[16] M. H. Vendeville, Sandrine, A. Tahri, T. H. M. Jonkers, P. J.-M. B. Raboisson, L. Hu, *WO2013/186335: 1,3-Dihydro-2H-Benzimidazol-2-One Derivatives Substituted with Heterocycles as Respiratory Syncytial Virus Antiviral Agents*, **2013**.

[17] K. J. Coffman, J. M. Duerr, N. Kaila, M. D. Parikh, M. R. Reese, T. Samad, S. Sciabola, *CA2899888A1 PYRROLO[2,3-D]PYRIMIDINE DERIVATIVES*, **2015**, 2,899,888.

[18] Y. Fu, R. Q. Li, L. Liu, Q. X. Guo, *Res. Chem. Intermed.* **2004**, *30*, 279–286.

[19] Y. D. Wu, C. L. Wong, K. W. K. Chan, G. Z. Ji, X. K. Jiang, *J. Org. Chem.* **1996**, *61*, 746–750.

[20] L. J. J. Laarhoven, P. Mulder, *J. Phys. Chem. B* **1997**, *101*, 73–77.

[21] J. B. I. Sap, N. J. W. Straathof, T. Knauber, C. F. Meyer, M. Médebielle, L. Buglioni, C. Genicot, A. A. Trabanco, T. Noël, C. W. am Ende, V. Gouverneur, *J. Am. Chem. Soc.* **2020**, *142*, 9181–9187.

[22] N. J. W. Straathof, S. E. Cramer, V. Hessel, T. Noël, *Angew. Chemie - Int. Ed.* **2016**, *55*, 15549–15553.

[23] A. K. Chandra, P. C. Nam, M. T. Nguyen, *J. Phys. Chem. A* **2003**, *107*, 9182–9188.

[24] S. M. Hell, C. F. Meyer, A. Misale, J. B. I. Sap, K. E. Christensen, M. C. Willis, A. A. Trabanco, V. Gouverneur, *Angew. Chemie Int. Ed.* **2020**, *59*, 11620–11626.

[25] J. YANG, S. ZHU, F. WANG, F.-L. QING, L. Chu, *Angew. Chemie Int. Ed.* **2020**, DOI

10.1002/anie.202014587.
[26] J. S. Lin, F. L. Wang, X. Y. Dong, W. W. He, Y. Yuan, S. Chen, X. Y. Liu, *Nat. Commun.* **2017**, *8*, 1–11.
[27] Y. Endo, K. Ishii, K. Mikami, *Tetrahedron* **2019**, *75*, 4099–4103.

Chapter 3 – Hydrochlorofluoro-methylation of Unactivated Alkenes with Chlorofluoroacetic Acid

The work discussed in this chapter was published in *Tetrahedron* as a contribution to the special issue to honour Prof. Stephen G. Davies. The work discussed in section **3.4** is unpublished to date.

Claudio F. Meyer, Sandrine M. Hell, Jeroen B. I. Sap, Antonio Misale, Aldo Peschiulli, Daniel Oehlrich, Andrés A. Trabanco, Véronique Gouverneur, *Tetrahedron* **2019**, *47*, 130679.

Author contributions: The project was designed by Claudio Meyer, Sandrine Hell, Jeroen Sap, Antonio Misale, Aldo Peschiulli, Daniel Oehlrich, Andrés A. Trabanco and Véronique Gouverneur. Reaction optimisations were performed by Claudio Meyer. Substrates were synthesised by Claudio Meyer with help of Sandrine Hell. The work described in Section **3.4** was performed by Claudio Meyer with help of Sandrine Hell and Sebastiano Ortalli.

3.1 Introduction to the Chlorofluoromethyl Group

Whilst the difluoromethyl group has recently become of interest in both academic as well as industrial research, investigations into the chlorofluoromethyl group have thus far been limited. Only recently, the chlorofluoromethyl group has been investigated as a precursor for F-18 radiolabelling, and as a reactive handle for cross-coupling reactions.[1–5] In recent years, several drug discovery programs exploited this functionality as a warhead for covalent inhibition.[6–9] This section will discuss the utility of the chlorofluoromethyl group, the traditional synthesis of chlorofluoromethyl containing compounds and our novel approach for the radical hydrochlorofluoromethylation of alkenes. Furthermore, the generation of the closely related bromofluoromethyl radical to access bromofluoromethylalkanes is discussed. To the best of our knowledge, these radicals have not been employed in organic synthesis thus far.

3.1.1 The Chlorofluoromethyl Group in Medicinal Chemistry

In 2007, Kuduk and co-workers reported a series of chlorinated and fluorinated acetamides as central nervous system (CNS) penetrant bradykinin B_1 receptor antagonists (Figure 3.1).[6] The authors investigated the binding of the respective compounds to the human bradikynin B1 receptor (K_ihB1) and the P-glycoprotein mediated efflux. Whilst the chlorofluoromethyl compound **3.1** outcompeted the non-fluorinated compound **3.2** and difluoromethylated compound **3.3**, the corresponding trifluoromethyl compound **3.4** was found to be more potent. The

dichloromethyl compound **3.5** showed subnanomolar binding but was not further investigated due to its low stability.

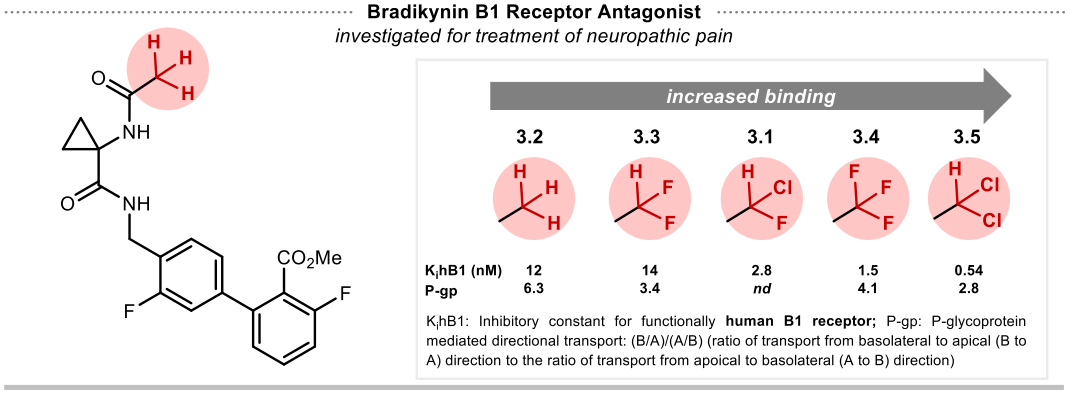


Figure 3.1. SAR of Bradikynin B1 receptor antagonists (**3.1** – **3.5**).

More recently, the chlorofluoromethyl group has acquired significant interests from the medicinal chemistry sector due to its ability to act as a warhead for covalent inhibition.[7–9] Traditionally, covalent inhibition is achieved by decorating a drug compound with an appropriate Michael-acceptor, that reacts with the target protein at a cysteine residue of the targeted protein (Figure 3.2).[10] However, due to the high reactivity of Michael-acceptors, low selectivity can result in undesired binding. To address this issue, Ojida and co-workers have reported a SAR study of different warheads towards cysteine residues.[8] A cysteine-containing peptide was used as nucleophile and reacted with tetranuclear zinc complexes bearing different electrophiles (**3.6** – **3.10**). They illustrated that these complexes were able to bind the target peptide at nanomolar concentrations (K_d = 73 nM), placing the warhead in close proximity to the targeted cysteine residue. The authors determined and compared the half-reaction time ($t_{1/2}$, h) of the different warheads. This data clearly demonstrates the high reactivity of the Michael-acceptor **3.7** towards cysteine residues ($t_{1/2}$(**3.7**) = 0.51 h). When changing

to a chloroacetamide (**3.6**), target binding proceeded more rapidly ($t_{1/2}$(**3.6**) = 0.04 h). In contrast, chlorofluoroacetamide **3.8** proved to engage in target binding with a moderate half-reaction time ($t_{1/2}$(**3.8**) = 4.4 h), whereas dichloroacetamide **3.9** and fluoroacetamide **3.10** were less reactive ($t_{1/2}$ ≥ 39 h).

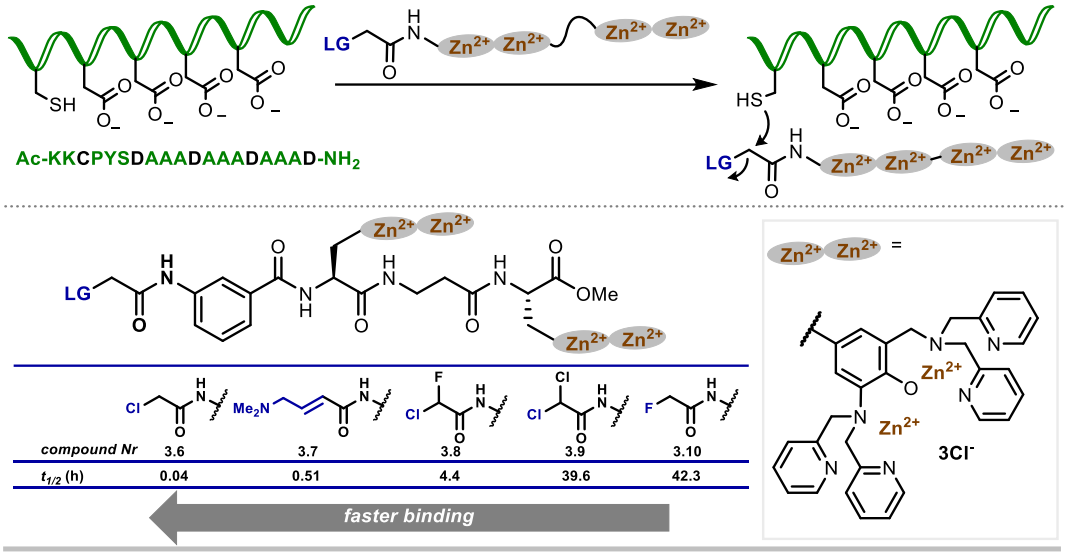
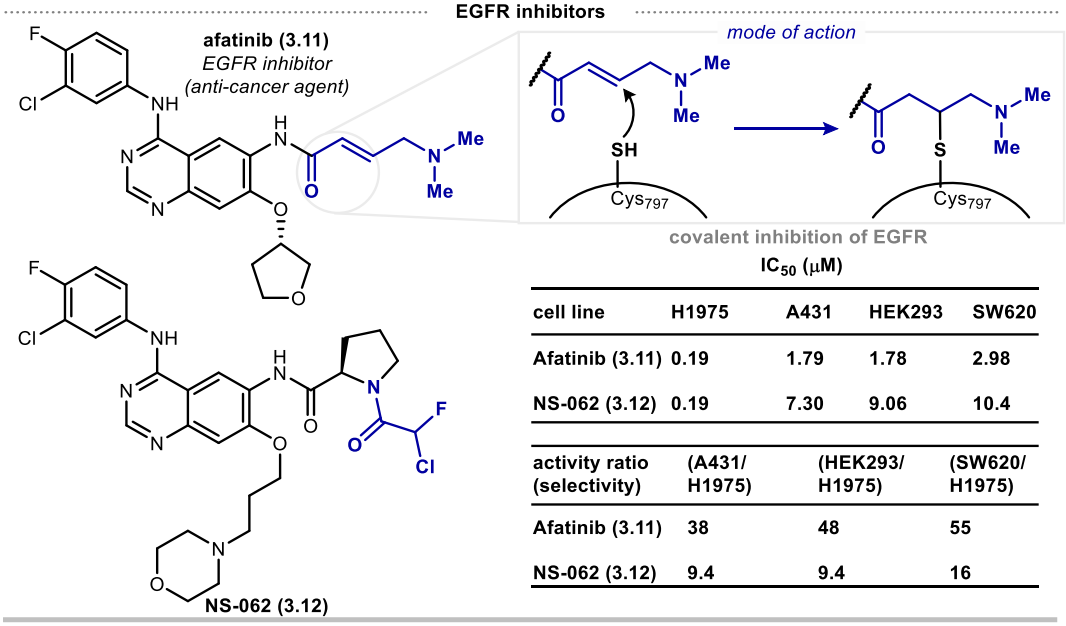


Figure 3.2. SAR study of zinc-complexes containing various warheads (**3.6** – **3.10**) towards cysteine residues.

Based on these results, the authors speculated that an inhibitor containing a chlorofluoroacetamide group could show increased selectivity compared to inhibitors containing Michael acceptors. They tested their hypothesis by comparing the anti-cancer drug afatinib (**3.11**) to the chlorofluoroacetamide analogue NS-062 (**3.12**) (Figure 3.3). These structurally related compounds are epidermal growth factor receptor (EGFR) inhibitors for mutated EGFR. In the active site of this enzyme, they react with Cys797 to covalently bind to the target protein. Ojida and co-workers found that both **3.11** and **3.12** show strong anti-proliferate activities towards H1975 cells (IC_{50} = 0.19 µM, H1975 cells expresses mutant EGFR). However, afatinib (**3.11**) showed off-target activity towards a range of

other cell lines (A431 (expresses wild-type EGFR); HEK293 and SW620 are EGFR independent), activity ratios ≤ 16), whereas NS-062 (**3.12**) was more selective towards the EGFR mutant-expressing H1975 cells (activity ratios ≥ 38).



IC_{50} (μM)

cell line	H1975	A431	HEK293	SW620
Afatinib (3.11)	0.19	1.79	1.78	2.98
NS-062 (3.12)	0.19	7.30	9.06	10.4

activity ratio (selectivity)	(A431/ H1975)	(HEK293/ H1975)	(SW620/ H1975)
Afatinib (3.11)	38	48	55
NS-062 (3.12)	9.4	9.4	16

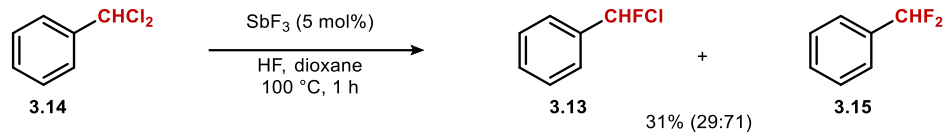
Figure 3.3. Comparison of anti-proliferate activities of afatinib (**3.11**) and chlorofluoroacetamide **3.12**.

3.1.2 Strategies to Access the Chlorofluoromethyl Group

Early strategies to access the chlorofluoromethyl motif relied on the addition of a nucleophile to chlorotrifluoroethylene.[11–14] More recent approaches for the synthesis of chlorofluoromethyl groups rely on either fluorination of a dichloromethyl group or *ipso*-chlorination of a fluoromethyl group.

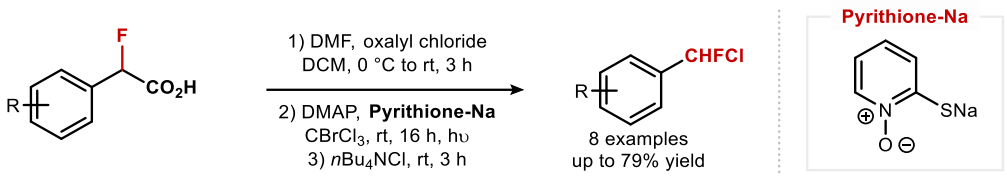
As such, Brunet and co-workers described the synthesis of chlorofluorotoluene (**3.13**) *via* nucleophilic fluorination of dichlorotoluene (**3.14**) with hydrogen fluoride using catalytic amounts of antimony trifluoride (Scheme 3.1).[15] The

reaction proceeded in low yield with low selectivity, affording difluorotoluene (**3.15**) as the major product.



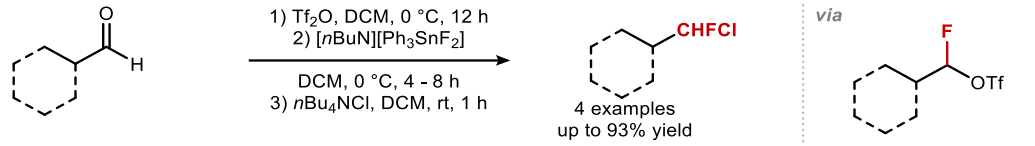
Scheme 3.1. Fluorination of dichlorotoluene (**3.14**) with HF and SbF_3.

In 2015, Gouverneur and co-workers disclosed a more general synthesis of chlorofluoromethylarenes *via* decarboxylative bromination of *α*,*α*-fluorophenylacetic acids followed by *in situ* chlorination (Scheme 3.2).[1] The carboxylic acid was first converted to the acid chloride, which was then reacted with sodium *N*-hydroxy-2-thiopyridone and catalytic amounts of 4-dimethylaminopyridine in bromotrichloromethane under UV-light irradiation to afford crude bromofluoromethylarene. This intermediate was treated with tetrabutylammonium chloride to afford the desired chlorofluoromethylarene.



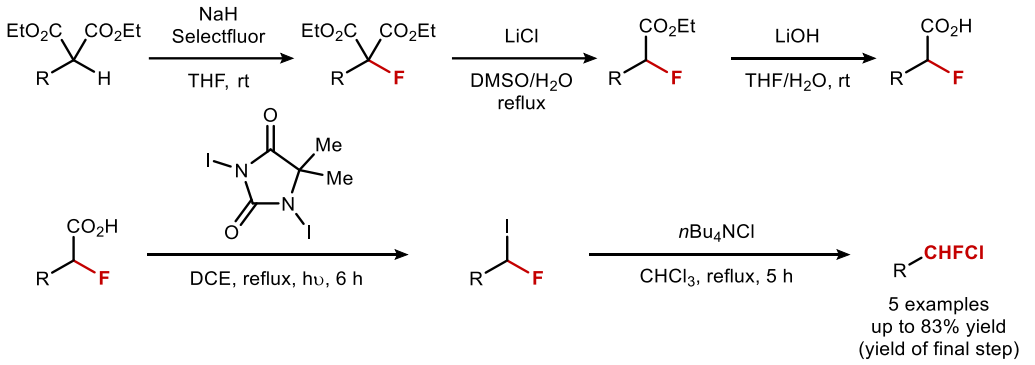
Scheme 3.2. Three-step synthesis of chlorofluoromethylarenes from *α*,*α*-fluorophenylacetic acids.

In 1993, Martínez and co-workers developed a synthesis towards chlorofluoromethylalkanes by nucleophilic substitution of *α*-fluorotriflates with tetrabutylammonium chloride (Scheme 3.3).[16] The synthesis of *α*-fluorotriflates from carbaldehydes required harsh conditions (triflic anhydride) and a highly toxic fluoride source (tetrabutylammonium difluorotriphenylstannane), limiting the scope and utility of this approach.



Scheme 3.3. Synthesis of chlorofluoromethylalkanes by nucleophilic substitution of α-fluorotriflates.

To overcome those limitations, Gandelman and co-workers more recently reported the synthesis of chlorofluoromethylalkanes by nucleophilic substitution of fluoroiodomethyl groups (Scheme 3.4).[2,3] They accessed the chlorofluoromethylalkanes by decarboxylative iodination of α-fluorocarboxylic acids. Despite the advantages of this strategy, the synthesis of the precursors required a multi-step procedure starting from alkylmalonates.

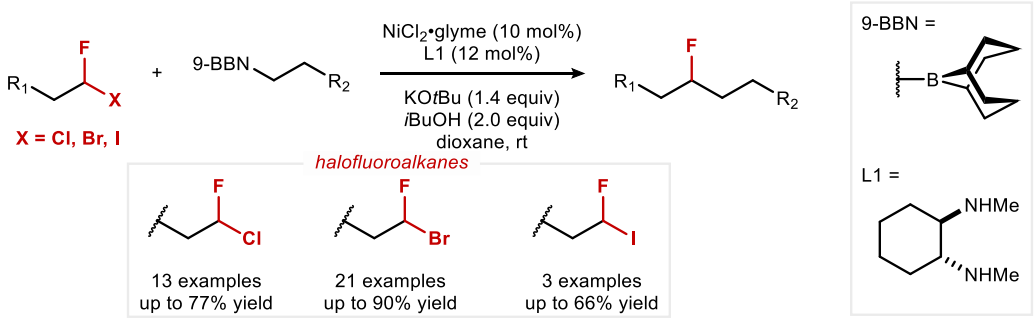


Scheme 3.4. General route to access chlorofluoromethylalkanes.

3.1.3 Cross-Coupling Reactions with the Chlorofluoromethyl Group

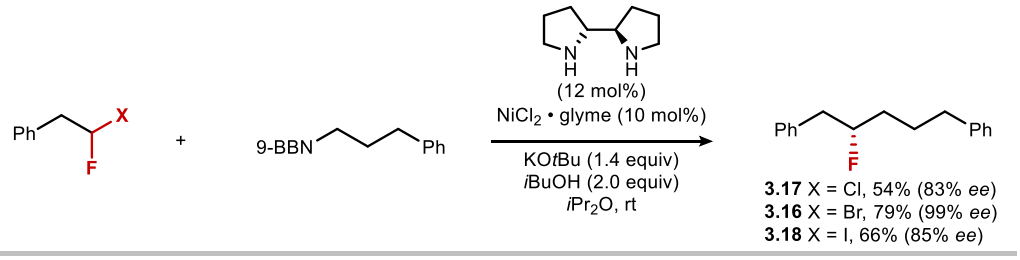
In addition to their application in medicinal chemistry, chlorofluoromethyl groups have been investigated as intermediates towards secondary alkyl fluorides. In 2014, Gandelman and co-workers demonstrated the Suzuki cross-coupling of terminal chlorofluoromethyl groups with alkyl boranes (Scheme 3.5).[2] This is a rare example of a nickel-catalysed C(sp^3)-C(sp^3) cross-coupling generating secondary alkyl fluorides. In addition to chlorofluoromethyl compounds, the

authors also investigated bromofluoromethyl and iodofluoromethyl analogues. As expected, the bromofluoromethyl substrates outperformed the chlorofluoromethyl substrates. However, reactions with iodofluoromethyl compounds suffered from catalyst poisoning, due to trace impurities in the starting materials, most likely iodine; addition of iodine under the standard reaction conditions was detrimental and shut down the reactivity.



Scheme 3.5. Synthesis of secondary alkyl fluorides *via* Suzuki cross-coupling from halofluoroalkanes.

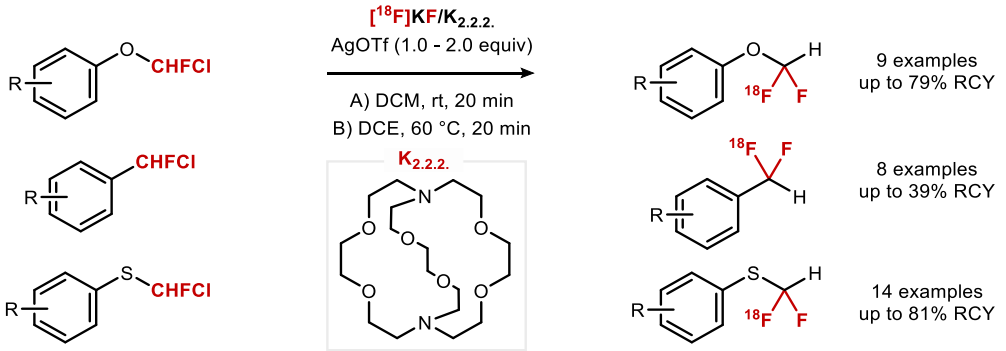
In 2015, the same authors expanded this protocol to an enantioselective variant (Scheme 3.6).[3] The use of a chiral bipyrrolidine ligand combined with catalytic nickel chloride allowed the construction of enantiomerically enriched secondary alkyl fluorides. Again, the bromofluoromethyl substrate **3.16** performed best. Chlorofluoromethyl substrate **3.17** as well as iodofluoromethyl substrate **3.18** suffered from low yield and lower enantiomeric excess.



Scheme 3.6. Catalytic asymmetric Suzuki cross-coupling of halofluoroalkanes (**3.16** – **3.18**).

3.1.4 The Chlorofluoromethyl Group as a Reactive Handle for F-18 Radiochemistry

In 2015 Gouverneur and co-workers developed a broadly applicable protocol for F-18 radiolabelling of trifluoromethyl ethers and difluoromethyl ethers (Scheme 3.7).[5] They found that in presence of silver salts various halo(di)fluoromethyl ethers efficiently underwent halogen exchange with non-carrier added [^{18}F]fluoride in chlorinated solvents. More specifically, chlorofluoromethylethers reacted with silver(I)triflate and [^{18}F]fluoride to afford [^{18}F]difluoromethylethers in dichloromethane at room temperature. Later, a similar strategy was used for the synthesis of [^{18}F]difluoromethylarenes and [^{18}F]difluoromethylthioethers.[1,4]



Scheme 3.7. Ag-mediated strategy to access [^{18}F]difluoromethylarenes and [^{18}F]difluoromethyl(thio)ethers.

3.2 Radical Halofluoromethylation Reactions

To the best of our knowledge, prior to the work outlined in this chapter, radical chlorofluoromethylation reactions were unexplored. However, halodifluoromethyl radicals, such as the bromodifluoromethyl and chlorodifluoromethyl radical have been studied in detail and used in various

transformations.[17–21] The following section presents an overview of the different halofluoromethyl radical precursors and their use in organic synthesis.

3.2.1 Previous Halofluoromethyl Radical Precursors

Early literature on halofluoromethylation mainly focused on the activation of dibromodifluoromethane, a non-flammable, ozone-depleting substance (Figure 3.4). More recent reports include novel reagents such as sulfilimino reagents reported by Masson and co-workers.[19] The field of chlorodifluoromethylation mainly relies on reagents derived from chlorodifluoroacetic acid (Zard and Maruoka),[17,22] chlorofluoroacetic anhydride (Stephenson) or bis(chlorofluoroacetyl)peroxide (Yoshida)[18,23,24].

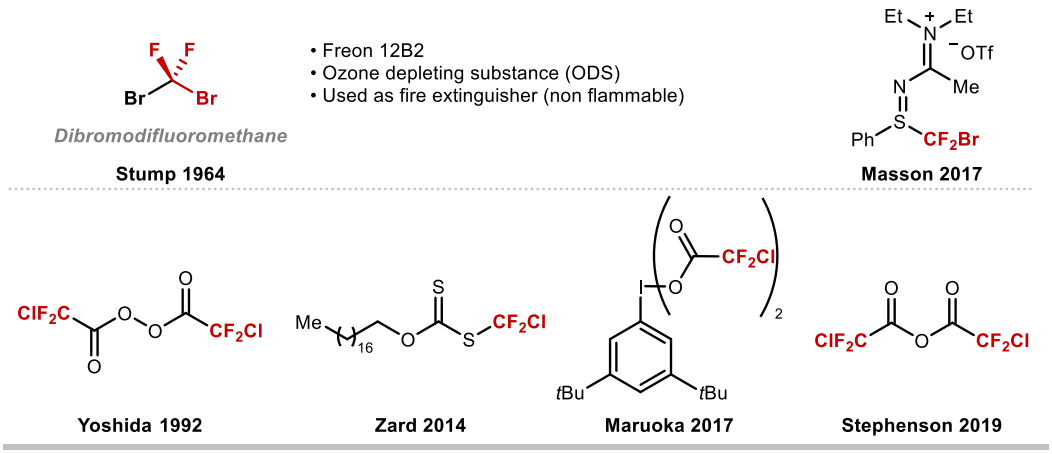
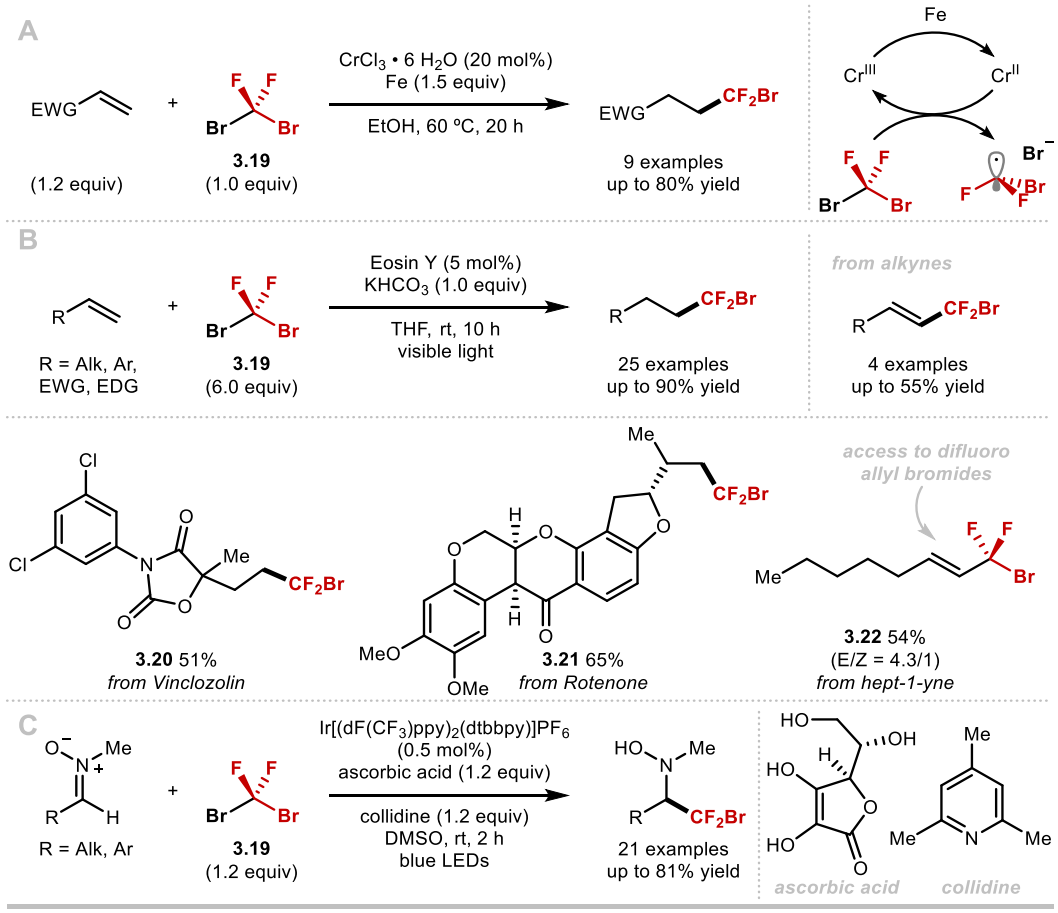


Figure 3.4. Commonly used halofluoromethyl radical precursors.

3.2.2 Bromodifluoromethylation Reactions

An early example of the use of the bromodifluoromethyl radical in synthesis was the Giese-type hydrobromodifluoromethylation of electron-deficient alkenes, reported by Hu and co-workers (Scheme 3.8A).[25] The bromodifluoromethyl radical was formed *via* a $CrCl_3$/Fe bimetallic redox system. In this system iron

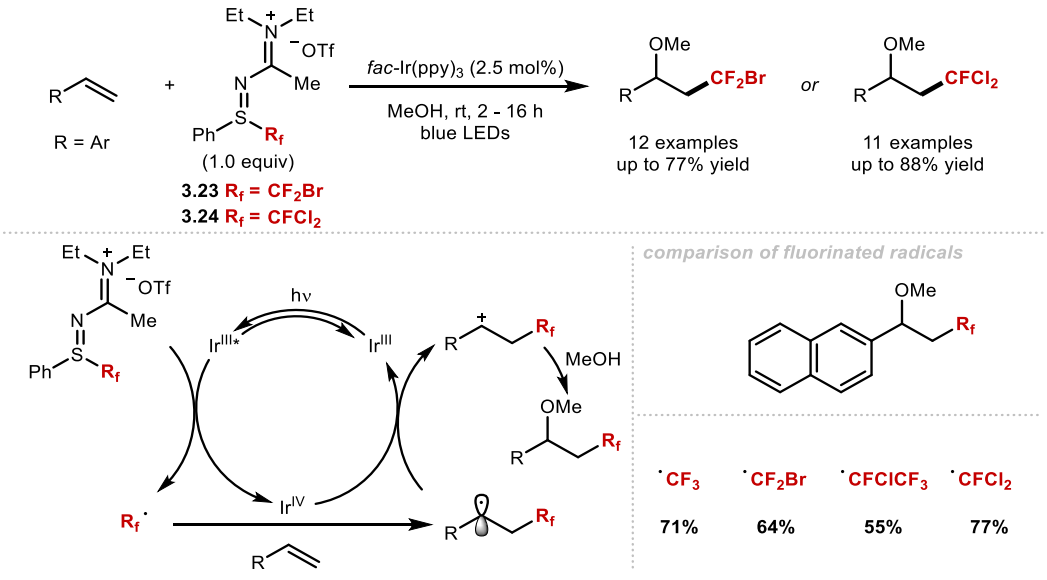
powder reduces Cr^{III} to Cr^{II}, which is a suitable activator of dibromodifluoromethane (**3.19**). More recently Qing and co-workers expanded the scope of hydrobromodifluoromethylation by developing a photocatalytic protocol employing the organophotocatalyst Eosin Y (Scheme 3.8B).[21] This method exhibited a broad substrate scope of a variety of alkenes with various functional groups and was applied to the late-stage functionalisation of complex biologically relevant alkenes (**3.20** – **3.21**). One limitation of this method is the requirement for **3.19** to be present in high excess. The method was further expanded to terminal alkynes, where predominantly *E*-configured allyl bromides were obtained (**3.22**).



Scheme 3.8. Hydrobromodifluoromethylation of alkenes with dibromodifluoromethane (**3.19**).

In 2019, Dilman and co-workers disclosed the bromodifluoromethylation of nitrones (Scheme 3.8C).[20] In this case, an iridium photocatalyst and ascorbate as reducing agent were required to access various bromodifluoromethyl-containing hydroxylamines.

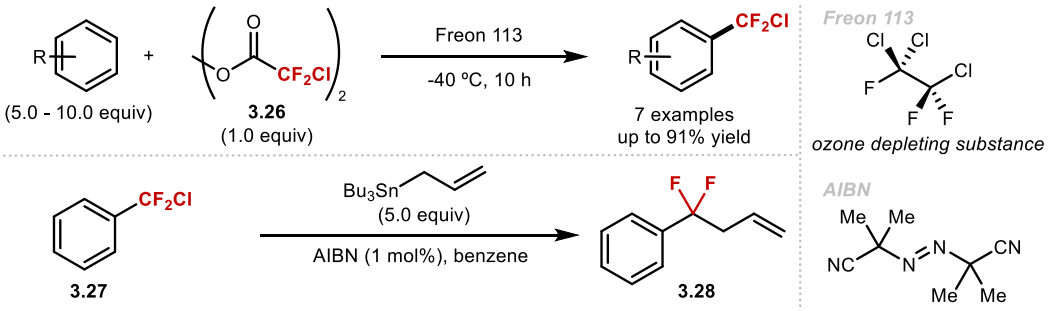
The above-mentioned reactions employ ozone-depleting dibromodifluoromethane (**3.19**). In 2017, Masson, Magnier and co-workers disclosed a series of sulfilimino reagents (**3.23, 3.24**) that allowed oxyfluoroalkylation of styrenes (Scheme 3.9).[19] Upon single-electron reduction by a photocatalyst, these reagents release fluoroalkyl radicals, which react with styrenes. Oxidation of the radical intermediate followed by trapping with methanol (solvent) affords the methoxyfluoroalkylated products in moderate to high yields. Other than the bromodifluoromethyl radical, the authors investigated the dichlorofluoromethyl radical, the trifluoromethyl radical and the 1-chloro-1,2,2,2-tetrafluoroethyl radical.



Scheme 3.9. Sulfilimino reagents **3.23** and **3.24** for photocatalytic methoxyfluoroalkylation of styrenes.

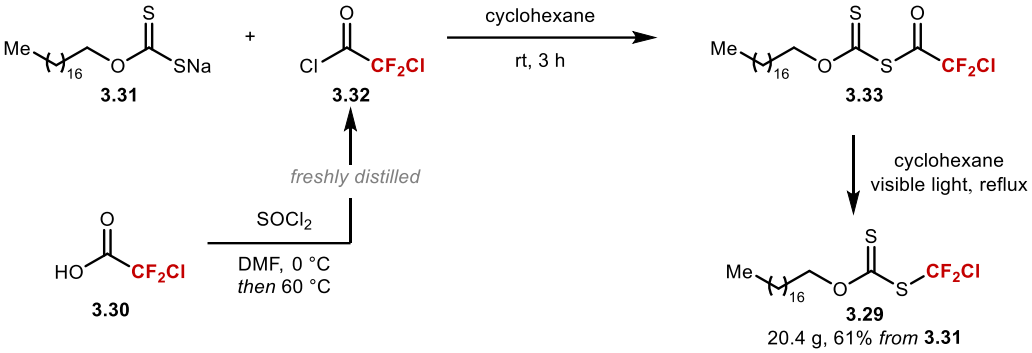
3.2.3 Chlorodifluoromethylation Reactions

In 1992, Yoshida and co-workers were the first to disclose a Minisci-type C-H chlorodifluoromethylation employing the reactivity of the chlorodifluoromethyl radical (Scheme 3.10).[24] Chlorodifluoroacetic anhydride (**3.25**) was reacted with 30% hydrogen peroxide to afford *bis*(chlorodifluoroacetyl)peroxide (**3.26**), which was directly engaged with various arenes to afford C-H chlorodifluoromethylated arenes. The authors further described the allylation of *α,α,α*-chlorodifluorotoluene (**3.27**) with allyltributylstannane to afford difluoromethylene compound **3.28**.



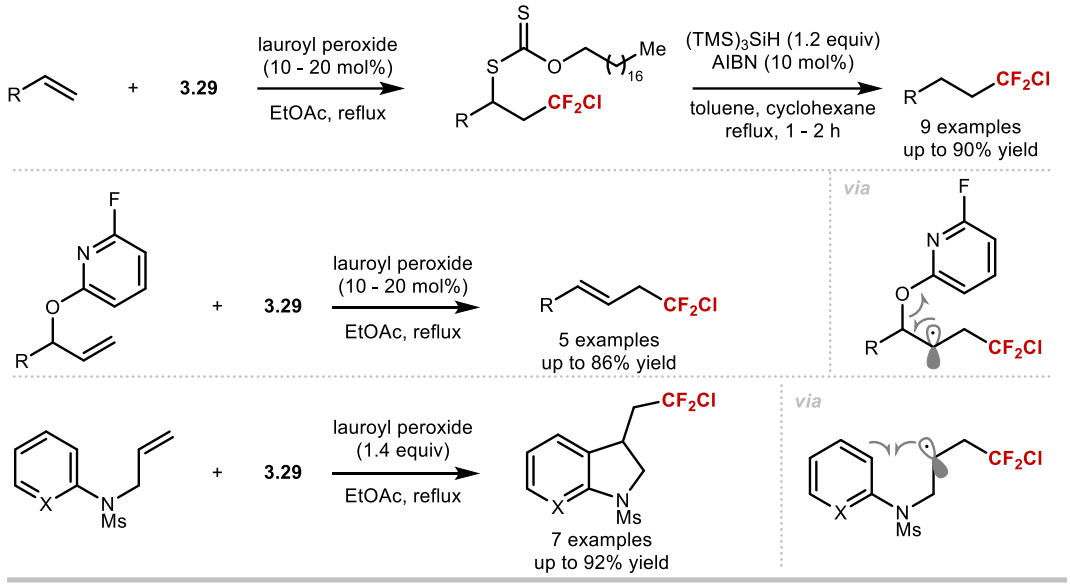
Scheme 3.10. Yoshida's report of the chlorodifluoromethyl radical generated from chlorodifluoroacetic anhydride (**3.26**).

In 2014, Salomon and Zard developed a chlorodifluoromethyl xanthate reagent (**3.29**) from commercial and inexpensive chlorodifluoroacetic acid (**3.30**, Scheme 3.11). **3.29** was synthesised in a two-step procedure from xanthate **3.31**. **3.31** was reacted with freshly-distilled chlorodifluoroacetyl chloride (**3.32**, afforded from the reaction of chlorodifluoroacetic acid **3.30** with thionyl chloride) to afford xanthate **3.33**. This intermediate was then irradiated with visible light which resulted in decarbonylation and afforded the desired xanthate **3.29** in 61% yield from **3.31**.



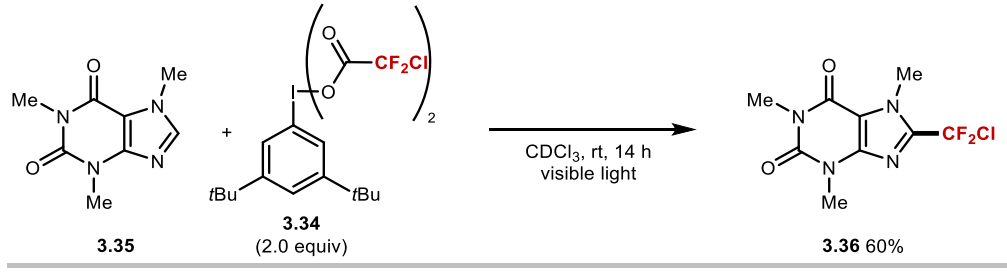
Scheme 3.11. Synthesis of the chlorodifluoromethyl xanthate **3.29**.

They then showed that xanthate **3.29** readily reacts with alkenes under initiation with substoichiometric amounts of lauroyl peroxide (Scheme 3.12). Under these conditions they were able to afford a variety of different products, depending on the substitution pattern of the alkene substrate. Unactivated terminal, or *gem*-disubstituted alkenes afforded the corresponding ATRA product in high yields. The resulting xanthates could be further reduced under radical conditions using AIBN as initiator and $(TMS)_3SiH$ as stoichiometric reducing agent. When the reaction was performed on 6-fluoropyridiyl allyl ethers, the reaction resulted in the chlorodifluoromethylated products with extrusion of the 2-hydroxypyridine. The authors propose a mechanism which involves homolytic bond cleavage of the carbon-oxygen bond from the C-centred radical intermediate. When the reaction was performed on *N*-aryl allyl amines protected with a mesylate moiety, the reaction afforded indolines in excellent yields. This reaction most likely proceeds through a radical addition of the C-centred radical intermediate to the arene. Stoichiometric amount of oxidant had to be used to obtain the product.



Scheme 3.12. Xanthate reagent **3.29** for the chlorodifluoromethylation of alkenes.

More recently, Maruoka and co-workers disclosed the use of a hypervalent iodine reagent with chlorodifluoroacetoxy ligands (**3.34**) for the C-H chlorodifluoromethylation of caffeine (**3.35**) to afford chlorofluoromethyl compound **3.36** (Scheme 3.13).



Scheme 3.13. Chlorodifluoromethylation of caffeine (**3.35**).

3.3 This Work - Hydrochlorofluoromethylation of Unactivated Alkenes with Chlorofluoroacetic Acid

To date, all methods used to access chlorofluoromethylalkanes rely on either a multistep procedure, toxic reagents, or suffer from a limited substrate scope. We set out to address these challenges by utilising the chlorofluoromethyl radical as a

reactive intermediate for the synthesis of a broad variety of chlorofluoromethylalkanes. Even though the chlorofluoromethyl radical was broadly studied in its role in ozone depletion, it was never investigated in the context of method development.[26] Structural computations by Schwartz and Marshall from 2003 showed that the chlorofluoromethyl radical has a pyramidal structure similar to other halogenated radicals (Figure 3.5).[26] Compared to the difluoromethyl radical (sum of interbond angles (Σ_χ) = 339°), the chlorofluoromethyl radical (Σ_χ = 348°) is more planar. Furthermore, owing to the higher electronegativity of fluorine (χ = 4.0, Pauling scale) compared to chlorine (χ = 3.2), the chlorofluoromethyl radical (sum of substituent electronegativies (Σ_χ) = 9.4) is also expected to be less electrophilic than the difluoromethyl radical (Σ_χ = 10.2). Overall, with respect to its reactivity, it is expected that the chlorofluoromethyl radical behaves similarly to the well-studied difluoromethyl radical.

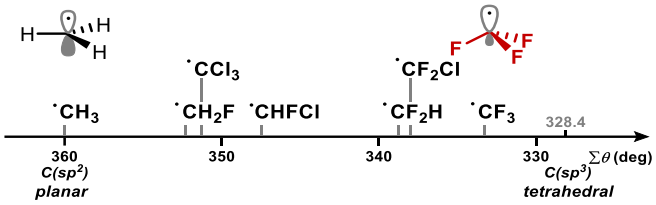


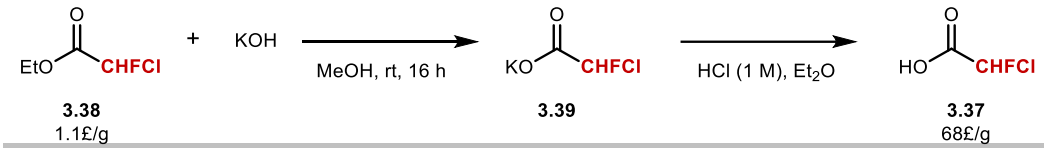
Figure 3.5. Structure of various halogenated methyl radicals.

We previously disclosed the hydrodifluoromethylation of alkenes (Chapter 2). This reaction relied on the activation of commercial and inexpensive difluoroacetic acid with a hypervalent iodine reagent.[27] Therefore, we initially investigated whether in a similar fashion, chlorofluoroacetic acid (**3.37**) could be used for hydrochlorofluoromethylation of unactivated alkenes. Chlorofluoroacetic acid

(**3.37**) is a commercial reagent mainly used for the synthesis of chlorofluoroacetamides *via* amide coupling.[6–9] However, to the best of our knowledge its use as a chlorofluoromethyl radical surrogate has not been investigated to date.

3.3.1 Synthesis of Starting Materials

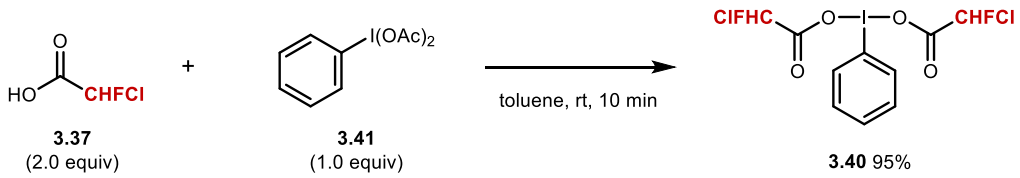
Chlorofluoroacetic acid (**3.37**) is commercially available but can also be prepared by hydrolysis of the much less expensive ethyl ester **3.38** (Scheme 3.14). Reacting equimolar amounts of potassium hydroxide and ethyl chlorofluoroacetate (**3.38**) in methanol at room temperature overnight affords potassium chlorofluoroacetate (**3.39**) in nearly quantitative yield. Excess **3.38** was removed by washing the crude salt with diethyl ether. The salt was then dissolved in water, the mixture was acidified, and extracted with diethyl ether to obtain chlorofluoroacetic acid (**3.37**) analytically pure.



3.38 1.1£/g **3.39** **3.37** 68£/g

Scheme 3.14. Synthesis of chlorofluoroacetic acid (**3.37**).

Iodine(III) derivative **3.40** was synthesised by stirring two equivalents of chlorofluoroacetic acid (**3.37**) with PIDA (**3.41**) in toluene at room temperature (Scheme 3.15). Removal of the solvent yields the desired reagent as a white solid, which is directly used in subsequent reactions without further purification.



3.37 (2.0 equiv) + **3.41** (1.0 equiv) → **3.40** 95%

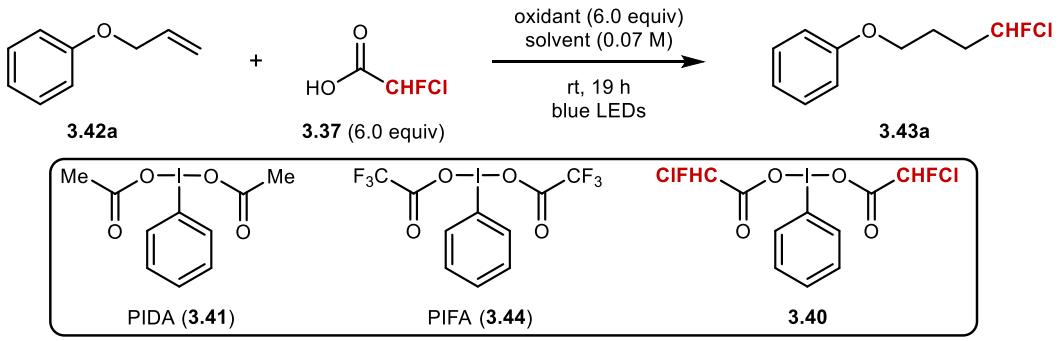
Scheme 3.15. Synthesis of reagent **3.40** from chlorofluoroacetic acid (**3.37**) and PIDA **3.41**.

3.3.2 Control Experiments and Optimisation

When allyl phenyl ether (**3.42a**) was reacted with phenyliodine(III) diacetate (**3.41**, 6.0 equiv, PIDA) and chlorofluoroacetic acid (**3.37**, 6.0 equiv) in THF at room temperature under visible light irradiation, the desired hydrochlorofluoromethylated compound **3.43a** was formed in 57% yield as determined by quantitative ^{19}F NMR spectroscopy (*α*,*α*,*α*-trifluorotoluene was used as an internal standard; Table 3.1, entry 1). Chlorofluoromethylalkanes display a characteristic doublet of triplets in ^{19}F NMR spectroscopy ($\delta_{(ppm)}$ −130 (dt, $^{2}J_{H\text{-}F}$ = 51 Hz, $^{3}J_{H\text{-}F}$ = 19 Hz)), coupling to both the CHFCl hydrogen and the neighbouring methylene hydrogens. A control experiment performed with *bis*(trifluoroacetoxy)iodobenzene (**3.44**) instead of PIDA (**3.41**) resulted in low yield (entry 2, 7%). The corresponding hydrotrifluoromethylated product (^{19}F NMR$_{(expected)}$: $\delta_{(ppm)}$ −66 (t, $^{3}J_{H\text{-}F}$ = 12 Hz)) was not observed in this reaction and the starting material (**3.42a**) was recovered. Furthermore, when the preformed iodine(III) reagent **3.40** was used in absence of chlorofluoroacetic acid (**3.37**) the reaction was significantly lower yielding (entry 3, 14%). When PIDA was added in two portions of three equivalents each (second portion added after five hours reaction time), the ^{19}F NMR yield was increased to 67% (entry 4). Other solvents such as *N*,*N*-dimethylformamide (DMF) and 1,4-dioxane proved to be less efficient

in this transformation and resulted in lower yields of **3.43a** (entries 5-6). The reaction was also successful in absence of light albeit in much lower yield (entry 7, 18%). When the radical scavenger (2,2,6,6-tetramethylpiperidin-1-yl)oxyl (TEMPO, **3.45**) was added under the standard reaction conditions, the hydrochlorofluoromethylation did not proceed and the alkene **3.42a** remained unreactive (entry 8).

Table 3.1 Optimisation of the Hydrochlorofluoromethylation of Alkenes.

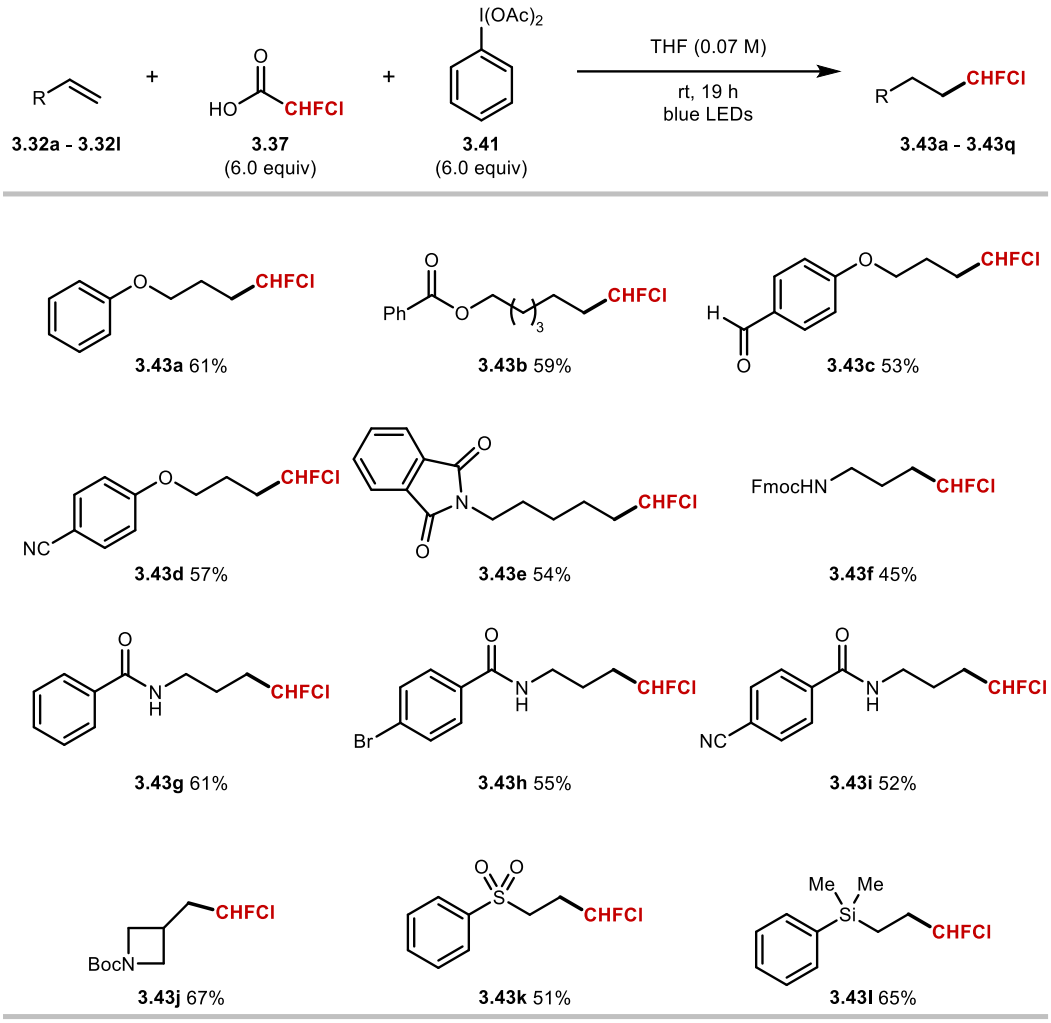


entry	solvent	oxidant	yield [%][a]
1	THF	**3.41**	57
2	THF	**3.44**	7
3[b]	THF	**3.40**	14
4[c]	**THF**	**3.41**	**67**
5[c]	DMF	**3.41**	30
6[c]	1,4-dioxane	**3.41**	16
7[d]	THF	**3.41**	18
8[e]	THF	**3.41**	0

[a]**3.42a** (0.1 mmol), oxidant (0.6 mmol), **3.37** (0.6 mmol), solvent (1.5 mL), blue LED irradiation (λ_{max} = 450 nm) at room temperature for 14 h. The yield was determined by ^{19}F NMR spectroscopy using *α*,*α*,*α*-trifluorotoluene as internal standard. [b]**3.40** was used in the absence of **3.37**. [c]**3.41** was added in two batches (0.3 mmol each). Second batch (3.0 equiv) was added after 5 h reaction time. [d]Reaction performed in the absence of light at 50 °C. [e]TEMPO (**3.45**, 0.6 mmol) was added to the standard reaction conditions. THF = tetrahydrofuran. DMF = *N*,*N*-dimethylformamide.

3.3.3 Substrate Scope for the Hydrochlorofluoromethylation of Alkenes

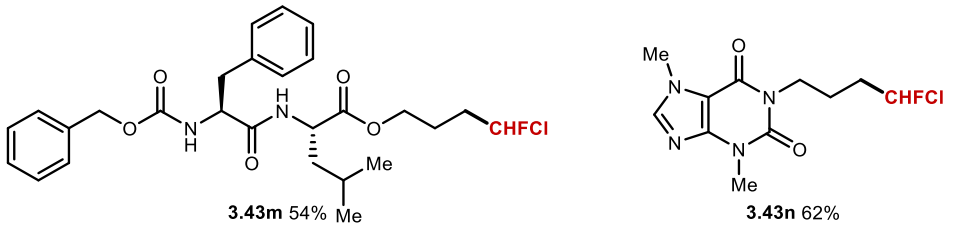
With the optimal reaction conditions in hand, the substrate scope of this transformation was investigated (Scheme 3.16). Ethers and esters bearing other functional groups such as aldehydes and nitriles were tolerated and yielded the desired products in moderate yields (**3.43b** – **3.43d**). Phtalimide protected 1-aminopent-4-ene yielded the desired hydrochlorofluoromethylated product **3.43e** in 54% yield. Notably, this product was previously synthesised in a six-step sequence (Scheme 3.4). With this hydrochlorofluoromethylation protocol, the same compound was obtained in two synthetic steps from commercial reagents. Other *N*-protected amines such as Fmoc and benzoyl protected allylamide yielded the hydrochlorofluoromethylated products **3.43f** and **3.43g** in moderate yields. Substitution in the 4-position of the benzoyl group had little effect on the reaction outcome. Bromo and nitrile substituents were tolerated and afforded the hydrochlorofluoromethylated products **3.43h** and **3.43i** in moderate yields. A representative *gem*-disubstituted alkene such as azetidine **3.42j** was suitable under the reaction conditions. Even though the reaction is performed in presence of excess chlorofluoroacetic acid (**3.37**), the *N*-protecting group remained intact. Phenyl vinyl sulfone (**3.42k**), an electron-deficient alkene yielded the desired product **3.43k** in 51% yield. Analogous to the hydrodifluoromethylation reaction described in Chapter 2, a side product which stems from THF radical addition to the alkene was observed by LC-MS. This side product was readily removed by flash column chromatography. Furthermore, a vinyl silane was hydrochlorofluoromethylated in 65% yield (**3.43l**).



Scheme 3.16. Substrate scope of the hydrochlorofluoromethylation of alkenes **3.42a** – **3.42l**. Yields of isolated products depicted.

The application of this protocol to more complex substrates of biological relevance was investigated next (Scheme 3.17). A dipeptide containing an allyl group was selectively functionalised and afforded the hydrochlorofluoromethylated product **3.43m** in 54% isolated yield. *N*-allyl-theobromine (**3.42n**) was reactive under the optimised conditions and chemoselectively afforded the desired product **3.43n** in 62% yield. Notably, caffeine derivatives have shown to react at the C_8-H position to undergo Minisci-type functionalisation under similar conditions.[22] Under the optimised hydrochlorofluoromethylation conditions, only trace amounts of C_8-H

chlorofluoromethylated were observed by quantitative ^{19}F NMR spectroscopy for *N*-allyl theobromine (**3.42n**). The product **3.43n** was purified by flash column chromatography on silica gel and the side product was removed. An estrone derivative (**3.43o**) underwent hydrochlorofluoromethylation in 46% yield. Finally, Vinclozolin (a fungizide) underwent the transformation in 72% yield to yield chlorofluoroalkane **3.43p**. The cyclic carbamate remained intact and no side products were observed.



Scheme 3.17. Late-stage hydrochlorofluoromethylation of alkenes with biological relevance.

3.3.4 Limitations of the Hydrochlorofluoromethylation Protocol

The hydrochlorofluoromethylation reaction performed well for the functionalisation of unactivated alkenes. However, electron-rich alkenes such as enol ethers, enamines, or enamides only afforded traces of the desired product under the hydrochlorofluoromethylation reaction conditions. Styrenes also proved unsuitable under the optimised conditions; ^{19}F NMR analysis of a crude mixture showed a mixture of various products that could result from polymerisation. Furthermore, some electron-deficient alkenes such as benzyl

acrylate only afforded low yields according to quantitative ^{19}F NMR analysis. A side reaction in case of electron-deficient alkenes is the competitive addition of the THF radical as observed in the reaction of phenyl vinyl sulfone (see Chapter 2, section 2.9). With regards to functional group compatibility, substrates containing unprotected primary, secondary or tertiary amines were not tolerated.

3.3.5 Proposed Mechanism for the Hydrochlorofluoromethylation of Alkenes

For this transformation, an analogous mechanism as for the hydrodifluoromethylation reaction is proposed (Figure 3.6). Acetate exchange on the iodine(III) reagent **3.41** with chlorofluoroacetic acid **3.37** leads to reagent **3.40**. Initiation by a homolytic carbon-iodine bond cleavage under blue light irradiation affords iodobenzene as well as the chlorofluoroacetoxy radical **3.46**. Decarboxylation of the latter releases the chlorofluoromethyl radical **3.47**, which can add in an anti-Markovnikov fashion onto an alkene (**3.42**). The C-centred radical intermediate **3.48** then abstracts a hydrogen atom from the solvent to form the desired product **3.43** and a THF radical (**3.49**). Oxidation of this radical by reagent **3.40** results in formation of a THF oxonium ion, iodobenzene, chlorofluoroacetate anion and a new species of chlorofluoroacetoxy radical **3.46** to close the chain propagation mechanism.

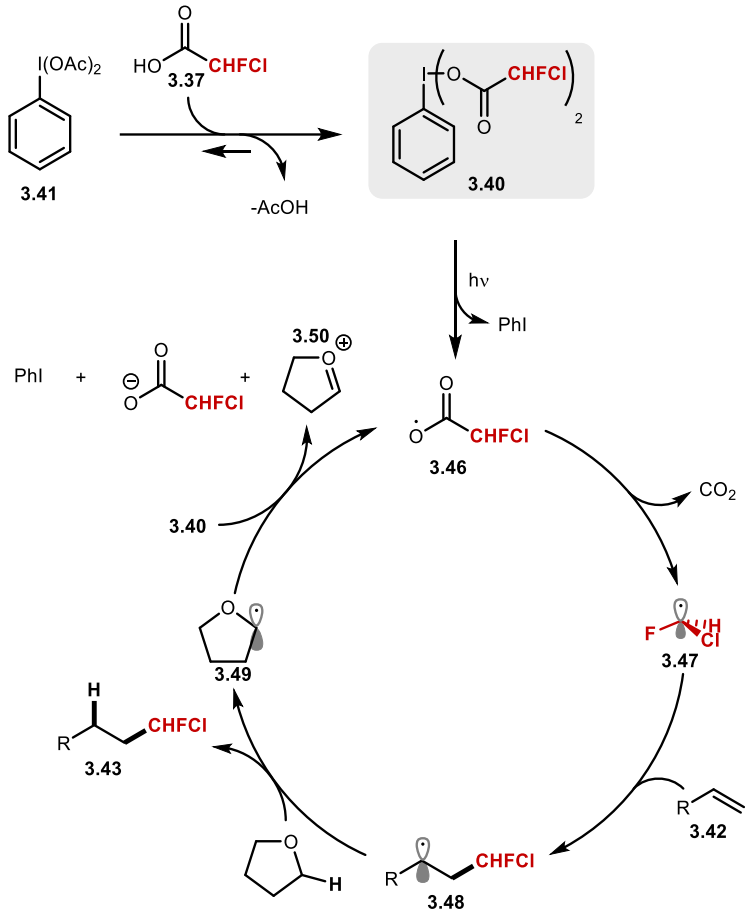
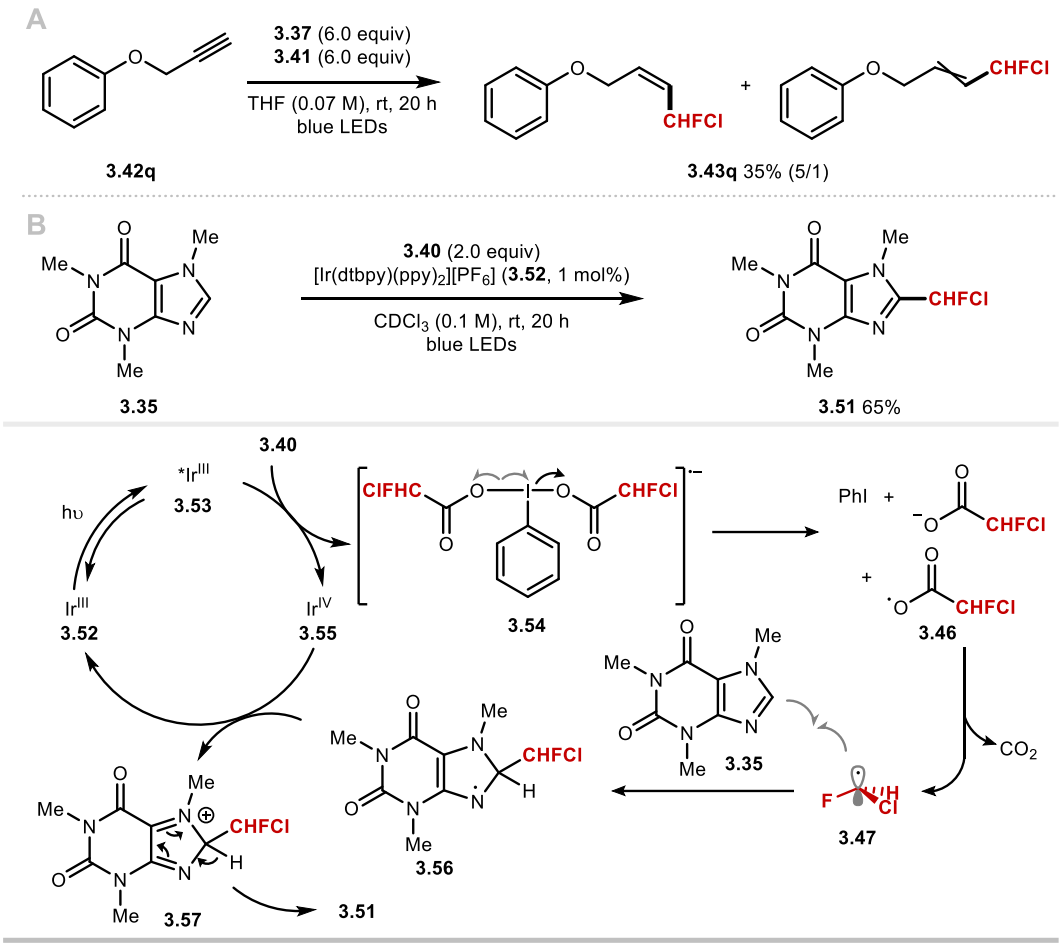


Figure 3.6. Proposed mechanism for the hydrochlorofluoromethylation of alkenes.

3.3.6 Further Applications of the Chlorofluoromethyl Radical

The reactivity of the chlorofluoromethyl radical towards other substrates was investigated next. When propargyl phenyl ether (**3.42q**) was used as substrate, a 1,2-disubstituted alkene containing chlorofluoromethyl group was obtained in low yield (**3.43q**) (Scheme 3.18A). Inspired by Maruoka's work on the direct C-H difluoromethylation of heteroarenes, we investigated whether chlorofluoroacetate containing reagent **3.40** could undergo direct C-H chlorofluoromethylation on caffeine (**3.35**) (Scheme 3.18B). Employing $[Ir(dtbpy)(ppy)_2][PF_6]$ (1 mol%, **3.52**) as photocatalyst and deuterated chloroform as solvent, C-H chlorofluoromethylated caffeine (**3.51**) was isolated in 65% yield.

However, when this methodology was used on other substrates such as 4-substituted pyridines, only traces of chlorofluoromethylated product were formed. Mechanistically, we suggest that blue light irradiation of iridium-based photocatalyst **3.52** affords the triplet excited state **3.53**. This highly reducing species could undergo single-electron reduction with the iodine(III) species **3.40** affording radical anion **3.54** and oxidised iridium **3.55**. Fragmentation of **3.54** results in iodobenzene, chlorofluoroacetate anion and chlorofluoroacetyl radical **3.46**. The latter readily undergoes decarboxylation to afford chlorofluoromethyl radical (**3.47**) that can add to the activated C-8 position of caffeine (**3.35**) to afford intermediate **3.56**. Oxidation of the radical intermediate with the photocatalyst would then afford **3.57** and finally the desired C-H chlorofluoromethylated product **3.51** after subsequent deprotonation.

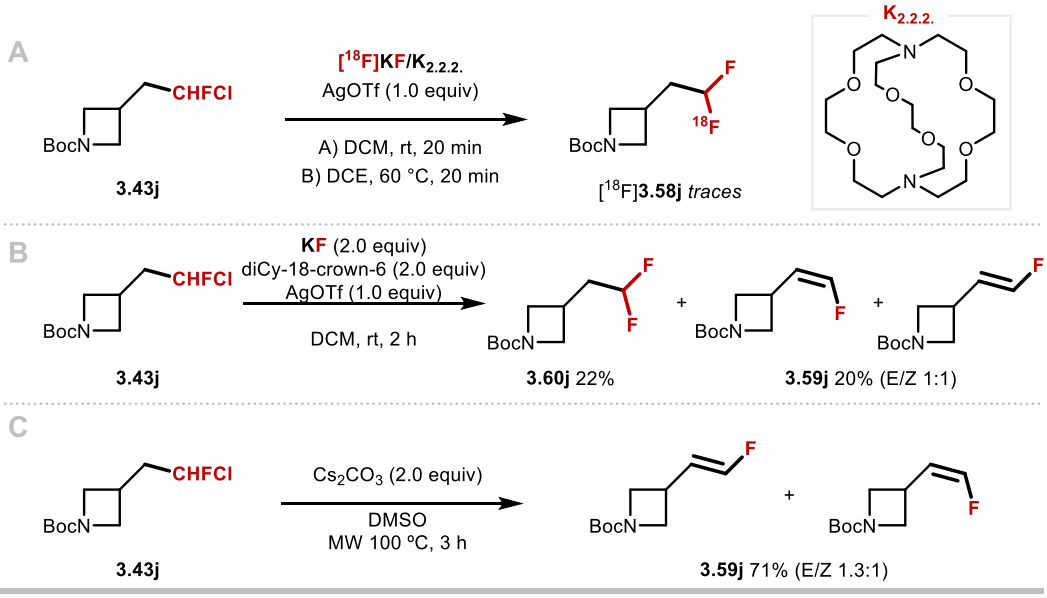


Scheme 3.18. Other substrates for radical chlorofluoromethylation.

3.3.7 Application of Chlorofluoromethyl Alkanes

Having a range of chlorofluoromethyl alkanes in hand, the possibility of using the chlorofluoromethyl group as a reactive synthon was investigated (Scheme 3.19). Given the literature precedence of F-18 radiolabelling of the C(sp^2)-linked chlorofluoromethyl group with [^{18}F]fluoride, the previously disclosed conditions were applied to the ^{18}F-fluorination of chlorofluoromethyl azetidine **3.43j** (Scheme 3.19A). Only traces of [^{18}F]fluoride incorporation was observed under any of the conditions ([^{18}F]**3.58j**). A possible explanation for this observation could stem from the presence of *α*-protons, which might result in elimination of hydrochloric acid rather than the desired halogen exchange reaction. Indeed, when an experiment

was performed with F-19 fluoride, three new products were observed by quantitative ^{19}F NMR spectroscopy (Scheme 3.19B). Two of them likely correspond to both the *E* and *Z* isomer of the vinyl fluoride **3.59j** ($\delta_{(ppm)}$ −127 (dd, $^{2}J_{H\text{-}F}$ = 84 Hz, $^{3}J_{H\text{-}F}$ = 43 Hz) and -128 (dd, $^{2}J_{H\text{-}F}$ = 84 Hz, $^{3}J_{H\text{-}F}$ = 18 Hz) in 20% yield, whilst the other new product corresponds to the desired fluorinated compound **3.60j** ($\delta_{(ppm)}$ −116 - −117 (m)) in 22% yield. This result is in agreement with literature showing that nucleophilic substitution is more challenging on halofluoroalkanes than haloalkanes.[28] In contrast, elimination of hydrogen halides occurs more readily on halofluoroalkanes. Therefore, the synthesis of vinyl fluorides from chlorofluoromethylalkanes under basic conditions was investigated. Vinyl fluoride **3.59j** could be accessed in 71% yield by treatment of **3.43j** with caesium carbonate at 100 °C for three hours (Scheme 3.19C).



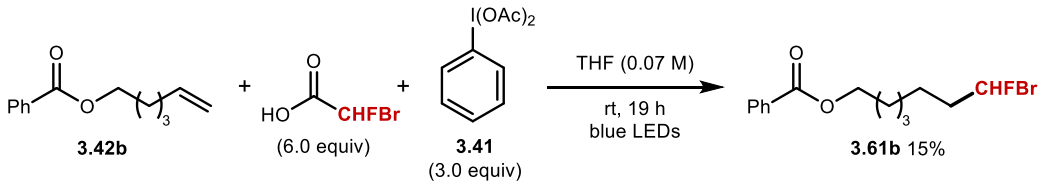
Scheme 3.19. Further applications of chlorofluoromethylalkanes.

3.4 The Bromofluoromethyl Radical

Similar to the chlorofluoromethyl radical, the bromofluoromethyl radical has not been investigated in organic synthesis. Therefore, the generation of the bromofluoromethyl radical to access bromofluoromethylalkanes was investigated next.

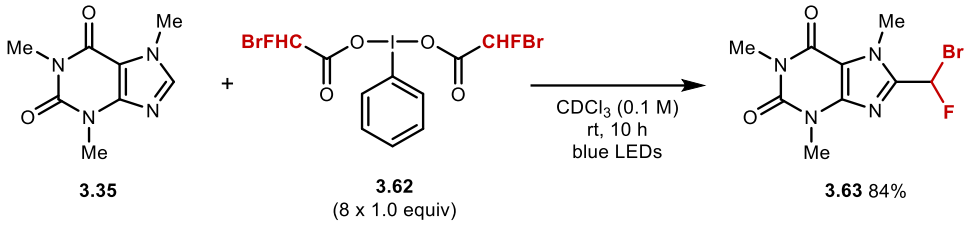
3.4.1 Generation of the Bromofluoromethyl Radical from Bromofluoroacetic Acid

When bromofluoroacetic acid was reacted with alkene **3.42b** and PIDA (**3.41**) in THF, low amounts of the desired bromofluoromethylalkane **3.61b** were observed by quantitative ^{19}F NMR spectroscopy (15%) (Scheme 3.20).



Scheme 3.20. Attempted hydrobromofluoromethylation of alkene **3.42b**.

On the other hand, when caffeine (**3.35**) was treated with a large excess of a bromofluoroacetate-containing iodine(III) reagent **3.62** the desired C-H bromofluoromethylated product **3.63** was observed in 84% yield according to quantitative ^{19}F NMR spectroscopy (Scheme 3.21). One limitation to this transformation is that the reagent was added in several batches, and the reaction mixture was degassed after each addition of reagent **3.62**.

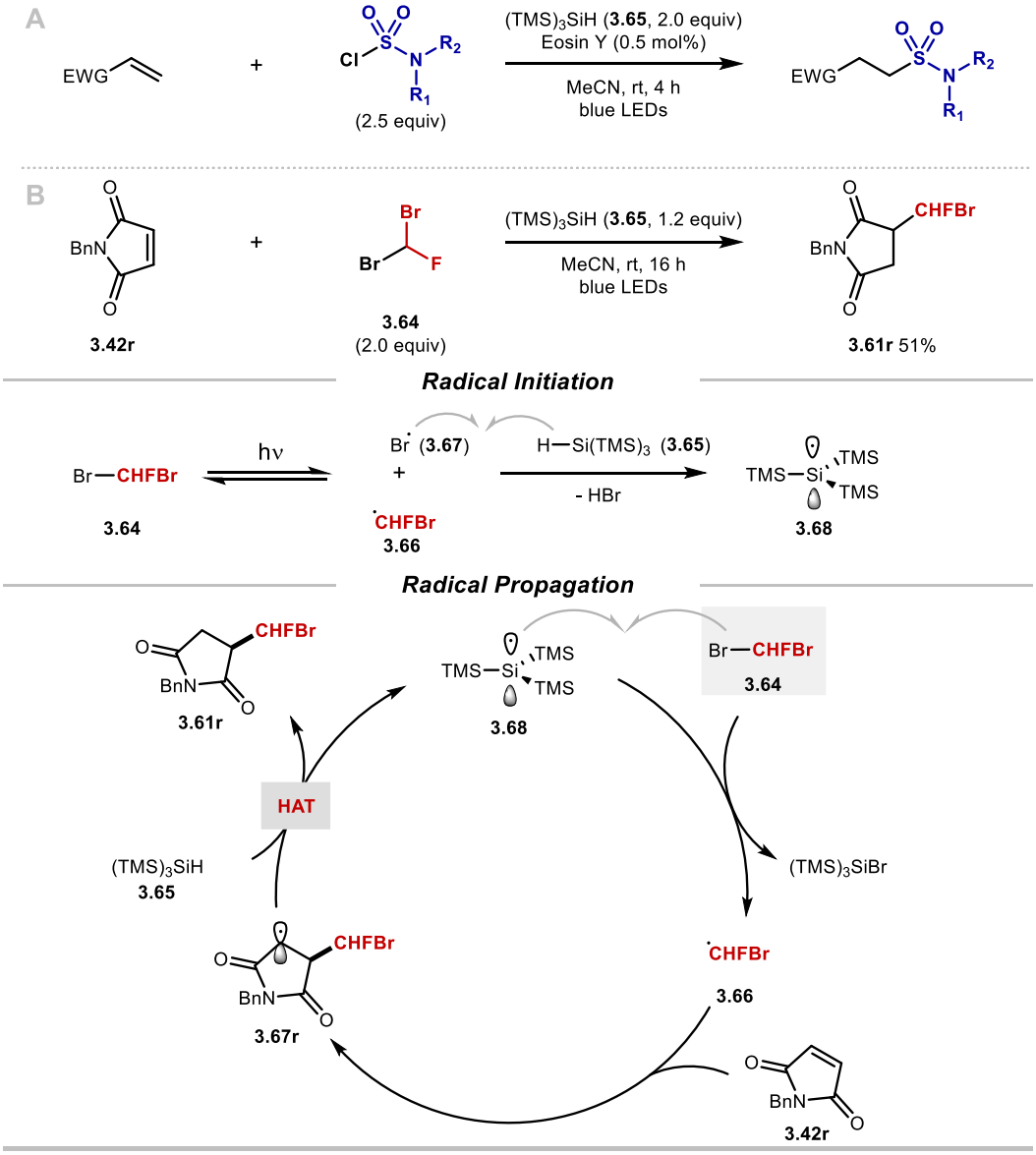


Scheme 3.21. C-H Bromofluoromethylation of caffeine (**3.35**) with reagent **3.62**.

When the C-H bromofluoromethylation conditions were applied to other heteroarenes such as substituted pyridines, the corresponding bromofluoromethylated products were not observed in quantitative ^{19}F NMR analysis of the crude reaction mixtures. Therefore, other bromofluoromethyl radical precursors were investigated next.

3.4.2 Generation of the Bromofluoromethyl Radical from Dibromofluoromethane

Recently, Gouverneur and co-workers reported the hydrosulfamoylation of electron-deficient alkenes.[29] This reaction relied on a silyl-radical mediated halogen-atom abstraction from sulfamoyl chlorides to generate sulfamoyl radicals (Scheme 3.22A). A similar strategy allowing the generation of the bromofluoromethyl radical was therefore investigated next (Scheme 3.22B). When dibromofluoromethane **3.64** was reacted with tris(trimethylsilyl)silane (**3.65**) and *N*-benzylmaleimide (**3.42r**) in acetonitrile under blue light irradiation, the desired hydrobromofluoromethylated product **3.61r** was afforded in moderate yield (51%). Dibromofluoromethane (**3.64**) is an ozone-depleting, commercial liquid reagent that has mainly been used in nucleophilic substitution reactions and carbene chemistry.[30]



Scheme 3.22. a) Hydrosulfamoylation of electron-deficient alkenes, b) Silyl radical-mediated hydrobromofluoromethylation of *N*-benzylmaleimide (**3.42r**).

Mechanistically, we suggest that initiation by blue light induced partial homolytic carbon-bromine bond cleavage of **3.64**, resulting in the release of trace amounts of bromofluoromethyl radical (**3.66**) and bromine (**3.67**) radical. The latter is known to undergo hydrogen atom abstraction with tris(trimethylsilyl)silane (**3.65**) to afford hydrogen bromide along with the tris(trimethylsilyl)silyl radical (**3.68**). This nucleophilic silyl radical **3.68** is a privileged halogen atom abstractor and could

abstract bromine from **3.64** to release the bromofluoromethyl radical (**3.66**). Giese-addition of **3.66** to alkene **3.42r** results in an electrophilic radical intermediate (**3.67r**), which can undergo hydrogen atom abstraction from tris(trimethylsilyl)silane (**3.65**) to afford the desired product **3.61r** and **3.68** to close the chain propagation mechanism.

3.5 Conclusion

In conclusion, we developed the first hydrochlorofluoromethylation of unactivated alkenes. The reaction relied on the use of commercially available chlorofluoroacetic acid in combination with commercial inexpensive (diacetoxyiodo)benzene as a mild oxidant. The hydrochlorofluoromethylation protocol was applied to a range of structurally diverse alkenes and the desired products were generally afforded in good yields. The utility of the chlorofluoromethyl group as a synthon for further functionalisation was investigated. We further developed reaction conditions for the generation of the bromofluoromethyl radical from a different precursors. Dibromofluoromethane, a commercial liquid reagent, reacted in a silyl-radical mediated hydrobromofluoromethylation to afford a bromofluoromethylalkane in good yield.

3.6 Outlook

The field of chlorofluoromethylation and bromofluoromethylation remains underexplored. Future developments in this field should focus on the introduction of the bromofluoromethyl radical to a broader range of substrates, including

alkenes (*via* hydrobromofluoromethylation) and (hetero)arenes (*via* Minisci-type chemistry). Bromofluoromethyl-containing compounds are more versatile than their chlorofluoromethyl analogues. Downstream applications of the bromofluoromethyl group should further be explored. The bromofluoromethyl group could be used for enantioselective Suzuki cross-couplings or for F-18 radiolabelling. Furthermore, the investigation of the bromofluoromethyl group as a warhead for covalent protein inhibition could be of interest to the pharmaceutical industry.

Considering that our attempts at F-18 radiofluorination of chlorofluoromethyl alkanes revealed unsuccessful, another approach to access the [^{18}F]difluoromethyl group will be investigated (Chapter 5).

3.7 References

[1] S. Verhoog, L. Pfeifer, T. Khotavivattana, S. Calderwood, T. L. Collier, K. Wheelhouse, M. Tredwell, V. Gouverneur, *Synlett* **2016**, *27*, 25–28.

[2] X. Jiang, S. Sakthivel, K. Kulbitski, G. Nisnevich, M. Gandelman, *J. Am. Chem. Soc.* **2014**, *136*, 9548–9551.

[3] X. Jiang, M. Gandelman, *J. Am. Chem. Soc.* **2015**, *137*, 2542–2547.

[4] Q. Zhao, P. G. Isenegger, T. C. Wilson, J. B. I. Sap, F. Guibbal, L. Lu, V. Gouverneur, Q. Shen, *CCS Chem.* **2020**, 1921–1028.

[5] T. Khotavivattana, S. Verhoog, M. Tredwell, L. Pfeifer, S. Calderwood, K. Wheelhouse, T. Leecollier, V. Gouverneur, *Angew. Chemie - Int. Ed.* **2015**, *54*, 9991–9995.

[6] S. D. Kuduk, C. N. Di Marco, R. K. Chang, M. R. Wood, K. M. Schirripa, J. J. Kim, J. M. C. Wai, R. M. DiPardo, K. L. Murphy, R. W. Ransom, C. M. Harrell, D. R. Reiss, M. A. Holahan, J. Cook, J. F. Hess, N. Sain, M. O. Urban, C. Tang, T. Prueksaritanont, D. J. Pettibone, M. G. Bock, *J. Med. Chem.* **2007**, *50*, 272–282.

[7] M. Sato, H. Fuchida, N. Shindo, K. Kuwata, K. Tokunaga, G. Xiao-Lin, R. Inamori, K. Hosokawa, K. Watari, T. Shibata, N. Matsunaga, S. Koyanagi, S. Ohdo, M. Ono, A. Ojida, *ACS Med. Chem. Lett.* **2020**, *11*, 1137–1144.

[8] N. Shindo, H. Fuchida, M. Sato, K. Watari, T. Shibata, K. Kuwata, C. Miura, K. Okamoto, Y. Hatsuyama, K. Tokunaga, S. Sakamoto, S. Morimoto, Y. Abe, M. Shiroishi, J. M. M. Caaveiro, T. Ueda, T. Tamura, N. Matsunaga, T. Nakao, S. Koyanagi, S. Ohdo, Y. Yamaguchi, I. Hamachi, M. Ono, A. Ojida, *Nat. Chem. Biol.* **2019**, *15*, 250–258.

[9] K. Tokunaga, M. Sato, K. Kuwata, C. Miura, H. Fuchida, N. Matsunaga, S. Koyanagi, S. Ohdo, N. Shindo, A. Ojida, *J. Am. Chem. Soc.* **2020**, DOI 10.1021/jacs.0c07490.

[10] A. K. Ghosh, I. Samanta, A. Mondal, W. R. Liu, *ChemMedChem* **2019**, *14*, 889–906.

[11] J. D. Park, D. K. Vail, K. R. Lea, J. R. Lacher, *J. Am. Chem. Soc.* **1948**, *70*, 1550–1552.

[12] D. C. England, L. R. Melby, M. A. Dietrich, R. V. Lindsey, *J. Am. Chem. Soc.* **1960**, *82*, 5116–5122.
[13] H. Rosenberg, J. B. Modrak, J. M. Hassing, W. A. Al-Turk, S. J. Stohs, *Biochem. Biophys. Res. Commun.* **1979**, *91*, 498–501.
[14] E. G. Locke, W. R. Erode, A. L. Henne, *J. Am. Chem. Soc.* **1934**, *56*, 1726–1728.
[15] A. Piou, S. Celerier, S. Brunet, *J. Fluor. Chem.* **2012**, *134*, 103–106.
[16] A. Garcia Martínez, J. Osío Barcina, A. Z. Rys, L. R. Subramanian, *Synlett* **1993**, *8*, 587–588.
[17] P. Salomon, S. Z. Zard, *Org. Lett.* **2014**, *16*, 2926–2929.
[18] S. Kawamura, C. J. Henderson, Y. Aoki, D. Sekine, S. Kobayashi, M. Sodeoka, *Chem. Commun.* **2018**, *54*, 11276–11279.
[19] M. Daniel, G. Dagousset, P. Diter, P. A. Klein, B. Tuccio, A. M. Goncalves, G. Masson, E. Magnier, *Angew. Chemie - Int. Ed.* **2017**, *56*, 3997–4001.
[20] I. A. Dmitriev, V. I. Supranovich, V. V. Levin, A. D. Dilman, *European J. Org. Chem.* **2019**, *2019*, 4119–4122.
[21] Q. Y. Lin, X. H. Xu, F. L. Qing, *Org. Biomol. Chem.* **2015**, *13*, 8740–8749.
[22] R. Sakamoto, H. Kashiwagi, K. Maruoka, *Org. Lett.* **2017**, *19*, 5126–5129.
[23] R. C. McAtee, J. W. Beatty, C. C. McAtee, C. R. J. Stephenson, *Org. Lett.* **2018**, *20*, 3491–3495.
[24] M. Yoshida, Y. Morinaga, M. Ueda, N. Kamigata, M. Iyoda, *Chem. Lett.* **1992**, *21*, 227–230.
[25] J. Chen, C.-M. Hu, *J. Org. Chem. Soc. Perkin Trans. 1* **1994**, 1111–1114.
[26] M. Schwartz, L. R. Peebles, R. J. Berry, P. Marshall, *J. Chem. Phys.* **2003**, *118*, 557–564.
[27] C. F. Meyer, S. M. Hell, A. Misale, A. A. Trabanco, V. Gouverneur, *Angew. Chemie - Int. Ed.* **2019**, *58*, DOI 10.1002/anie.201903801.
[28] W. R. Dolbier, M. Okamoto, *J. Fluor. Chem.* **2014**, *179*, 33–41.
[29] S. M. Hell, C. F. Meyer, G. Laudadio, A. Misale, M. C. Willis, T. Noël, A. A. Trabanco, V. Gouverneur, *J. Am. Chem. Soc.* **2020**, *142*, 720–725.
[30] L. Trump, A. Lemos, B. Lallemand, P. Pasau, J. Mercier, C. Lemaire, A. Luxen, C. Genicot, *Angew. Chemie - Int. Ed.* **2019**, *58*, 13149–13154.

Chapter 4 – Introduction to Positron Emission Tomography and F-18 Radiochemistry

4.1 Positron Emission Tomography

4.1.1 Introduction to Positron Emission Tomography

Positron emission tomography (PET) is a powerful, non-invasive tool for *in vivo* imaging of biological events.[1–6] PET relies on the administration of a radioactive compound (radiotracer) to an organism to provide physiological information. The precise detection and quantification of the radioactivity over specific parts of the organism reveals a 3D image of the radiotracer distribution. Thus, PET can be used to understand disease states of patients or to reveal information about biodistribution and receptor occupancy of preclinical compounds for drug discovery. In PET, a range of positron-emitting radioactive isotopes can be used. Figure 4.1 describes the basic physical events resulting from positron emission by the example of radioactive F-18 decaying to O-18. When a radioactive positron emitting isotope (e.g. F-18) decays, the positron (β^+) travels a certain range (depending on its energy) before it collides with an electron and annihilates. Annihilation of a positron and electron results in the release of two anti-parallel (angle of 180° to each other) gamma ray photons (γ) with an energy of approximately 511 keV. These gamma ray photons are detected by the PET scanner and are the main readout information for the PET image. A software is then used to reconstruct an image using these inputs.

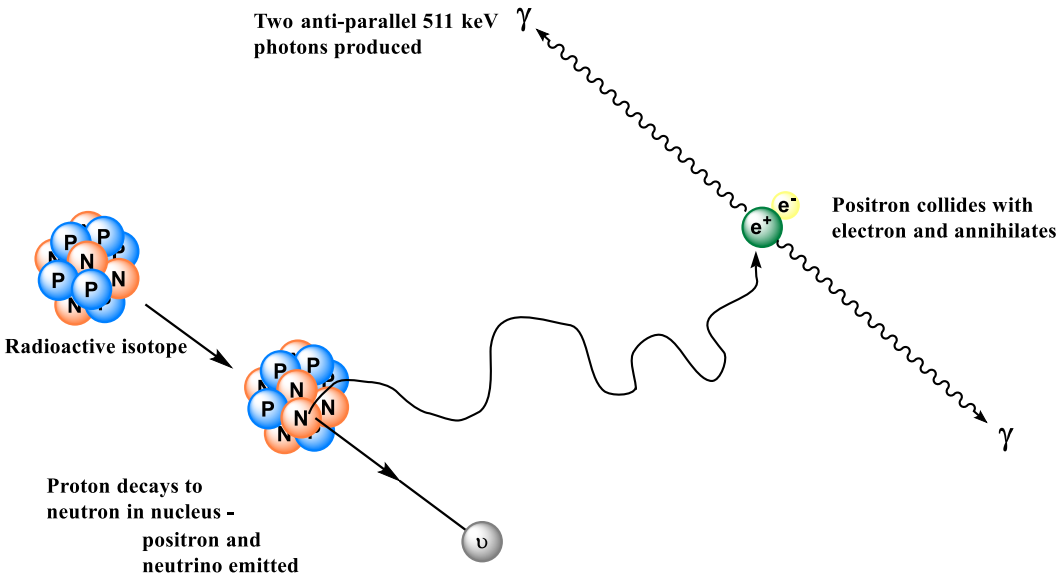


Figure 4.1. Principle of positron emission tomography. P = proton, N = neutron, ν = neutrino, γ = photon, e^+ = positron, e^- = electron.

4.1.2 Radionuclides for Positron Emission Tomography

The choice of radionuclide is often dependent on the availability of methods to access the labelled compound, as well as the desired application. Key factors in the choice of radionuclide are half-life time, decay profile, positron energy, and maximal positron range (Table 4.1).[1,4] The short-lived isotopes ^{11}C, ^{13}N, ^{15}O and ^{18}F have very clean decay profiles (all >96% β^+ decay). A clean decay profile is crucial for a strong signal and therefore high sensitivity. These isotopes mainly differ in their half-lives ($t_{1/2}$), their maximal positron energies (E_{max}), and their mean positron ranges (R_{mean}). A short half-life is preferred for *in vivo* injection to reduce damage induced by radioactive deposition in the organism. All the isotopes shown in Table 4.1 have a short enough half-life to allow for injection in humans. On the other hand, in terms of logistics, C-11, N-13 and O-15 have too short half-lives to allow for transport of a radiotracer from off-site production facilities to an imaging centre. Consecutively, radiotracers employing these isotopes must be

produced at the imaging site. The maximal positron energy (E_{max}) has a direct influence on the maximal positron range (R_{max}) and mean positron range (R_{mean}); high energy positrons travel further than low energy positrons. Too long a positron range can have a negative influence on the spatial resolution of a PET image. However, present generation whole-body PET scanners only have a spatial resolution of around 4 mm. Therefore, spatial blurring due to positron range is barely measurable for the isotopes shown in Table 4.1. Notably, with the development of more precise PET scanners and therefore increased spatial resolution, it is preferential to employ isotopes with short positron ranges.

Table 4.1. Common radioisotopes for applications in PET. [a]Maximal range of positron in water. [b]Average range of a positron in water.

Isotope	Half-life	% β^+ decay	E_{max} (MeV)	R_{max} (mm)[a]	R_{mean} (mm)[b]
^{11}C	20.4 min	99.8	0.960	4.2	1.2
^{13}N	10.0 min	99.8	1.199	5.5	1.8
^{15}O	2.04 min	99.9	1.732	8.4	3.0
^{18}F	110 min	96.9	0.634	2.4	0.6
^{64}Cu	12.7 h	17.5	0.653	2.5	0.7
^{89}Zr	78.4 h	22.7	0.902	3.8	1.3

To date, the most commonly employed radionuclides for PET imaging in humans are F-18 and C-11.[2,6] These isotopes have very similar properties, the main difference being that C-11 radiotracers need to be produced at the imaging site due to their short half-life. Apart from logistics, the longer half-life of F-18 is advantageous in that an efficient procedure for the preparation of an F-18 radiotracer allows for multiple patient doses. F-18 is commonly produced in cyclotrons from O-18 enriched water by bombardment with high energy protons (approximately 18 MeV), resulting in the release of a neutron. This process affords

[^{18}F]fluoride in [^{18}O]water. The fluoride is then usually trapped on an anion exchange cartridge to remove any radioactive impurities and the O-18 enriched target water. Common radioactive impurities are tritium enriched water and transition metals originating from the target. The [^{18}F]fluoride is then eluted with a solution containing a suitable counter ion to afford fluoride salts such as [^{18}F]potassium fluoride ([^{18}F]KF) or [^{18}F]tetraethylammonium fluoride ([^{18}F]TEAF). Another way to generate F-18 is by bombardment of Ne-20 with high energy deuterons in the presence of elemental fluorine. This process results in emission of an α-particle to afford F-18 in the form of elemental [^{18}F]fluorine ([^{18}F]F_2). However, due to the required presence of F-19 fluorine in the target gas, this process results in low molar activity (see section 4.2.3). The commonly used carbon isotope in PET is C-11, which is produced by bombardment of N-14 with high energy protons, releasing He-4. Depending on whether the bombardment is performed in the presence of small amounts (0.5% – 5%) of H_2 or O_2, this process affords either [^{11}C]CH_4 or [^{11}C]CO_2. These reagents are often subsequently converted to more reactive species such as [^{11}C]CH_3I, [^{11}C]CH_3OH or [^{11}C]CO.

4.2 Concepts and Important Factors in F-18 Radiochemistry

4.2.1 Stoichiometry in F-18 Radiochemistry

The stoichiometry in F-18 radiochemistry is very different from that in traditional organic chemistry.[1,6] Due to the half-life of F-18 ($t_{1/2}$ = 110 min), the maximal amount of [^{18}F]fluoride that can be produced by a standard cyclotron in a single run ranges from 200 GBq to 400 GBq. This corresponds to amounts of [^{18}F]fluoride in the picomolar to nanomolar range. This has an obvious influence on the

reactivity of [^{18}F]fluoride in terms of reaction kinetics. Due to the high excess of the other reaction components (usually 0.01 M to 0.1 M) compared to [^{18}F]fluoride, radiochemical reactions are often much quicker than classical reactions. This is an important factor due to radioactive decay over time. Therefore, F-18 reactions are traditionally performed in reaction times of 1 to 20 min.

4.2.2. Radiochemical Yield and Activity Yield

Since [^{18}F]fluoride is generally the limiting reagent in F-18 radiochemistry, yields in radiochemistry are based on the conversion of the radioactive component. These yields are indicated as radiochemical yields (RCY). RCY are calculated as the fraction of the desired ^{18}F-product divided by all ^{18}F-species in the crude reaction mixture. It is important to note that in most cases the final compounds are not isolated, and the radiochemical yield is always calculated based on radioHPLC analysis of the crude reaction mixture. In the case of radiotracers for imaging, it is however crucial to have chemically pure compounds. The crude reaction mixtures are therefore purified either by cartridges (for example C18, silica, ion-exchange) or by semipreparative HPLC (reversed phase). Isolated yields of radiochemical reactions are indicated as activity yields (AY). AY is calculated as the radioactivity of the desired isolated product divided by the starting radioactivity of the radiosynthesis. Reported AY are never decay corrected (see Section 4.2.4). Due to losses in purification and radioactive decay over time, the AY is generally significantly lower than the RCY. It is important to note that activity yields as low as 1% are acceptable for clinical purposes. For example, the method for production

of [^{18}F]Flumazenil in clinics results in an AY of 1% and has been used for clinical studies in humans.

4.2.3 Molar Activity

Other than the choice of radionuclide, an important factor for the quality of a PET image is the molar activity (MA). Molar activity is a descriptor of the isotopic enrichment of a radioactive compound (given as radioactivity per mole, which effectively represents the ratio of non-radioactive isotopologue compared to radioactive isotopologue, Figure 4.2). High molar activity is required for certain applications such as for the imaging of low tissue density targets (e.g. neuroreceptors).[7] Since the separation of two isotopologues is nearly impossible in radiolaboratories, reactions that afford high molar activity products are often desirable. On the other hand, if a specific application requires low molar activity, the radioactive compound can be diluted with the non-radioactive isotopologue. MA can be assessed by injection of a known amount of radioactivity into a UV HPLC. Using a calibration curve, the total amount of compound present in the sample can be determined by integration of the compound peak in the UV trace. Molar activity values are described as radioactivity per mole of compound (e.g. GBq/µmol).



Figure 4.2. Pictorial representation of molar activity.

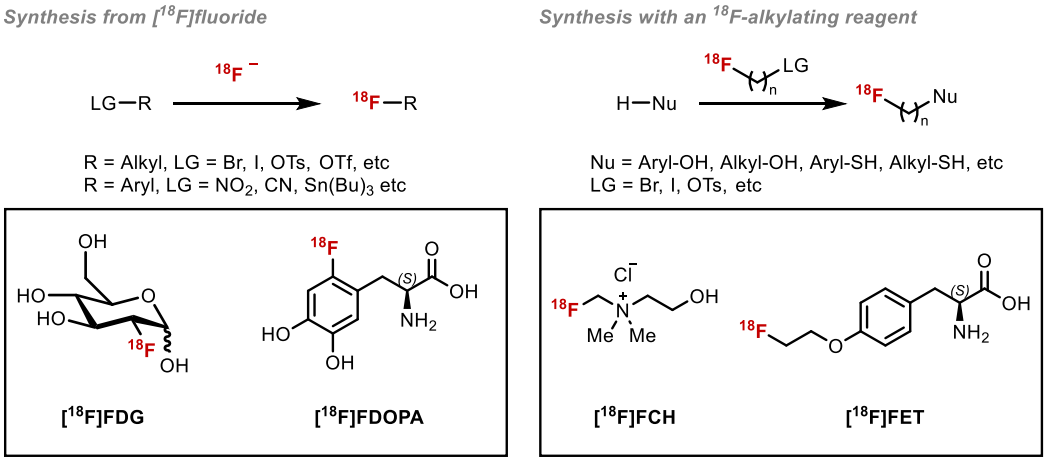
4.2.4 Decay Correction

In order to allow for better comparison between different radiochemistry methods, chemists often perform a decay correction (dc) for specific descriptors. Conventionally, molar activity is decay corrected to the end of synthesis (EoS) timepoint unless otherwise noted. This prevents underestimated molar activity values due to analysis time. Furthermore, radiochemical yields are based on radiochemical conversions, without including a factor for radioactive decay. Therefore, it can always be assumed that radiochemical yields are decay corrected unless otherwise noted. This allows for better comparison of radiochemical processes but should be considered when changing reaction times.

4.3 F-18 Radiochemistry

Due to its favourable physicochemical properties (*vide supra*), F-18 is currently the radionuclide of choice for PET radiochemistry.[6] The synthesis of F-18 containing radiotracers can be broadly divided into two categories: labelling from [^{18}F]fluoride or labelling from an [^{18}F]alkylation reagent (Scheme 4.1). Apart from a few exceptions, these two categories account for all relevant F-18 radiotracers used to date. Common reactions using [^{18}F]fluoride are nucleophilic substitution (mainly

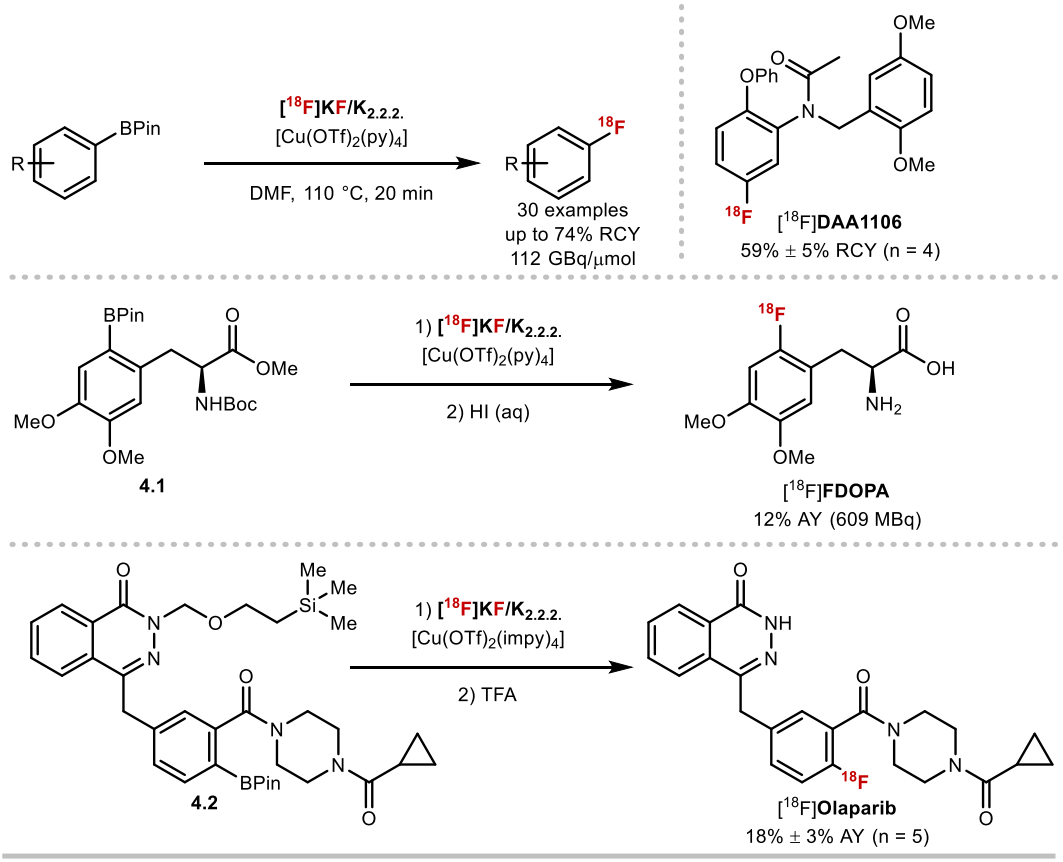
S_N2 and S_NAr), cross-coupling reactions (from aryl stannanes, etc) and isotopic exchange reactions on silicon, boron or aluminium. Relevant radiotracers synthesized from [^{18}F]fluoride are the oncological PET tracer [^{18}F]Fluorodeoxyglucose ([^{18}F]FDG, LG = OTf), and [^{18}F]Fluorodopa ([^{18}F]FDOPA), a tracer of high relevance for the detection of Parkinson disease.[8,9] On the other hand, the field of ^{18}F-fluoroalkylation is mainly focused on alkylation of (thio)phenols and amines with reagents such as [^{18}F]fluorobromomethane, [^{18}F]fluorobromoethane, [^{18}F]fluoroiodomethane, [^{18}F]fluoroiodoethane, [^{18}F]fluoromethyltosylate, [^{18}F]fluoroethyltosylate.[10–12] These reagents are readily available by a simple (pseudo)halogen exchange reaction and can then be used in S_N2 alkylations of nucleophiles. Relevant examples of radiotracers synthesised *via* ^{18}F-fluoroalkylation are the neuro-oncological PET tracer [^{18}F]fluoroethyl-L-tyrosine ([^{18}F]FET) and the oncological PET tracer [^{18}F]fluorocholine ([^{18}F]FCH).[13,14]



Scheme 4.1. Synthesis of ^{18}F-radiotracers from [^{18}F]fluoride or *via* ^{18}F-fluoroalkylation.

In contrast to ^{18}F-fluoroalkylation, radiofluorination reactions from [^{18}F]fluoride have become an increasingly populated field of interest and many developments

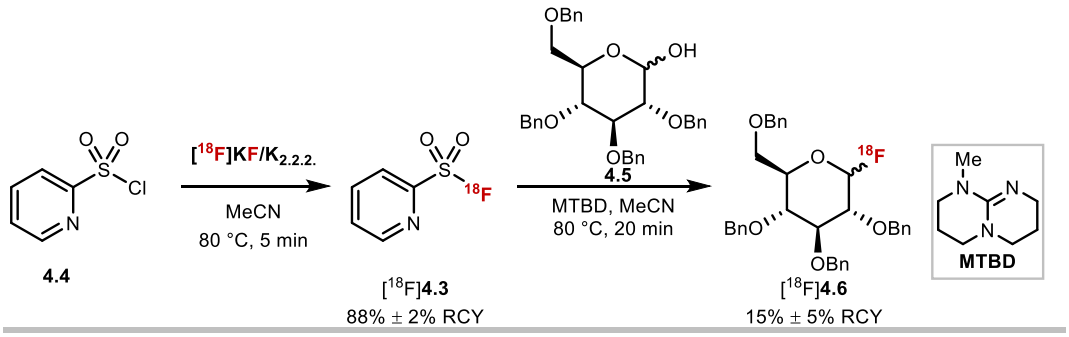
have been made to advance this field.[15,16] A relevant recent contribution to this field is the copper-mediated ^{18}F-fluorination of (hetero)aryl boronic esters reported by Gouverneur and co-workers in 2014 (Scheme 4.2).[16] This reaction allowed for the synthesis of [^{18}F](hetero)aryl fluorides that are hard to access by classical S_NAr chemistry. This method has been used to improve the radiosynthesis of existing radiotracers such as [^{18}F]DAA1106 (one step) and [^{18}F]FDOPA (two steps from **4.1**). More recently, a similar method has been employed for the radiosynthesis of [^{18}F]Olaparib from **4.2**.[17]



Scheme 4.2. Copper-mediated ^{18}F-fluorination of (hetero)aryl boronic esters (n = number of repetitions).

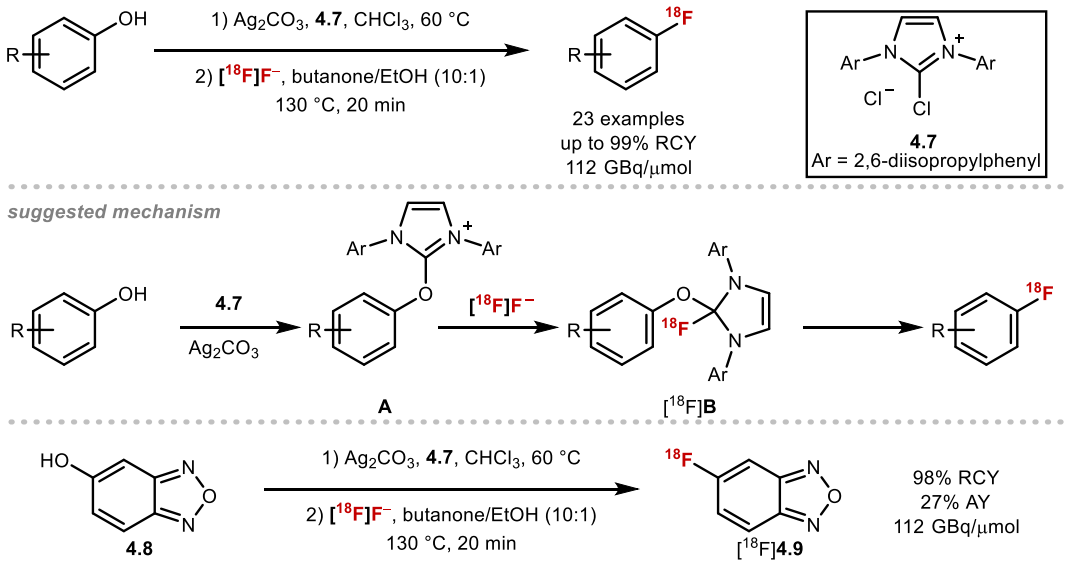
More recently, Doyle and co-workers reported the synthesis and application of [^{18}F]2-pyridinesulfonyl fluoride ([^{18}F]PyFluor, [^{18}F]**4.3**, Scheme 4.3).[18] This reagent

could be synthesised from the corresponding sulfonyl chloride (**4.4**) *via* halogen exchange in high RCY. The authors have demonstrated the use of [^{18}F]**4.3** for the direct ^{18}F-deoxyfluorination of alcohol **4.5** to afford [^{18}F]**4.6** in low RCY. Notably, the radiosynthesis of analogous ^{18}F-1-deoxyfluorinated sugars is underexplored.



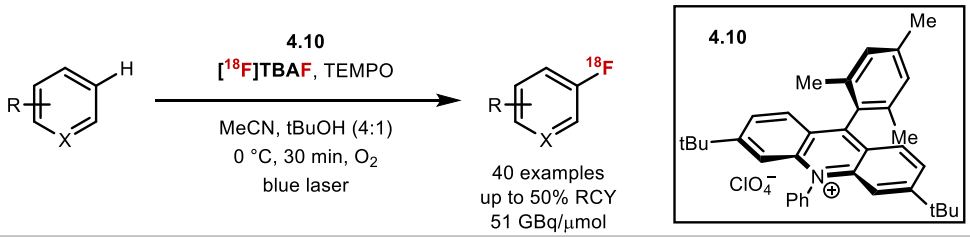
Scheme 4.3. ^{18}F-Deoxyfluorination of alcohols with [^{18}F]PyFluor ([^{18}F]**4.3**). Reactions were performed with n = 3 (n = number of repetitions).

In 2016, Ritter and co-workers reported a direct ^{18}F-deoxyfluorination of phenols (Scheme 4.4).[19] The reaction was demonstrated on a broad range of phenols and the corresponding [^{18}F]aryl fluorides were obtained in excellent RCY. Their method required preformation of a uronium species (**A**) from **4.7** and a phenol, that was then treated with [^{18}F]fluoride to afford intermediate [^{18}F]**B**. Upon heating, [^{18}F]**B** could afford the desired [^{18}F]aryl fluorides in high radiochemical yields. The authors were able to perform the deoxyfluorination of 5-hydroxybenzofurazan (**4.8**) to afford ([^{18}F]**4.9**) in high activity yield and high molar activity (112 GBq/µmol).



Scheme 4.4. ^{18}F-Deoxyfluorination of phenols from [^{18}F]fluoride.

In the past decade, photochemistry has received immense interest. In 2019, Nicewicz, Li and co-workers reported a photocatalytic C-H ^{18}F-fluorination of arenes to merge the fields of photochemistry with F-18 radiochemistry (Scheme 4.5).[15] Their method relies on the oxidation of electron-rich (hetero)arenes using **4.10** as an organophotocatalyst. This method represents an important conceptual advance in the field of ^{18}F-fluorination of arenes as it does not require prefunctionalised starting materials. The reaction was successful on a broad range of (hetero)arenes and a high degree of regiocontrol was observed for most substrates.

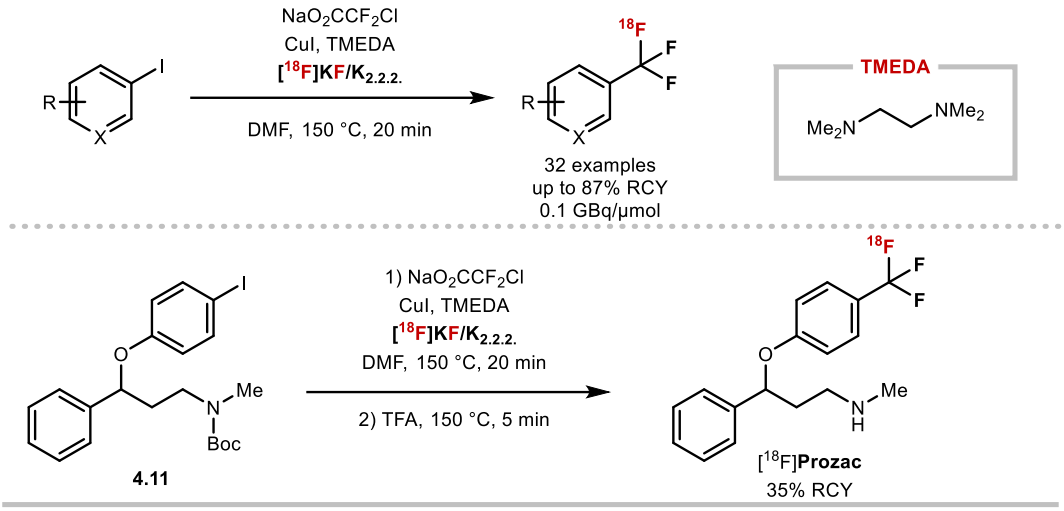


Scheme 4.5. Photocatalytic C-H ^{18}F-fluorination of (hetero)arenes from [^{18}F]fluoride.

4.3.1 New Motifs in F-18 Radiochemistry

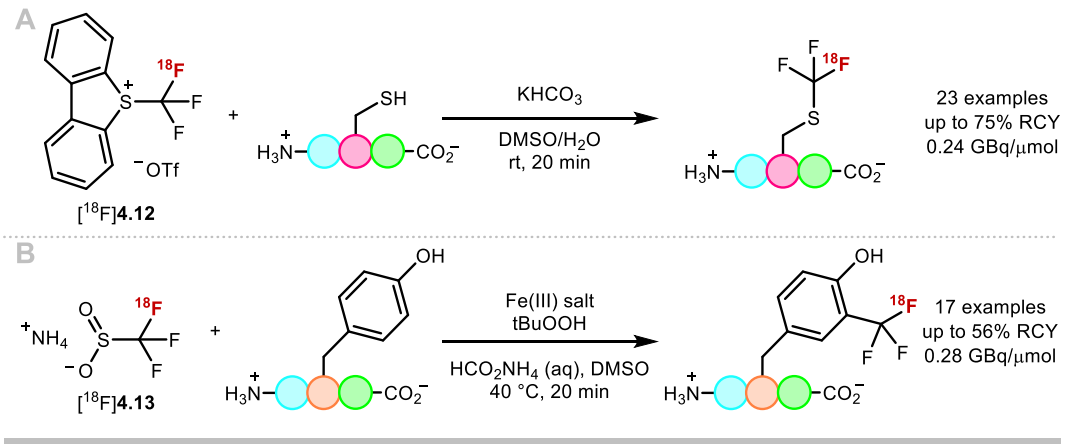
Given the relevance of polyfluorinated groups (mainly the trifluoromethyl and difluoromethyl group) in medicinal chemistry, radiochemists have recently investigated methods to access F-18 isotopologues of these motifs. A general challenge associated with the radiosynthesis of polyfluorinated compounds is the low molar activity obtained. The synthesis of polyfluorinated compounds often requires highly reactive starting materials that are prone to release trace amounts of F-19 fluoride. As a result, isotopic dilution of the radiolabelled products can be observed (low MA), hampering the utility of the final compounds. Furthermore, the synthesis of precursors for these radiosyntheses are often challenging and/or limited in substrate scope.

An early contribution to the field of ^{18}F-trifluoromethylation has been disclosed by Gouverneur and co-workers in 2013, describing the copper-mediated trifluoromethylation of (hetero)aryl iodides (Scheme 4.6).[20] This reaction relied on the *in situ* formation of an [^{18}F]$CuCF_3$ species from [^{18}F]fluoride, which reacted with a range of aryl iodides to afford the corresponding [^{18}F]trifluoromethylarenes in good radiochemical yields albeit in low molar activity (0.1 GBq/µmol). The authors demonstrated the utility of this protocol by the ^{18}F-trifluoromethylation of aryl iodide **4.11** to afford the ^{18}F-isotopologue of the anti-depressant Prozac ([^{18}F]**Prozac**).



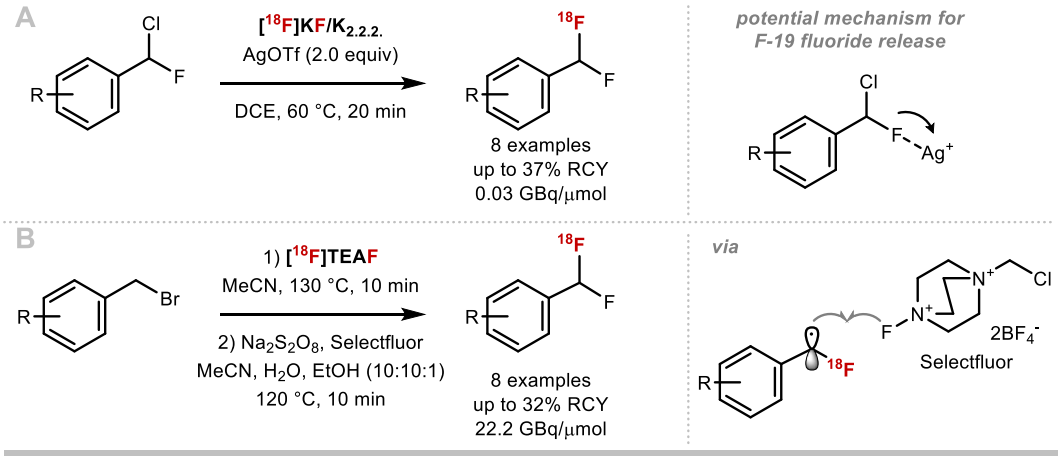
Scheme 4.6. Copper-mediated ^{18}F-trifluoromethylation of aryl iodides from [^{18}F]fluoride.

Building up on this work, Gouverneur and co-workers reported the ^{18}F-trifluoromethylation of cysteine residues in peptides (Scheme 4.7A).[21] This transformation was achieved using an ^{18}F-analogue of the well-known Umemoto reagent ([^{18}F]**4.12**). [^{18}F]**4.12** is an electrophilic ^{18}F-trifluoromethylating reagent that reacts with cysteine residues under basic conditions to afford the corresponding [^{18}F]trifluoromethylthioether in up to 72% RCY. More recently, Gouverneur and co-workers also developed an ^{18}F-analogue of the Langlois reagent ([^{18}F]**4.13**), a radical ^{18}F-trifluoromethylating reagent (Scheme 4.7B).[22] Under oxidizing conditions, [^{18}F]**4.13** efficiently reacts with tyrosine and tryptophan residues of peptides to afford the C-H ^{18}F-trifluoromethylated compounds in high RCY. Due to their different preferential reaction sites, these reagents are complementary and allow the synthesis of various ^{18}F-trifluoromethylated peptides, albeit in low molar activity (0.24 – 0.28 GBq/µmol).



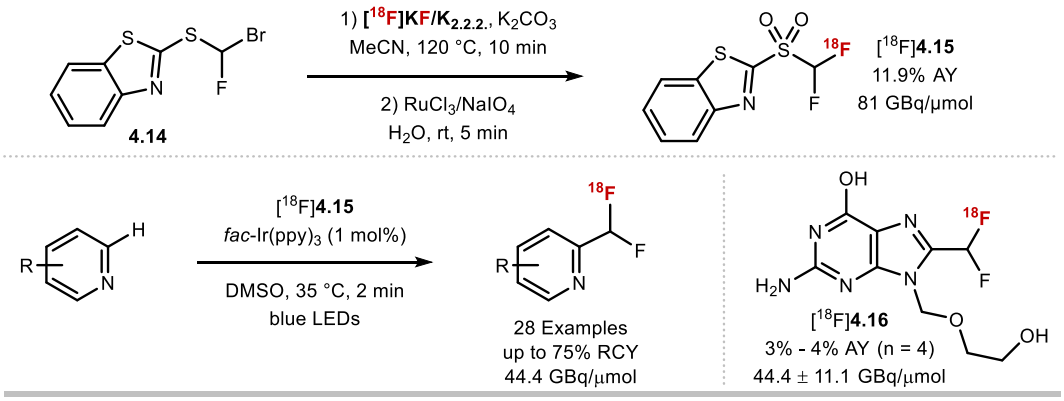
Scheme 4.7. Electrophilic and radical ^{18}F-trifluoromethylation of peptides with [^{18}F]**4.12** and [^{18}F]**4.13**.

In 2016, Gouverneur and co-workers reported a silver-mediated halogen exchange reaction of chlorofluoromethylarenes to the corresponding [^{18}F]difluoromethylarenes (Scheme 4.8A).[23] However, due to partial release of [^{19}F]fluoride from the starting materials, this method suffered from low molar activity. As an alternative to access [^{18}F]difluoromethylarenes in high molar activity, Liang and co-workers developed a two-step process to convert benzyl bromides to the corresponding [^{18}F]difluoromethylarenes (Scheme 4.8B).[24] Since the ^{18}F-halogen exchange reaction is performed on non-fluorinated substrates, no isotopic dilution was observed. The [^{18}F]fluoromethylarenes were then subjected to electrophilic C-H fluorination to obtain [^{18}F]difluoromethylarenes under radical conditions, which resulted in a molar activity of 22.2 GBq/µmol.



Scheme 4.8. Synthesis of [^{18}F]difluoromethylarenes from [^{18}F]fluoride.

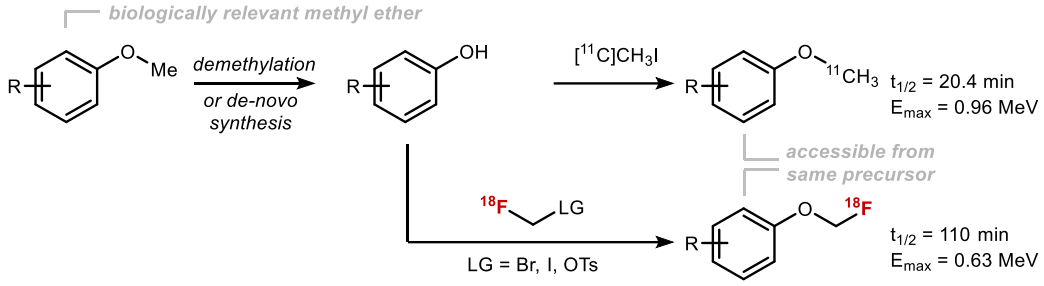
Recently, Genicot, Luxen and co-workers reported the radiosynthesis of an [^{18}F]difluoromethyl sulfone in high MA (Scheme 4.9).[25] The authors showed that bromofluoromethylsulfide **4.14** reacts with [^{18}F]fluoride in the absence of silver additives. Subsequently, they performed a ruthenium-mediated oxidation of the [^{18}F]difluoromethyl sulfide to afford the [^{18}F]difluoromethyl sulfone [^{18}F]**4.15**. The authors reported the use of this reagent for a Minisci-type C-H ^{18}F-difluoromethylation of a broad range of (hetero)arenes. The reaction had a broad functional group tolerance which was demonstrated by the synthesis of [^{18}F]**4.16** from acyclovir. This reaction resulted in very high molar activity (the value was decay corrected to the end of bombardment).



Scheme 4.9. ^{18}F-Difluoromethylation of heteroarenes with [^{18}F]**4.15**. n = number of reactions.

4.3.2. ^{18}F-Fluoroalkylation of Phenols

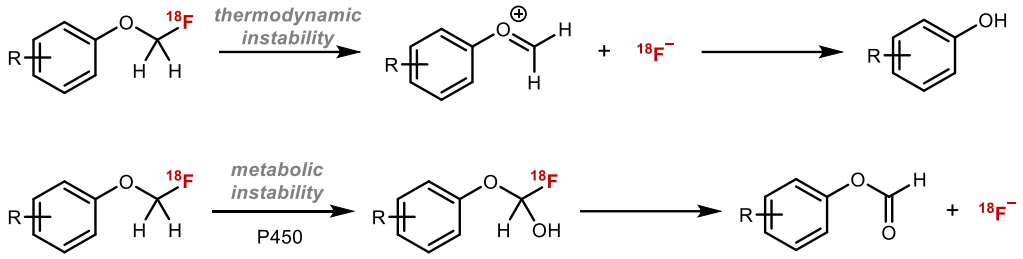
Due to the high prevalence of methoxy(hetero)arenes in biologically relevant compounds, one of the most straightforward ways to radiolabel an isotopologue of a biologically active molecule is treatment of the corresponding phenol with [^{11}C]iodomethane (Scheme 4.10).[26] This strategy has been widely adopted and is generally very robust. However, due to the reasons given in section 4.1.2, when looking for an improved radiotracer, chemists often attempt to introduce F-18 rather than C-11. An obvious strategy to access ^{18}F-fluorinated analogues is the use of [^{18}F]fluoroiodomethane or analogues thereof.[10,11] [^{18}F]fluoroiodomethane is easily accessible from diiodomethane and [^{18}F]fluoride in high MA. Similar procedures have been adopted for the synthesis of [^{18}F]bromofluoromethane and [^{18}F]fluoromethyltosylate. Treatment of the phenol precursor with such a reagent generally results in high RCY of the desired [^{18}F]fluoromethylether.



Scheme 4.10. Radiolabelling of phenols *via* ^{11}C-methylation or ^{18}F-fluoromethylation.

The problem of this strategy is the inherent instability of many [^{18}F]fluoromethyl ethers.[27] Some [^{18}F]fluoromethyl ethers are thermodynamically unstable which results in release of [^{18}F]fluoride and formation of the corresponding phenol after hydrolysis (Scheme 4.11). Furthermore, some [^{18}F]fluoromethyl ethers are metabolically unstable and undergo cytochrome P450-mediated oxidation to

afford thermodynamically unstable [^{18}F]fluorohydroxymethylethers that decompose to the corresponding formate after loss of [^{18}F]fluoride.



Scheme 4.11. Instability of [^{18}F]fluoromethyl ethers.

Release of [^{18}F]fluoride can prove detrimental in PET imaging due to the highly efficient bone uptake of fluoride. This results in problematically high background signals during PET scans. Radiochemists have found two potential solutions for this problem: 1) the use of deuterated [^{18}F]fluoroiodomethane to afford deuterated [^{18}F]fluoromethyl ethers (increased metabolic stability); and 2) the use of ^{18}F-fluoroalkylating reagents with a longer linker (to afford thermodynamically more stable [^{18}F]fluoroethylethers or [^{18}F]fluoropropylethers, Figure 4.3). Such strategies have been used for numerous radiotracers, with two relevant examples being [^{18}F]**FMeNER-D2** and [^{18}F]**FET**.[13,28]

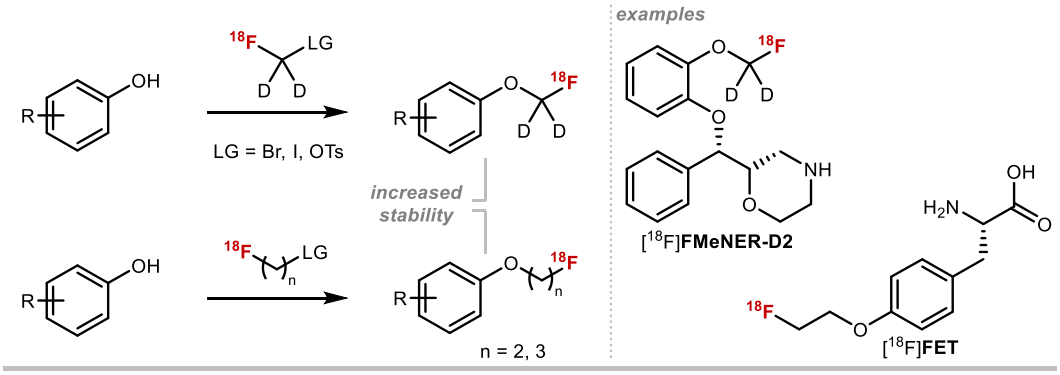
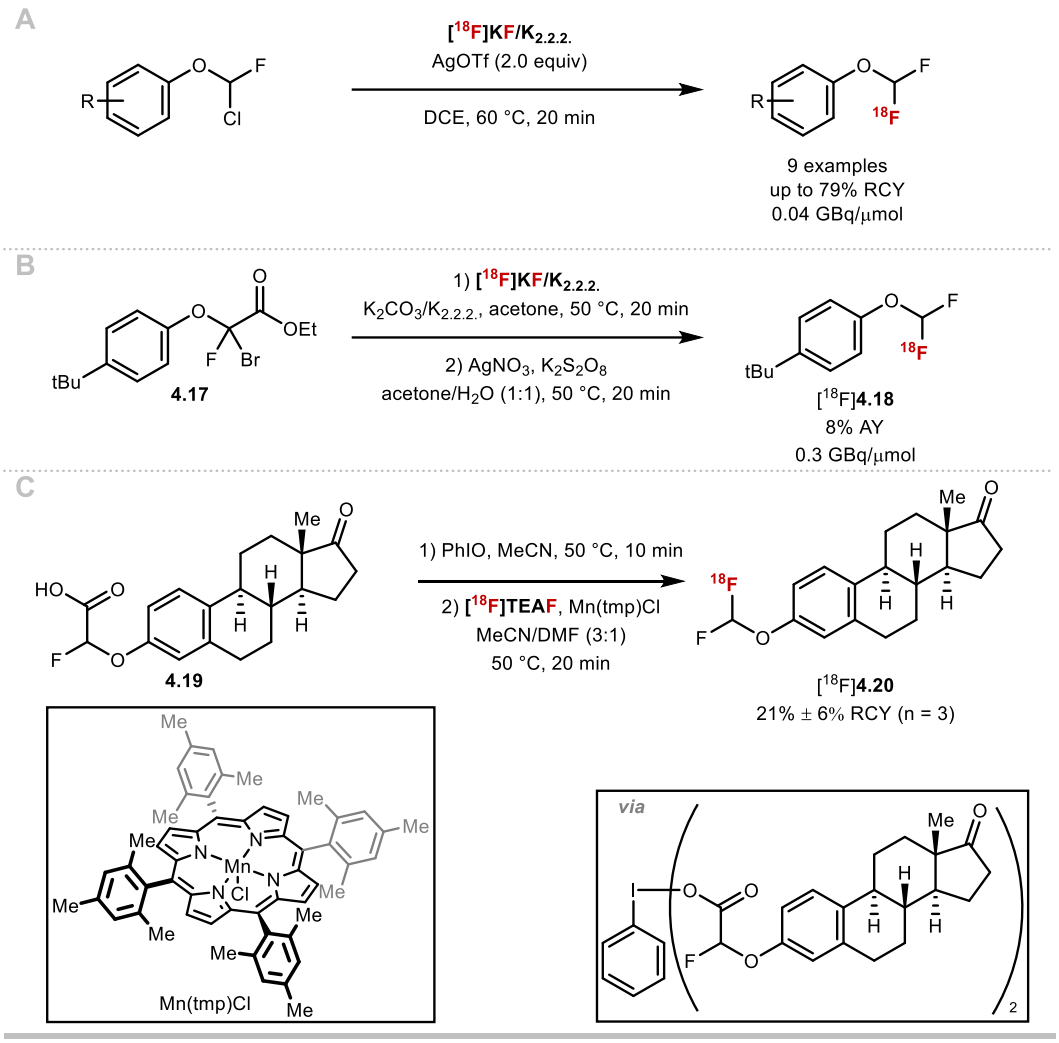


Figure 4.3. Current solutions for the stability problem of [^{18}F]fluoromethylethers.

These two strategies however have several other disadvantages. Deuteration is often ineffective in preventing thermodynamic decomposition of [^{18}F]fluoromethylethers. Alternative use of increased linker lengths results in more steric bulk that can be problematic depending on the compound.

An alternative approach to overcome these limitations is the synthesis of [^{18}F]difluoromethylethers. The introduction of additional fluorine atoms often positively impacts metabolic stability and could therefore prevent decomposition and fluoride release. A first radiosynthesis of [^{18}F]difluoromethylethers was reported by Gouverneur and co-workers in 2015 (Scheme 4.12A).[29] Starting from chlorofluoromethylethers, a silver-mediated halogen exchange reaction afforded the corresponding [^{18}F]difluoromethylethers in high RCY (up to 79% RCY) albeit in low molar activity (0.04 to 0.17 GBq/µmol). More recently, a two-step ^{18}F-fluorination-protodecarboxylation of bromofluoroalkylether **4.17** was shown to yield the corresponding [^{18}F]difluoromethylether [^{18}F]**4.18** in moderate AY (8% starting from [^{18}F]fluoride) and low MA (0.3 GBq/µmol; Scheme 4.12B).[30] An alternative method for the synthesis of [^{18}F]difluoromethylethers was reported by Gouverneur and co-workers in 2019 (Scheme 4.12C).[31] They disclosed an isolated example of decarboxylative ^{18}F-fluorination of fluoroacetatic acid derivative **4.19** to access [^{18}F]*O*-difluoromethyl estrone ([^{18}F]**4.20**) in low RCY.



Scheme 4.12. Radiosynthetic approaches towards [^{18}F]difluoromethylethers.

Whilst these strategies have been demonstrated to yield [^{18}F]difluoromethylethers, they are severely limited by the following factors: requirement for prefunctionalisation of the phenol substrate (and therefore limited accessibility of the starting materials), limited substrate scope and low molar activity. To this end we developed a direct procedure for the ^{18}F-difluoromethylation of readily available phenols to afford the corresponding [^{18}F]difluoromethylethers. This method will be discussed in Chapter 5.

4.4 References

[1] A. Alavi, S. S. Huang, *Cancer Imaging* **2008**, *31*, 39–44.
[2] P. W. Miller, N. J. Long, R. Vilar, A. D. Gee, *Angew. Chemie - Int. Ed.* **2008**, *47*, 8998–9033.
[3] J. J. Vaquero, P. Kinahan, *Annu. Rev. Biomed. Eng.* **2015**, *17*, 385–414.
[4] M. Conti, L. Eriksson, *EJNMMI Phys.* **2016**, *3*, DOI 10.1186/s40658-016-0144-5.
[5] T. C. Wilson, T. Cailly, V. Gouverneur, *Chem. Soc. Rev.* **2018**, *47*, 6990–7005.
[6] S. Preshlock, M. Tredwell, V. Gouverneur, *Chem. Rev.* **2016**, *116*, 719–766.
[7] M. Sergeev, M. Lazari, F. Morgia, J. Collins, M. R. Javed, O. Sergeeva, J. Jones, M. E. Phelps, J. T. Lee, P. Y. Keng, R. M. van Dam, *Commun. Chem.* **2018**, *1*, 1–10.
[8] A. d'Amico, *Radiol. Medica* **2015**, *120*, 345–351.
[9] F. Somme, L. Bender, I. J. Namer, G. Noël, C. Bund, *Cancer Imaging* **2020**, *20*, 1–13.
[10] L. Zheng, M. S. Berridge, *Appl. Radiat. Isot.* **2000**, *52*, 55–61.
[11] T. R. Neal, S. Apana, M. S. Berridge, *J. Label. Compd. Radiopharm.* **2005**, *48*, 557–568.
[12] T. Kniess, M. Laube, P. Brust, J. Steinbach, *Medchemcomm* **2015**, *6*, 1714–1754.
[13] M. Hutterer, M. Nowosielski, D. Putzer, N. L. Jansen, C. Fouge, M. Seiz, M. Schocke, M. McCoy, G. Go, I. J. Virgolini, E. Trinka, A. H. Jacobs, G. Göbel, C. La Fougère, I. J. Virgolini, E. Trinka, A. H. Jacobs, G. Stockhammer, *Neuro. Oncol.* **2013**, *15*, 341–351.
[14] M. H. Poulsen, K. Bouchelouche, P. F. Høilund-Carlsen, H. Petersen, O. Gerke, S. I. Steffansen, N. Marcussen, N. Svolgaard, W. Vach, U. Geertsen, S. Walter, *BJU Int.* **2012**, *110*, 1666–1671.
[15] W. Chen, Z. Huang, N. E. S. Tay, B. Giglio, M. Wang, H. Wang, Z. Wu, D. A. Nicewicz, Z. Li, *Science (80-.).* **2019**, *364*, 1170–1174.
[16] M. Tredwell, S. M. Preshlock, N. J. Taylor, S. Gruber, M. Huiban, J. Passchier, J. Mercier, C. Génicot, V. Gouverneur, *Angew. Chemie - Int. Ed.* **2014**, *53*, 7751–7755.
[17] T. C. Wilson, M. A. Xavier, J. Knight, S. Verhoog, J. B. Torres, M. Mosley, S. L. Hopkins, S. Wallington, P. D. Allen, V. Kersemans, R. Hueting, S. Smart, V. Gouverneur, B. Cornelissen, *J. Nucl. Med.* **2019**, *60*, 504–510.
[18] M. K. Nielsen, C. R. Ugaz, W. Li, A. G. Doyle, *J. Am. Chem. Soc.* **2015**, *137*, 9571–9574.
[19] C. N. Neumann, J. M. Hooker, T. Ritter, *Nature* **2016**, *534*, 369–373.
[20] M. Huiban, M. Tredwell, S. Mizuta, Z. Wan, X. Zhang, T. L. Collier, V. Gouverneur, J. Passchier, *Nat. Chem.* **2013**, *5*, 941–944.
[21] S. Verhoog, C. W. Kee, Y. Wang, T. Khotavivattana, T. C. Wilson, V. Kersemans, S. Smart, M. Tredwell, B. G. Davis, V. Gouverneur, *J. Am. Chem. Soc.* **2018**, *140*, 1572–1575.
[22] C. W. Kee, O. Tack, F. Guibbal, T. C. Wilson, P. G. Isenegger, M. Imiołek, S. Verhoog, M. Tilby, G. Boscutti, S. Ashworth, J. Chupin, R. Kashani, A. W. J. Poh, J. K. Sosabowski, S. Macholl, C. Plisson, B. Cornelissen, M. C. Willis, J. Passchier, B. G. Davis, V. Gouverneur, *J. Am. Chem. Soc.* **2020**, *142*, 1180–1185.
[23] S. Verhoog, L. Pfeifer, T. Khotavivattana, S. Calderwood, T. L. Collier, K. Wheelhouse, M. Tredwell, V. Gouverneur, *Synlett* **2016**, *27*, 25–28.
[24] H. Shi, A. Braun, L. Wang, S. H. Liang, N. Vasdev, T. Ritter, *Angew. Chemie - Int. Ed.* **2016**, *55*, 10786–10790.
[25] L. Trump, A. Lemos, B. Lallemand, P. Pasau, J. Mercier, C. Lemaire, A. Luxen, C. Genicot, *Angew. Chemie - Int. Ed.* **2019**, *58*, 13149–13154.
[26] P. Larsen, J. Ulin, K. Dahlstrøm, M. Jensen, *Appl. Radiat. Isot.* **1997**, *48*, 153–157.
[27] M. Kuchar, C. Mamat, *Molecules* **2015**, *20*, 16186–16220.
[28] C. Rami-Mark, M. R. Zhang, M. Mitterhauser, R. Lanzenberger, M. Hacker, W. Wadsak, *Nucl. Med. Biol.* **2013**, *40*, 1049–1054.
[29] T. Khotavivattana, S. Verhoog, M. Tredwell, L. Pfeifer, S. Calderwood, K. Wheelhouse, T. Leecollier, V. Gouverneur, *Angew. Chemie - Int. Ed.* **2015**, *54*, 9991–9995.
[30] T. Khotavivattana, S. Calderwood, S. Verhoog, L. Pfeifer, S. Preshlock, N. Vasdev, T. L. Collier, V. Gouverneur, *Org. Lett.* **2017**, *19*, 568–571.
[31] J. B. I. Sap, T. C. Wilson, C. W. Kee, N. J. W. Straathof, C. W. a. Ende, P. Mukherjee, L. Zhang, C. Genicot, V. Gouverneur, *Chem. Sci.* **2019**, *10*, 3237–3241.

Chapter 5 – [^{18}F]Difluorocarbene Unlocks New Motifs for F-18 Radiochemistry

The work discussed in this chapter is unpublished to date.

Author contributions: Claudio Meyer, Dr. Jeroen Sap and Prof. Véronique Gouverneur conceived the project. Claudio Meyer investigated the chlorofluorocarbene halogen exchange reaction. Claudio Meyer performed all ^{19}F-experiments with $PhSO_2CF_2H$ and 4-*t*Bu-$PhSO_2CF_2H$ unless otherwise noted. Jeroen Sap prepared the precursor for the synthesis of [^{18}F]4-*t*Bu-$PhSO_2CF_2H$. Dr. Natan Straathof and Dr. Jeroen Sap performed the first radiosynthesis of [^{18}F]4-*t*Bu-$PhSO_2CF_2H$, which was further optimised by Claudio Meyer and Dr. Jeroen Sap. Claudio Meyer and Dr. Jeroen Sap performed all further F-18 experiments. Precursors for radiolabelling were synthesised by Claudio Meyer, Dr. Jeroen Sap and Sandrine Hell or provided by Dr. Andrés Trabanco (Janssen, ES) and Dr. Christopher Am Ende (Pfizer, US). Claudio Meyer, Dr. Jeroen Sap and Sandrine Hell synthesised the ^{19}F references. Claudio Meyer, Dr. Jeroen Sap and Dr. Natan Straathof wrote the automation procedure with the help of Dr. Matthew Tredwell.

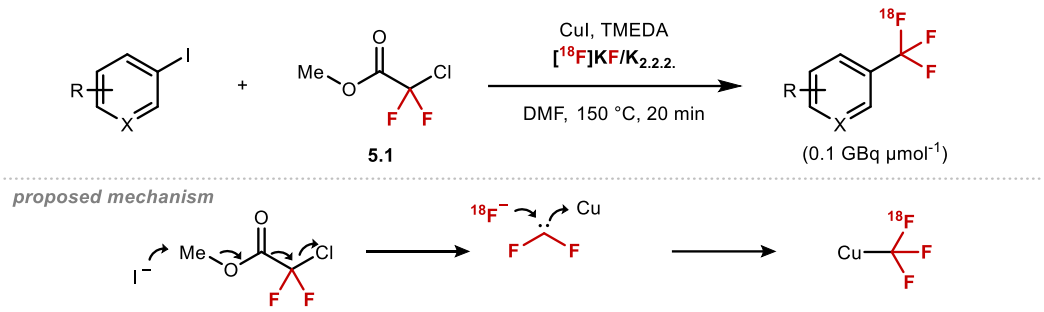
5.1 Introduction

5.1.1 Aim of this Project

PET has played an instrumental role in medical imaging, as well as drug discovery and development. In recent years, an impressive range of reactions that enable C(sp^2)-^{18}F radiofluorination from a variety of precursors have been developed. However, methods which can access equally desirable [^{18}F]fluoroalkyl motifs remain underdeveloped. Although the use of native functional groups (for example, (thio)alcohols and amines) has allowed facile access to these moieties *via* S_N2 alkylation chemistry, considerable limitations still exist. As such, alternative technologies that combat the problems of metabolic and thermodynamic stability traditionally associated with [^{18}F]fluoromethyl ethers have long been sought after. A general and widely applicable platform for the preparation of more stable [^{18}F]difluoromethyl ethers has up to this point not been realised. A key challenge to overcome is the low molar activity observed in many radiochemistry methods addressing polyfluorinated motifs. Herein, the first fully-automated radiosynthesis of an [^{18}F]difluorocarbene reagent to access [^{18}F]difluoromethyl (thio)ethers is described. Harnessing the chemistry of [^{18}F]difluorocarbene unlocks a wide selection of medicinally relevant [^{18}F]difluoromethyl motifs for applications in PET radiochemistry. Biologically relevant molecules and radiotracer analogues readily underwent site-selective ^{18}F-difluoromethylation in a single step, through the functionalisation of innate or easy-to-install reactive handles such as (thio)phenols and *N*-heterocycles.

5.1.2 Difluorocarbene in F-18 Radiochemistry

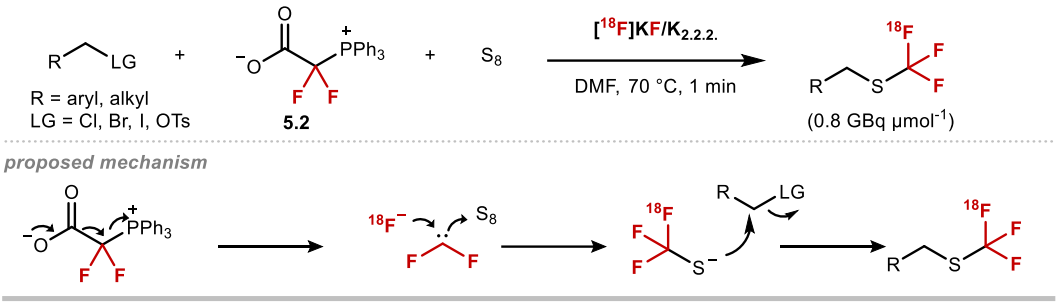
Difluorocarbene has recently found application in the realm of F-18 radiochemistry. Gouverneur, Passchier and co-workers demonstrated that the reaction of difluorocarbene (generated from methyl chlorodifluorocaetate (**5.1**)) and [^{18}F]fluoride results in the formation of [^{18}F]CF_3^- (Scheme 5.1).[1] This intermediate was trapped with copper and the resulting [^{18}F]$CuCF_3$ species was used for the ^{18}F-trifluoromethylation of aryl iodides. This method represents the first example of difluorocarbene being used for radiochemistry method development and the products obtained are of high relevance to PET radiochemists. A limitation that remains unsolved however, is the low molar activity associated with these processes (MA = 0.1 GBq µmol^{-1}).



Scheme 5.1. Copper-mediated ^{18}F-trifluoromethylation of aryl iodides from [^{18}F]fluoride.

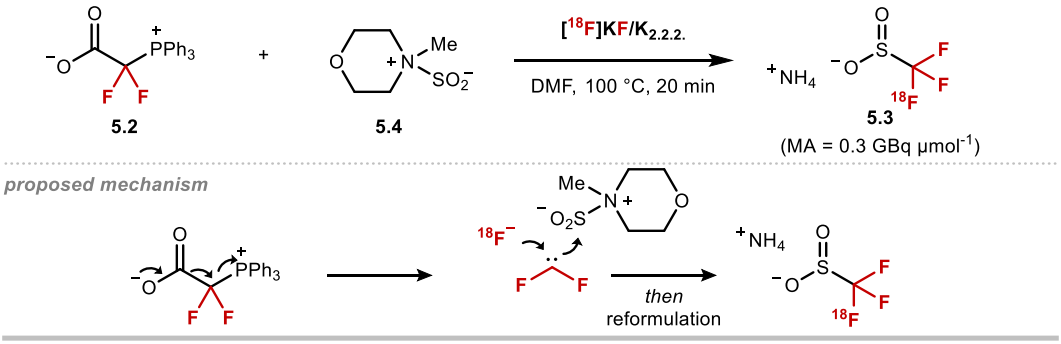
More recently, a similar strategy was adopted by Xiao, Liang and co-workers for the ^{18}F-trifluoromethylthiolation of alkyl halides (Scheme 5.2).[2] In this transformation, [^{18}F]fluoride reacts with difluorocarbene (generated from 2-(triphenylphosphonium)-2,2-difluoroacetate (**5.2**)) and elemental sulfur to afford [^{18}F]SCF_3^-, which is an efficient intermediate for the nucleophilic substitution of alkyl halides to afford [^{18}F]trifluoro thioethers. This reaction was applied to a broad range of primary alkyl halide substrates and generally resulted in high RCY.

However, the molar activity of a model trifluoromethyl thioether was low (MA = 0.8 GBq µmol^{-1}).



Scheme 5.2. ^{18}F-Trifluoromethylthiolation of alkyl halides.

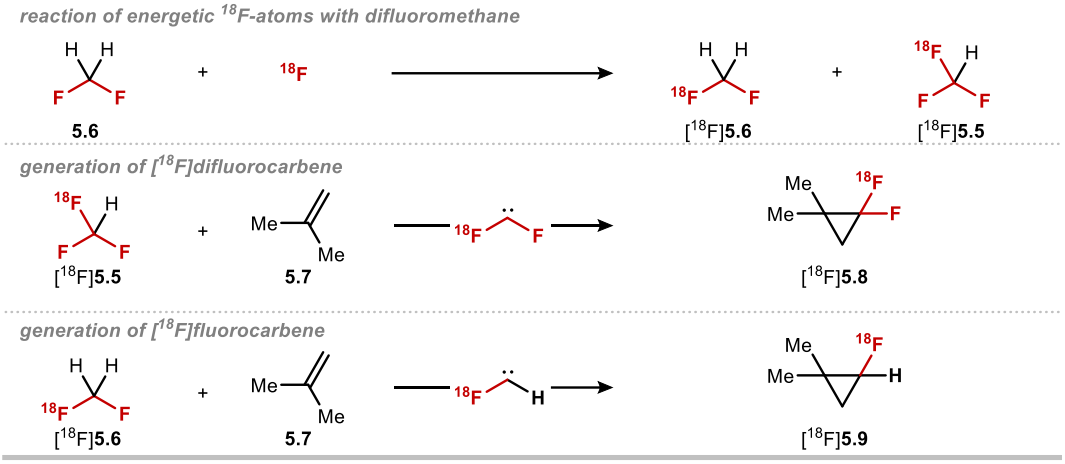
Gouverneur and co-workers recently used an analogous strategy for the synthesis of [^{18}F]ammonium trifluoromethanesulfinate (**5.3**) (Scheme 5.3).[3] This synthesis relied on the reaction of [^{18}F]fluoride with difluorocarbene (also generated from **5.2**) and the sulfur dioxide adduct of *N*-methylmorpholine (**5.4**). The [^{18}F]trifluoromethanesulfinate was employed for the direct trifluoromethylation of native amino acid residues in peptides. However, this reaction did not provide a solution for the low molar activity observed amongst radiosyntheses of polyfluorinated F-18 motifs (MA = 0.3 GBq µmol^{-1}).



Scheme 5.3. Synthesis of [^{18}F]ammonium trifluoromethanesulfinate (**5.3**).

5.2 Generation of [^{18}F]Difluorocarbene and [^{18}F]Fluorocarbene

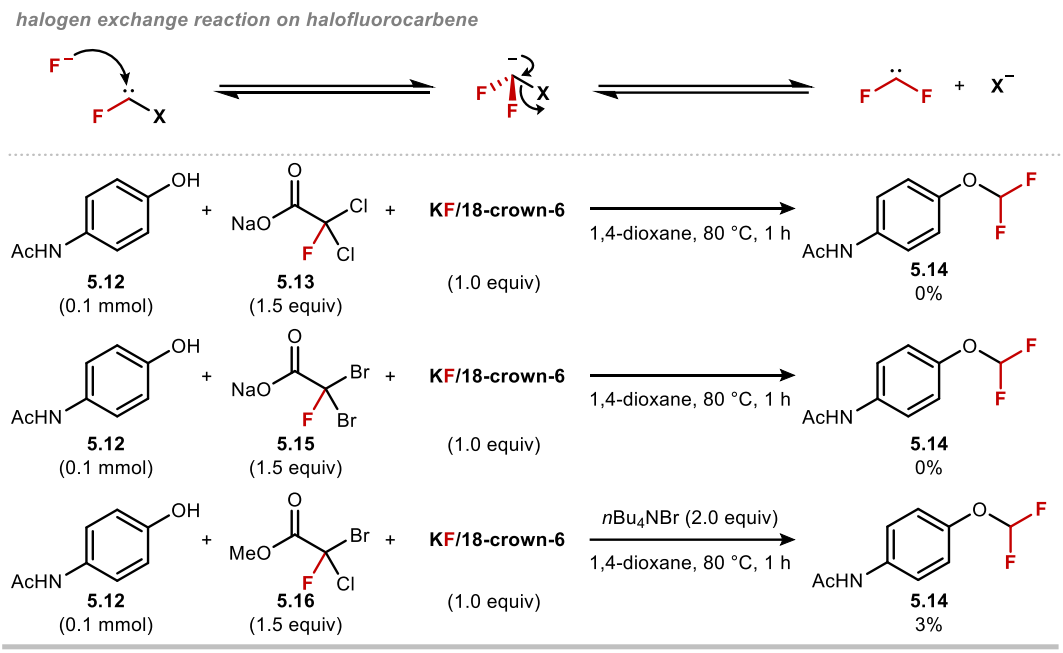
An early report by Tang, Smail and Rowland from 1968, reported the generation of [^{18}F]difluorocarbene ([^{18}F]DFC) from [^{18}F]fluoroform ([^{18}F]**5.5**) and [^{18}F]fluorocarbene from [^{18}F]difluoromethane ([^{18}F]**5.6**) (Scheme 5.4).[4,5] Bombardment of difluoromethane (**5.6**) with neutrons affords energetic ^{18}F-atoms that can in turn react with difluoromethane. This reaction affords [^{18}F]difluoromethane ([^{18}F]**5.6**) (exchange with fluorine) and [^{18}F]fluoroform ([^{18}F]**5.5**) (exchange with hydrogen). The latter has been shown to release [^{18}F]difluorocarbene, which was trapped with isobutylene (**5.7**) to afford [^{18}F]difluorocyclopropane [^{18}F]**5.8**. [^{18}F]Difluoromethane ([^{18}F]**5.6**) released [^{18}F]fluorocarbene, that was scavenged with isobutylene (**5.7**) to afford fluorocyclopropane [^{18}F]**5.9**. Other alkenes, such as propylene (**5.10**) and 2-butene (**5.11**) were less efficient in trapping [^{18}F]DFC under the reported conditions. Due to the harsh conditions of these experiments, this strategy was not further pursued in F-18 method development. Furthermore, as this radiosynthesis is based on an isotopic exchange reaction, the molar activity is expected to be low.



Scheme 5.4. First report of [^{18}F]DFC from [^{18}F]**5.5** and [^{18}F]fluorocarbene from [^{18}F]**5.6**.

5.2.1 *In Situ* Fluorination of Halofluorocarbene

Building on previous work, the halogen exchange reaction of fluoride with a halofluorocarbene to generate [^{18}F]difluorocarbene was investigated (Scheme 5.5). This strategy would directly use [^{18}F]fluoride rather than relying on the synthesis of a [^{18}F]difluorocarbene reagent. Initial experiments focused on the reaction of phenol **5.12** with sodium dichlorofluoroacetate (**5.13**), a chlorofluorocarbene precursor, and potassium fluoride in 1,4-dioxane. A crown ether (18-crown-6) was added to improve the solubility of fluoride in the organic solvent. However, after running the reaction at 80 °C for one hour, the desired difluoromethyl ether **5.14** was not formed. Similarly, when the bromofluorocarbene precursor sodium dibromofluoroacetate (**5.15**) was used under analogous reaction conditions, the desired difluoromethyl ether was not formed and the phenol remained unreacted.

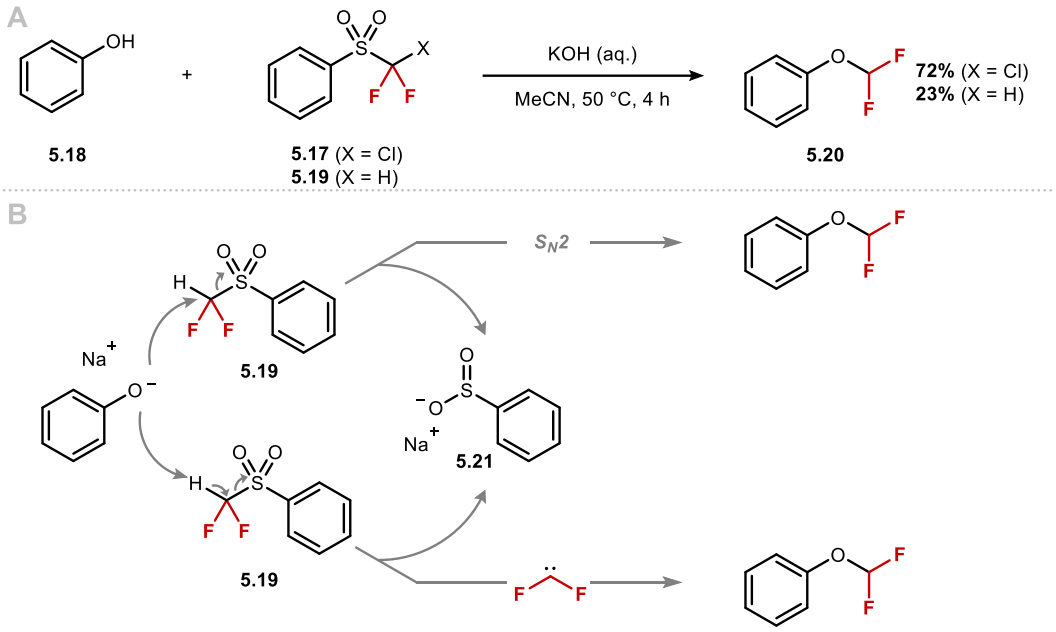


Scheme 5.5. Generation of difluorocarbene from fluoride and halofluorocarbene precursors.

However, when methyl bromochlorofluoroacetate (**5.16**), a more reactive chlorofluorocarbene precursor, was treated with phenol **5.12**, potassium fluoride, 18-crown-6 and tetrabutyl ammonium bromide in 1,4-dioxane at 80 °C for one hour, the corresponding difluoromethyl ether **5.14** was observed in low yield according to quantitative ^{19}F NMR spectroscopy. Due to the low yield of these reactions, further investigations focused on an alternative strategy, relying on a [^{18}F]difluorocarbene reagent.

5.2.2 $PhSO_2CF_2H$ as a Difluorocarbene Reagent

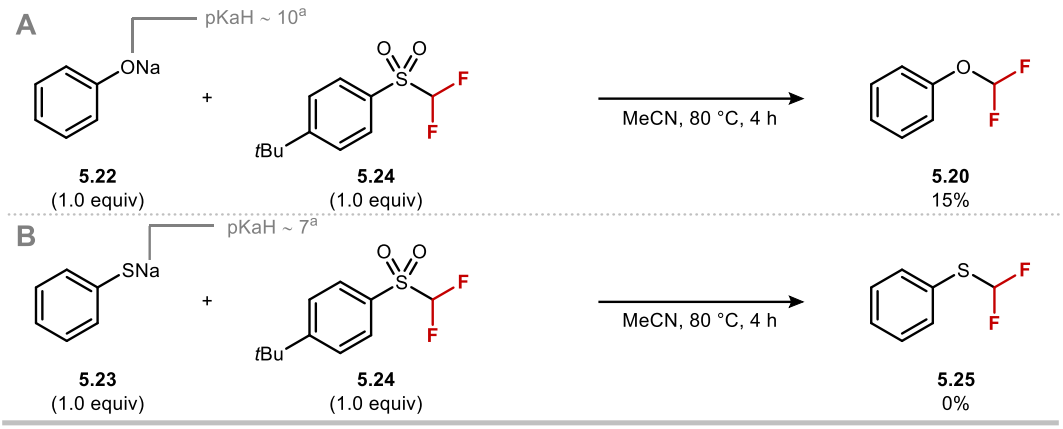
Recently, Hu and co-workers disclosed the use of phenyl chlorodifluoromethyl sulfone (**5.17**) for the difluoromethylation of phenol **5.18** (Scheme 5.6A).[6]



Scheme 5.6. a) Synthesis of difluoromethyl ethers with difluoroalkylsulfones. b) Potential mechanisms for the difluoromethylation of **5.18** with **5.19**.

In their optimisation studies, phenyl difluoromethyl sulfone (**5.19**) was shown to be a competent reagent for this transformation. However, the authors did not investigate the mechanism of this process. The reaction might either follow an S_N2 pathway or proceed *via* a difluorocarbene mechanism. Either case would afford the desired difluoromethyl ether (**5.20**) and result in the release of sodium benzenesulfinate (**5.21**) (Scheme 5.6B).

To investigate this reaction mechanism, sodium phenoxide (**5.22**) and sodium thiophenolate (**5.23**) were reacted independently with a difluoromethyl sulfone reagent (**5.24**) (Scheme 5.7). When equimolar amounts of phenoxide **5.22** and sulfone **5.24** were reacted, the corresponding difluoromethyl ether **5.20** was observed in low yield (Scheme 5.7A). In contrast, the reaction of thiophenolate **5.23** and sulfone reagent **5.24** failed to afford the corresponding difluoromethyl thioether **5.25** under the same conditions (Scheme 5.7B).



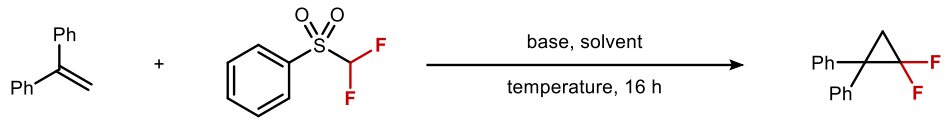
Scheme 5.7. Control experiment: reaction of a) sodium phenoxide and b) sodium thiophenolate with sulfone **5.24**. [a]pKa value of (thio)phenol in water.

Sodium phenoxide (**5.22**) is a stronger base (pKa(PhOH) ~ 10.0 in water) than sodium thiophenolate (**5.23**, pKa(PhSH) ~ 7.0 in water). The proposed carbene mechanism (Scheme 5.6B), is initiated by deprotonation of the difluoromethyl sulfone **5.24**. Therefore, the successful difluoromethylation of the more basic sodium phenoxide and the unsuccessful difluoromethylation of less basic sodium thiophenolate, supports a difluorocarbene mechanism, initiated by deprotonation of difluoromethyl sulfone **5.24**.

Difluorocyclopropanation reactions are typically performed *via* the addition of difluorocarbene to an alkene. To demonstrate that phenyl difluoromethyl sulfone indeed is a difluorocarbene precursor, the difluorocyclopropanation of 1,1-diphenylethylene (**5.26**) to afford difluorocyclopropane **5.27** was investigated. The reactions were analysed by quantitative ^{19}F NMR spectroscopy using *α,α,α*-trifluorotoluene as an internal standard. The desired product shows a characteristic triplet peak in ^{19}F NMR spectroscopy (coupling to the cyclopropane methylene protons; $\delta_{(ppm)}$ -130 (t, $^{3}J_{H\text{-}F}$ = 8.7 Hz)). An initial reaction was performed with sodium hydride (60% in mineral oil) as a base and toluene as a high boiling

non-polar solvent. However, after 16 hours reaction time, the quantitative ^{19}F NMR spectrum of the crude reaction mixture showed unreacted difluoromethyl sulfone **5.19** (Table 5.1, entry 1). This lack of reactivity might be due to two reasons: either the deprotonation and consecutive *α*-elimination to release difluorocarbene does not occur at this temperature, or the release of difluorocarbene is reversible. The reaction of sodium benzenesulfinate with difluorocarbene has been reported.[7] Due to the high electrophilicity of difluorocarbene and the low nucleophilicity of alkenes, difluorocyclopropanation reactions typically require harsh reaction conditions and are performed at elevated temperatures.[7,8] Therefore, a high boiling solvent (propylene carbonate) was used, and the reaction was run at 200 °C for 16 hours, which resulted in the formation of the difluorocyclopropane **5.27** in low yield (entry 2).

Table 5.1. Difluorocyclopropanation of 1,1-diphenylethylene with phenyl difluoromethyl sulfone.[a]



5.26 (5.0 equiv) **5.19** (1.0 equiv) **5.27**

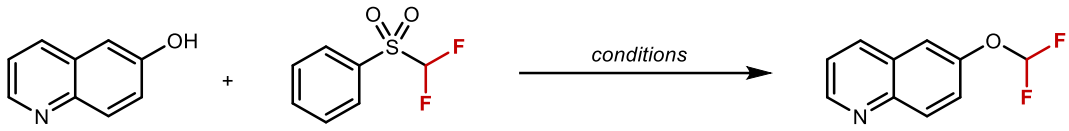
entry	base/additive	solvent	temperature	yield
1	NaH	toluene	110 °C	0%
2	NaH	propylene carbonate	200 °C	14%
3	NaOH	propylene carbonate	200 °C	20%
4	K_2CO_3	propylene carbonate	200 °C	6%

[a]Reaction conditions: **5.26** (0.5 mmol), base (0.11 mmol), solvent (5.0 mL), **5.19** (0.1 mmol), 110 - 200 °C, 16 h. Yield determined *via* quantitative ^{19}F NMR spectroscopy of the crude mixture using *α*,*α*,*α*-trifluorotoluene as an internal standard.

Further experiments showed that other bases such as sodium hydroxide and potassium carbonate also afforded the difluorocyclopropane **5.27** albeit in low yield (entries 3, 4).

Next, the difluoromethylation of a model phenol (6-hydroxyquinoline, **5.18b**) was optimised with phenyl difluoromethyl sulfone (**5.19**) as difluorocarbene reagent. Difluoromethyl ethers show a characteristic doublet in ^{19}F NMR spectroscopy ($\delta_{(ppm)}$ -80 (d, $^{2}J_{H\text{-}F}$ ~ 75 Hz)), coupling to the CF_2H proton. After the given reaction time, trifluoroacetic acid was added to the crude mixture as an internal standard and the reaction was analysed by quantitative ^{19}F NMR spectroscopy. The conditions disclosed by Hu and co-workers[6] (Table 5.2, entry 1) afforded the difluoromethyl ether **5.20b** in 8% yield after 4 hours. When the reaction time was increased to 18 hours, **5.20b** was formed in 24% yield (entry 2). When the reaction was performed at higher temperature (80 °C) with a reaction time of 4 hours, the yield was significantly increased to 55% (entry 3). Performing the reaction at 80 °C for 18 hours increased the yield of the difluoromethyl ether **5.20b** to 63% (entry 4). Notably, reducing the excess of difluoromethyl sulfone **5.19** to equimolar amounts still afforded the desired difluoromethyl ether **5.20b** in moderate yield (entry 5). When the reaction was performed in deuterated water, the yield decreased to 42%, and the product **5.20b** showed 38% deuterium incorporation (entry 6). Running the reaction in fully deuterated solvents (D_2O and [D_3]MeCN) resulted in similar yield (41%) albeit with 96% deuterium incorporation in the product (entry 7).

Table 5.2. Optimisation of the difluoromethylation of phenol **5.18b**.[a]



5.18b (1.0 equiv) **5.19** (mmol) **5.20b**

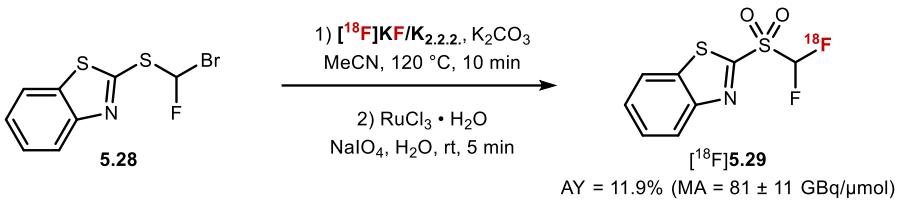
entry	solvent	XY	base	temperature	time	yield
1	MeCN	2.3 equiv	KOH (30% in H_2O)	50 °C	4 h	8%
2	MeCN	2.3 equiv	KOH (30% in H_2O)	50 °C	18 h	24%
3	MeCN	2.3 equiv	KOH (30% in H_2O)	80 °C	4 h	55%
4	MeCN	2.3 equiv	KOH (30% in H_2O)	80 °C	18 h	63%
5	MeCN	1.0 equiv	KOH (30% in H_2O)	80 °C	18 h	41%
6	MeCN	2.3 equiv	KOH (30% in D_2O)	80 °C	18 h	42%[b]
7	[D_3]MeCN	2.3 equiv	KOH (30% in D_2O)	80 °C	18 h	41%[c]

[a]Reaction conditions: **5.18b** (0.25 mmol), KOH (30% aq, 500 µL), MeCN (1.75 mL), **5.19** (given mmol), 50 - 80 °C, 4 – 18 h. Yield determined *via* quantitative ^{19}F NMR spectroscopy of the crude mixture using trifluoroacetic acid as an internal standard. [b]The product showed 38% deuterium incorporation (determined by quantitative ^{19}F NMR spectroscopy); experiment performed by Dr. Jeroen Sap. [c]The product showed 96% deuterium incorporation (determined by quantitative ^{19}F NMR spectroscopy); experiment performed by Dr. Jeroen Sap.

5.2.3 Radiosynthesis of [^{18}F]4-*t*Bu-PhSO$_2$CF$_2$H

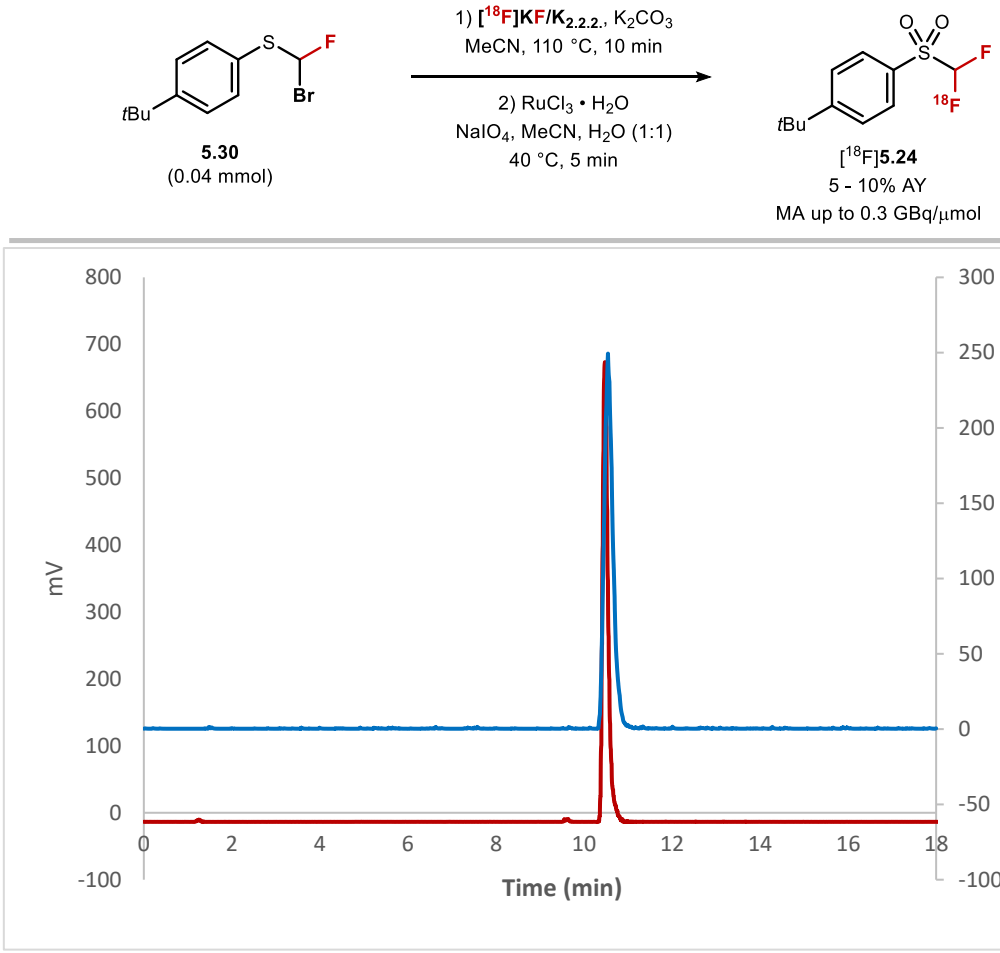
Encouraged by these preliminary results, the synthesis of an [^{18}F]difluoromethyl sulfone reagent was investigated. In 2019, Luxen, Genicot and co-workers reported the synthesis of an [^{18}F]difluoromethyl benzothiazole sulfone reagent (Scheme 5.8).[9] The reaction of heteroaryl bromofluoromethyl sulfide **5.28** with [^{18}F]fluoride and Kryptofix® 222 (to enhance the solubility of [^{18}F]fluoride in acetonitrile), followed by ruthenium-mediated oxidation afforded the desired [^{18}F]difluoromethyl sulfone [^{18}F]**5.29** in high molar activity (81 ± 11 GBq µmol^{-1}). This result is remarkable, as it is the first example for the synthesis of the [^{18}F]difluoromethyl group in high molar activity.[10–14] Notably, the molar activity

value was decay corrected to the end of [^{18}F]fluoride production (end of bombardment), a factor that has to be taken into account when comparing to other molar activity values (conventionally decay corrected to the end of synthesis).



Scheme 5.8. High molar activity synthesis of a ^{18}F-sulfone reagent as reported by Luxen, Genicot and co-workers.

These conditions were adapted for the synthesis of a different sulfone reagent ([^{18}F]**5.24**; Scheme 5.9). To reduce the volatility of the reagent, a *tert*-butyl group was installed at the *para*-position of the phenyl group. Volatile reagents are more challenging to handle in the radio laboratory, since the radioactive compound is only available in low amounts (picomolar to nanomolar range). Notably, [^{18}F]**5.24** was obtained in high activity yield of up to 25% after a simple purification on C18 cartridge. However, to remove the side product (mainly oxidised **5.30**), the mixture was purified by semipreparative reversed-phase HPLC to afford [^{18}F]difluoromethyl sulfone [^{18}F]**5.24** as a chemically pure reagent (radiochemical purity >99%) in a mixture of acetonitrile and water. The product was reformulated *via* C18 cartridge followed by elution with dry acetonitrile to afford [^{18}F]**5.24** (5 – 10% AY) in acetonitrile. The molar activity for this reaction was significantly lower (0.3 GBq µmol^{-1}) than the value reported by Genicot and Luxen (75 GBq µmol^{-1}).



Scheme 5.9. Synthesis of [^{18}F]**5.24** by halogen exchange followed by ruthenium-mediated oxidation. RadioHPLC trace [^{18}F]**5.24** (red), overlaid with the UV HPLC (λ = 220 nm) trace of an authentic sample of **5.24** (blue).

In part, this can be explained by the much lower starting activity used in this case (starting activity of 4.0 GBq) compared to Genicot and Luxens' synthesis (starting activity = 150 GBq). The major source of F-19 product arises from fluoride release of bromofluoromethylsulfide **5.30**. The amount of generated F-19 product is therefore independent of the starting activity. Accordingly, the molar activity is dependent on the amount of starting activity.

5.2.4 Automated synthesis of [^{18}F]4-tBuPhSO$_2$CF$_2$H

Radiosyntheses are often automated to facilitate reproducibility. There are several commercial synthesisers such as Eckert & Ziegler's Modular-Lab, Advion's NanoTek or Trasis' AllinOne platform. The Trasis AllinOne platform, stands out as it is a cassette-based synthesiser, which has been previously employed for the automated radiosynthesis of numerous radiotracers such as [^{18}F]FDG, [^{18}F]FET and [^{18}F]FDOPA.[15,16]

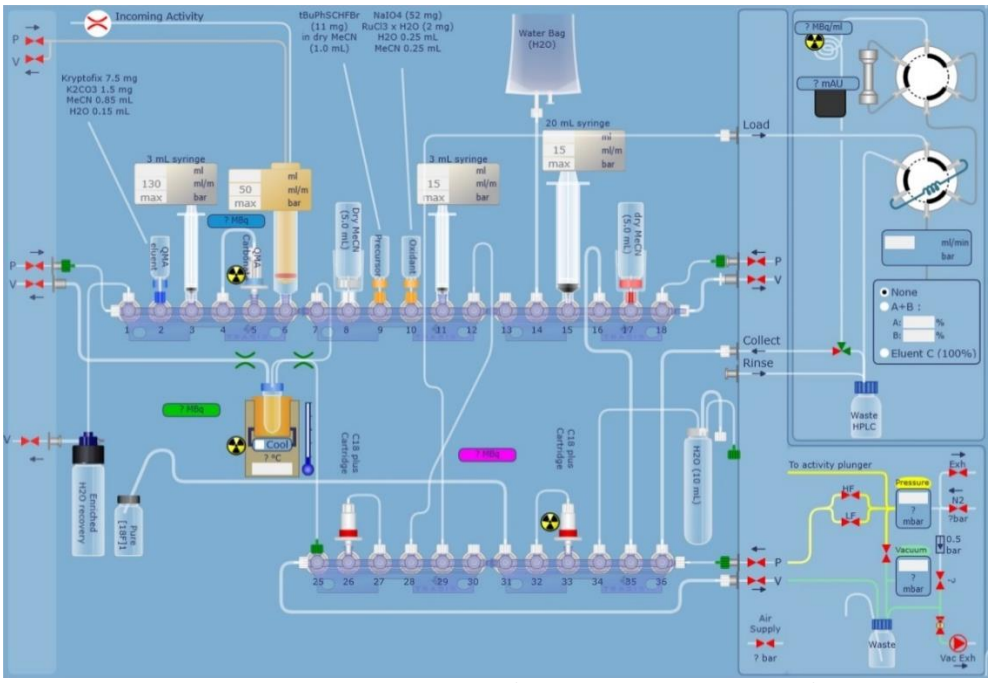


Figure 5.1. Layout for the automated synthesis of [^{18}F]difluoromethyl sulfone [^{18}F]**5.24** on the Trasis AllInOne platform. The figure was generated using the Tracerlab software.

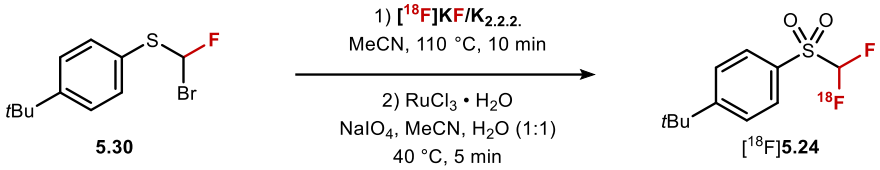
The synthesis starts with the delivery of [^{18}F]fluoride in O-18-enriched water. The [^{18}F]fluoride is then trapped on a strong anion exchange cartridge and the [^{18}O]water and other impurities from the F-18 production are collected into a waste container. A mixture of Kryptofix® 222 and potassium carbonate in an acetonitrile/water mixture (4:1) is then passed through the anion exchange cartridge to elute the [^{18}F]fluoride into the reactor. The [^{18}F]fluoride is dried at 110

°C under a constant flow of nitrogen (600 mBar pressure) for 12 minutes to afford a mixture of dry [^{18}F]potassium fluoride with Kryptofix® 222. Subsequently, the reactor is cooled to 40 °C and a solution of bromofluoromethyl sulfide **5.30** in acetonitrile is added to the reactor. The mixture is reacted at 110 °C for 10 minutes, after which it is cooled to 40 °C. A solution of ruthenium chloride and sodium periodate in a mixture of water and acetonitrile (1:1) is added to the reactor and the mixture is reacted at 40 °C for 5 minutes. The mixture is then diluted with water to allow trapping on a C18 cartridge to remove inorganic impurities. The C18 cartridge is washed with water, dried with air and the desired product is eluted into the reactor with pure acetonitrile. The mixture is injected into the integrated reversed-phase HPLC column and the product is eluted with a mixture of acetonitrile/water (55:45). In this solvent system, the product elutes with a retention time of 25 minutes (Phenomenex HydroRP C18 column). Notably, when a higher amount of acetonitrile was used, the product coeluted with oxidised starting material. After elution, [^{18}F]**5.24** is further diluted with water to allow for trapping on a C18 cartridge for reformulation. The diluted mixture is loaded on a C18 cartridge and the cartridge is washed with water. [^{18}F]**5.24** is then eluted with dry acetonitrile into the target vial.

An initial experiment afforded the desired [^{18}F]difluoromethyl sulfone [^{18}F]**5.24** in low yield (AY = 5.7%), calculated from the starting activity delivered from the cyclotron (Table 5.3, entry 1). The molar activity of the [^{18}F]difluoromethyl sulfone [^{18}F]**5.24** was 2.62 GBq/µmol (following conventional decay correction to the end of synthesis). Further efforts focused on the optimisation of the molar activity

value. Since the bromofluoromethyl sulfide **5.30** is the major source of F-19 fluoride in this transformation, the effect of precursor loading was investigated. Decreasing the precursor loading from 0.04 mmol to 0.013 mmol resulted in a slightly lower activity yield (4.0%) but increased the molar activity (4.84 GBq µmol^{-1}) (entry 2). When the reaction was performed with an increased starting activity (137 GBq of [^{18}F]fluoride) the desired product [^{18}F]**5.24** was isolated in 3.2% activity yield with an increased molar activity (11.9 GBq µmol^{-1}) (entry 3). The lower activity yield in this case might be due to radiolysis occurring at a high loading of [^{18}F]fluoride.

Table 5.3. Optimisation of the automated synthesis of difluoromethyl sulfone [^{18}F]**5.24**.

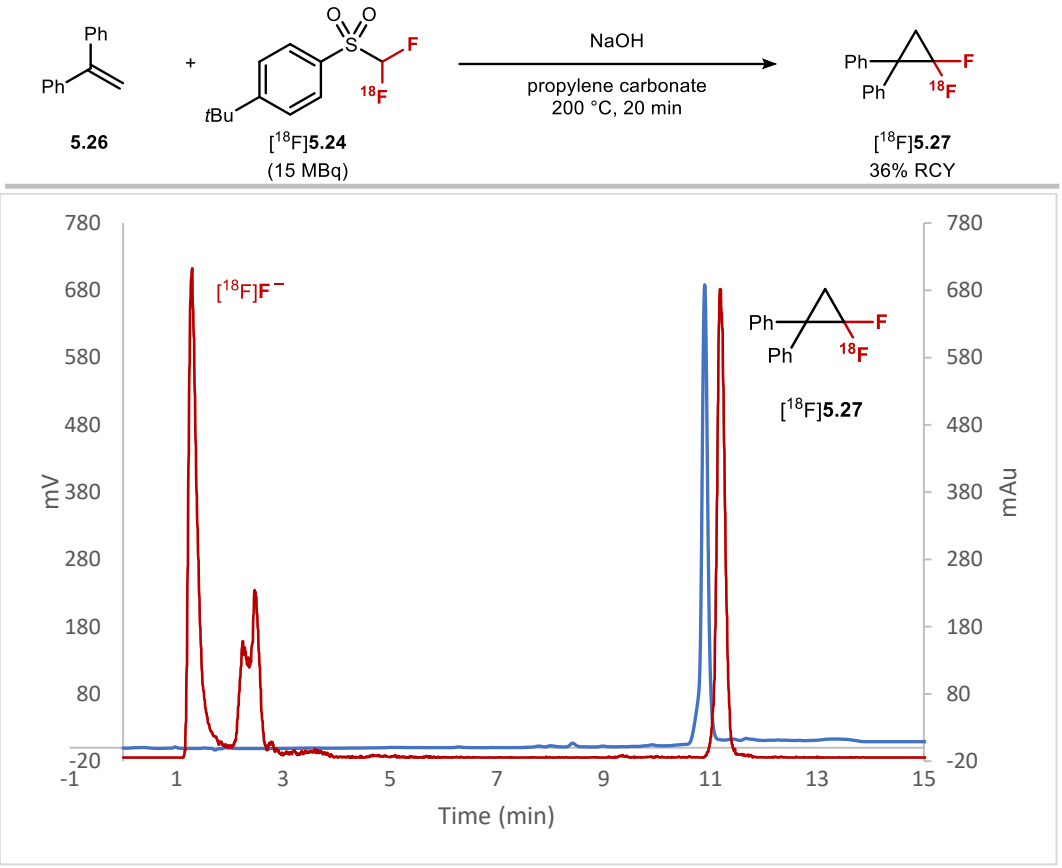


entry	loading (5.30)	[^{18}F]fluoride	isolated	AY	MA [GBq µmol^{-1}]
1	0.04 mmol	42.7 GBq	2.44 GBq	5.7%	2.62
2	0.013 mmol	47.0 GBq	1.86 GBq	4.0%	4.84
3	**0.013 mmol**	**137 GBq**	**4.40 GBq**	**3.2%**	**11.9**

5.2.5 ^{18}F-Difluorocyclopropanation

With [^{18}F]**5.24** in hand, the ability of this reagent to generate [^{18}F]DFC was examined. Based on the results obtained with F-19 difluoromethyl sulfone **5.19** (Table 5.1), analogous conditions were tested for the ^{18}F-difluorocyclopropanation of 1,1-diphenylethylene (**5.26**). When [^{18}F]difluoromethyl sulfone [^{18}F]**5.24** was treated with sodium hydroxide and olefin **5.26** in propylene carbonate at 200 °C for 20 min, complete consumption of the [^{18}F]difluoromethyl sulfone [^{18}F]**5.24** was

observed and the desired [^{18}F]difluorocyclopropane [^{18}F]**5.27** was formed in moderate yield (36% RCY). The major side product of this reaction was assigned as [^{18}F]fluoride due to its low retention time (t_R = 1-2 min). The nature of the other fluorinated side product remains to be investigated.



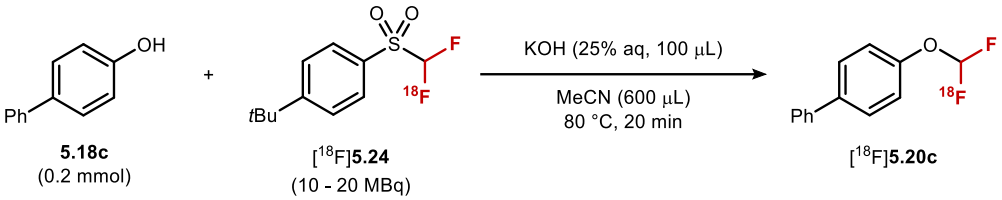
Scheme 5.10. Generation of [^{18}F]DFC from [^{18}F]**5.24** trapped by 1,1-diphenylethylene (**5.26**). Radiochemical yield calculated on crude mixture *via* RadioHPLC. RadioHPLC trace [^{18}F]**5.27** (red), overlaid with the UV HPLC (λ = 220 nm) trace of an authentic sample of **5.27** (blue).

5.2.6 ^{18}F-Difluoromethylation of (thio)phenols

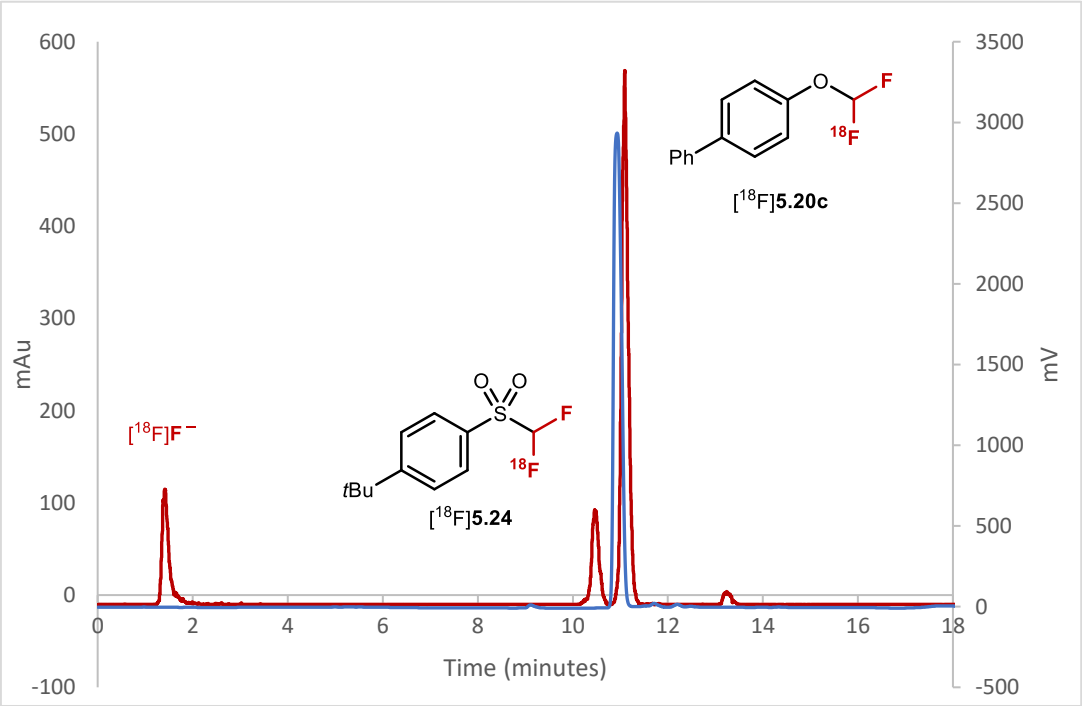
As part of a growing interest from the radiochemistry field in [^{18}F]difluoromethyl ethers, we sought to investigate the ^{18}F-difluoromethylation of phenols and thiophenols under milder reaction conditions. Translation of F-19 chemistry to

F-18 radiochemistry is often difficult. This can be attributed to the different stoichiometries of F-19 chemistry compared to F-18 radiochemistry. However, experiments with F-19 can serve as a starting point for F-18 reaction optimisation. Building on the results obtained with the F-19 difluoromethyl sulfone reagent **5.19** (Table 5.2), model substrate 4-phenylphenol **5.18c** was treated with [^{18}F]**5.24** in a mixture of 25% aqueous potassium hydroxide and acetonitrile (1:6). Under these conditions, the desired [^{18}F]difluoromethyl ether [^{18}F]**5.20c** was observed in high RCY (71% ± 10%) (Table 5.4, entry 1). Lowering the amount of phenol **5.18c** resulted in similar RCY (65% ± 7%) (entry 2). Lowering the amount of base was detrimental and the desired [^{18}F]difluoromethyl ether was not formed (entry 3). [^{18}F]Difluoromethyl sulfone [^{18}F]**5.24** remained unreacted. In contrast, when the amount of base was increased, the ^{18}F-difluoromethylation proceeded in good RCY (62% ± 3%) (entry 4). When dimethylsulfoxide (DMSO) was used as a solvent the [^{18}F]difluoromethyl ether [^{18}F]**5.20c** was observed in low RCY (entry 5). A control experiment showed that the presence of water is strictly necessary for the reaction to proceed (entry 6). This might be attributed to the low solubility of potassium hydroxide in organic solvents. When the reaction was performed on 0.1 mmol scale with lower substrate loading but a similar concentration, [^{18}F]**5.20c** was obtained in good RCY (entry 7). The crude radioHPLC analysis shows remaining [^{18}F]**5.24** and formation of a polar side product with a short retention time, that was assigned as [^{18}F]fluoride (t_R = 1-2 min).

Table 5.4. Optimisation of the reaction conditions for the ^{18}F-difluoromethylation of phenol 5.18c.[a]

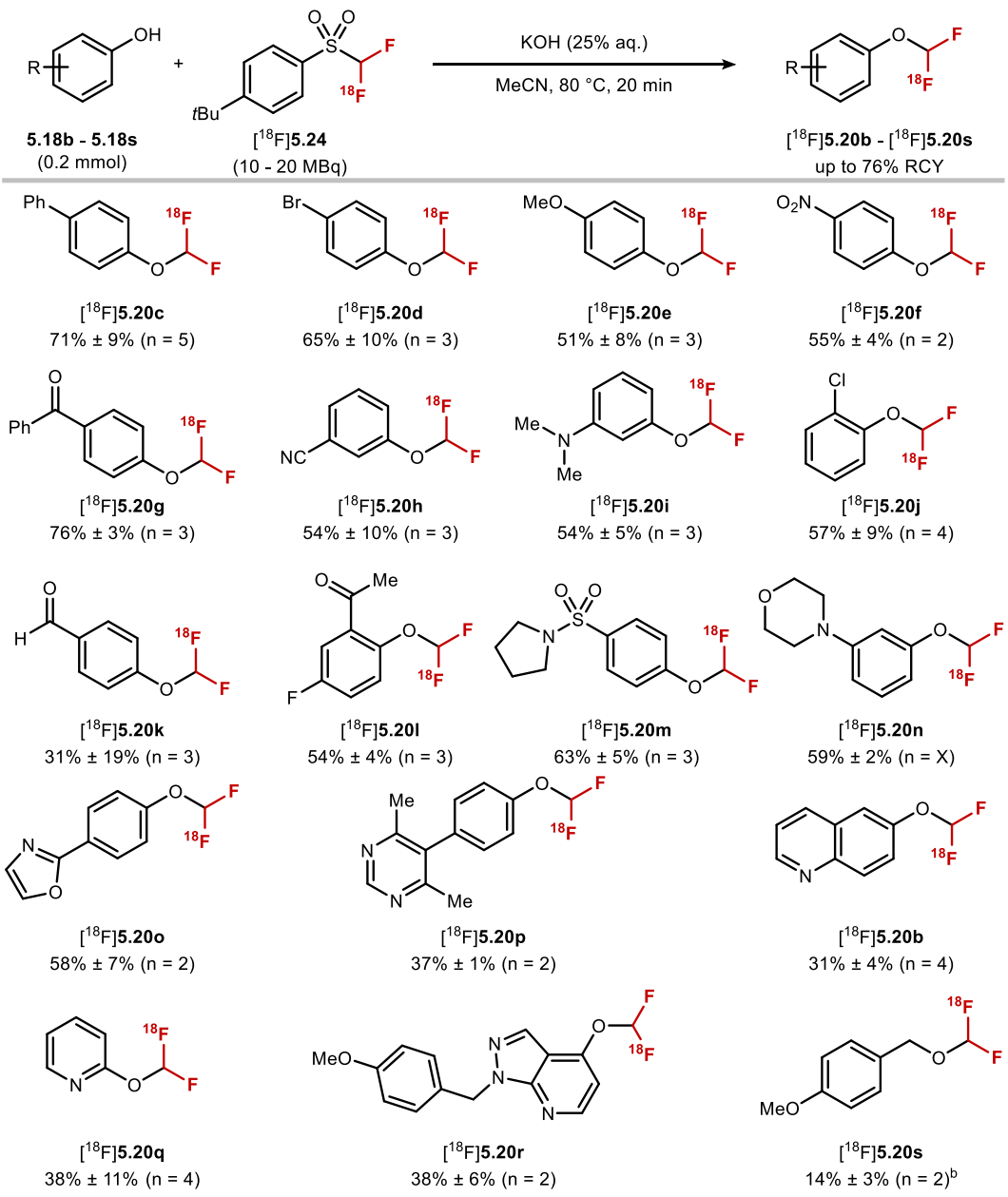


Entry	Alterations to conditions	RCY (n = 2)
1	**No alteration**	**71% ± 9%**[b]
2	**5.18c** (0.1 mmol)	65% ± 7%
3	KOH (25% aq, 50 µL)	Trace
4	KOH (25% aq, 150 µL)	62% ± 3%
5	DMSO (600 µL) instead of MeCN	25% ± 1%
6	KOH (3 mg) instead of KOH (aq)	0%
7	**5.18c** (0.1 mmol), KOH (25% aq, 50 µL), MeCN (300 µL)	66% ± 14%



[a]Reaction conditions: **5.18c** (0.2 mmol), KOH (25% aq, 100 µL), MeCN (600 µL), [^{18}F]**5.24** (10 – 20 MBq), 80 °C, 20 min. Radiochemical yield calculated on crude mixture *via* RadioHPLC. [b]Reaction performed in n = 5. n = number of reactions. RadioHPLC trace [^{18}F]**5.20c** (red), overlaid with the UV HPLC (λ = 220 nm) trace of an authentic sample of **5.20** (blue).

The optimised reaction conditions (Table 5.4; entry 1) were applied to the ^{18}F-difluoromethylation of a range of phenols (Scheme 5.12).



Scheme 5.11. Substrate scope of the ^{18}F-difluoromethylation of phenols. a) Reaction conditions: phenol **5.18b** – **5.18r** (0.2 mmol), KOH (25% aq, 100 µL), MeCN (600 µL), [^{18}F]**2** (10 – 20 MBq), 80 °C, 20 min. b) Reaction conditions: alcohol **5.18s** (0.2 mmol), NaH (0.1 mmol), DMF (300 µL), [^{18}F]**5.24** (10 – 20 MBq), 60 °C, 20 min. Radiochemical yield calculated on crude mixture *via* RadioHPLC. n = number of reactions.

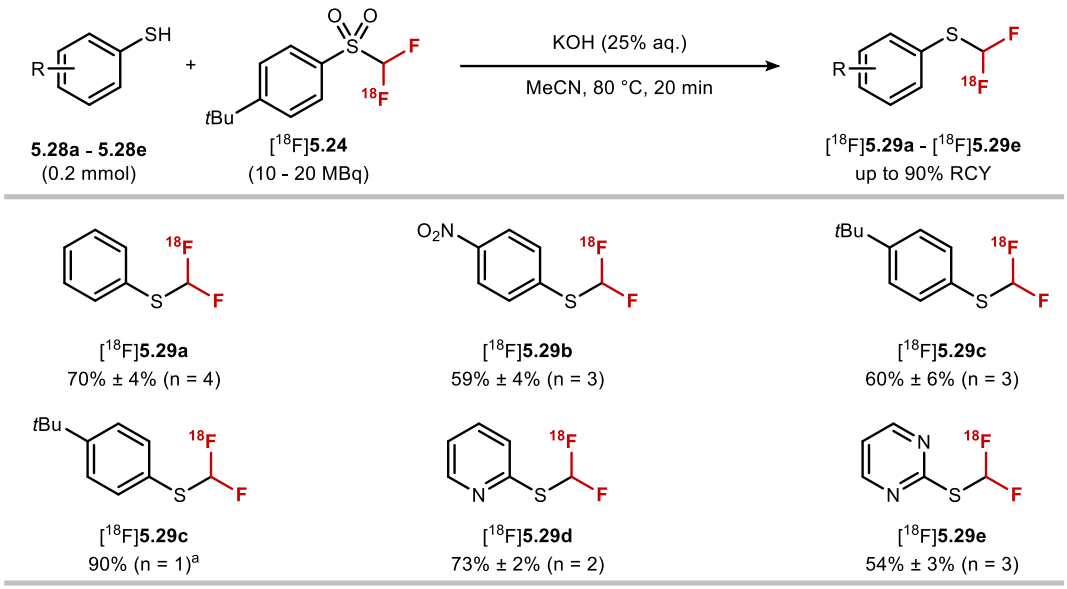
Phenols with various substitution patterns reacted under the optimised reaction conditions and afforded the desired [^{18}F]difluoromethyl ethers in moderate to high RCY ([^{18}F]**5.20b** – [^{18}F]**5.20s**). *Para*-substituted phenols with different electronic properties, containing bromo, methoxy, nitro or ketone functionalities yielded the

desired product in good RCY ([^{18}F]**5.20c** – [^{18}F]**5.20g**). Electronically different *meta*-substituted phenols afforded the desired ^{18}F-difluoromethyl ethers in moderate RCY ([^{18}F]**5.20h** – [^{18}F]**5.20i**). Furthermore, a more sterically hindered 2-substituted phenol yielded the desired product in similar RCY ([^{18}F]**5.20j**). Phenols containing a potentially reactive functional group, such as aldehyde or ketone, yielded the products in moderate RCY ([^{18}F]**5.20g**, [^{18}F]**5.20k**, [^{18}F]**5.20l**). Next, the ^{18}F-difluoromethylation of phenols decorated with motifs of relevance to drug discovery were tested under the optimised reaction conditions. A pyrrolidine sulfonamide-containing phenol and a morpholine-containing phenol afforded the desired products in good RCY ([^{18}F]**5.20m**, [^{18}F]**5.20n**). Due to the relevance of heteroarenes to medicinal chemistry, the ^{18}F-difluoromethylation of substrates containing an oxazole and pyrimidine motif were investigated. Whilst the oxazole substituent was tolerated ([^{18}F]**5.20o**), a pyrimidine substituent proved to be problematic and the difluoromethyl ether [^{18}F]**5.20p** was observed in only moderate RCY. Other hydroxy-heteroarenes, such as 6-hydroxyquinoline, 2-hydroxypyridine and a hydroxypyrazolopyridine underwent ^{18}F-difluoromethylation under the optimised reaction conditions. These substrates were less efficient, and the desired product was formed in low RCY ([^{18}F]**5.20q**, [^{18}F]**5.20b**, [^{18}F]**5.20r**). When the benzylic alcohol **5.18s** was reacted under the standard reaction conditions, the desired [^{18}F]difluoromethyl ether [^{18}F]**5.20s** was not obtained, and the [^{18}F]difluoromethyl sulfone [^{18}F]**5.24** remained unreacted. This could be explained by the higher pKa of benzylic alcohols (pKa ~ 16 in water) compared to phenols (pKa ~ 10 in water), resulting in inefficient formation of the alkoxide. The formation of alkoxide is required for the efficient activation of the

[^{18}F]difluoromethyl sulfone [^{18}F]**5.24**. Therefore, alternative reaction conditions, with sodium hydride as base in *N*,*N*-dimethylformamide (DMF) (60 °C for 20 minutes) were applied for the ^{18}F-difluoromethylation of benzylic alcohol **5.18s**. Sodium hydride (pKa(H_2) ~ 35) is a suitable base for efficient deprotonation of alcohol **5.18s**. DMF was chosen as a non-protic solvent to prevent the reverse protonation of alcohol **5.18s**. Under these modified reaction conditions, [^{18}F]difluoromethyl ether [^{18}F]**5.20s** was formed in low RCY. Lowering or increasing the reaction temperature did not increase the RCY of the benzylic [^{18}F]difluoromethyl ether. The activation of [^{18}F]**5.24** was found to be inefficient at lower temperature (remaining [^{18}F]**5.24** observed in crude reaction mixture) and the desired product [^{18}F]**5.20s** likely decomposed at higher reaction temperature (complete consumption of [^{18}F]**5.24** and formation of [^{18}F]fluoride). Overall, the evaluation of the scope demonstrated the high functional group tolerance of this transformation, a key factor in the context of the radiolabelling of structurally complex bioactive molecules or tracers for PET imaging.

When thiophenols (**5.28a** – **5.28e**) were treated under the optimised reaction conditions (Table 5.4, entry 1), the corresponding [^{18}F]difluoromethyl thioethers [^{18}F]**5.29a** – [^{18}F]**5.29e** were obtained in high RCY (Scheme 5.12). The RCY of [^{18}F]**5.29c** was further increased by performing the reaction at higher temperature (100 °C instead of 80 °C). Interestingly, 2-mercaptopyridine afforded the desired product [^{18}F]**5.29d** in significantly higher RCY than the corresponding 2-hydroxypyridine (Scheme 5.11, [^{18}F]**5.20q**). Furthermore, the ^{18}F-

difluoromethylation of 2-mercaptopyrimidine afforded the [^{18}F]difluoromethyl thioether [^{18}F]**5.29e** in moderate RCY.

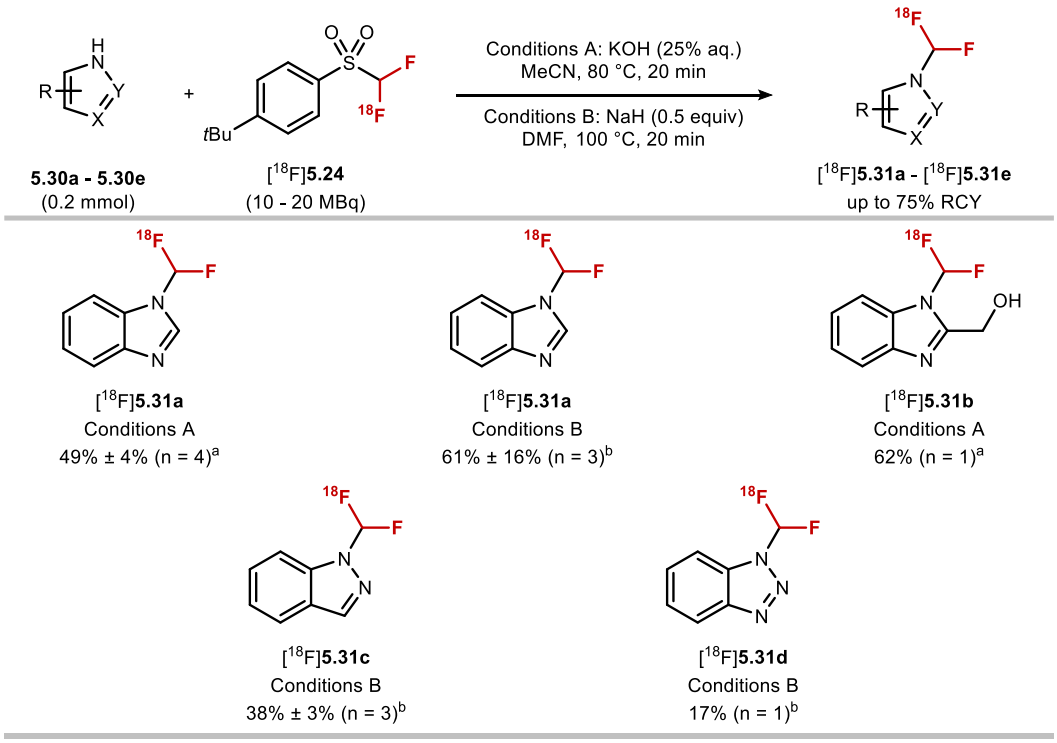


Scheme 5.12. Substrate scope of the ^{18}F-difluoromethylation of thiophenols. Reaction conditions: thiophenol **5.28a** – **5.28e** (0.2 mmol), KOH (25% aq, 100 µL), MeCN (600 µL), [^{18}F]**5.24** (10 – 20 MBq), 80 °C, 20 min. Radiochemical yield calculated on crude mixture *via* RadioHPLC. n = number of reactions. [a]The reaction was performed at 100 °C.

5.2.7 ^{18}F-Difluoromethylation of *N*-heterocycles

Owing to the importance of heterocyclic fragments to drug discovery, the difluoromethylation of *N*-heterocycles (**5.30a** – **5.30e**) was investigated under the standard reaction conditions (KOH (25% aq.), MeCN, 80 °C). When benzimidazole was treated with [^{18}F]**5.24**, the desired [^{18}F]*N*-CF_2H compound [^{18}F]**5.31a** was formed in moderate RCY. Benzimidazole is less acidic (pKa ~ 12.8 in water) than phenol (pKa ~ 10 in water). Therefore, alternative conditions employing sodium hydride as base in DMF (analogous to the difluoromethylation of benzylic alcohol **5.18s**) were tested. When benzimidazole was treated with sodium hydride and [^{18}F]difluoromethyl sulfone [^{18}F]**5.24** in DMF at 100 °C, the RCY of the desired [^{18}F]*N*-CF_2H compound [^{18}F]**5.31a** was increased. 2-(Hydroxymethyl)benzimidazole

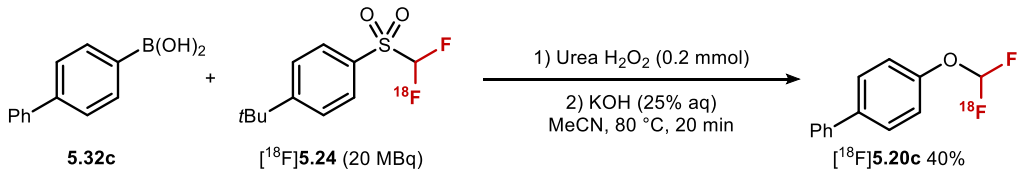
(**5.30b**) afforded the desired [^{18}F]*N*-CF_2H compound [^{18}F]**5.31b** in high RCY under aqueous conditions (KOH (25% aq.), MeCN, 80 °C). In contrast, the reaction of 2-(hydroxymethyl)benzimidazole with sodium hydride, afforded [^{18}F]fluoride as the major product. This could be due to competitive ^{18}F-difluoromethylation of the alcohol under these conditions (pKa(H_2) ~ 35; pKa(MeOH) ~ 27.9 in DMSO). The corresponding [^{18}F]*O*-CF_2H compound however, is unstable at high temperature and decomposes to [^{18}F]fluoride. Indazole and 2-phenylimidazole underwent ^{18}F-difluoromethylation to afford the corresponding [^{18}F]*N*-CF_2H compounds [^{18}F]**530c** and [^{18}F]**530e** in high RCY. In contrast, the ^{18}F-difluoromethylation of benzotriazole was significantly less efficient ([^{18}F]**5.30d**).



Scheme 5.13. Substrate scope of the ^{18}F-difluoromethylation of *N*-heterocycles. Radiochemical yield calculated on crude mixture *via* RadioHPLC. n = number of reactions. [a]Reaction conditions: *N*-heterocycle **5.30a**, **5.30b** (0.2 mmol), KOH (25% aq, 100 µL), MeCN (600 µL), [^{18}F]**2** (15 – 20 MBq), 80 °C, 20 min. [b]Reaction conditions: *N*-heterocycle **5.30a** – **5.30d** (0.2 mmol), NaH (0.1 mmol), DMF (300 µL), [^{18}F]**2** (15 – 20 MBq), 100 °C, 20 min.

5.2.8 ^{18}F-Difluoromethoxylation of an Aryl Boronic Acid

A recent report from Hartwig and co-workers illustrated the two-step one-pot transformation from an arylboronic acid to the corresponding difluoromethoxyarene.[17] Arylboronic acids are readily available starting materials and can easily be prepared by Miyaura borylation of aryl(pseudo)halides.[18] Treatment of the arylboronic acid with urea hydroperoxide resulted in the formation of the corresponding phenol, which could then undergo difluoromethylation with difluorocarbene to afford the difluoromethoxyarene. A similar transformation was performed using [^{18}F]difluoromethyl sulfone [^{18}F]**5.24** for the formal ^{18}F-difluoromethoxylation of aryl boronic acid **5.32c**. The reaction sequence afforded the [^{18}F]difluoromethyl ether [^{18}F]**5.20c** in moderate RCY.

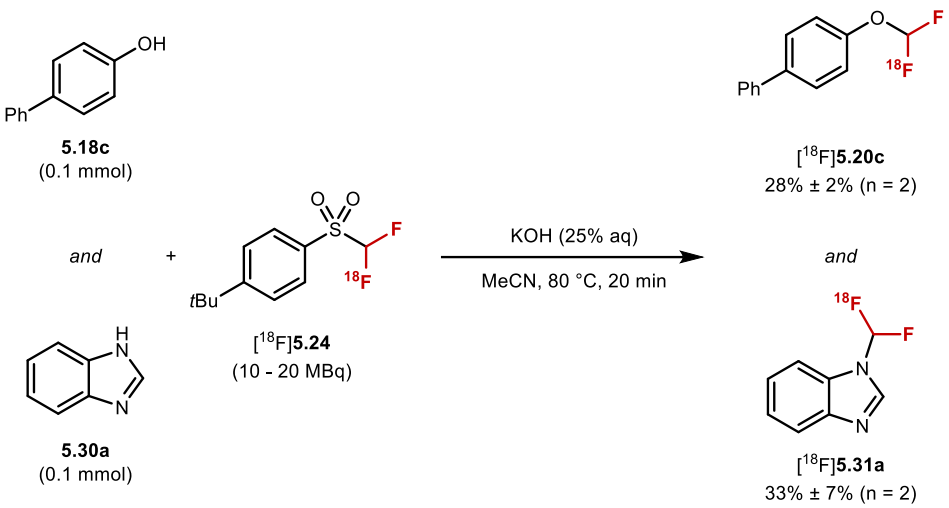


5.32c [^{18}F]**5.24** (20 MBq) [^{18}F]**5.20c** 40%

Scheme 5.14. Two-step one-pot formal difluoromethoxylation of arylboronic acid **5.32c**.

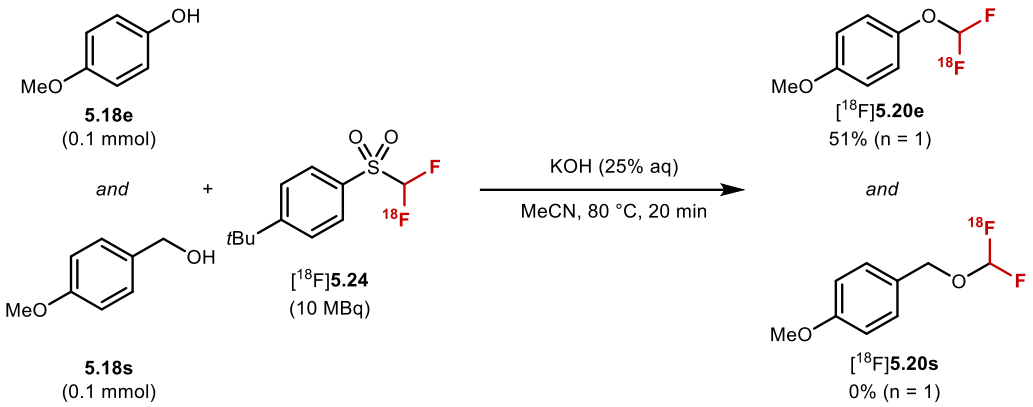
4.2.9 Competition experiments

To investigate the selectivity of this novel ^{18}F-difluoromethylation protocol, competition experiments between different substrates were performed. When equimolar amounts of benzimidazole (**5.30a**) and 4-phenylphenol (**5.18c**) were reacted with [^{18}F]**5.24** under the standard reaction conditions, the reaction was unselective and a mixture of [^{18}F]**5.20c** and [^{18}F]**5.31a** was obtained (Scheme 5.15).



Scheme 5.15. Competition experiment between benzimidazole (**5.30a**) and 4-phenyl-phenol (**5.18c**).

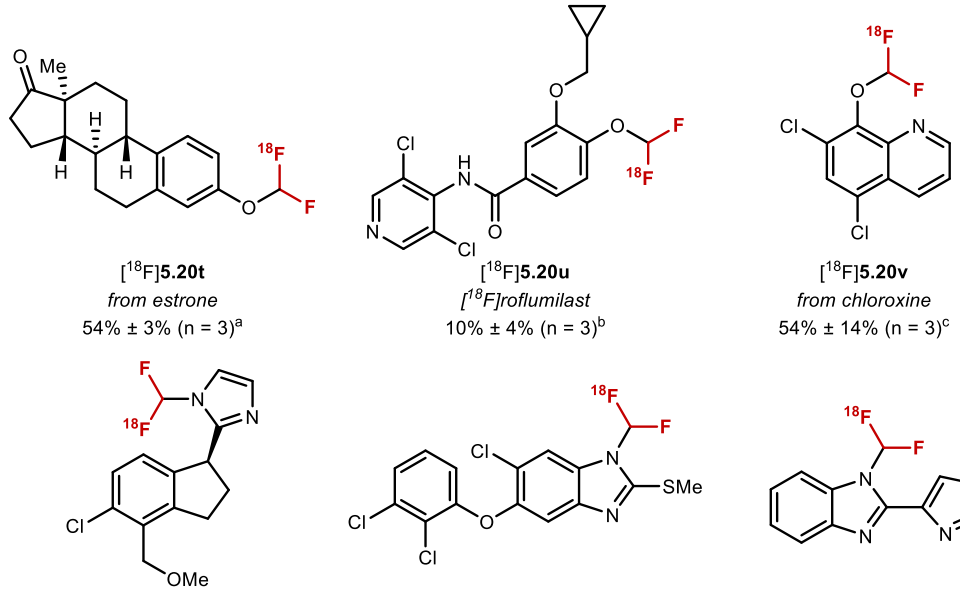
In contrast, in a competition experiment between equimolar amounts of benzylic alcohol **5.18s** and phenol **5.18e**, the reaction proceeded with high selectivity towards [^{18}F]**5.20e** (Scheme 5.16). Although reagent [^{18}F]**5.24** is activated under these reaction conditions and [^{18}F]DFC is formed, the benzylic alcohol **5.18s** did not react with [^{18}F]DFC. This could be explained by the higher acidity of phenols (pKa ~ 10) compared to aliphatic alcohols (pKa ~ 16). Phenols are more readily deprotonated and the resulting highly nucleophilic phenolate outcompetes the less nucleophilic benzylic alcohol.



Scheme 5.16. Competition experiment between phenol **5.18e** and alcohol **5.18s**.

5.2.10 ^{18}F-Difluoromethylation of Biologically Relevant Molecules

With the different procedures for ^{18}F-*O*- and ^{18}F-*N*-difluoromethylation in hand, the ^{18}F-difluoromethylation of biologically relevant molecules was further investigated. Estrone was ^{18}F-difluoromethylated at the phenol position in good RCY ([^{18}F]**5.20t**). When the ^{18}F-difluoromethylation protocol was applied to the synthesis of the ^{18}F-isotopologue of the anti-inflammatory drug roflumilast, the desired [^{18}F]*O*-CF_2H compound [^{18}F]**5.20u** was formed, albeit in low RCY.



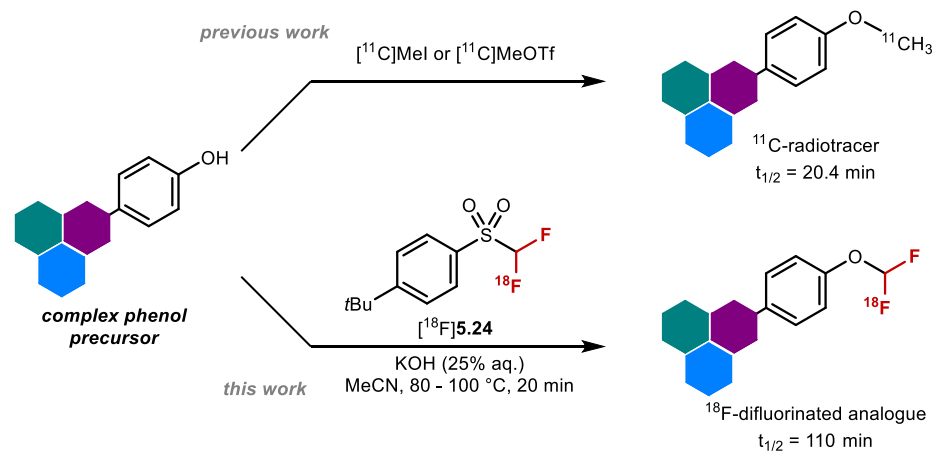
Scheme 5.17. Substrate scope of the ^{18}F-difluoromethylation of biologically relevant molecules. [a]Reaction conditions: nucleophile (**5.18t**, **5.30e**, **5.30f**) (0.2 mmol), KOH (25% aq, 100 µL), MeCN (600 µL), [^{18}F]**5.24** (10 – 20 MBq), 80 °C, 20 min. [b]Reaction conditions: phenol **5.18u** (0.1 mmol), KOH (25% aq, 100 µL), MeCN (600 µL), [^{18}F]**5.24** (10 – 20 MBq), 100 °C, 20 min. [c]Reaction conditions: chloroxine (**5.18v**) (0.2 mmol), KOH (25% aq, 100 µL), MeCN (600 µL), [^{18}F]**5.24** (10 – 20 MBq), 100 °C, 20 min. [d]Regioselectivity was not determined. [e]Reaction conditions: thiabendazole (**5.30g**) (0.2 mmol), NaH (0.1 mmol), DMF (300 µL), [^{18}F]**5.24** (10 – 20 MBq), 140 °C, 20 min. Radiochemical yield calculated on crude mixture *via* RadioHPLC. n = number of reactions.

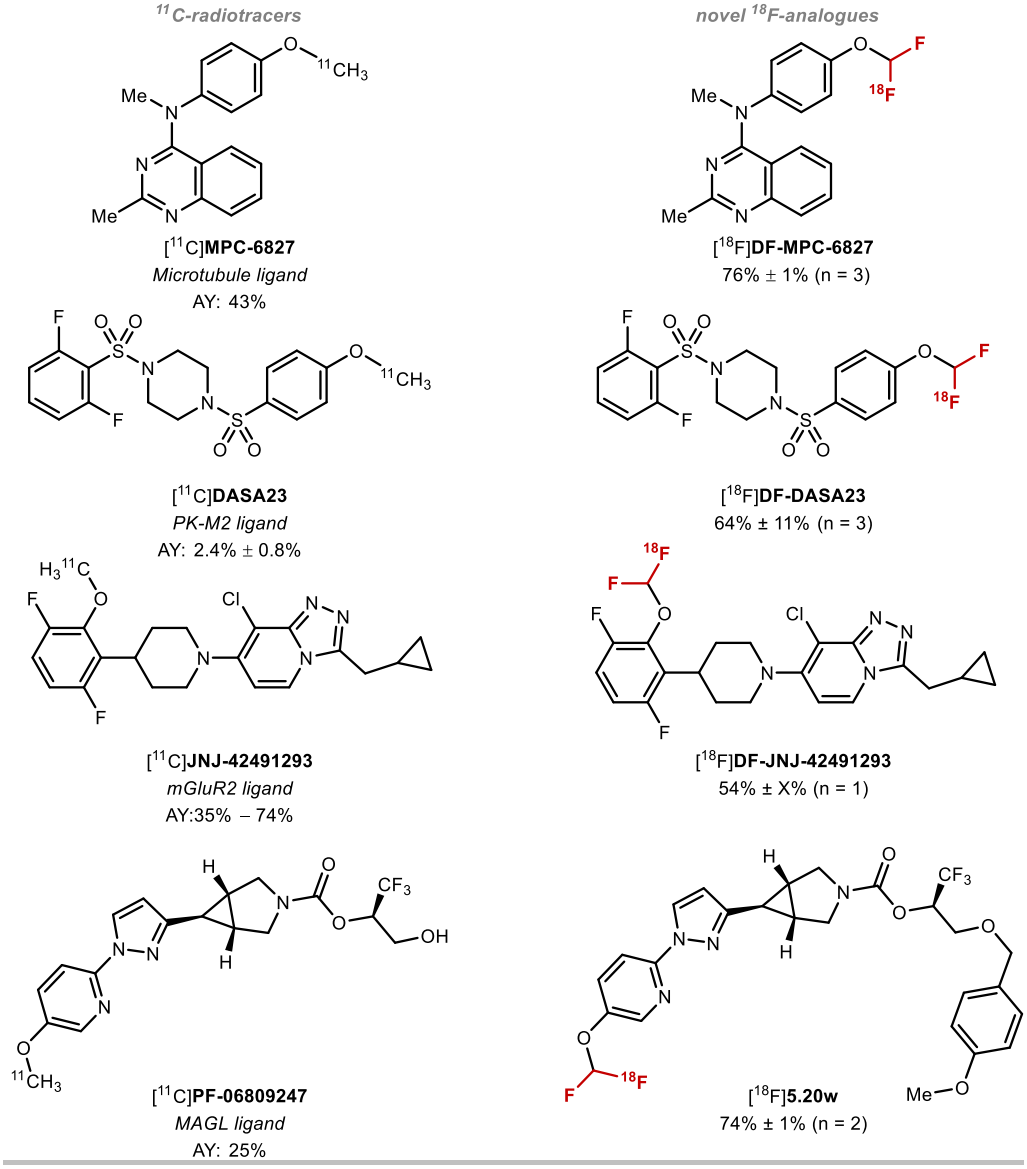
The antibacterial drug chloroxine was ^{18}F-difluoromethylated in moderate RCY ([^{18}F]**5.20v**). Furthermore, PF-3774076, a brain penetrant CNS drug, underwent

^{18}F-difluoromethylation at the imidazole moiety to afford [^{18}F]**5.31e** in moderate RCY. The antiparasitic drug triclabendazole underwent ^{18}F-difluoromethylation at the benzimidazole core in moderate RCY ([^{18}F]**5.31f**). Similarly, the antiparasitic agent thiabendazole underwent ^{18}F-*N*-difluoromethylation, albeit a higher reaction temperature was required for the reaction to proceed in good RCY ([^{18}F]**5.31g**).

Next, the ^{18}F-difluoromethylation method was applied to the radiosynthesis of PET radiotracer analogues, that have previously been labelled *via* ^{11}C-methylation of a phenol with [^{11}C]iodomethane or [^{11}C]methyl triflate. [^{11}C]**MPC-6827** is a brain-penetrant microtubule ligand.[19] Microtubule are expected to play a significant role in cell division. Alcohol use disorder (AUD) can lead to disturbance of the structural integrity of microtubule, which in turn can lead to neurological and psychiatric disorders such as Alzheimer's disease, multiple sclerosis, or cancer. [^{11}C]**MPC-6827** has been used *in vivo* in mouse models, where alcohol dependent mice have shown reduced microtubule binding in the brain compared to the liver and heart. Based on these results, it is suggested that [^{11}C]**MPC-6827** could be used as a PET tracer for AUD and related neurodegenerative diseases in humans. The corresponding [^{18}F]fluoromethyl ether has not been reported to date. This might be due to low stability of [^{18}F]4-(fluoromethoxy)anilines. Therefore, the ^{18}F-difluoromethylation conditions were applied to the synthesis of an [^{18}F]difluorinated analogue. Starting from the same phenol precursor as used in the synthesis of [^{11}C]**MPC-6827**, the reaction afforded the [^{18}F]difluoro-analogue [^{18}F]**DF-MPC-6827** in high RCY. Next, the synthesis of an ^{18}F-difluoro analogue of

the oncological PET tracer [^{11}C]**DASA23** was investigated. [^{11}C]**DASA23** can be synthesised *via* ^{11}C-methylation of the corresponding phenol using [^{11}C]methyl triflate.[20] However, this reaction is very low yielding (AY = 2.4% ± 0.8%). The ^{18}F-isotopologue [^{18}F]**DASA23** has been synthesised by S_NAr of the corresponding nitrobenzene derivative.[21] However, also this reaction was low yielding (AY = 2.6% ± 1.5%). Using the novel ^{18}F-difluoromethylation protocol the difluorinated analogue [^{18}F]**DF-DASA23** was afforded in high RCY (64% ± 11%). Analogously, an ^{18}F-variant of the metabotropic glutamate receptor subtype 2 (mGluR2) positive allosteric modulator (PAM) [^{11}C]**JNJ-42491293** was synthesised.[22] mGluR2 plays a significant role in CNS processes and is therefore an attractive target for neuropharmacology. [^{11}C]**JNJ-42491293** was previously synthesised with [^{11}C]iodomethane in high AY (ranging from 25% to 74%).[22] An ^{18}F-variant of the compound has not been synthesised to date. When the ^{18}F-difluoromethylation procedure was applied to the same precursor, [^{18}F]**DF-JNJ-42491293** was obtained in moderate RCY. Similarly, the ^{18}F-difluoromethylation conditions were applied to the synthesis of paramethoxybenzene protected analogue of [^{11}C]**PF-06809247**, a covalent, irreversible monoacylglycerol lipase (MAGL) inhibitor.[23] Inhibition of MAGL is suggested to positively affect numerous neurological disorders. In the active site of MAGL, serine 122 irreversibly displaces the 3,3,3-trifluoro-2-hydroxypropanol group, which links the target covalently to MAGL. Applying the novel ^{18}F-difluoromethylation procedure to this compound afforded the desired [^{18}F]*O*-CF_2H compound [^{18}F]**5.20w** in high RCY.





Scheme 5.18. Previous synthesis of [^{11}C]radiotracers and the novel synthesis of ^{18}F-difluorinated analogues starting from the same precursors.

5.2.11 Proposed Mechanism for the ^{18}F-Difluoromethylation

The following mechanism is proposed for the ^{18}F-difluoromethylation of (thio)phenols and *N*-heterocycles. Deprotonation of the nucleophile ($pKa_{(PhOH)}$ ~ 10; $pKa_{(PhSH)}$ ~ 7.0; $pKa_{(benzimidazole)}$ ~ 13) affords the anionic species **A**. **A** can then deprotonate [^{18}F]**5.24** to afford [^{18}F]**B**, which can release 4-*tert*-butylphenylsulfinate (**5.32**) and [^{18}F]DFC ([^{18}F]**C**). [^{18}F]DFC is then attacked by species **A** to afford the desired product ([^{18}F]**5.20**, [^{18}F]**5.29**, [^{18}F]**5.31**) after protonation.

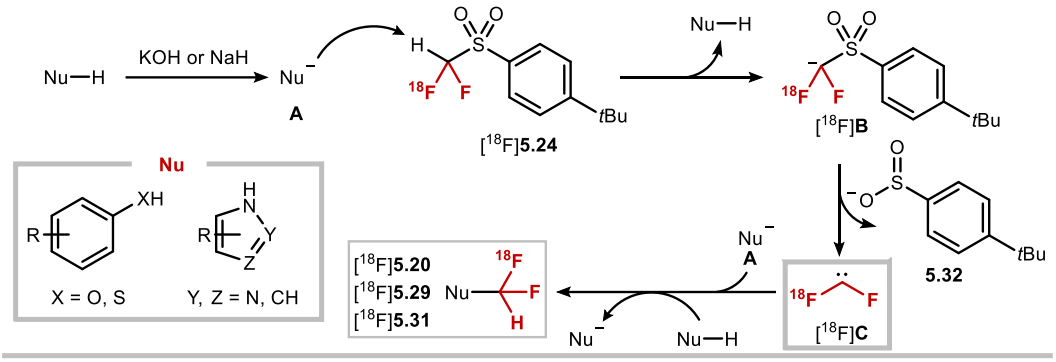


Figure 5.2. Proposed mechanism for the ^{18}F-difluoromethylation with [^{18}F]**5.24**.

For the ^{18}F-difluorocyclopropanation the following mechanism is proposed. Deprotonation of [^{18}F]**5.24** with a suitable base (such as sodium hydride or sodium hydroxide) affords the anionic species [^{18}F]**B**, which releases [^{18}F]DFC ([^{18}F]**C**) and 4-*tert*-butylphenylsulfinate (**5.32**). [^{18}F]**C** undergoes concerted ^{18}F-difluorocyclopropanation with the alkene **5.26** to afford difluorocyclopropane [^{18}F]**5.27**.

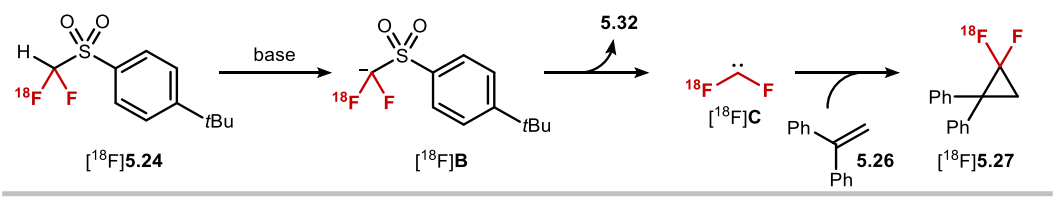


Figure 5.3. Proposed mechanism for the ^{18}F-difluorocyclopropanation of olefin **5.26**.

5.3 Conclusion

In conclusion, the manual and fully automated radiosynthesis of a novel [^{18}F]difluoromethyl sulfone reagent is described. The reagent is synthesised in low AY and moderate MA (11.9 GBq μmol^{-1}). For the first time, this reagent allows for direct ^{18}F-difluoromethylation of various nucleophiles including (thio)phenols and *N*-heterocycles. The reaction shows a broad functional group tolerance and is high yielding. The reaction conditions were applied to the ^{18}F-difluoromethylation of a wide range of substrates including biologically relevant phenols and (benz)imidazoles. PET radiotracer analogues, that have previously been labelled with C-11, underwent ^{18}F-difluoromethylation to afford F-18 labelled analogues. Competition experiments show a high selectivity for the ^{18}F-difluoromethylation of phenols over aliphatic alcohols. Limitations of the protocol include inefficient difluoromethylation of aliphatic alcohols and low selectivity in substrates containing an *N*-heterocycle and a phenol. Mechanistic experiments suggest an ^{18}F-difluorocarbene mechanism based on deprotonation followed by α-elimination of a sulfinate. Based on these observations the ^{18}F-difluorocyclopropanation of 1,1-diphenylethylene was demonstrated.

5.4 Outlook

We have successfully synthesised F-18-analogues of a selection of known PET radiotracers. Future work will focus on the biological evaluation of these compounds. Specifically, we will investigate whether the ^{18}F-difluoromethyl motif shows increased *in vivo* stability compared to classical fluoromethyl groups, which

could increase the signal-to-noise ratio in PET images. Furthermore, we will attempt to automate the full sequence (reagent synthesis and ^{18}F-difluoromethylation) to allow for other radio laboratories to implement this ^{18}F-difluoromethylation protocol.

DFC has recently been employed for Csp^2-CF_2H bond formation using transition metal-catalysed cross-coupling with aryl boronic acids. Experiments to determine whether such a transformation could be achieved using the novel ^{18}F-difluorocarbene reagent described in this chapter are currently ongoing in our laboratory.

5.5 References

[1] M. Huiban, M. Tredwell, S. Mizuta, Z. Wan, X. Zhang, T. L. Collier, V. Gouverneur, J. Passchier, *Nat. Chem.* **2013**, *5*, 941–944.

[2] J. Zheng, L. Wang, J. H. Lin, J. C. Xiao, S. H. Liang, *Angew. Chemie - Int. Ed.* **2015**, *54*, 13236–13240.

[3] C. W. Kee, O. Tack, F. Guibbal, T. C. Wilson, P. G. Isenegger, M. Imiołek, S. Verhoog, M. Tilby, G. Boscutti, S. Ashworth, J. Chupin, R. Kashani, A. W. J. Poh, J. K. Sosabowski, S. Macholl, C. Plisson, B. Cornelissen, M. C. Willis, J. Passchier, B. G. Davis, V. Gouverneur, *J. Am. Chem. Soc.* **2020**, *142*, 1180–1185.

[4] Y. N. Tang, T. Small, F. S. Rowland, *J. Am. Chem. Soc.* **1969**, *91*, 2130–2131.

[5] T. Smail, F. S. Rowland, *J. Phys. Chem.* **1970**, *74*, 1866–1871.

[6] J. Zheng, Y. Li, L. Zhang, J. Hu, G. J. Meuzelaar, H. J. Federsel, *Chem. Commun.* **2007**, 5149–5151.

[7] L. Li, F. Wang, C. Ni, J. Hu, *Angew. Chemie - Int. Ed.* **2013**, *52*, 12390–12394.

[8] D. M. Gill, N. McLay, M. J. Waring, C. T. Wilkinson, J. B. Sweeney, *Synlett* **2014**, *25*, 1756–1758.

[9] L. Trump, A. Lemos, B. Lallemand, P. Pasau, J. Mercier, C. Lemaire, A. Luxen, C. Genicot, *Angew. Chemie - Int. Ed.* **2019**, *58*, 13149–13154.

[10] H. Shi, A. Braun, L. Wang, S. H. Liang, N. Vasdev, T. Ritter, *Angew. Chemie - Int. Ed.* **2016**, *55*, 10786–10790.

[11] Q. Zhao, P. G. Isenegger, T. C. Wilson, J. B. I. Sap, F. Guibbal, L. Lu, V. Gouverneur, Q. Shen, *CCS Chem.* **2020**, 1921–1028.

[12] T. Khotavivattana, S. Verhoog, M. Tredwell, L. Pfeifer, S. Calderwood, K. Wheelhouse, T. Leecollier, V. Gouverneur, *Angew. Chemie - Int. Ed.* **2015**, *54*, 9991–9995.

[13] S. Verhoog, L. Pfeifer, T. Khotavivattana, S. Calderwood, T. L. Collier, K. Wheelhouse, M. Tredwell, V. Gouverneur, *Synlett* **2016**, *27*, 25–28.

[14] J. B. I. Sap, T. C. Wilson, C. W. Kee, N. J. W. Straathof, C. W. a. Ende, P. Mukherjee, L. Zhang, C. Genicot, V. Gouverneur, *Chem. Sci.* **2019**, *10*, 3237–3241.

[15] E. Schopf, C. M. Waldmann, J. Collins, C. Drake, R. Slavik, R. M. van Dam, *J. Vis. Exp.* **2018**, 1–12.

[16] S. Li, A. Schmitz, H. Lee, R. H. Mach, *EJNMMI Radiopharm. Chem.* **2017**, *1*, 1–19.

[17] P. S. Fier, J. F. Hartwig, *Angew. Chemie - Int. Ed.* **2013**, *52*, 2092–2095.

[18] G. A. Molander, S. L. J. Trice, S. M. Kennedy, S. D. Dreher, M. T. Tudge, *J. Am. Chem. Soc.* **2012**, *134*, 11667–11673.

[19] N. Damuka, P. W. Czoty, A. T. Davis, M. A. Nader, S. H. Nader, S. Craft, S. L. Macauley, L. K. Galbo, P. M. Epperly, C. T. Whitlow, A. T. Davenport, T. J. Martin, J. B. Daunais, A. Mintz, K. K. S. Sai, *Molecules* **2020**, *25*, 1–7.

[20] T. H. Witney, M. L. James, B. Shen, E. Chang, C. Pohling, N. Arksey, A. Hoehne, A. Shuhendler, J. H. Park, D. Bodapati, J. Weber, G. Gowrishankar, J. Rao, F. T. Chin, S. S. Gambhir, *Sci. Transl. Med.* **2015**, *7*, DOI 10.1126/scitranslmed.aac6117.

[21] T. Haywood, C. Beinat, G. Gowrishankar, C. B. Patel, I. S. Alam, S. Murty, S. S. Gambhir, *Proc. Natl. Acad. Sci. U. S. A.* **2019**, *166*, 11402–11407.

[22] J. I. Andrés, J. Alcázar, J. M. Cid, M. De Angelis, L. Iturrino, X. Langlois, H. Lavreysen, A. A. Trabanco, S. Celen, G. Bormans, *J. Med. Chem.* **2012**, *55*, 8685–8699.

[23] L. Zhang, C. R. Butler, K. P. Maresca, A. Takano, S. Nag, Z. Jia, R. Arakawa, J. R. Piro, T. Samad, D. L. Smith, D. M. Nason, S. O'Neil, L. McAllister, K. Schildknegt, P. Trapa, T. J. McCarthy, A. Villalobos, C. Halldin, *J. Med. Chem.* **2019**, *62*, 8532–8543.

6. Supporting Information

6.1 General Information

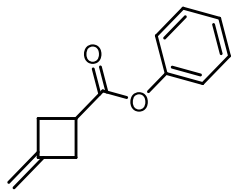
All NMR spectra were recorded on Bruker DPX200, DPX400, AV400, AV500 and DRX500 spectrometers. ^{1}H and ^{13}C NMR spectral data are reported as chemical shifts (δ) in parts per million (ppm) relative to the solvent peak using the Bruker internal referencing procedure (edlock). $^{19}FNMR$ spectra are referenced relative to $CFCl_3$ in $CDCl_3$. Coupling constants (J) are measured in hertz (Hz). The following abbreviations are used to describe multiplicities s=singlet, d=doublet, t=triplet, q=quartet, pent=pentet, br=broad, m=multiplet. NMR spectra were processed in MestreNova/ACD. High resolution mass spectra (HRMS, m/z) were recorded on a Bruker MicroTOF spectrometer using positive electrospray ionization (ESI) or on a Micromass GCT spectrometer using field ionization (EI/FI). IR spectra were recorded on a Bruker Tensor 27 FT-IR spectrometer. Absorptions are measured in wavenumbers and only peaks of interest are reported. Melting points of solids were measured on a Griffin apparatus. IUPAC names were obtained using the ChemDraw service. Weighing was performed with a 4 decimal place balance. All reactions for hydrodifluoromethylation of alkenes were conducted in non-dried glassware with magnetic stirring. All solvents were used as received without further purification. Flash column chromatography was performed over Merck silica gel C60 (40−60 µm) using the eluent system described for each experiment. Difluoroacetic acid was purchased from Sigma-Aldrich, TCI and FluoroChem. PIDA

was purchased from Sigma-Aldrich and Carbosynth. All commercially available substrates were purchased from commercial suppliers or otherwise synthesized according to literature.[1-6] Reactions were performed in 7 mL vials in a EvoluChem^{TM} PhotoRedOx Box with a 18W blue LED lamp (λ = 450 nm). The large scale hydrodifluoromethylation was performed using a Radleys Reactor Ready of 2 Liters and the temperature controlled using a Julabo A80 unit. The yields were determined by either ^{19}F NMR spectroscopy or by the isolation on SiO_2 gel column chromatography. If the purity of the compounds was not satisfying an analytical sample was further purified by reverse phase HPLC purification.

6.2 Supporting information for Chapter 2

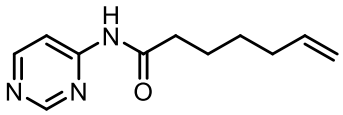
6.2.1 Synthesis of starting materials

Phenyl 3-methylenecyclobutane-1-carboxylate (2.20m)



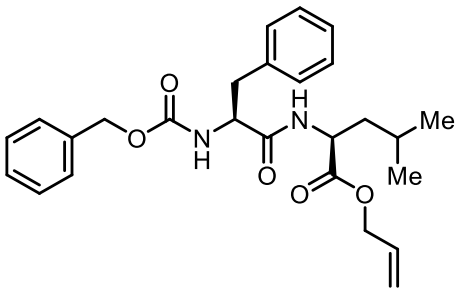
To a suspension of 3-methylenecyclobutanecarboxylic acid (590 mg, 5.26 mmol, 1.0 equiv), *N*,*N*'-dicyclohexylcarbodiimide (1.19 g, 5.79 mmol, 1.1 equiv) and 4-dimethylaminopyridine (128 mg, 1.05 mmol, 0.2 equiv) in DMF (40 mL) was added a solution of phenol (594 mg, 6.31 mmol, 1.2 equiv) in DMF (10 mL). The mixture was stirred at rt for 18 h. The mixture was concentrated *in vacuo*, redissolved in EtOAc (20 mL), filtered through a celite pad and concentrated *in vacuo*. The crude product was purified by column chromatography (silica, EtOAc in heptane 0/100 to 10/90) to yield **2.20m** (660 mg, 3.51 mmol, 67%) as a colourless oil. **^{1}H NMR** (500 MHz, $CDCl_3$) δ 7.41 – 7.35 (m, 2H), 7.25 – 7.21 (m, 1H), 7.12 – 7.07 (m, 2H), 4.88 – 4.85 (m, 2H), 3.38 (tt, *J* = 9.1, 7.4 Hz, 1H), 3.21 – 3.12 (m, 2H), 3.08 – 3.00 (m, 2H); **^{13}C NMR** (126 MHz, $CDCl_3$) δ 173.7, 150.9, 143.9, 129.6, 125.9, 121.6, 107.4, 35.7, 33.5; **HRMS** (ESI-TOF): calculated for $C_{12}H_{13}O_2$ $[M+H]^+$: 189.0910; found: 189.0910; **IR** (neat): 1751, 1594, 1493, 1347, 1194, 1160, 1133, 1025, 917, 878, 835, 748, 688 cm^{-1}.

_N_-(pyrimidin-4-yl)hept-6-enamide (2.20r)



To a solution of pyrimidin-4-amine (190 mg, 2.00 mmol, 1.0 equiv) in DMF (4 mL) was added 6-heptenoic acid (307 mg, 2.40 mmol, 1.2 equiv), EDCl (458 mg, 2.40 mmol, 1.2 equiv) and 4-(dimethylamino)-pyridine (24 mg, 0.20 mmol, 0.1 equiv). The reaction mixture was stirred at 30 °C for 24 h. Water (20 mL) was added and the mixture was extracted with EtOAc (3 x 10 mL), dried (Na_2SO_4), filtered, and concentrated *in vacuo*. Pentane/Et_2O (1:1, 5 mL) was added and the mixture was cooled to -18 °C. The solids were collected by filtration and dried under air to yield **2.20r** (227 mg, 1.11 mmol, 55%) as an off-white solid. **^{1}H NMR** (400 MHz, $CDCl_3$) δ 8.93 (s, 1H), 8.85 (d, *J* = 1.3 Hz, 1H), 8.61 (d, *J* = 5.8 Hz, 1H), 8.19 (dd, *J* = 5.8, 1.4 Hz, 1H), 5.75 (ddt, *J* = 16.9, 10.2, 6.7 Hz, 1H), 5.01 – 4.90 (m, 2H), 2.44 (t, *J* = 7.5 Hz, 2H), 2.05 (q, *J* = 7.1 Hz, 2H), 1.77 – 1.66 (m, 2H), 1.44 (tt, *J* = 10.1, 6.5 Hz, 2H); **^{13}C NMR** (101 MHz, $CDCl_3$) δ 172.8, 158.5, 158.2, 157.4, 138.1, 115.1, 110.5, 37.6, 33.4, 28.4, 24.5; **HRMS** (ESI-TOF): calculated for $C_{11}H_{16}N_3O$ ($[M+H]^+$): 206.1293; found: 206.1292; **IR** (neat): 2942, 1718, 1567, 1511, 1459, 1415, 1393, 1367, 1305, 1212, 1164, 1114, 1065, 995, 902, 839, 777, 642, 618 cm^{-1}; **MP**: 78 – 80 °C.

Allyl ((benzyloxy)carbonyl)-*L*-phenylalanyl-*L*-leucinate (2.20w)



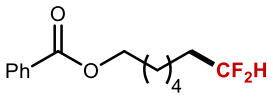
Allyl bromide (1.17 g, 9.70 mmol, 8.0 equiv) was added dropwise to a suspension of Z-Phe-Leu-OH (500 mg, 1.21 mmol, 1.0 equiv) and $NaHCO_3$ (407 mg, 4.85 mmol, 4.0 equiv) in DMF (5 mL). The mixture was stirred at rt for 48 h. Water (25 mL) was added and the mixture was extracted with DCM (3 x 10 mL). The organic layer was separated, dried (Na_2SO_4), filtered and concentrated *in vacuo* to yield **2.20w** (483 mg, 1.07 mmol, 88%) as a white solid; **^{1}H NMR** (400 MHz, $CDCl_3$) δ 7.36 – 7.13 (m, 10H), 6.58 (d, J = 6.4 Hz, 1H), 5.88 (ddt, J = 16.5, 11.0, 5.8 Hz, 1H), 5.55 (d, J = 8.3 Hz, 1H), 5.35 – 5.19 (m, 2H), 5.05 (d, J = 2.6 Hz, 2H), 4.62 – 4.48 (m, 4H), 3.09 – 3.02 (m, 2H), 1.68 – 1.39 (m, 3H), 0.96 – 0.74 (m, 6H); **^{13}C NMR** (101 MHz, $CDCl_3$) δ 172.2, 170.9, 156.0, 136.4, 131.6, 129.4, 128.6, 128.5, 128.2, 128.0, 127.0, 118.8, 67.0, 65.9, 56.0, 50.9, 41.4, 38.5, 24.8, 22.8, 22.0; **HRMS** (ESI-TOF): calculated for $C_{26}H_{33}O_5N_2$ ($[M+H]^+$): 453.2384; found: 453.2385; **IR** (neat): 3328, 3303, 2924, 1734, 1697, 1650, 1534, 1251, 1201, 1137, 1029, 919, 751, 734, 697, 655 cm^{-1}; **MP**: 84 – 85 °C.

6.2.2 Synthesis of Hydrodifluoromethylated Compounds

General procedure 1: Hydrodifluoromethylation of alkenes (2.24a – 2.24y)

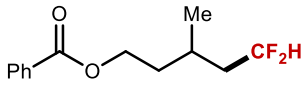
Difluoroacetic acid **2.23** (113 uL, 1.80 mmol, 6.0 equiv) was added to a suspension of (diacetoxyiodo)benzene **2.21** (290 mg, 0.90 mmol, 3.0 equiv) and alkene **2.20** (0.30 mmol) in THF (4.5 mL). The vial was stirred under blue LED irradiation at 50 °C for 6 h after which a second portion of **2.21** (diacetoxyiodo)benzene (290 mg, 1.80 mmol, 3.0 equiv) was added. The solution was stirred under blue LED irradiation for another 8 h. The solvents were removed *in vacuo* and the residue was purified by column chromatography (silica, EtOAc in heptane 0/100 to 100/0) to yield the desired product **2.24**. Reactions were performed in 7 mL vials in a EvoluChem^{TM} PhotoRedOx Box with a 18W blue LED lamp (λ = 450 nm).

7,7-difluoroheptyl benzoate (2.24a)



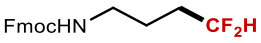
General procedure 1 was followed to obtain **2.24a** (48 mg, 0.19 mmol, 62%) as a colourless oil. **^{1}H NMR** (500 MHz, $CDCl_3$) δ 8.07 – 8.02 (m, 2H), 7.59 – 7.52 (m, 1H), 7.47 – 7.41 (m, 2H), 5.80 (tt, J = 56.6, 4.3 Hz, 1H), 4.32 (t, J = 6.7 Hz, 2H), 1.90 – 1.74 (m, 4H), 1.53 – 1.38 (m, 6H); **^{13}C NMR** (126 MHz, $CDCl_3$) δ ppm 166.6, 132.8, 130.4, 129.5, 128.3, 117.3 (t, $J_{C\text{-}F}$ = 238.6 Hz), 64.8, 34.0 (t, $J_{C\text{-}F}$ = 20.7 Hz), 28.7, 28.5, 25.8, 22.0 (t, $J_{C\text{-}F}$ = 5.3 Hz); **^{19}F NMR** (471 MHz, $CDCl_3$) δ ppm -115.8 (dt, J = 57.2, 17.0 Hz, 2F); **HRMS** (ESI-TOF): calculated for $C_{14}H_{19}O_2F_2$ ($[M+H]^+$): 257.1348; found: 257.1348. Spectroscopic data were in accordance with previous reports.[1]

5,5-difluoro-3-methylpentyl benzoate (2.24b)



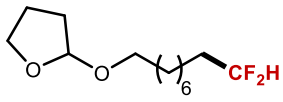
General procedure 1 was followed to obtain **2.24b** (42 mg, 0.17 mmol, 57%, [NMR yield: 71%]) as a colourless oil. **^{1}H NMR** (500 MHz, $CDCl_3$) δ 8.02 – 8.06 (m, 2H), 7.55 – 7.60 (m, 1H), 7.43 – 7.48 (m, 2H), 5.91 (tt, J = 57.2, 4.9 Hz, 1H), 4.35 – 4.44 (m, 2H), 1.65 – 2.06 (m, 5H), 1.09 (d, J = 6.7 Hz, 3H); **^{13}C NMR** (126 MHz, $CDCl_3$) δ 166.6, 132.9, 130.2, 129.5, 128.4, 116.7 (t, $J_{C\text{-}F}$ = 239.0 Hz), 62.6, 40.8 (t, $J_{C\text{-}F}$ = 20.3 Hz), 35.5, 25.2 (t, $J_{C\text{-}F}$ = 5.3 Hz), 19.6; **^{19}F NMR** (471 MHz, $CDCl_3$) δ -114.8 (dt, J = 57.2, 19.1 Hz, 2F); **MS** (EI): m/z = 241.9 $[M]^+$. Spectroscopic data were in accordance with previous reports.[1]

(9*H*-fluoren-9-yl)methyl (4,4-difluorobutyl)carbamate (2.24c)



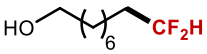
General procedure 1 was followed to obtain **2.24c** (64 mg, 0.19 mmol, 64%, [NMR yield: 76%]) as a white solid. **^{1}H NMR** (500 MHz, $CDCl_3$) δ 7.77 (d, J = 7.8 Hz, 2H), 7.59 (d, J = 7.5 Hz, 2H), 7.40 (t, J = 7.5 Hz, 2H), 7.33 – 7.30 (m, 2H), 5.96 – 5.71 (m, 1H), 4.90 – 4.58 (m, 1H), 4.54 – 4.38 (m, 2H), 4.29 – 4.18 (m, 1H), 3.32 – 2.92 (m, 2H), 1.96 – 1.76 (m, 2H), 1.74 – 1.57 (m, 2H); **^{13}C** NMR (126 MHz, $CDCl_3$) δ ppm 156.5, 143.9, 141.4, 127.7, 127.1, 125.0, 120.0, 116.9 (br t, $J_{C\text{-}F}$ = 239.0 Hz), 66.6, 47.4, 40.3, 31.3 (br t, $J_{C\text{-}F}$ = 21.6 Hz), 22.7 (br t, $J_{C\text{-}F}$ = 5.3 Hz); **^{19}F NMR** (471 MHz, $CDCl_3$) δ -116.0 (dt, J = 56.2, 18.5 Hz, 2F); **HRMS** (ESI-TOF): calculated for $C_{19}H_{19}O_2NF_2{}^{23}Na$ ($[M+Na]^+$): 354.1276; found: 354.1276; **IR** (neat): 3336, 1690, 1541, 1449, 1405, 1267, 1081, 1013, 988, 758, 741, 645 cm^{-1}; **MP**: 97 – 100 °C.

2-((9,9-difluorononyl)oxy)tetrahydrofuran (2.24d)



General procedure 1 was followed using alcohol **2.20d** to obtain **2.24d** (45 mg, 0.18 mmol, 60%, [NMR yield: 79%]) as a colourless oil. **^{1}H NMR** (400 MHz, $CDCl_3$) δ 5.77 (tt, J = 57.0, 4.6 Hz, 1H), 5.09 (dd, J = 4.5, 1.7 Hz, 1H), 3.85 (pd, J = 8.0, 6.0 Hz, 2H), 3.63 (dt, J = 9.6, 6.8 Hz, 1H), 3.35 (dt, J = 9.5, 6.6 Hz, 1H), 2.05 – 1.69 (m, 6H), 1.54 (dd, J = 9.2, 4.8 Hz, 2H), 1.48 – 1.23 (m, 10H); **^{13}C NMR** (101 MHz, $CDCl_3$) δ 117.4 (t, $J_{C\text{-}F}$ = 239.0 Hz), 103.8, 67.2, 66.7, 34.0 (t, $J_{C\text{-}F}$ = 20.4 Hz), 32.3, 29.7, 29.3, 29.2, 29.0, 26.1, 23.5, 22.1 (t, $J_{C\text{-}F}$ = 5.5 Hz); **^{19}F NMR** (377 MHz, $CDCl_3$) δ -115.8 (dt, J = 57.2, 17.7 Hz, 2F); **HRMS** (ESI-TOF): calculated for $C_{13}H_{24}O_2F_2{}^{23}Na$ ($[M+Na]^+$): 273.1637; found: 273.1636; **IR** (neat): 2931, 2858, 2160, 2031, 1122, 1092, 1038, 920 cm^{-1}.

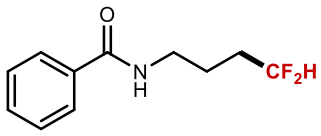
9,9-difluorononan-1-ol (2.24e)



General procedure 1 was followed using alcohol **2.20d** with the following modification: After reaction completion, HCl (conc, 0.5 mL) was added and the mixture was stirred at rt for 5 min. α,α,α-Trifluorotoluene (12.3 µL, 0.10 mmol, 0.33 equiv) was added and the mixture was analyzed by ^{19}F NMR spectroscopy. The solvents were removed *in vacuo* and the residue was purified by column chromatography (silica, EtOAc in heptane 0/100 to 100/0) to yield **2.24e** (39 mg, 0.22 mmol, 72%, [NMR yield: 76%]) as a colourless oil. **^{1}H NMR** (400 MHz, $CDCl_3$)

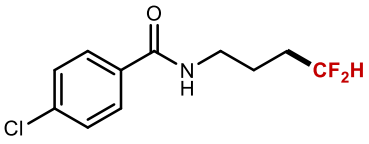
δ 5.77 (tt, J = 57.0, 4.5 Hz, 1H), 3.61 (t, J = 6.6 Hz, 2H), 1.91 – 1.63 (m, 3H), 1.60 – 1.50 (m, 2H), 1.47 – 1.38 (m, 2H), 1.31 (s, 8H); **^{13}C NMR** (101 MHz, $CDCl_3$) δ 117.6 (t, $J_{C\text{-}F}$ = 238.6 Hz), 63.0, 34.2 (t, $J_{C\text{-}F}$ = 20.5 Hz), 32.8, 29.4, 29.3, 29.1, 25.8, 22.2 (t, $J_{C\text{-}F}$ = 5.4 Hz); **^{19}F NMR** (377 MHz, $CDCl_3$) δ -115.8 (dt, J = 56.9, 17.6 Hz, 2F); **HRMS** (ESI-TOF): calculated for $C_9H_{18}OF_2{}^{23}Na$ ($[M+Na]^+$): 203.1218; found: 203.1220; **IR** (neat): 3332, 2930, 2858, 1465, 1403, 1123, 1050, 724 cm^{-1}.

_N_-(4,4-difluorobutyl)benzamide (2.24f)



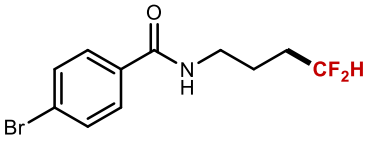
General procedure 1 was followed to obtain **2.24f** (42 mg, 0.20 mmol, 66%, [NMR yield: 76%]) as a colourless oil. **^{1}H NMR** (500 MHz, $CDCl_3$) δ ppm 7.84 – 7.72 (m, 2H), 7.53 – 7.48 (m, 1H), 7.45 – 7.40 (m, 2H), 6.38 (br s, 1H), 6.04 – 5.72 (m, 1H), 3.52 (q, J = 6.8 Hz, 2H), 1.99 – 1.86 (m, 2H), 1.84 – 1.76 (m, 2H); **^{13}C NMR** (126 MHz, $CDCl_3$) δ 167.7, 134.4, 131.5, 128.6, 126.8, 116.9 (t, $J_{C\text{-}F}$ = 239.4 Hz), 39.2, 31.5 (t, $J_{C\text{-}F}$ = 21.1 Hz), 22.4 (t, $J_{C\text{-}F}$ = 5.3 Hz); **^{19}F NMR** (471 MHz, $CDCl_3$) δ ppm -116.0 (dt, J = 57.2, 17.0 Hz, 2F); **HRMS** (ESI-TOF): calculated for $C_{11}H_{14}F_2NO$ ($[M+H]^+$): 214.1044; found: 214.1050; **IR** (neat): 3311, 3067, 2934, 1637, 1603, 1578, 1541, 1489, 1438, 1406, 1366, 1310, 1204, 1121, 1080, 1023, 876, 804, 696 cm^{-1}.

4-chloro-*N*-(4,4-difluorobutyl)benzamide (2.24g)



General procedure 1 was followed to obtain **2.24g** (54 mg, 0.22 mmol, 72%, [NMR yield: 73%]) as a colourless oil. **^{1}H NMR** (500 MHz, $CDCl_3$) δ 7.72 – 7.67 (m, 2H), 7.43 – 7.38 (m, 2 H), 6.23 (br s, 1 H), 5.88 (tt, J = 56.4, 4.3 Hz, 1 H), 3.51 (q, J = 6.9 Hz, 2 H), 2.00 – 1.87 (m, 2 H), 1.84 – 1.77 (m, 2 H); **^{13}C NMR** (126 MHz, $CDCl_3$) δ 166.6, 137.8, 132.8, 128.9, 128.3, 116.8 (t, $J_{C\text{-}F}$ = 239.0 Hz), 39.3, 31.5 (t, $J_{C\text{-}F}$ = 21.6 Hz), 22.4 (t, $J_{C\text{-}F}$ = 5.3 Hz); **^{19}F NMR** (471 MHz, $CDCl_3$) δ -116.0 (dt, J = 56.2, 18.5 Hz, 2F); **HRMS** (ESI-TOF): calculated for $C_{11}H_{13}ClF_2NO$ ($[M+H]^+$): 248.0654; found: 248.0655; **IR** (neat): 3311, 2931, 1637, 1597, 1544, 1487, 1439, 1404, 1315, 1204, 1121, 1093, 1014, 847, 758, 624 cm^{-1}.

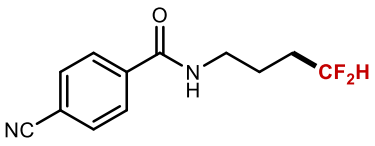
4-bromo-*N*-(4,4-difluorobutyl)benzamide (2.24h)



General procedure 1 was followed to obtain **2.24h** (51 mg, 0.17 mmol, 58%, [NMR yield: 65%]) as a white solid. **^{1}H NMR** (400 MHz, $CDCl_3$) δ 7.59 – 7.54 (m, 2H), 7.53 – 7.48 (m, 2H), 6.18 (s, 1H), 5.81 (tt, J = 56.6, 4.2 Hz, 1H), 3.44 (td, J = 7.0, 6.0 Hz, 2H), 1.94 – 1.79 (m, 2H), 1.79 – 1.68 (m, 2H); **^{13}C NMR** (101 MHz, $CDCl_3$) δ 166.8, 133.3, 132.0, 128.6, 126.4, 116.9 (t, $J_{C\text{-}F}$ = 239.2 Hz), 39.5, 31.6 (t, $J_{C\text{-}F}$ = 21.1 Hz), 22.5 (t, $J_{C\text{-}F}$ = 5.2 Hz); **^{19}F NMR** (377 MHz, $CDCl_3$) δ -116.0 (dt, J = 56.7, 17.7 Hz, 2F); **HRMS** (ESI-TOF): calculated for $C_{11}H_{13}ON^{79}BrF_2$ ($[M+H]^+$):

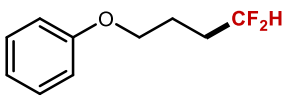
292.0143; found: 292.0143; **IR** (neat): 3306, 1629, 1591, 1539, 1391, 1279, 1118, 1095, 1056, 1021, 1010, 989, 952, 872, 840, 749, 706, 675, 623 cm^{-1}; **MP**: 86 – 88 °C.

4-cyano-N-(4,4-difluorobutyl)benzamide (2.24i)



General procedure 1 was followed to obtain **2.24i** (48 mg, 0.20 mmol, 67%, [NMR yield: 79%]) as a colourless oil. **^{1}H NMR** (500 MHz, $CDCl_3$) δ 7.84 – 7.89 (m, 2H), 7.70 – 7.75 (m, 2H), 6.54 (br s, 1H), 5.88 (tt, J = 56.93, 4.33 Hz, 1H), 3.52 (td, J = 6.94, 4.07 Hz, 2H), 1.87 – 2.00 (m, 2H), 1.78 – 1.86 (m, 2H); **^{13}C NMR** (126 MHz, $CDCl_3$) δ 165.9, 138.3, 132.4, 127.6, 117.9, 115.0, 116.7 (t, J_{C-F} = 239.0 Hz), 39.5, 31.4 (t, J_{C-F} = 21.6 Hz), 22.1 (t, J_{C-F} = 5.3 Hz); **^{19}F NMR** (471 MHz, $CDCl_3$) δ -116.1 (dt, J = 57.2, 19.1 Hz, 2F); **HRMS** (ESI-TOF): calculated for $C_{12}H_{13}F_2N_2O$ ($[M+H]^+$): 237.0920; found 237.0842; **IR** (neat): 3308, 2940, 2231, 1641, 1543, 1498, 1439, 1404, 1305, 1204, 1120, 1081, 1018, 982, 857, 765, 670, 637 cm^{-1}.

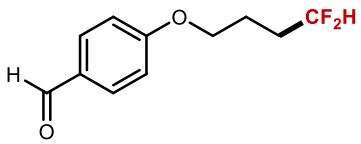
(4,4-difluorobutoxy)benzene (2.24j)



General procedure 1 was followed to obtain **2.24j** (34 mg, 0.18 mmol, 61%, [NMR yield: 69%]) as a colourless oil. **^{1}H NMR** (500 MHz, $CDCl_3$) δ 7.27 – 7.20 (m, 2H), 6.90 (tt, J = 7.4, 1.1 Hz, 1H), 6.85 – 6.81 (m, 2H), 5.86 (tt, J = 56.7, 4.3 Hz, 1H), 3.96 (t, J = 6.0 Hz, 2H), 2.06 – 1.94 (m, 2H), 1.94 – 1.87 (m, 2H); **^{13}C NMR** (126 MHz,

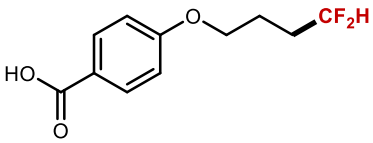
$CDCl_3$) δ 157.7, 128.5, 119.9, 116.0 (t, J_{C-F} = 238.9 Hz), 114.5, 65.6, 30.0 (t, J_{C-F} = 21.3 Hz), 21.1 (t, J_{C-F} = 5.7 Hz); **^{19}F NMR** (377 MHz, $CDCl_3$) δ -116.1 (dt, J = 56.6, 17.4 Hz, 2F); **MS** (ESI): m/z = 204.0 ($[M+NH_4]^+$). Spectroscopic data were in accordance with previous reports.[1]

4-(4,4-difluorobutoxy)benzaldehyde (2.24k)



General procedure 1 was followed to obtain **2.24k** (33 mg, 0.15 mmol, 51%, [NMR yield: 52%]) as a colourless oil. **^{1}H NMR** (500 MHz, $CDCl_3$) δ 9.90 (s, 1H), 7.85 (d, J = 9.0 Hz, 2H), 7.00 (d, J = 8.8 Hz, 2H), 5.94 (tt, J = 56.4, 4.4 Hz, 1H), 4.09 – 4.15 (m, 2H), 1.98 – 2.22 (m, 4H); **^{13}C NMR** (126 MHz, $CDCl_3$) δ 190.7, 163.7, 132.0, 130.1, 116.8 (t, J_{C-F} = 239.0 Hz), 114.7, 67.2, 30.9 (t, J_{C-F} = 21.6 Hz), 21.9 (t, J_{C-F} = 5.3 Hz); **^{19}F NMR** (471 MHz, $CDCl_3$) δ -116.3 (dt, J = 57.2, 17.0 Hz, 2F); **MS** (EI): m/z = 214.0 ($[M]^+$); **IR** (neat): 2926, 1687, 1601, 1578, 1510, 1404, 1313, 1259, 1215, 1161, 1119, 1025, 832, 619 cm^{-1}.

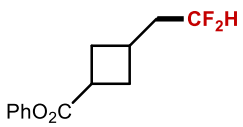
4-(4,4-difluorobutoxy)benzoic acid (2.24l)



General procedure 1 was followed to obtain **2.24l** (38 mg, 0.17 mmol, 55%, [NMR yield: 67%]) as a colourless oil. **^{1}H NMR** (500 MHz, MeOD) δ 8.00 – 7.94 (m, 2H), 7.01 – 6.94 (m, 2H), 5.97 (tt, J = 57.6, 4.2 Hz, 1H), 4.10 (t, J = 5.9 Hz, 2H), 2.11 – 1.89 (m, 4H); **^{13}C NMR** (126 MHz, MeOD) δ 169.9, 164.4, 133.0, 124.3, 118.8 (t,

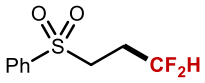
J_{C-F} = 237.2 Hz), 115.3, 68.5, 32.1 (t, J_{C-F} = 21.6 Hz), 23.3 (t, J_{C-F} = 6.2 Hz); **^{19}F NMR** (471 MHz, MeOD) δ -117.8 (dt, J = 57.2, 17.0 Hz, 2F); **HRMS** (ESI-TOF): calculated for $C_{11}H_{11}F_2O_3$ ([M-H]$^-$): 229.0675; found 229.0675; **IR** (neat): 2922, 1678, 1607, 1580, 1514, 1429, 1293, 1253, 1203, 1171, 1122, 1032, 989, 936, 846, 769, 693, 646 cm^{-1}.

Phenyl 3-(2,2-difluoroethyl)cyclobutane-1-carboxylate (2.24m)



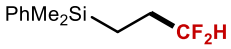
General procedure 1 was followed to obtain **2.24m** (60 mg, 0.23 mmol, 75%, [NMR yield: 83%]) as a colourless oil; d.r: 70/30 (Stereochemistry of major diastereomer not assigned). **^{1}H NMR** (500 MHz, $CDCl_3$) δ 7.41 – 7.35 (m, 2H), 7.25 – 7.21 (m, 1H), 7.11 – 7.06 (m , 2H), 5.78 (tt, J = 56.06, 4.62 Hz, 1H), 3.39 – 3.24 (m, 1H), 2.82 – 2.49 (m, 3H), 2.21 – 2.12 (m, 2H), 2.11 – 1.95 (m, 2H); **^{13}C NMR** (126 MHz, $CDCl_3$) δ 174.1, 173.2, 150.8, 150.7, 129.4, 125.8, 121.4, 116.7 (t, J_{C-F} = 237.7 Hz), 116.5 (t, J_{C-F} = 240.3 Hz), 40.4 (t, J_{C-F}= 21.1 Hz), 40.1 (t, J_{C-F} = 20.3 Hz), 35.4, 35.2, 31.5, 30.3, 26.6 (t, J_{C-F} = 5.3 Hz), 25.5 (t, J_{C-F} = 5.3 Hz); **^{19}F NMR** (471 MHz, $CDCl_3$) δ -115.62 (dt, J = 55.1, 17.0 Hz, 0.65F), -116.2 (dt, J = 57.2, 17.0 Hz, 1.35F); **HRMS** (ESI-TOF): calculated for $C_{13}H_{15}O_2F_2$ ([M+H]$^+$): 241.1035; found: 241.1034; **IR** (neat): 2980, 1750, 1593, 1492, 1457, 1434, 1402, 1377, 1242, 1196, 1162, 1140, 1122, 1073, 1014, 833, 737, 689 cm^{-1}.

((3,3-difluoropropyl)sulfonyl)benzene (2.24n)



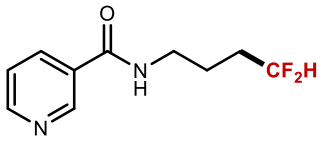
General procedure 1 was followed to obtain **2.24n** (38 mg, 0.17 mmol, 58%, [NMR yield: 66%]) as a white solid. **^{1}H NMR** (500 MHz, $CDCl_3$) δ 7.91 – 7.97 (m, 2H), 7.68 – 7.73 (m, 1H), 7.58 – 7.64 (m, 2H), 6.00 (tt, J = 56.1, 4.1 Hz, 1H), 3.20 – 3.30 (m, 2H), 2.22 – 2.40 (m, 2H); **^{13}C NMR** (126 MHz, $CDCl_3$) δ 138.5, 134.2, 129.5, 128.0, 114.6 (t, $J_{C\text{-}F}$ = 240.8 Hz), 49.2 (t, $J_{C\text{-}F}$ = 5.7 Hz), 27.7 (t, $J_{C\text{-}F}$ = 22.9 Hz); **^{19}F NMR** (471 MHz, $CDCl_3$) δ -117.0 (dt, J = 55.1, 17.0 Hz, 2F); **MS** (EI): m/z = 220.0 ($[M]^+$); **IR** (neat): 2981, 1585, 1447, 1407, 1308, 1280, 1239, 1172, 1146, 1119, 1086, 1044, 999, 938, 910, 798, 744, 689 cm^{-1}. Spectroscopic data were in accordance with previous reports.[1]

(3,3-difluoropropyl)dimethyl(phenyl)silane (2.24o)



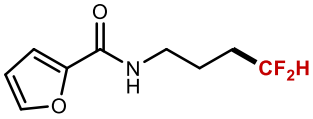
General procedure 1 was followed to obtain **2.24o** (38 mg, 0.18 mmol, 60%, [NMR yield: 92%]) as a colourless oil. **^{1}H NMR** (500 MHz, $CDCl_3$) δ 7.55 – 7.48 (m, 2H), 7.43 – 7.36 (m, 3H), 5.73 (tt, J = 57.5, 4.6 Hz, 1H), 1.87 – 1.73 (m, 2H), 0.92 – 0.84 (m, 2H), 0.32 (s, 6 H); **^{13}C NMR** (126 MHz, $CDCl_3$) δ 138.0, 133.5, 129.2, 127.9, 118.2 (t, $J_{C\text{-}F}$ = 239.9 Hz) 28.8 (t, $J_{C\text{-}F}$ = 21.6 Hz), 7.48 (t, $J_{C\text{-}F}$ = 4.0 Hz), -3.4; **^{19}F NMR** (471 MHz, $CDCl_3$) δ ppm -116.6 (dt, J = 57.2, 17.0 Hz, 2F); **HRMS**: the compound did not ionise under various ionisation techniques; **MS** (EI): m/z = 135.0 [M-$CH_2CH_2CHF_2$], 199.0 [M-CH_3]; **IR** (neat): 3071, 2956, 2927, 2356, 1957, 1427, 1395, 1363, 1251, 1175, 1115, 1043, 873, 837, 816, 779, 731, 700, 634, 632, 613 cm^{-1}.

***N*-(4,4-difluorobutyl)nicotinamide (2.24p)**



General procedure 1 was followed to obtain **2.24p** (42 mg, 0.20 mmol, 65%, [NMR yield: 77%]) as a colourless oil. **^{1}H NMR** (500 MHz, $CDCl_3$) δ 8.96 (d, J = 1.7 Hz, 1H), 8.70 (dd, J = 4.9, 1.5 Hz, 1H), 8.11 (dt, J = 8.1 Hz, 2.0 Hz, 1H), 7.42 – 7.34 (m, 1H), 6.72 (br s , 1H), 5.87 (td, J = 57.5, 4.3 Hz, 1H), 3.56 – 3.50 (m, 2H), 2,01 – 1.87 (m, 2H), 1.85 – 1.77 (m, 2H); **^{13}C NMR** (126 MHz, $CDCl_3$) δ 165.8, 152.2, 147.7, 135.1, 130.1, 123.5, 116.7 (t, $J_{C\text{-}F}$ = 239.0 Hz), 39.3, 31.4 (t, $J_{C\text{-}F}$ = 21.6 Hz), 22.3 (t, $J_{C\text{-}F}$ = 5.3 Hz); **^{19}F NMR** (471 MHz, $CDCl_3$) δ -116.1 (dt, J = 56.2, 18.5 Hz, 2F); **HRMS** (ESI-TOF): calculated for $C_{10}H_{13}F_2N_2O$ ($[M+H]^+$): 215.0920; found 215.0995; **IR** (neat): 3289, 2939, 1643, 1594, 1548, 1476, 1440, 1418, 1314, 1198, 1165, 1121, 1082, 1026, 877, 828, 707 cm^{-1}.

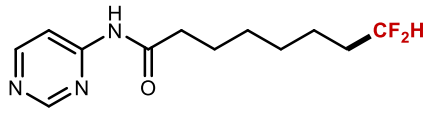
***N*-(4,4-difluorobutyl)furan-2-carboxamide (2.24q)**



General procedure 1 was followed to obtain **2.24q** (37 mg, 0.18 mmol, 61%, [NMR yield: 67%]) as a light brown oil. **^{1}H NMR** (400 MHz, $CDCl_3$) δ 7.42 (dd, J = 1.8, 0.8 Hz, 1H), 7.10 (dd, J = 3.5, 0.9 Hz, 1H), 6.49 (qt, J = 4.0, 2.4 Hz, 2H), 5.86 (tt, J = 56.6, 4.2 Hz, 1H), 3.48 (q, J = 6.7 Hz, 2H), 2.12 – 1.73 (m, 6H); **^{13}C NMR** (101 MHz, $CDCl_3$) δ 158.7, 147.9, 144.0, 117.0 (t, $J_{C\text{-}F}$ = 239.2 Hz), 114.4, 112.3, 38.4, 31.5 (t, $J_{C\text{-}F}$ = 21.4 Hz), 22.6 (t, $J_{C\text{-}F}$ = 5.4 Hz); **^{19}F NMR** (377 MHz, $CDCl_3$) δ -116.1

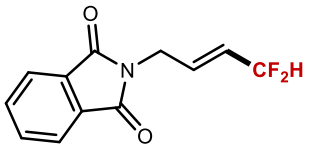
(dt, *J* = 56.8, 17.6 Hz, 2F); **HRMS** (ESI-TOF) calculated for $C_9H_{12}O_2NF_2$ ([M+H]$^+$): 204.0831; found: 204.0832; **IR** (neat): 3306, 2939, 1645, 1594, 1574, 1530, 1476, 1440, 1407, 1381, 1303, 1228, 1186, 1121, 1080, 1009, 932, 885, 861, 758, 701 cm^{-1}.

8,8-difluoro-*N*-(pyrimidin-4-yl)octanamide (2.24r)



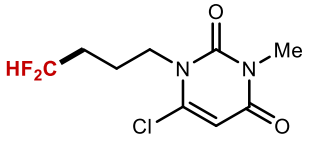
General procedure 1 was followed to obtain **2.24r** (42 mg, 0.16 mmol, 54%, [NMR yield: 56%]) as a white solid. **^{1}H NMR** (400 MHz, $CDCl_3$) δ 8.87 (d, *J* = 1.1 Hz, 1H), 8.64 (d, *J* = 5.7 Hz, 1H), 8.43 – 8.32 (m, 1H), 8.19 (dd, *J* = 5.8, 1.2 Hz, 1H), 5.79 (tt, *J* = 56.9, 4.5, 1H), 2.45 (t, *J* = 7.5 Hz, 2H), 1.96 – 1.71 (m, 4H), 1.50 – 1.21 (m, 6H); **^{13}C NMR** (101 MHz, $CDCl_3$) δ 172.5, 158.4, 158.2, 157.2, 117.3 (t, $J_{C\text{-}F}$ = 238.8 Hz), 110.4, 37.5, 33.9 (t, $J_{C\text{-}F}$ = 20.5 Hz), 28.9, 28.8, 24.7, 21.9 (t, $J_{C\text{-}F}$ = 5.5 Hz); **^{19}F NMR** (377 MHz, $CDCl_3$) δ -115.8 (dt, *J* = 57.0, 17.7 Hz, 2F); **HRMS** (ESI-TOF) calculated for $C_{12}H_{18}F_2N_3O$ ([M+H]$^+$): 258.1418; found: 258.1422**; IR** (neat): 2936, 2863, 2361, 1717, 1584, 1514, 1474, 1460, 1398, 1378, 1356, 1307, 1267, 1224, 1198, 1175, 1123, 1094, 1063, 1018, 995, 957, 920, 852, 822, 785, 722, 671, 617 cm^{-1}; **MP**: 103 – 104 °C.

(*E*)-2-(4,4-difluorobut-2-en-1-yl)isoindoline-1,3-dione (2.24s)



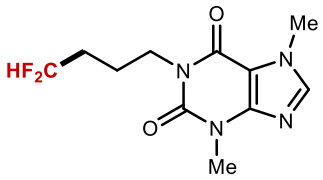
General procedure 1 was followed to obtain **2.24s** (23 mg, 0.10 mmol, 32%, [NMR yield: 46%]) as a colourless oil. **^{1}H NMR** (500 MHz, $CDCl_3$) δ 7.88 (dd, J = 5.4, 3.1 Hz, 2H), 7.75 (dd, J = 5.5, 3.0 Hz, 2H), 6.19 – 5.94 (m, 2H), 5.81 (dtdt, J = 15.4, 8.6, 5.0, 1.6 Hz, 1H), 4.48 – 4.27 (m, 2H); **^{13}C NMR** (126 MHz, $CDCl_3$) δ 167.6, 134.3, 132.1 (t, $J_{C\text{-}F}$ = 11.5 Hz), 131.9, 125.9 (t, $J_{C\text{-}F}$ = 24.0 Hz), 123.5, 113.9 (t, $J_{C\text{-}F}$ = 235.2 Hz), 38.1; **^{19}F NMR** (377 MHz, $CDCl_3$) δ -111.5 – -113.3 (m, 2F); **HRMS** (ESI-TOF): calculated for $C_{12}H_9O_2NF_2Na$ ($[M+Na]^+$): 260.0494; found: 260.0495; **IR** (neat): 2361, 2341, 1710, 1389, 1012, 722 cm^{-1}.

6-chloro-1-(4,4-difluorobutyl)-3-methylpyrimidine-2,4(1*H*,3*H*)-dione (2.24t)



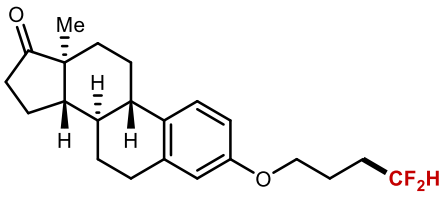
General procedure 1 was followed to obtain **2.24t** (46 mg, 0.18 mmol, 61%, [NMR yield: 65%]) as a white solid. **^{1}H NMR** (500 MHz, $CDCl_3$) δ 6.01 – 5.74 (m, 2H), 4.13 (t, J = 7.5 Hz, 2H), 3.33 (s, 3H), 2.01 – 1.86 (m, 4H); **^{13}C NMR** (126 MHz, $CDCl_3$) δ 160.7, 151.0, 145.1, 116.3 (t, $J_{C\text{-}F}$ = 239.4 Hz), 102.2, 46.2, 31.0 (t, $J_{C\text{-}F}$ = 22.0 Hz), 28.3, 21.4 (t, $J_{C\text{-}F}$ = 5.3 Hz); **^{19}F NMR** (471 MHz, $CDCl_3$) δ -116.2 (dt, J = 55.6, 17.8 Hz, 2F); **HRMS** (ESI-TOF): calculated for $C_9H_{12}O_2N_2{}^{35}ClF_2$ ($[M+H]^+$): 253.0550; found 253.0550; **IR** (neat): 1711, 1659, 1606, 1441, 1407, 1360, 1203, 1121, 1077, 972, 811, 757 cm^{-1}; **MP**: 70 – 72 °C.

1-(4,4-difluorobutyl)-3,7-dimethyl-3,7-dihydro-1*H*-purine-2,6-dione (2.24u)



General procedure 1 was followed to obtain **2.24u** (41 mg, 0.15 mmol, 50%, [NMR yield: 89%]) as a white solid. **^{1}H NMR** (500 MHz, $CDCl_3$) δ 7.52 (s, 1H), 6.00 – 5.72 (m, 1H), 4.07 (t, J = 6.94 Hz, 2H), 3.99 (s, 3H), 3.58 (s, 3H), 1.98 – 1.79 (m, 4H); **^{13}C NMR** (126 MHz, $CDCl_3$) δ 155.2, 151.5, 148.9, 141.6, 117.0 (t, $J_{C\text{-}F}$ = 239.0 Hz), 107.6, 40.4, 33.6, 31.6 (t, $J_{C\text{-}F}$ = 21.1 Hz), 29.7, 21.0 (t, $J_{C\text{-}F}$ = 5.7 Hz); **^{19}F NMR** (471 MHz, $CDCl_3$) δ -115.9 (dt, J = 57.2, 17.0 Hz, 2F); **HRMS** (ESI-TOF): calculated for $C_{11}H_{15}F_2N_4O_2$ ($[M+H]^+$): 273.1163; found: 273.1165; **IR** (neat): 2957, 1701, 1654, 1605, 1550, 1456, 1413, 1358, 1325, 1287, 1235, 1188, 1120, 1052, 1014, 846, 763, 749, 613 cm^{-1}; **MP**: 100 – 104 °C.

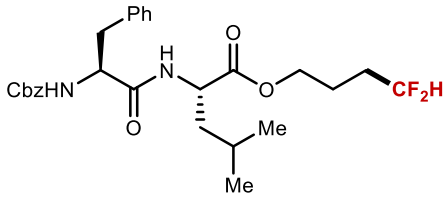
(8*S*,9*R*,13*R*,14*R*)-3-(4,4-difluorobutoxy)-13-methyl-6,7,8,9,11,12,13,14,15,16-decahydro-17*H*-cyclopenta[*a*]phenanthren-17-one (2.24v)



General procedure 1 was followed to obtain **2.24v** (46 mg, 0.13 mmol, 42%, [NMR yield: 60%]) as a white solid. **^{1}H NMR** (400 MHz, $CDCl_3$) δ 7.21 (d, J = 8.6 Hz, 1H), 6.71 (d, J = 8.8 Hz, 1H), 6.65 (s, 1H), 5.92 (tt, J = 56.6, 4.9, Hz, 1H), 4.00 (t, J = 5.8 Hz, 2H), 2.95 – 2.86 (m 2H), 2.51 (dd, J = 18.4, 8.4 Hz, 1H), 2.45 – 2.36 (m, 1H), 2.32 – 2.22 (m, 1H), 2.20 – 1.88 (m, 8H), 1.71 – 1.58 (m, 2H), 1.55 – 1.35 (m, 4H),

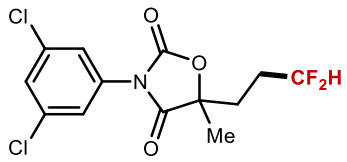
0.92 (s, 3H); **^{13}C NMR** (101 MHz, $CDCl_3$) δ 220.9, 156.9, 138.0, 132.4, 126.5, 117.2 (t, J_{C-F} = 239.0 Hz), 114.7, 112.2, 66.9, 50.6, 48.1, 44.1, 38.5, 36.0, 31.7, 31.2 (t, J_{C-F} = 21.5 Hz), 29.8, 26.7, 26.1, 22.3 (t, J_{C-F} = 5.5 Hz), 21.7, 14.0; **^{19}F NMR** (471 MHz, MeOD) δ -116.1 (dt, J = 56.2, 18.5 Hz, 2F); **HRMS** (ESI-TOF): calculated for $C_{22}H_{29}O_2F_2$ ([M+H]$^+$): 363.2130; found 363.2130; **IR** (neat): 3730, 2928, 2862, 2360, 2340, 1737, 1609, 1574, 1500, 1475, 1452, 1406, 1374, 1281, 1256, 1162, 1120, 1056, 1031, 1006, 870, 817, 668, 619 cm^{-1}; **MP**: 101 – 103 °C.

4,4-difluorobutyl ((benzyloxy)carbonyl)-*L*-phenylalanyl-*L*-leucinate (2.24w)



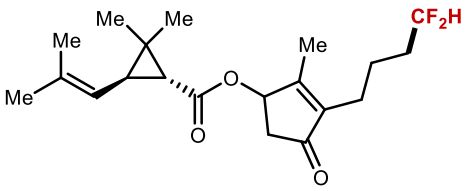
General procedure 1 was followed to obtain **2.24w** (77 mg, 0.15 mmol, 51%, [NMR yield: 62%]) as a white solid. **^{1}H NMR** (400 MHz, $CDCl_3$) δ 7.34 – 7.09 (m, 10H), 6.11 (d, J = 8.0 Hz, 1H), 5.79 (tt, J = 56.3, 4.1 Hz, 1H), 5.28 – 5.13 (m, 1H), 5.02 (d, J = 1.3 Hz, 2H), 4.45 (td, J = 8.4, 5.3 Hz, 1H), 4.37 (q, J = 7.3 Hz, 1H), 4.15 – 4.00 (m, 2H), 3.02 (qd, J = 13.9, 6.7 Hz, 2H), 1.97 – 1.78 (m, 4H), 1.63 – 1.41 (m, 3H), 0.82 (dd, J = 6.1, 4.6 Hz, 6H); **^{13}C NMR** (101 MHz, $CDCl_3$) δ 172.3, 170.6, 155.9, 136.2, 136.1, 129.4, 128.7, 128.6, 128.3, 128.1, 127.1, 116.6 (t, J_{C-F} = 239.2 Hz), 67.2, 64.2, 56.0, 50.9, 41.4, 38.2, 30.7 (t, J_{C-F} = 21.6 Hz), 24.8, 22.7, 21.9, 21.3 (t, J_{C-F} = 5.6 Hz); **^{19}F NMR** (376 MHz, $CDCl_3$) δ -116.4 (dt, J = 56.3, 17.3 Hz, 2F); **HRMS** (ESI-TOF): calculated for $C_{27}H_{35}F_2N_2O_5$ ([M+H]$^+$): 505.2514; found: 505.2509; **IR** (neat): 3306, 3065, 2959, 1739, 1701, 1658, 1539, 1454, 1369, 1258, 1124, 1051, 1027, 743, 698 cm^{-1}; **MP**: 64 – 65 °C.

3-(3,5-dichlorophenyl)-5-(3,3-difluoropropyl)-5-methyloxazolidine-2,4-dione (2.24x)



General procedure 1 was followed to obtain **2.24x** (90 mg, 0.27 mmol, 89%, [NMR yield: 96%]) as a white solid. **^{1}H NMR** (500 MHz, $CDCl_3$) δ 7.44 – 7.46 (m, 2H), 7.42 – 7.44 (m, 1H), 5.90 (tt, J = 56.1 Hz, 3.8 Hz, 1H), 1.86 – 2.19 (m, 4H), 1.70 (s, 3H); **^{13}C NMR** (126 MHz, $CDCl_3$) δ 173.0, 152.0, 135.5, 132.4, 129.1, 123.7, 115.6 (t, J_{C-F} = 239.9 Hz), 84.7, 29.0 (t, J_{C-F} = 5.7 Hz), 28.0 (t, J_{C-F} = 22.5 Hz), 22.3; **^{19}F NMR** (471 MHz, $CDCl_3$) δ -116.9 (dt, J = 57.2, 17.0 Hz, 2F); **MS** (EI): m/z = 337.0 ($[M]^+$). Spectroscopic data were in accordance with previous reports.[1]

3-(4,4-difluorobutyl)-2-methyl-4-oxocyclopent-2-en-1-yl (1R,3R)-2,2-dimethyl-3-(2-methylprop-1-en-1-yl)cyclopropane-1-carboxylate (2.24y)



General procedure 1 was followed to obtain **2.24y** (46 mg, 0.13 mmol, 43%, [NMR yield: 62%]) as a colourless oil; d.r: 1/1. **^{1}H NMR** (500 MHz, $CDCl_3$) δ 5.94 – 5.64 (m, 2H), 4.90 (ddq, J = 9.1, 5.7, 1.4 Hz, 1H), 2.85 (ddd, J = 18.6, 13.5, 6.3 Hz, 1H), 2.33 – 2.24 (m, 3H), 2.11 – 2.07 (m, 1H), 2.03 (dd, J = 10.3, 0.9 Hz, 3H), 1.89 – 1.69 (m, 8H), 1.64 – 1.55 (m, 2H), 1.41 (dd, J = 6.4, 5.4 Hz, 1H), 1.30 (d, J = 13.1 Hz, 3H), 1.15 (d, J = 5.9 Hz, 3H); **^{13}C NMR** (126 MHz, $CDCl_3$) δ 204.5, 204.4, 172.44, 172.40,

165.8, 165.7, 143.1, 143.0,136.11, 136.08, 120.9, 120.8, 117.2 (t, $J_{C\text{-}F}$ = 239.0 Hz), 116.5, 73.0, 72.7, 42.2, 41.8, 34.73, 34.68, 33.89 (t, $J_{C\text{-}F}$ = 21.0 Hz), 33.1, 33.2, 29.9, 29.3, 25.7, 22.5, 22.3, 22.2, 20.72 (t, $J_{C\text{-}F}$ = 5.7 Hz), 20.7, 20.6, 18.7, 14.2, 14.1; **^{19}F NMR** (377 MHz, $CDCl_3$) δ -115.9 (dt, J = 57.0, 17.5 Hz, 2F); **MS** (ESI): m/z = 377.2 ($[M+Na]^+$). Spectroscopic data were in accordance with previous reports.[1]

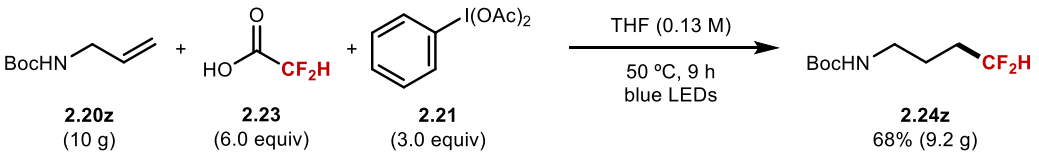
6.2.3 Scale-up experiments

General procedure 2: Large scale hydrodifluoromethylation 2.24z, 2.24aa

The reaction was performed in a 2000 mL reactor with a water heating jacket, internal temperature control and mechanical overhead stirring.

In the reactor, difluoroacetic acid **2.23** (6.0 equiv) was added dropwise to a suspension of PIDA **2.21** (1.0 equiv) and alkene **2.20** (10 g) in THF (500 mL) at 10 °C. The mixture was warmed to 50 °C under stirring and irradiated with two Kessil H150-Blue LED lights (34 W, 3 cm distance, see picture above) for 3 h, after which a second portion of PIDA (1.0 equiv) was added. Irradiation was continued for 3 h, after which a third portion of PIDA (1.0 equiv) was added and the mixture was stirred under irradiation for another 3 h. The mixture was cooled to 0 °C and quenched by addition of $NaHSO_3$ (sat. aq. 500 mL). EtOAc (100 mL) was added and the layers were separated. The aqueous layer was extracted with EtOAc (2 x 250 mL). The combined organic layers were dried (Na_2SO_4), filtered and concentrated *in vacuo*. The crude product was purified by flash column chromatography (silica, EtOAc in heptane 0/100 to 20/80).

***tert*-butyl (4,4-difluorobutyl)carbamate (2.24z)**

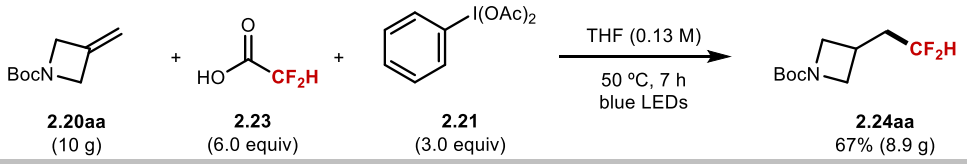


2.20z (10 g) + **2.23** (6.0 equiv) + **2.21** (3.0 equiv) → **2.24z** 68% (9.2 g)

General procedure 2 was followed to obtain *tert*-butyl (4,4-difluorobutyl)carbamate **2.24z** (9.1 g, 43.49 mmol, 68%) as a colourless oil. **^{1}H NMR** (400 MHz, $CDCl_3$) δ 5.84 (tt, J = 56.8, 4.2 Hz, 1H), 4.60 (br s, 1H), 3.18 (q, J =

6.5 Hz, 2H), 1.92 – 1.80 (m, 2H), 1.69 – 1.62 (m, 2H), 1.45 (s, 9H); **^{13}C NMR** (126 MHz, $CDCl_3$) δ 156.0, 117.0 (t, $J_{C\text{-}F}$ = 238.8 Hz), 79.3, 39.8, 31.3 (t, $J_{C\text{-}F}$ = 21.3 Hz), 28.3, 22.8 (t, $J_{C\text{-}F}$ = 5.1 Hz); **^{19}F NMR** (377 MHz, $CDCl_3$) δ -116.0 (dt, J = 56.7, 17.3, 2F); **HRMS**: the compound did not ionise under various ionisation techniques; **IR** (neat): 3352, 2980, 1687, 1518, 1366, 1251, 1168, 1121, 1081, 1047, 780 cm^{-1}.

***tert*-butyl 3-(2,2-difluoroethyl)azetidine-1-carboxylate (2.24aa)**

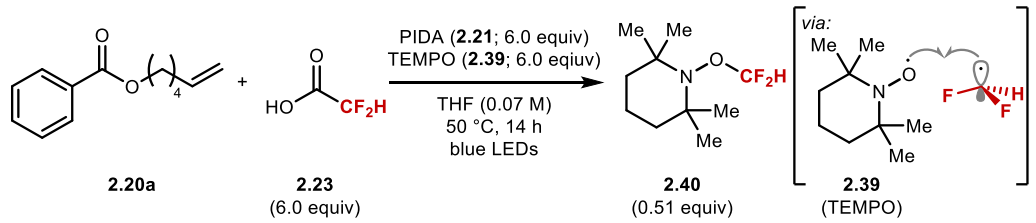


2.20aa (10 g) + **2.23** (6.0 equiv) + **2.21** (3.0 equiv) → **2.24aa** 67% (8.9 g)

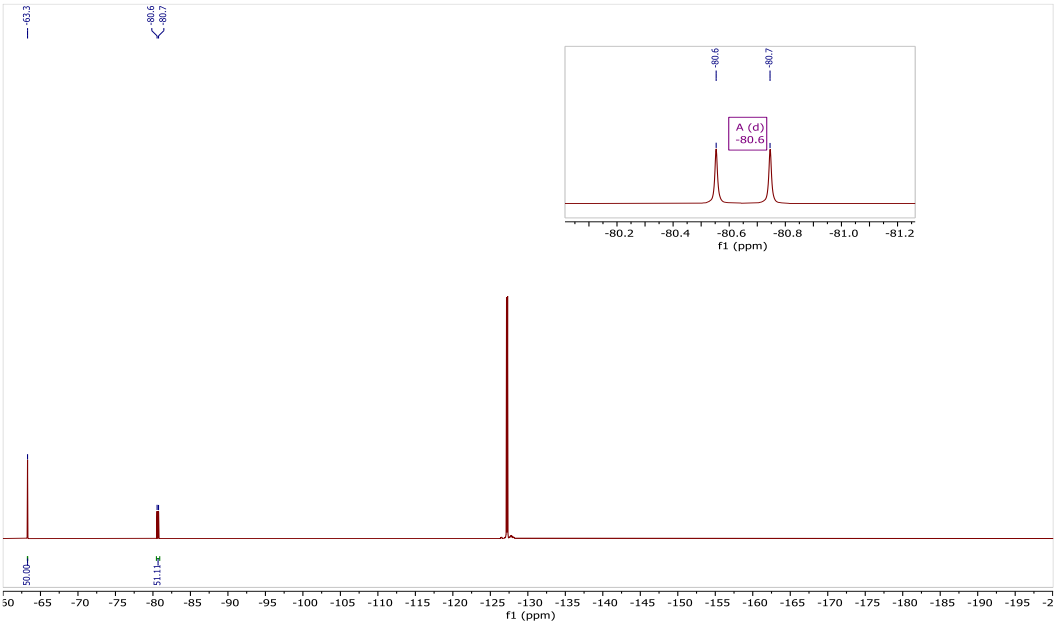
General procedure 2 was followed to obtain *tert*-butyl 3-(2,2-difluoroethyl)azetidine-1-carboxylate **2.24aa** (8.80 g, 39.80 mmol, 67%) as a colourless oil. **^{1}H NMR** (400 MHz, $CDCl_3$) δ 5.75 (tt, J = 56.1, 4.1 Hz, 1H), 4.02 (t, J = 8.6 Hz, 2H), 3.59 (dd, J = 8.7, 5.7 Hz, 2H), 2.78 – 2.66 (m, 1H), 2.08 (tdd, J = 17.6, 7.6, 4.1 Hz, 2H), 1.37 (s, 9H); **^{13}C NMR** (101 MHz, $CDCl_3$) δ 156.2, 116.0 (t, $J_{C\text{-}F}$ = 239.5 Hz), 79.5, 54.4 (br s), 38.2 (t, $J_{C\text{-}F}$ = 20.9 Hz), 28.3, 22.9 (t, $J_{C\text{-}F}$ = 5.5 Hz); **^{19}F NMR** (377 MHz, $CDCl_3$) δ -116.4 – -117.3 (m, 2F); **HRMS** (ESI-TOF): calculated for $C_{10}H_{18}NF_2$ ($[M+H]^+$): 222.1301; found: 222.1300; **IR** (neat): 2976, 1737, 1698, 1406, 1366, 1245, 1119, 1071, 997, 952, 861, 773 cm^{-1}.

6.2.4 Mechanistic experiments

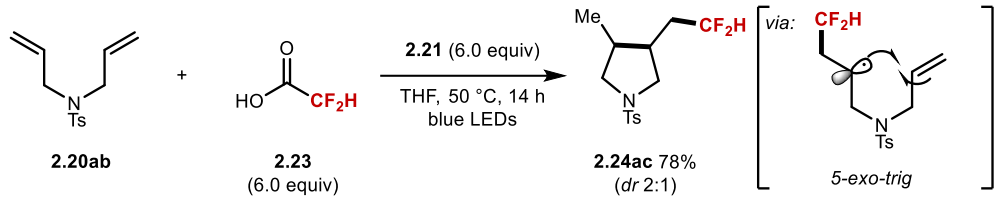
Tempo trapping



Difluoroacetic acid **2.23** (113 µL, 1.80 mmol, 6.0 equiv) was added to a suspension of PIDA (**2.21**) (293 mg, 0.90 mmol, 3.0 equiv), TEMPO (281 mg, 1.80 mmol, 6.0 equiv) and alkene **2.20a** (61 mg, 0.30 mmol, 1.0 equiv) in THF (4.5 mL) in a 7 mL vial. The vial was put in 5 cm distance of a 18 W blue LED light (λ = 450 nm) and stirred under irradiation at 50 °C for 5 h. PIDA (293 mg, 0.90 mmol, 3.0 equiv) was added and the mixture was stirred for another 10 h under blue LED irradiation. *α*,*α*,*α*-Trifluorotoluene (12.3 µL, 0.10 mmol, 1.0 equiv) was added and the mixture was analyzed by ^{19}F NMR spectroscopy. **^{19}F NMR** (377 MHz, $CDCl_3$) δ -80.4 (d, J = 72.4 Hz, 2F). Spectroscopic data is in accordance with previous reports.[1]

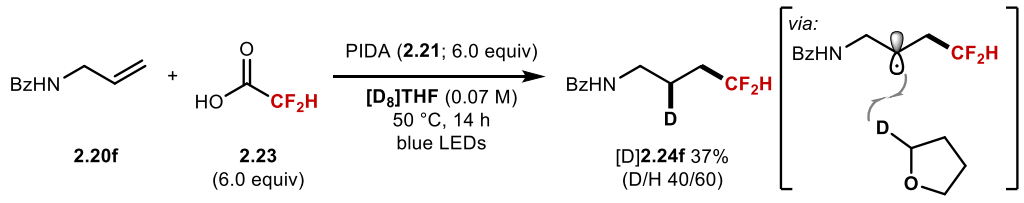


Radical clock



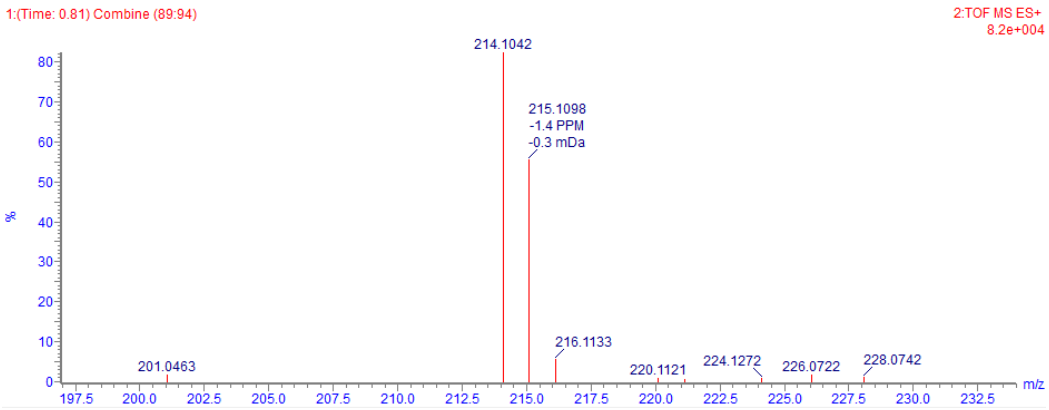
General procedure 1 was followed to obtain **2.24ac** (71 mg, 0.23 mmol, 78%) as a colourless oil. d.r: 2/1 (Stereochemistry of major diastereomer not assigned). **^{1}H NMR** (400 MHz, $CDCl_3$) δ ppm 7.71 (d, J = 7.7 Hz, 2H), 7.34 (d, J = 7.6 Hz, 2H), 5.79 (tt, J = 56.3, 4.2 Hz, 1H), 3.61 (dd, J = 10.2, 6.9 Hz, 1H), 3.51 (dd, J = 9.9, 7.0 Hz, 1H), 2.93 (dd, J = 10.1, 8.6 Hz, 1H), 2.77 (br dd, J = 9.8, 9.1 Hz, 1H), 2.44 (s, 3H), 2.08 – 1.87 (m, 1H), 1.81 – 1.54 (m, 3H), 0.95 (d, J = 6.2 Hz, 3H); **^{13}C NMR** (126 MHz, $CDCl_3$) δ 143.5, 133.7, 129.7, 127.4, 116.0 (t, $J_{C\text{-}F}$ = 239.9 Hz), 54.0, 53.2, 39.7 (t, $J_{C\text{-}F}$ = 4.4 Hz), 36.0 (t, $J_{C\text{-}F}$ = 21.3 Hz), 21.5, 15.7; **^{19}F NMR** (471 MHz, $CDCl_3$) δ -114.8 (dddd, J = 283.1, 55.2, 21.1, 19.1 Hz, 1F), -116.0 (ddt, J = 283.1, 56.2, 18.1 Hz, 1F); **MS** (EI): m/z = 303.1 $[M]^+$. Spectroscopic data is in accordance with previous reports.[1]

Deuteration experiment

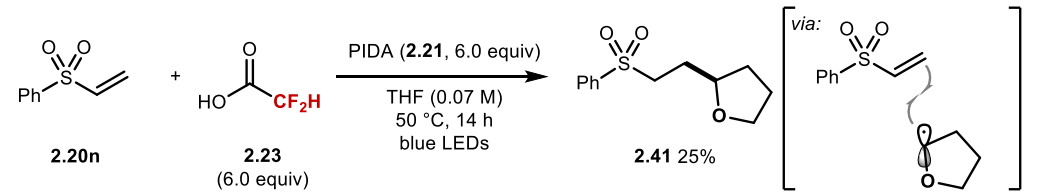


General procedure 1 was followed with the exception that THF-d8 was used as the solvent. [D]**4f** (24 mg, 0.11 mmol, 37%) was obtained as a colourless oil with a D/H ratio of 40/60. **^{1}H NMR** (400 MHz, MeOD) δ ppm 7.91 – 7.78 (m, 2H), 7.58

– 7.42 (m, 3H), 5.95 (tt, *J* = 57.2, 4.3 Hz, 1H), 3.60 – 3.35 (m, 2H), 1.99 – 1.85 (m, 2H), 1.83 – 1.72 (m, 1.6H); **HRMS** (ESI-TOF): calculated for $C_{11}H_{13}DF_2NO$ ($[M+H]^+$): 215.1101; found: 215.1098.



THF radical trapping



General procedure 1 was followed to obtain **2.41** (19 mg, 0.08 mmol, 25%) as a colourless oil. **^{1}H NMR** (400 MHz, $CDCl_3$) δ 7.92 (d, *J* = 7.7 Hz, 2H), 7.68 – 7.54 (m, 3H), 3.88 – 3.75 (m, 2H), 3.71 – 3.64 (m, 1H), 3.34 – 3.25 (m, 1H), 3.18 – 3.05 (m, 1H), 2.04 – 1.78 (m, 5H), 1.52 – 1.42 (m, 1H); **^{13}C NMR** (126 MHz, $CDCl_3$) δ 139.2, 133.7, 129.3, 128.0, 77.3, 67.9, 53.6, 31.2, 28.5, 25.6; **MS** (EI): *m/z* = 239.9 $[M]^+$. Spectroscopic data were in accordance with previous reports.[2]

6.3 Supporting Information Chapter 3

General information

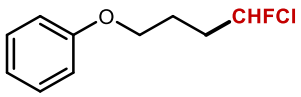
The experiments in this chapter were performed at the Janssen sites in Toledo (Spain) and Beerse (Belgium). High resolution mass spectra (HRMS, m/z) were recorded on a Bruker MicroTOF spectrometer using positive electrospray ionization (ESI). Compounds that did not ionise in ESI, were analysed on an Intuvo GC 9000 - MSD 5977B (Agilent Technologies) using electron impact ionisation (EI). Exact masses for these compounds were calculated with MassWorks software (from Cerno Bioscience) through a correction of the mass with a calibration file. Melting points of solids were measured on a DSC823^{e} (Differential Scanning Analysis) Mettler Toledo apparatus. All reactions for the hydrochlorofluoromethylation of alkenes were conducted in non-dried glassware with magnetic stirring. Chlorofluoroacetic acid was purchased from Apollo Scientific. PIDA was purchased from Carbosynth. All commercially available substrates were purchased from commercial suppliers or otherwise synthesized according to literature. Reactions were performed in 7 mL vials in a SynLED photoreactor (λ_{max} = 465-470 nm). The yields were determined by either ^{19}F NMR spectroscopy or by the isolation on silica gel column chromatography. If the purity of the compounds was not satisfying an analytical sample was further purified by reverse phase HPLC purification. **Note**: The compounds for this chapter were synthesised at the Janssen sites in Toledo (Spain) and Beerse (Belgium). There was no IR machine available on these sites and therefore these data could not be generated.

6.3.1 Hydrochlorofluoromethylation of Alkenes

General procedure 1: Hydrochlorofluoromethylation of alkenes and alkynes

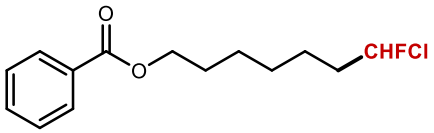
Chlorofluoroacetic acid **3.37** (133 uL, 1.80 mmol, 6.0 equiv) was added to a suspension of phenyliodine(III) diacetate **3.41** (290 mg, 0.90 mmol, 3.0 equiv) and alkene **3.42** (0.30 mmol) in THF (4.5 mL). The mixture was stirred under blue LED irradiation (SynLED photoreactor) at rt for 5 h, after which a second portion of phenyliodine(III) diacetate **3.41** (290 mg, 1.80 mmol, 3.0 equiv) was added. The suspension was stirred under blue LED irradiation for another 14 h. The solvent was removed *in vacuo* and the residue was purified by silica gel column chromatography (EtOAc in heptane 0/100 to 100/0) to yield the desired product.

(4-chloro-4-fluorobutoxy)benzene (3.43a)



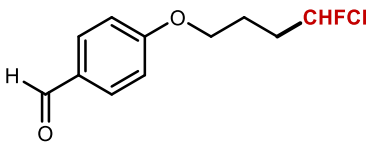
General procedure A was followed to obtain **3.43a** (37 mg, 0.18 mmol, 61%) as a colourless oil. **^{1}H NMR** (500 MHz, $CDCl_3$) δ 7.34 – 7.27 (m, 2H), 6.97 (tt, J = 7.3, 1.1 Hz, 1H), 6.93 – 6.88 (m, 2H), 6.29 (dt, J = 50.8, 5.3 Hz, 1H), 4.03 (t, J = 6.0 Hz, 2H), 2.40 – 2.20 (m, 2H), 2.09 – 1.96 (m, 2H); **^{13}C NMR** (126 MHz, $CDCl_3$) δ 158.8, 129.6, 121.0, 114.6, 102.7 (d, J = 241.4 Hz), 66.7, 36.4 (d, J = 20.3 Hz), 24.2 (d, J = 4.5 Hz); **^{19}F NMR** (471 MHz, $CDCl_3$) δ -130.3 (dt, J = 50.6, 18.5 Hz); **HRMS** (EI): calculated for $C_{10}H_{12}ClFO^{\bullet+}$ ($M^{\bullet+}$): 202.0555; observed: 202.0570.

7-chloro-7-fluoroheptyl benzoate (3.43b)



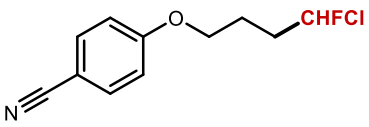
General procedure A was followed to obtain **3.43b** (48 mg, 0.18 mmol, 59%) as a colourless oil. **^{1}H NMR** (500 MHz, $CDCl_3$) δ 8.06 – 8.02 (m, 2H), 7.58 – 7.53 (m, 1H), 7.47 – 7.42 (m, 2H), 6.16 (dt, *J* = 51.0, 5.4 Hz, 1H), 4.32 (t, *J* = 6.6 Hz, 2H), 2.20 – 1.97 (m, 2H), 1.85 – 1.74 (m, 2H), 1.58 – 1.38 (m, 6H); **^{13}C NMR** (126 MHz, $CDCl_3$) δ 166.6, 132.9, 130.4, 129.5, 128.3, 102.8 (d, *J* = 241.3 Hz), 64.9, 39.2 (d, *J* = 20.1 Hz), 28.6, 28.5, 25.9, 24.0 (d, *J* = 4.4 Hz); **^{19}F NMR** (471 MHz, $CDCl_3$) δ -129.7 – -129.9 (m); **HRMS** (EI): calculated for $C_{14}H_{18}ClFO_2^{\bullet+}$ ($M^{\bullet+}$): 272.0974; observed: 272.1022.

4-(4-chloro-4-fluorobutoxy)benzaldehyde (3.43c)



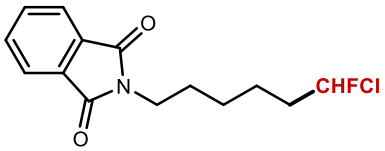
General procedure A was followed to obtain **3.43c** (37 mg, 0.16 mmol, 53%) as a colourless oil. **^{1}H NMR** (500 MHz, $CDCl_3$) δ 9.89 (s, 1H), 7.89 – 7.79 (m, 2H), 7.02 – 6.96 (m, 2H), 6.29 (dt, *J* = 50.8, 5.1 Hz, 1H), 4.11 (t, *J* = 6.0 Hz, 2H), 2.40 – 2.20 (m, 2H), 2.13 – 2.00 (m, 2H); **^{13}C NMR** (126 MHz, $CDCl_3$) δ 190.9, 163.8, 132.2, 130.3, 114.9, 102.4 (d, *J* = 241.5 Hz), 67.2, 36.1 (d, *J* = 20.6 Hz), 23.9 (d, *J* = 4.4 Hz); **^{19}F NMR** (471 MHz, $CDCl_3$) δ -130.5 (dt, *J* = 50.8, 18.4 Hz); **HRMS** (ESI-TOF): calculated for $C_{11}H_{13}ClFO_2^{+}$ ($[M+H]^{+}$): 231.0588, observed: 231.0586.

4-(4-chloro-4-fluorobutoxy)benzonitrile (3.43d)



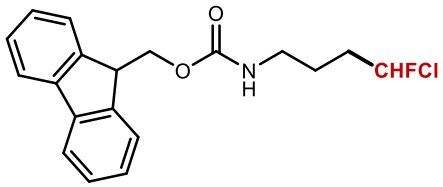
General procedure A was followed to obtain **3.43d** (39 mg, 0.17 mmol, 57%) as a white solid. **^{1}H NMR** (500 MHz, $CDCl_3$) δ 7.63 – 7.57 (m, 2H), 6.98 – 6.92 (m, 2H), 6.29 (dt, *J* = 50.7, 5.1 Hz, 1H), 4.07 (t, *J* = 6.0 Hz, 2H), 2.37 – 2.23 (m, 2H), 2.11 – 2.01 (m, 2H); **^{13}C NMR** (126 MHz, $CDCl_3$) δ 162.1, 134.2, 119.3, 115.3, 104.4, 102.3 (d, *J* = 241.5 Hz), 67.2, 36.0 (d, *J* = 20.5 Hz), 23.8 (d, *J* = 4.4 Hz); **^{19}F NMR** (471 MHz, $CDCl_3$) δ -130.6 (dt, *J* = 50.5, 18.6 Hz); **HRMS** (EI): calculated for $C_{11}H_{11}ClFNO^{\bullet+}$ ($M^{\bullet+}$): 227.0508; observed: 227.0430; **MP**: 31 - 33 °C.

2-(6-chloro-6-fluorohexyl)isoindoline-1,3-dione (3.43e)



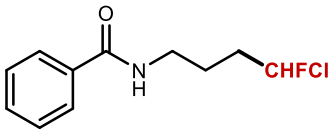
General procedure A was followed to obtain **3.43e** (46 mg, 0.16 mmol, 54%) as a colourless oil. **^{1}H NMR** (500 MHz, $CDCl_3$) δ 7.85 – 7.77 (m, 2H), 7.73 – 7.66 (m, 2H), 6.13 (dt, *J* = 50.9, 5.4 Hz, 1H), 3.67 (t, *J* = 7.2 Hz, 2H), 2.14 – 1.94 (m, 2H), 1.73 – 1.64 (m, 2H), 1.60 – 1.46 (m, 2H), 1.44 – 1.33 (m, 2H); **^{13}C NMR** (126 MHz, $CDCl_3$) δ 168.6, 134.1, 132.3, 123.3, 102.8 (d, *J* = 241.6 Hz), 39.2 (d, *J* = 19.8 Hz), 37.8, 28.5, 26.2, 23.8 (d, *J* = 4.2 Hz); **^{19}F NMR** (471 MHz, $CDCl_3$) δ -129.8 – -130.0 (m). Data in accordance with literature values.[7]

(9*H*-fluoren-9-yl)methyl (4-chloro-4-fluorobutyl)carbamate (3.43f)



General procedure A was followed to obtain **3.43f** (47 mg, 0.14 mmol, 45%) as a white solid. **^{1}H NMR** (500 MHz, $CDCl_3$) δ 7.77 (d, *J* = 7.5 Hz, 2H), 7.59 (d, *J* = 7.4 Hz, 2H), 7.41 (t, *J* = 7.5 Hz, 2H), 7.32 (td, *J* = 7.5, 1.2 Hz, 2H), 6.20 (dt, *J* = 50.7, 5.1 Hz, 1H), 4.82 (br s, 0.8H), 4.64 (br s, 0.2H), 4.55 (br s, 0.2H), 4.44 (br d, *J* = 6.7 Hz, 1.8H), 4.21 (t, *J* = 6.8 Hz, 1H), 3.25 (q, *J* = 6.7 Hz, 1.7H), 3.01 (s, 0.3H), 2.17 – 2.02 (m, 1.7H), 1.90 (br s, 0.3H), 1.80 – 1.67 (m, 1.7H), 1.50 (br s, 0.3H); **^{13}C NMR** (126 MHz, $CDCl_3$) δ 156.6, 144.0, 141.5, 127.8, 127.2, 125.1, 120.1, 102.4 (d, *J* = 241.5 Hz), 66.7, 47.4, 40.2, 36.4 (d, *J* = 20.3 Hz), 24.8 (d, *J* = 4.0 Hz); **^{19}F NMR** (471 MHz, $CDCl_3$) δ -130.2 (dt, *J* = 50.9, 18.6 Hz); **HRMS**: the compound did not ionise under various ionisation techniques; **MP**: 116 - 119 °C.

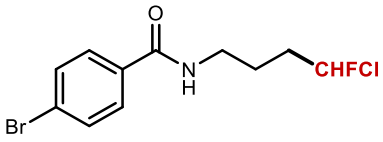
***N*-(4-chloro-4-fluorobutyl)benzamide (3.43g)**



General procedure A was followed to obtain **3.43g** (42 mg, 0.18 mmol, 61%) as a colourless oil. **^{1}H NMR** (500 MHz, $CDCl_3$) δ 7.78 – 7.73 (m, 2H), 7.52 – 7.46 (m, 1H), 7.45 – 7.38 (m, 2H), 6.47 (br s, 1H), 6.22 (dt, *J* = 50.8, 5.2 Hz, 1H), 3.50 (q, *J* = 6.8 Hz, 2H), 2.23 – 2.06 (m, 2H), 1.90 – 1.79 (m, 2H); **^{13}C NMR** (126 MHz, $CDCl_3$) δ 167.9, 134.5, 131.7, 128.7, 127.0, 102.4 (d, *J* = 241.5 Hz), 39.1, 36.6 (d, *J* = 20.3

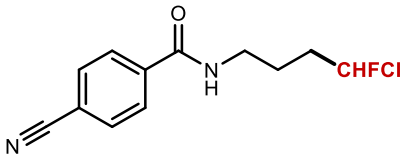
Hz), 24.5 (d, *J* = 4.1 Hz); **^{19}F NMR** (471 MHz, $CDCl_3$) *δ* -130.2 (dt, *J* = 51.0, 19.0 Hz); **HRMS** (ESI-TOF): calculated for $C_{11}H_{12}ClFNO^-$ ([M-H]$^-$): 228.0591; observed: 228.0589.

4-bromo-*N*-(4-chloro-4-fluorobutyl) benzamide (3.43h)



General procedure A was followed to obtain **3.43h** (51 mg, 0.17 mmol, 55%) as a white solid. **^{1}H NMR** (400 MHz, $CDCl_3$) δ 7.66 – 7.60 (m, 2H), 7.59 – 7.53 (m, 2H), 6.32 (s, 1H), 6.23 (dt, *J* = 50.8, 5.1 Hz, 1H), 3.50 (q, *J* = 6.9 Hz, 2H), 2.25 – 2.05 (m, 2H), 1.94 – 1.80 (m, 2H); **^{13}C NMR** (101 MHz, $CDCl_3$) *δ* 166.9, 133.3, 132.0, 128.6, 126.4, 102.4 (d, *J* = 241.6 Hz), 39.3, 36.6 (d, *J* = 20.4 Hz), 24.4 (d, *J* = 4.0 Hz); **^{19}F NMR** (377 MHz, $CDCl_3$) *δ* -130.3 (dt, *J* = 50.8, 18.7 Hz); **HRMS** (ESI-TOF): calculated for $C_{11}H_{11}BrClFNO^-$ ([M-H]$^-$): 305.9697; observed: 305.9692; **MP**: 85 – 88 °C.

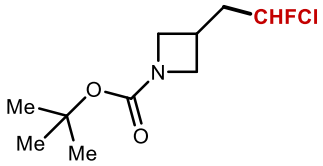
***N*-(4-chloro-4-fluorobutyl)-4-cyanobenzamide (3.43i)**



General procedure A was followed to obtain **3.43i** (40 mg, 0.16 mmol, 52%) as a white solid. **^{1}H NMR** (500 MHz, $CDCl_3$) *δ* 7.88 – 7.84 (m, 2H), 7.75 – 7.71 (m, 2H), 6.48 (s, 1H), 6.24 (dt, *J* = 50.7, 5.0 Hz, 1H), 3.53 (q, *J* = 6.7 Hz, 2H), 2.22 – 2.09 (m, 2H), 1.92 – 1.82 (m, 2H); **^{13}C NMR** (126 MHz, $CDCl_3$) *δ* 165.9, 138.3, 132.5, 127.6, 118.0, 115.1, 102.2 (d, *J* = 241.6 Hz), 39.3, 36.4 (d, *J* = 20.3 Hz), 24.2 (d, *J* = 3.8 Hz);

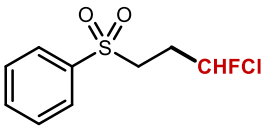
^{19}F NMR (471 MHz, $CDCl_3$) δ -130.4 (dt, J = 51.2, 19.0 Hz); **HRMS** (ESI-TOF): calculated for $C_{12}H_{11}ClFN_2O^-$ ([M-H]$^-$): 253.0544; observed: 253.0538. MP: 120 - 122 °C.

***tert*-butyl 3-(2-chloro-2-fluoroethyl) azetidine-1-carboxylate (3.43j)**



General procedure A was followed to obtain **3.43j** (48 mg, 0.20 mmol, 67%) as a colourless oil. **^{1}H NMR** (500 MHz, $CDCl_3$) δ 6.16 (dt, J = 50.4, 5.0 Hz, 1H), 4.08 (t, J = 8.5 Hz, 2H), 3.67 (ddd, J = 8.3, 5.8, 1.9 Hz, 2H), 2.88 – 2.77 (m, 1H), 2.46 – 2.30 (m, 2H), 1.43 (s, 9H); **^{13}C NMR** (126 MHz, $CDCl_3$) δ 156.3, 101.2 (d, J = 241.8 Hz), 79.7, 54.4 (br s), 43.3 (d, J = 19.9 Hz), 28.5, 24.7 (d, J = 3.9 Hz); **^{19}F NMR** (471 MHz, $CDCl_3$) δ -131.8 (br s); **HRMS** (EI): calculated for $C_{10}H_{17}ClFNO_2^{\bullet+}$ ($M^{\bullet+}$): 237.0926; observed: 237.0869.

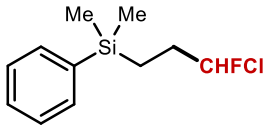
((3-chloro-3-fluoropropyl)sulfonyl)benzene (3.43k)



General procedure A was followed to obtain **3.43k** (36 mg, 0.15 mmol, 51%) as a white solid. **^{1}H NMR** (500 MHz, $CDCl_3$) δ 7.96 – 7.89 (m, 2H), 7.73 – 7.67 (m, 1H), 7.64 – 7.57 (m, 2H), 6.34 (dt, J = 50.3, 4.8 Hz, 1H), 3.38 – 3.23 (m, 2H), 2.60 – 2.44 (m, 2H); **^{13}C NMR** (126 MHz, $CDCl_3$) δ 138.6, 134.3, 129.7, 128.1, 100.0 (d, J = 242.5 Hz), 50.8 (d, J = 3.9 Hz), 32.5 (d, J = 22.1 Hz); **^{19}F NMR** (471 MHz, $CDCl_3$) δ -132.5 –

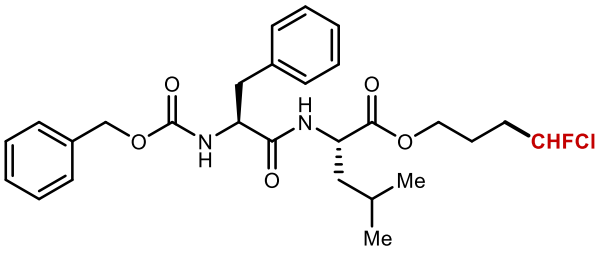
-132.7 (m); **HRMS** (EI): calculated for $C_9H_{10}ClFO_2S^{\bullet+}$ ($M^{\bullet+}$): 236.0069; observed: 236.0016; **MP**: 45 - 47 °C.

(3-chloro-3-fluoropropyl)dimethyl(phenyl) silane (3.43l)



General procedure A was followed to obtain **3.43l** (45 mg, 0.20 mmol, 65%) as a colourless oil. **^{1}H NMR** (500 MHz, $CDCl_3$) δ 7.53 – 7.49 (m, 2H), 7.41 – 7.36 (m, 3H), 6.08 (dt, *J* = 51.2, 5.2 Hz, 1H), 2.12 – 1.96 (m, 2H), 1.01 – 0.87 (m, 2H), 0.32 (s, 6H); **^{13}C NMR** (126 MHz, $CDCl_3$) δ 138.1, 133.6, 129.4, 128.1, 104.5 (d, *J* = 243.4 Hz), 34.3 (d, *J* = 20.4 Hz), 10.1 (d, *J* = 3.0 Hz), -3.1; **^{19}F NMR** (471 MHz, $CDCl_3$) δ -130.0 (dt, *J* = 51.2, 17.8 Hz); **HRMS**: the compound did not ionise under various ionisation techniques.

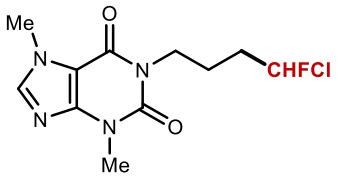
4-chloro-4-fluorobutyl ((benzyloxy) carbonyl)-*L*-phenylalanyl-*L*-leucinate (3.43m)



General procedure A was followed to obtain **3.43m** (84 mg, 0.16 mmol, 54%) as a white solid. **^{1}H NMR** (500 MHz, $CDCl_3$) δ 7.39 – 7.16 (m, 10H), 6.30 – 6.14 (m, 2H), 5.33 – 5.23 (m, 1H), 5.09 (d, *J* = 1.7 Hz, 2H), 4.52 (td, *J* = 8.4, 5.3 Hz, 1H), 4.44 (q, *J* = 7.3 Hz, 1H), 4.21 – 4.09 (m, 2H), 3.09 (qd, *J* = 13.9, 6.7 Hz, 2H), 2.14 (dddd,

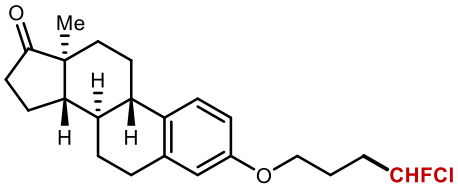
J = 18.4, 9.3, 6.9, 4.8 Hz, 2H), 1.94 – 1.81 (m, 2H), 1.62 – 1.40 (m, 3H), 0.89 (dd, *J* = 6.2, 4.9 Hz, 6H); **^{13}C NMR** (126 MHz, $CDCl_3$) *δ* 172.4, 170.7, 156.1, 136.3, 136.2, 129.5, 128.8, 128.7, 128.4, 128.2, 127.2, 102.2 (d, *J* = 241.9 Hz), 67.3, 64.2, 56.2, 51.1, 41.6, 38.3, 35.9 (d, *J* = 20.7 Hz), 24.9, 23.4 (d, *J* = 4.4 Hz), 22.8, 22.1; **^{19}F NMR** (471 MHz, $CDCl_3$) *δ* -130.5 – -130.9 (m); **HRMS** (ESI-TOF): calculated for $C_{27}H_{35}ClFN_2O_5^+$ ([M+H]$^+$): 521.2219; observed: 521.2216; **MP**: 80 - 84 °C.

1-(4-chloro-4-fluorobutyl)-3,7-dimethyl-3,7-dihydro-1H-purine-2,6-dione (3.43n)



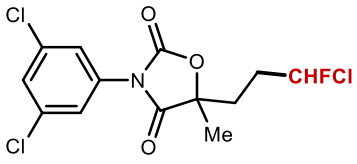
General procedure A was followed to obtain **3.43n** (54 mg, 0.19 mmol, 62%) as a white solid. **^{1}H NMR** (400 MHz, $CDCl_3$) *δ* 7.51 (s, 1H), 6.21 (dt, *J* = 50.8, 5.3 Hz, 1H), 4.05 (t, *J* = 7.2 Hz, 2H), 3.97 (s, 3H), 3.56 (s, 3H), 2.23 – 2.02 (m, 2H), 1.96 – 1.82 (m, 2H); **^{13}C NMR** (126 MHz, $CDCl_3$) *δ* 155.3, 151.5, 149.0, 141.7, 107.7, 102.4 (d, *J* = 241.7 Hz), 40.3, 36.7 (d, *J* = 20.6 Hz), 33.7, 29.8, 23.0 (d, *J* = 4.4 Hz); **^{19}F NMR** (471 MHz, $CDCl_3$) *δ* -130.0 – -130.2 (m); **HRMS** (ESI-TOF): calculated for $C_{11}H_{15}ClFN_4O_2$ (M+H)$^+$: 289.0868; observed: 289.0883; **MP**: 111 - 115 °C

(8*R*,9*S*,13*S*,14*S*)-3-(4-chloro-4-fluorobutoxy)-13-methyl-6,7,8,9,11,12,13,14,15,16-decahydro-17*H*-cyclopenta[*a*]phenanthren-17-one (3.43o)



General procedure A was followed to obtain **3.43o** (52 mg, 0.14 mmol, 46%) as a white solid. **^{1}H NMR** (400 MHz, $CDCl_3$) δ 7.20 (d, J = 8.6 Hz, 1H), 6.70 (dd, J = 8.6, 2.8 Hz, 1H), 6.64 (d, J = 2.7 Hz, 1H), 6.27 (dt, J = 50.9, 5.3 Hz, 1H), 3.99 (t, J = 6.0 Hz, 2H), 2.95 – 2.85 (m, 2H), 2.50 (dd, J = 18.8, 8.6 Hz, 1H), 2.44 – 1.90 (m, 10H), 1.71 – 1.38 (m, 6H), 0.91 (s, 3H); **^{13}C NMR** (126 MHz, $CDCl_3$) δ 221.0, 156.9, 138.0, 132.5, 126.5, 114.7, 112.2, 102.7 (d, J = 241.3 Hz), 66.8, 50.6, 48.2, 44.1, 38.5, 36.4 (d, J = 20.9 Hz), 36.0, 31.7, 29.8, 26.7, 26.1, 24.2 (d, J = 4.7 Hz), 21.7, 14.0; **^{19}F NMR** (471 MHz, $CDCl_3$) δ -130.2 (dt, J = 51.5, 18.8 Hz); **HRMS** (ESI-TOF): calculated for $C_{22}H_{29}ClFO_2^+$ ([M+H]$^+$): 379.1840; observed: 379.1839; **MP**: 107 - 110 °C.

5-(3-chloro-3-fluoropropyl)-3-(3,5-dichlorophenyl)-5-methyloxazolidine-2,4-dione (3.43p)

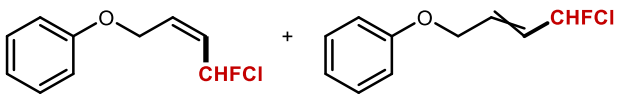


General procedure A was followed to obtain **3.43p** (76 mg, 0.21 mmol, 71%) as a sticky oil; d.r: 1:1. **^{1}H NMR** (400 MHz, $CDCl_3$) δ 7.47 – 7.44 (m, 2H), 7.44 – 7.42 (m, 1H), 6.35 – 6.15 (m, 1H), 2.38 – 2.05 (m, 4H), 1.71 (s, 3H); **^{13}C NMR** (101 MHz,

$CDCl_3$) δ 173.2, 152.1, 135.8, 132.6, 129.3, 123.8, 101.1 (dd, J = 242.3, 3.5 Hz), 84.9, 32.9 (d, J = 21.3 Hz), 31.1 (d, J = 4.4 Hz, 0.5C), 31.0 (d, J = 4.3 Hz, 0.5C), 22.5; **^{19}F NMR** (471 MHz, $CDCl_3$) δ -131.5 – -131.7 (m, 0.5F), -131.8 – -132.0 (m, 0.5F); **HRMS** (ESI-TOF): calculated for $C_{13}H_{10}Cl_3FNO_3^-$ ([M-H]$^-$): 351.9710; observed: 351.9719.

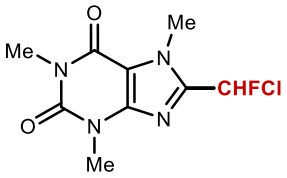
6.3.2 Chlorofluoromethylation of other substrates

((4-chloro-4-fluorobut-2-en-1-yl)oxy) benzene (3.43q)



General procedure A was followed to obtain **3.43q** (21 mg, 0.11 mmol, 35%) as a colourless oil. Mixture of stereoisomers (86:14). **^{1}H NMR** (500 MHz, $CDCl_3$) δ 7.33 – 7.28 (m, 2H), 7.05 – 7.02 (m, 0.14H), 6.99 (tt, J = 7.4, 1.1 Hz, 0.86H), 6.94 – 6.89 (m, 2H), 6.64 – 6.50 (m, 1H), 6.24 – 6.11 (m, 1.86H), 5.97 – 5.93 (m, 0.14H), 4.72 – 4.60 (m, 2H); **^{13}C NMR** (126 MHz, $CDCl_3$) δ 158.2, 130.7 (d, J = 10.2 Hz), 129.7, 128.2 (d, J = 21.2 Hz), 121.5, 114.8, 99.3 (d, J = 239.2 Hz), 66.3; **^{19}F NMR** (471 MHz, $CDCl_3$) δ -128.3 – -128.5 (m); **HRMS** (EI): calculated for $C_{10}H_{10}ClFO^{\bullet+}$ ($M^{\bullet+}$): 200.0399; observed: 200.0364.

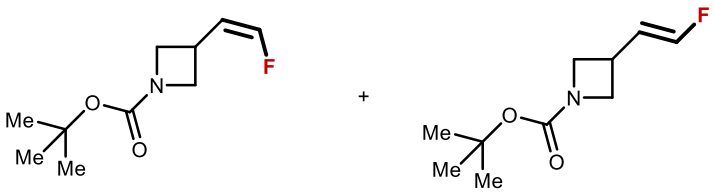
8-(chlorofluoromethyl)-1,3,7-trimethyl-3,7-dihydro-1*H*-purine-2,6-dione (3.51)



Chlorofluoroacetic acid **3.37** (30 µL, 0.40 mmol, 4.0 equiv) was added to a suspension of phenyliodine(III) diacetate **3.41** (64 mg, 0.20 mmol, 2.0 equiv) in toluene (5 mL). The mixture was concentrated *in vacuo* and azeotropically dried with toluene. To this crude iodine reagent **3.40** was added caffeine (19 mg, 0.10 mmol, 1.0 equiv), $[Ir(dtbbpy)(ppy)_2][PF_6]$ (1 mg, 0.001 mmol, 1 mol%) and $CDCl_3$ (1.0 mL). The mixture was degassed by nitrogen bubbling for 5 min whilst cooling in a water bath. The mixture was stirred under blue LED irradiation (SynLED photoreactor) at rt for 20 h. *α,α,α*-Trifluorotoluene (123 µL, 1.00 mmol, 10.0 equiv) was added and the mixture was analyzed by ^{19}F NMR spectroscopy. The solvents were removed *in vacuo* and the residue was purified by silica gel column chromatography (EtOAc in heptane 0/100 to 100/0) to yield **3.51** (17 mg, 0.07 mmol, 65%) as a white solid. **^{1}H NMR** (500 MHz, $CDCl_3$) *δ* 7.15 (d, *J* = 47.3 Hz, 1H), 4.19 (d, *J* = 1.4 Hz, 3H), 3.55 (s, 3H), 3.41 (s, 3H); **^{13}C NMR** (126 MHz, $CDCl_3$) *δ* 155.6, 151.6, 146.8, 145.0 (d, *J* = 24.9 Hz), 109.7, 93.4 (d, *J* = 240.5 Hz), 33.3 (d, *J* = 3.3 Hz), 29.9, 28.3; **^{19}F NMR** (471 MHz, $CDCl_3$) *δ* -135.1 (d, *J* = 47.8 Hz); **HRMS** (ESI-TOF): calculated for $C_9H_{11}ClFN_4O_2^+$ ($[M+H]^+$): 261.0555; observed: 261.0554; **MP**: 200 – 202 °C.

6.3.3 Synthesis of Vinyl Fluorides

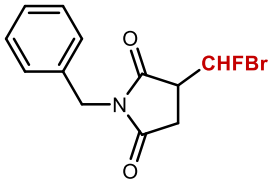
tert-butyl 3-(2-fluorovinyl)azetidine-1-carboxylate (3.59j)



Cs_2CO_3 (165 mg, 0.51 mmol, 2.0 equiv) was added to a solution of **3.43j** (60 mg, 0.25 mmol, 1.0 equiv) in DMSO (2 mL). The mixture was stirred at 100 °C for 3 h. Water was added and the mixture was extracted with EtOAc. The organic layer was separated, dried (Na_2SO_4), filtered and concentrated *in vacuo*. The crude product was purified by silica gel column chromatography (EtOAc in heptane 0/100 to 60/40) to yield **3.59j** (36 mg, 0.18 mmol, 71%) as a colourless oil. E/Z 57:43; **^{1}H NMR** (500 MHz, $CDCl_3$) δ 6.55 (ddd, *J* = 83.5, 11.1, 0.8 Hz, 0.57H), 6.44 (ddd, *J* = 83.9, 4.8, 1.2 Hz, 0.43H), 5.56 (ddd, *J* = 17.6, 11.1, 9.6 Hz, 0.57H), 5.00 (ddd, *J* = 41.5, 9.0, 4.7 Hz, 0.43H), 4.16 – 4.05 (m, 2H), 3.72 – 3.65 (m, 2H), 3.62 – 3.50 (m, 0.43H), 3.17 – 3.02 (m, 0.57H), 1.42 (s, 9H); **^{13}C NMR** (126 MHz, $CDCl_3$) δ 156.3, 156.3, 149.8 (d, *J* = 258.0 Hz), 148.5 (d, *J* = 260.6 Hz), 112.9 (d, *J* = 11.5 Hz), 112.4 (d, *J* = 4.1 Hz), 79.7, 79.6, 55.1 (br s), 28.5, 28.5, 25.5 (d, *J* = 10.6 Hz), 23.1 (d, *J* = 5.4 Hz); **^{19}F NMR** (471 MHz, $CDCl_3$) δ -127.6 (dd, *J* = 84.0, 41.8 Hz, 0.43F), -128.3 (dd, *J* = 83.5, 17.6 Hz, 0.57F); **HRMS** (EI): calculated for $C_{10}H_{16}FNO_2^{\bullet+}$ ($M^{\bullet+}$): 201.1160; observed: 201.1084.

6.3.4 Hydrobromofluoromethylation of Alkenes

1-benzyl-3-(bromofluoromethyl)pyrrolidine-2,5-dione (3.61r)

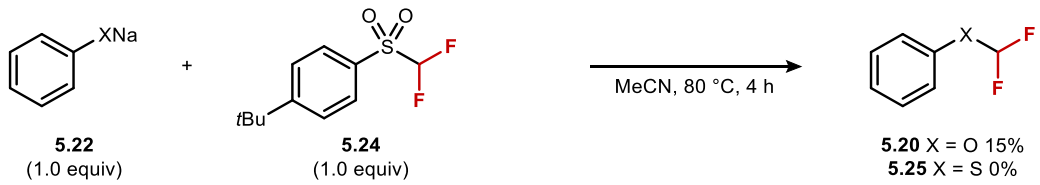


To a 7 mL vial equipped with a magnetic stir bar, was added alkene **3.42r** (0.50 mmol, 1.0 equiv), MeCN (dry, 3.0 mL), $(TMS)_3SiH$ (**3.65**, 185 uL, 0.6 mmol, 1.2 equiv) and $CHFBr_2$ (**3.64**, 191 mg, 1.0 mmol, 2.0 equiv). The vial was sealed with a septum, degassed by nitrogen bubbling for 10 seconds and wrapped with parafilm. The reaction mixture was stirred in a SynLED Parallel Photoreactor with a 12W blue LED lamp (λ_{max} = 470 nm) at room temperature (using a fan) for 16 hours. The solvent was removed *in vacuo* and the residue was purified by preparative thin layer chromatography (Et_2O in pentane 30/70) to yield **3.61r** (66 mg, 0.26 mmol, 51%) as a colourless oil as a mixture of diastereomers (1:1). **^{1}H NMR** (400 MHz, $CDCl_3$) δ 6.92 - 6.88 (m, 5H), 6.93 - 6.87 (m, 0.5H), 6.81 - 6.75 (m, 0.5H), 4.64 - 4.52 (m, 2H), 3.59 - 3.49 (m, 0.5H), 3.35 (dddd, J = 31.7, 9.3, 5.6, 1.8 Hz, 0.5H), 3.07 - 2.70 (m, 2H); **^{13}C NMR** (101 MHz, $CDCl_3$) δ 174.5, 174.1, 173.2, 172.9 (d, $J_{C\text{-}F}$ = 14.4 Hz), 135.2, 135.1, 128.9, 128.8, 128.7, 128.7, 128.2, 93.2 (d, $J_{C\text{-}F}$ = 256.2 Hz), 90.1 (d, $J_{C\text{-}F}$ = 254.1 Hz), 49.8 (d, $J_{C\text{-}F}$ = 21.4 Hz), 47.5 (d, $J_{C\text{-}F}$ = 22.6 Hz), 42.9 (d, $J_{C\text{-}F}$ = 6.9 Hz), 30.7, 29.8; **^{19}F NMR** (377 MHz, $CDCl_3$) δ -139.5 (dd, J = 48.0, 7.1 Hz, 0.5F), -147.0 (dd, J = 49.3, 31.8 Hz, 0.5F); **HRMS**: the compound did not ionise under various ionisation techniques; **IR** (neat): 1180, 1705, 1497, 1432, 1399, 1345, 1249, 1170, 1119, 1083, 1028, 951 cm^{-1}; **MP**: 64 - 66 °C.

6.4 Supporting Information Chapter 5

6.4.1 Mechanistic Experiments

Difluoromethylation of sodium phenoxide and sodium thiophenolate

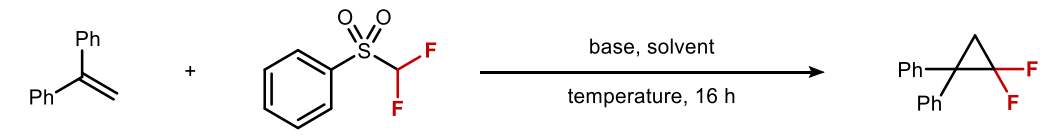


5.22 (1.0 equiv) + **5.24** (1.0 equiv) → **5.20** X = O 15%, **5.25** X = S 0%

1-(*Tert*-butyl)-4-((difluoromethyl)sulfonyl)benzene (248 mg, 1.0 mmol, 1.0 equiv) was added to a suspension of sodium (thio)phenolate (1.0 mmol, 1.0 equiv) in dry MeCN (10 mL) at room temperature. The mixture was heated to 80 °C for 4 hours and cooled to room temperature. The mixture was diluted with ethanol (10.0 mL) and *α*,*α*,*α*-trifluorotolouene (123 µL, 1.0 mmol, 1.0 equiv) was added as an internal standard. The mixture was analysed by quantitative ^{19}F NMR spectroscopy.

6.4.2 Optimisation Data

Difluorocyclopropanation of 1,1-diphenylethylene (Table 5.1; entry 3)

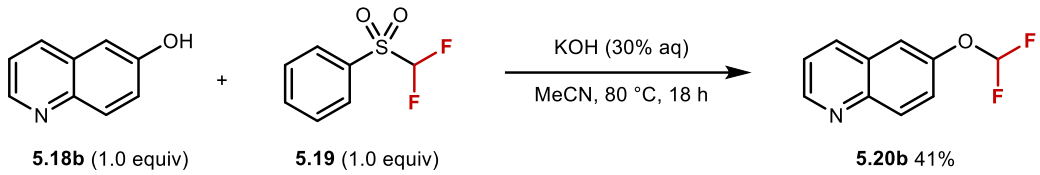


5.26 (5.0 equiv) + **5.19** (1.0 equiv) → **5.27**

((Difluoromethyl)sulfonyl)benzene (19 mg, 0.1 mmol, 1.0 equiv) was added to a suspension of 1,1-diphenylethylene (90 mg, 0.5 mmol, 5.0 equiv) and sodium hydroxide (4.5 mg, 0.11 mmol, 1.1 equiv) in dry propylene carbonate (5.0 mL) at room temperature. The mixture was heated to 200 °C for 16 hours and cooled to

room temperature. The mixture was diluted with ethanol (2.0 mL) and *α*,*α*,*α*-trifluorotolouene (123 µL, 1.0 mmol, 1.0 equiv) was added as an internal standard. The mixture was analysed by quantitative ^{19}F NMR spectroscopy.

Difluoromethylation of 6-hydroxyquinoline (Table 5.2; entry 5)

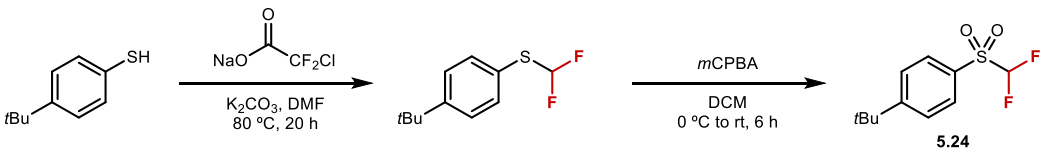


5.18b (1.0 equiv) **5.19** (1.0 equiv) **5.20b** 41%

((Difluoromethyl)sulfonyl)benzene (48 mg, 0.25 mmol, 1.0 equiv) was added to 6-hydroxyquinoline (36 mg, 0.25 mmol, 1.0 equiv) in a mixture of KOH (30%, 500 µL) and MeCN (1.75 mL) at room temperature. The mixture was heated to 80 °C for 18 hours and cooled to room temperature. The mixture was homogenised by addition of ethanol (2.0 mL) and trifluoroacetic acid (76.5 µL, 1.0 mmol, 1.0 equiv) was added as an internal standard. The mixture was analysed by quantitative ^{19}F NMR spectroscopy.

6.4.3 Synthesis of F-19 Compounds

Synthesis of 1-(*tert*-butyl)-4-((difluoromethyl)sulfonyl)benzene (5.24)



5.24

Step 1: According to a modified literature procedure:[8] 4-*tert*-butyl-thiophenol (16.6 g, 100 mmol, 1.0 equiv) was added to a suspension of K_2CO_3 (20.7 g, 150 mmol, 1.5 equiv) and sodium chlorodifluoroacetate (30.5 g, 200 mmol, 2.0 equiv) in dry DMF (250 mL). The mixture was slowly heated to 80 °C behind a blast shield

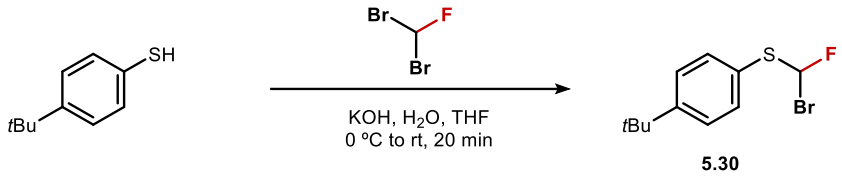
and stirred until completion (20 h). The mixture was cooled to room temperature, diluted with water (200 mL), extracted with EtOAc (3 x 150 mL) and washed with LiCl (10% aq., 200 mL). The organic layer was dried (Na_2SO_4), filtered and concentrated *in vacuo*. The crude product (19.4 g) was used as such in the next synthetic step without further purification.

Step 2: To a mixture of crude (4-(tert-butyl)phenyl)(difluoromethyl)sulfane (9.0 g, 42 mmol, 1.0 equiv) in DCM (180 mL) was carefully added mCPBA (21.5 g (in 5 g portions every 10 min), 87 mmol, 2.1 equiv) at 0 °C behind a blast shield. The mixture was allowed to warm to room temperature and stirred until completion (6 - 16 h). The mixture was quenched by addition of Na_2SO_3 (sat. aq., 200 mL) at 0 °C, basified (pH 10) with NaOH (1 M) and extracted with DCM (3 x 200 mL). The mixture was dried (Na_2SO_4), filtered and concentrated *in vacuo* to yield **5.24** (9.96 g, 40 mmol, 96%) as a white solid.

^{1}H NMR (400 MHz, $CDCl_3$) δ 7.92 – 7.88 (m, 2H), 7.67 – 7.62 (m, 2H), 6.18 (t, J = 53.49 Hz, 1H), 1.36 (s, 9H); **^{13}C NMR** (101 MHz, $CDCl_3$) δ 160.3, 130.6, 128.7, 126.8, 114.8 (t, J = 285.4 Hz), 35.6, 31.0; **^{19}F NMR** (377 MHz, $CDCl_3$) δ -121.9 (d, J = 53.6 Hz); **MS** (ESI-TOF): 271.0 ($[M+Na]^+$).

Spectroscopic data in accordance with literature.[9]

Synthesis of (bromofluoromethyl)(4-(*tert*-butyl)phenyl)sulfane (5.30)



5.30

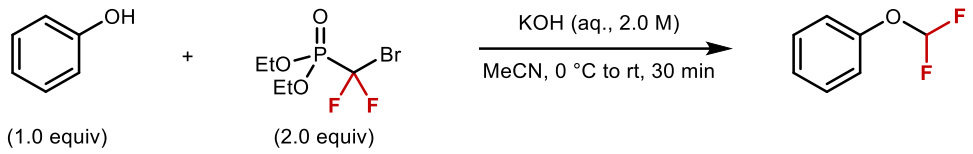
This reaction was performed by Dr. Jeroen Sap. A solution of KOH (3.36 g, 60 mmol, 10.0 equiv) in H_2O (8.0 mL) was added to a round-bottomed flask (under air) and cooled to 0 ˚C. To this solution was added, 4-(*tert*-butyl)benzenethiol (6.0 mmol, 1.0 equiv) in THF (6.0 mL). The resulting mixture was warmed to room temperature and stirred for 20 minutes. A solution of dibromofluoromethane (1.43 mL, 18.0 mmol, 3.0 equiv) in THF (2.0 ml) was subsequently added dropwise. The reaction mixture was stirred at room temperature for a 20 minutes, after which it was quenched by the addition of H_2O (40 mL). The crude product was extracted with DCM (3 x 50 mL). The combined organic layers were washed with brine (50 mL) and dried over $MgSO_4$. After filtration, the crude compound was concentrated *in vacuo*. The crude product was purified by silica gel column chromatography (pentane) and (bromofluoromethyl)(4-(*tert*-butyl)phenyl)sulfane (**5.30**) was isolated as a colourless oil. **^{1}H NMR** (400 MHz, $CDCl_3$) δ 7.55 – 7.51 (m, 2H), 7.46 – 7.42 (m, 2H), 7.21 (d, J = 56.10 Hz) 1.35 (s, 9H); **^{13}C NMR** (101 MHz, $CDCl_3$) δ 153.5, 134.5, 127.3, 126.5, 92.9 (d, J = 293.9 Hz), 34.9, 31.2; **^{19}F NMR** (376 MHz, $CDCl_3$) δ -99.5 (d, J = 56.2 Hz); **HRMS**: the compound did not ionise under various ionisation techniques; **IR (neat)**: 2963, 2869, 1596, 1489, 1461, 1398, 1364, 1294, 1268, 1175, 1151, 1117, 995, 830.

Note: prolonged reaction times lead to consumption of the product and result in (fluoromethylene)*bis*((4-(*tert*-butyl)phenyl)sulfane).

6.4.4 Synthesis of Reference Compounds

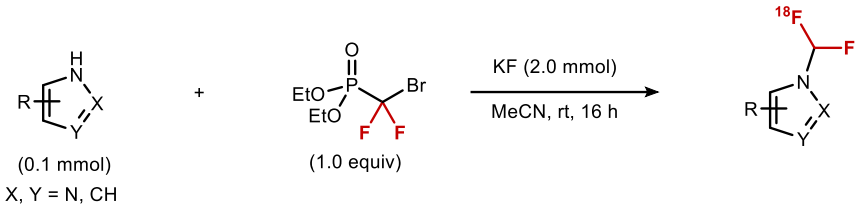
Compounds **5.27**, **5.20c** – **5.20h**, **5.20j**, **5.20k**, **5.20q**, **5.20s**, **5.29a** – **5.29e**, **5.31a** – **5.31e**, **5.20t** are known in literature and were synthesised accordingly.[1,4–11] Compound **5.20u** was obtained from a commercial supplier (ABCR).

General procedure 1 (GP1): Difluoromethylation of phenols with diethyl bromodifluoromethylphosphonate



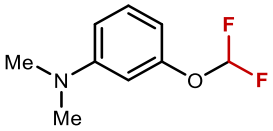
According to a modified literature procedure.[5] Diethyl bromodifluoromethylphosphonate (356 µL, 2.0 mmol, 2.0 equiv) was added to a stirred mixture of phenol (1.0 mmol, 1.0 equiv) in MeCN (5.0 mL) and KOH (aq., 2.0 M, 5.0 mL) at 0 °C. The mixture was allowed to warm to room temperature and stirred for 30 min or until complete consumption of starting material. The mixture was extracted with Et_2O (3 x 5.0 mL) and the organic layer was dried (Na_2SO_4), filtered and concentrated *in vacuo*. The crude product was purified by silica gel column chromatography.

General procedure 2 (GP2): Difluoromethylation of *N*-heterocycles with diethyl bromodifluoromethylphosphonate



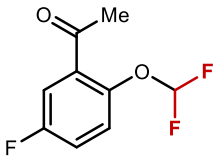
According to a modified literature procedure.[11] Diethyl bromodifluoromethylphosphonate (178 µL, 1.0 mmol, 1.0 equiv) was added to a stirred mixture of *N*-heterocycle (1.0 mmol, 1.0 equiv) and KF (116 mg, 2.0 mmol, 2.0 equiv) in MeCN (8.0 mL). The mixture was stirred overnight and concentrated. The crude product was purified by silica gel column chromatography.

3-(difluoromethoxy)-*N*,*N*-dimethylaniline (5.20i)



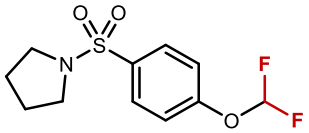
GP1 was followed (1.0 mmol scale) to yield compound **5.20i** (140 mg, 0.75 mmol, 75%) as a colourless oil. **^{1}H NMR** (400 MHz, $CDCl_3$) δ 7.11 – 7.03 (m, 1H), 6.46 – 6.42 (m, 1H), 6.36 – 6.30 (m, 2H), 2.84 (s, 6H); **^{13}C NMR** (101 MHz, $CDCl_3$) δ 152.8 (t, J = 2.7 Hz), 152.0, 130.1, 116.4 (t, J = 257.3 Hz), 109.4, 106.2, 103.3, 40.3; **^{19}F NMR** (377 MHz, $CDCl_3$) δ -79.8 (d, J = 74.9 Hz); **HRMS** (ESI-TOF): calculated for $C_9H_{11}F_2NO$ ($[M+H]^+$): 188.0881; found: 188.0881; **IR** (neat): 1683, 1507, 1441,1357, 1214, 1176, 1158, 1119, 1041.

1-(2-(difluoromethoxy)-4-fluorophenyl)ethan-1-one (5.20l)



This reaction was performed by Sandrine Hell. GP1 was followed (1.0 mmol scale) to yield compound **5.20l** (135 mg, 0.66 mmol, 66%) as a white solid. **^{1}H NMR** (400 MHz, $CDCl_3$) δ 7.81 (dd, J = 8.79, 6.57 Hz, 1H), 6.97 (ddd, J = 8.79, 7.54, 2.40 Hz, 1H), 6.93 – 6.87 (m, 1H), 6.62 (t, J = 72.85 Hz, 1H), 2.58 (s, 3H); **^{13}C NMR** (101 MHz, $CDCl_3$) δ 196.7, 165.1 (d, J = 255.5 Hz), 151.0 (dt, J = 10.9, 3.2 Hz), 132.8 (d, J = 10.3 Hz), 127.5 (d, J = 3.6 Hz), 115.9 (t, J = 261.5 Hz), 112.9 (d, J = 21.2 Hz), 107.5 (d, J = 25.6 Hz), 31.2; **^{19}F NMR** (377 MHz, $CDCl_3$) δ -81.7 (d, J = 73.1 Hz), -103.1 – -103.3 (m); **HRMS**: the compound did not ionise under various ionisation techniques; **IR** (neat): 3056, 1669, 1594, 1494, 1428, 1386, 1359, 1307, 1256, 1171, 1091, 1057, 1040, 985, **MP**: 52 – 54 °C.

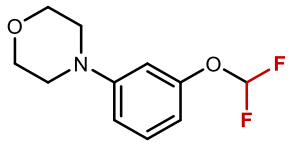
1-((4-(difluoromethoxy)phenyl)sulfonyl)pyrrolidine (5.20m)



This reaction was performed by Sandrine Hell. GP1 was followed (1.0 mmol scale) to yield compound **5.20m** (199 mg, 0.72 mmol, 72%) as a white solid. **^{1}H NMR** (400 MHz, $CDCl_3$) δ 7.84 – 7.79 (m, 2H), 7.25 – 7.20 (m, 2H), 6.61 (t, J = 72.79 Hz, 1H), 3.28 – 3.14 (m, 4H), 1.83 – 1.70 (m, 4H); **^{13}C NMR** (101 MHz, $CDCl_3$) δ 154.2 (t, J = 2.7 Hz), 133.9, 129.7, 119.4, 115.3 (t, J = 262.0 Hz), 48.0, 25.3; **^{19}F NMR** (377 MHz, $CDCl_3$) δ -82.1 (d, J = 73.0 Hz); **HRMS** (ESI-TOF): calculated for

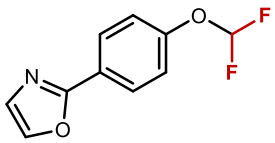
$C_{11}H_{14}F_2NO_3S$ ([M+H]$^+$): 278.0657; found: 278.0658; **IR** (neat): 1598, 1493, 1398, 1351, 1329, 1299, 1245, 1206, 1168, 1094, 1070, 1047, 1009, 834, **MP**: 63 – 64 °C.

4-(3-(difluoromethoxy)phenyl)morpholine (5.20n)



This reaction was performed by Sandrine Hell. GP1 was followed (1.0 mmol scale) to yield compound **5.20n** (156 mg, 0.68 mmol, 68%) as a colourless oil. **^{1}H NMR** (400 MHz, $CDCl_3$) δ 7.22 (t, J = 8.17 Hz, 1H), 6.78 – 6.27 (m, 4H), 3.88 – 3.79 (m, 4H), 3.17 – 3.10 (m, 4H); **^{13}C NMR** (101 MHz, $CDCl_3$) δ 152.9, 152.6 (t, J = 2.9 Hz), 130.3, 116.3 (t, J = 258.5 Hz), 112.3, 109.9, 106.7, 66.8, 48.9; **^{19}F NMR** (377 MHz, $CDCl_3$) δ -80.2 (d, J = 74.3 Hz); **HRMS** (ESI-TOF): calculated for $C_{11}H_{13}F_2NO_2$ ([M+H]$^+$): 230.0987; found: 230.0988; **IR** (neat): 2858, 1605, 1582, 1494, 1380, 1352, 1331, 1302, 1265, 1249, 1188, 1114, 1040, 996.

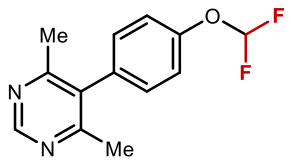
2-(4-(difluoromethoxy)phenyl)oxazole (5.20o)



GP1 was followed (1.0 mmol scale) to yield compound **5.20o** (166 mg, 0.79 mmol, 79%) as a yellow oil. **^{1}H NMR** (400 MHz, $CDCl_3$) δ 7.86 (d, J = 0.96 Hz, 1H), 7.82 (d, J = 0.95 Hz, 1H), 7.65 – 7.59 (m, 2H), 7.09 – 7.00 (m, 2H), 6.44 (t, J = 73.80 Hz, 1H); **^{13}C NMR** (101 MHz, $CDCl_3$) δ 151.4, 151.0 (t, J = 2.8 Hz), 139.5, 133.7, 128.1, 127.1, 119.9, 115.8 (t, J = 260.1 Hz); **^{19}F NMR** (377 MHz, $CDCl_3$) δ -80.9 (d, J = 73.9 Hz);

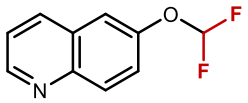
HRMS (ESI-TOF): calculated for $C_{10}H_8F_2NO_2$ ($[M+H]^+$): 212.0518; found: 212.0518; **IR** (neat): 1575, 1514, 1502, 1381, 1217, 1177, 1113, 1038, 936, 912, 860.

5-(4-(difluoromethoxy)phenyl)-4,6-dimethylpyrimidine (5.20p)



GP1 was followed (1.0 mmol scale) to yield compound **5.20p** (59 mg, 0.24 mmol, 24%) as an orange oil. **^{1}H NMR** (400 MHz, $CDCl_3$) δ 8.92 (s, 1H), 7.34 – 7.07 (m, 4H), 6.58 (t, J = 73.52 Hz, 1H), 2.25 (s, 6H); **^{13}C NMR** (101 MHz, $CDCl_3$) δ 164.7, 156.8, 151.0 (t, J = 2.8 Hz), 133.6, 133.1, 130.4, 120.2, 115.8 (t, J = 260.7 Hz), 23.1; **^{19}F NMR** (377 MHz, $CDCl_3$) δ -81.1 (d, J = 73.7 Hz); **HRMS** (ESI-TOF): calculated for $C_{13}H_{13}ON_2F_2$ ($[M+H]^+$): 251.0990; found: 251.0990; **IR:** 1510, 1445, 1393, 1265, 1224, 1265, 1445, 840, 730, 704.

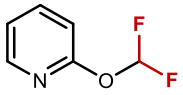
6-(difluoromethoxy)quinoline (5.20b)



GP1 was followed (1.0 mmol scale) to yield compound **5.20b** (55 mg, 0.28 mmol, 28%) as a yellow-brown oil. **^{1}H NMR** (400 MHz, $CDCl_3$) δ 8.89 (dd, J = 4.43, 1.68 Hz, 1H), 8.20 – 8.12 (m, 2H), 7.56 – 7.49 (m, 2H), 7.45 (dd, J = 8.36, 4.32 Hz, 1H), 6.65 (t, J = 73.30 Hz, 1H)., **^{13}C NMR** (101 MHz, $CDCl_3$) δ 149.5, 149.1 (t, J = 2.9 Hz), 145.1, 136.4, 131.1, 128.7, 123.7, 121.9, 115.7 (t, J = 262.6 Hz) 115.0; **^{19}F NMR** (377 MHz, $CDCl_3$) δ -81.4 (d, J = 73.4 Hz); **HRMS** (ESI-TOF): calculated for

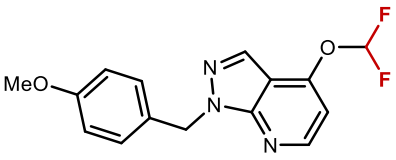
$C_{10}H_7F_2NO$ ([M+H]$^+$): 196.0568; found: 196.0569; **IR** (neat): 1504, 1218, 1171, 1126, 1056, 904, 724.

2-(difluoromethoxy)pyridine (5.20q)



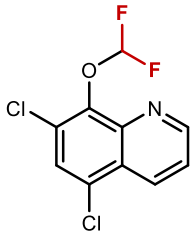
This reaction was performed by Dr. Jeroen Sap. GP1 was followed (1.0 mmol scale) to yield compound **5.20q** (65 mg, 0.45 mmol, 45%) as a pale-yellow oil. **^{1}H NMR** (400 MHz, $CDCl_3$) δ 8.21 (dd, J = 5.0, 2.1 Hz, 1H), 7.77 – 7.71 (m, 1H), 7.49 (t, J = 73.5 Hz, 1H), 7.11 (ddd, J = 7.3, 5.0, 0.9 Hz, 1H), 6.91 (dt, J = 8.2, 0.9 Hz, 1H); **^{19}F NMR** (377 MHz, $CDCl_3$) δ -88.86 (d, J = 73.2 Hz); **MS** (ESI-TOF): 146.0 ([M+H]$^+$). Spectroscopic data is in accordance with literature.[12]

4-(difluoromethoxy)-1-(4-methoxybenzyl)-1*H*-pyrazolo[3,4-*b*]pyridine (5.20r)



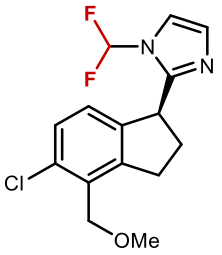
GP1 was followed (0.5 mmol scale) to yield compound **5.20r** (105 mg, 0.34 mmol, 68%) as a colourless oil. **^{1}H NMR** (400 MHz, $CDCl_3$) δ 8.48 (d, J = 5.30 Hz, 1H), 8.08 (s, 1H), 7.34 – 7.30 (m, 2H), 7.01 – 6.62 (m, 4H), 5.64 (s, 2H), 3.74 (s, 3H); **^{13}C NMR** (101 MHz, $CDCl_3$) δ 159.4, 152.6, 152.3 (t, J = 3.3 Hz), 150.4, 129.9, 129.6, 128.9, 115.1 (t, J = 263.4 Hz), 114.1, 107.8, 103.3, 55.3, 50.7; **^{19}F NMR** (377 MHz, $CDCl_3$) δ -83.1 (d, J = 72.5 Hz); **HRMS** (ESI-TOF): calculated for $C_{15}H_{14}O_2N_3F_2$ ([M+H]$^+$): 306.1049; found: 306.1048; **IR** (neat): 1573, 1514, 1422, 1333, 1265, 1145, 1067, 908, 730, 704, 650.

5,7-dichloro-8-(difluoromethoxy)quinoline (5.20v)



This reaction was performed by Dr. Jeroen Sap. GP1 was followed (2.0 mmol scale) to yield compound **5.20v** (262 mg, 1.0 mmol, 50%) as an off-white solid. **^{1}H NMR** (500 MHz, $CDCl_3$) δ 9.01 (dd, J = 4.23, 1.62 Hz, 1H), 8.56 (dd, J = 8.63, 1.61 Hz, 1H), 7.71 (s, 1H), 7.59 (dd, J = 8.57, 4.20 Hz, 1H), 7.34 (t, J = 76.28 Hz, 1H); **^{13}C NMR** (126 MHz, $CDCl_3$) δ 151.8, 142.9 (t, J = 3.8 Hz), 142.4, 133.7, 129.0, 128.2, 128.1, 126.3, 122.7, 117.0 (t, J = 263.2 Hz); **^{19}F NMR** (377 MHz, $CDCl_3$) δ -82.4 (d, J = 76.3 Hz); **HRMS** (ESI-TOF): calculated for $C_9H_{11}F_2NO$ ($[M+H]^+$): 263.9789; found: 263.9790; **IR** (neat): 1603, 1584, 1488, 1458, 1375, 1349, 1081, 1056, 950; **MP:** 123 – 124 ˚C.

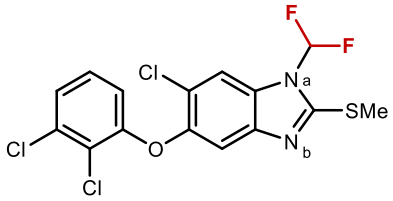
(*S*)-2-(5-chloro-4-(methoxymethyl)-2,3-dihydro-1*H*-inden-1-yl)-1-(difluoromethyl)-1*H*-imidazole (5.31e)



This reaction was performed by Dr. Jeroen Sap. GP2 was followed (0.5 mmol scale) to yield compound **5.31e** (75 mg, 0.48 mmol, 48%) as a yellow-brown oil. **^{1}H NMR** (400 MHz, $CDCl_3$) δ 7.23 (d, J = 8.1 Hz, 1H), 7.21 (d, J = 1.7 Hz, 1H), 7.06

(d, *J* = 1.7 Hz, 1H), 7.02 (t, *J* = 59.4 Hz, 1H), 6.95 (dd, *J* = 8.2, 1.1 Hz, 1H), 4.70 (t, *J* = 8.6 Hz, 1H), 4.67 – 4.55 (m, 2H), 3.41 (s, 3H), 3.27 (m, 1H), 3.08 (m, 1H), 2.67 (m, 1H), 2.34 (m, 1H); **^{13}C NMR** (101 MHz, $CDCl_3$) *δ* 149.7, 146.6, 141.6, 134.7, 132.1, 129.4, 128.9, 125.6, 116.2, 108.3 (t, *J* = 250.6 Hz), 69.8, 58.8, 44.1, 33.5, 31.0; **^{19}F NMR** (377 MHz, $CDCl_3$) *δ* -89.8 (dd, *J* = 229.2, 60.4 Hz), -91.8 (dd, *J* = 229.3, 59.2 Hz); **HRMS** (ESI-TOF): calculated for $C_{15}H_{15}ClF_2N_2O$ ($[M+H]^+$): 313.0914; found: 313.0914; **IR** (neat): 2921, 1446, 1401, 1350, 1289, 1262, 1192, 1126, 1086, 1052, 1030, 942, 921, 908.

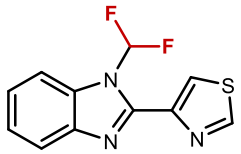
6-chloro-5-(2,3-dichlorophenoxy)-1-(difluoromethyl)-2-(methylthio)-1*H*-benzo[*d*]imidazole (5.31f)



This reaction was performed by Dr. Jeroen Sap. GP2 was followed (1.0 mmol scale) to yield compound **5.31f** (253 mg, 0.62 mmol, 62%) as a mixture of regioisomers (N_a/N_b: 1:1) as a white solid. **^{1}H NMR** (400 MHz, $CDCl_3$) *δ* 7.70 – 7.58 (m, 1H), 7.31 – 6.95 (m, 4H), 6.67 – 6.45 (m, 1H), 2.74 (s, 1.5H), 2.71 (s, 1.5H); **^{13}C NMR** (101 MHz, $CDCl_3$) δ 154.7, 154.2, 153.1, 152.9, 148.7 (d, *J* = 3.1 Hz), 147.3, 143.1, 141.3, 134.5 (d, *J* = 4.1 Hz), 131.8, 129.7, 127.6, 127.5, 125.4, 124.8, 124.1, 123.1, 122.9, 121.6, 120.4, 116.9, 115.2, 113.2, 109.9, 108.8 (t, *J* = 250.7 Hz), 104.8 (t, *J* = 2.9 Hz), 15.2, 15.1; **^{19}F NMR** (377 MHz, $CDCl_3$) *δ* -95.7 (d, *J* = 58.6 Hz), -95.9 (d, *J* = 58.5 Hz); **HRMS** (ESI-TOF): calculated for $C_{15}H_9Cl_3F_2N_2OS$ ($[M+H]^+$): 408.9547; found: 408.9542; **IR** (neat): 2921, 1575, 1473, 1445, 1401, 1349, 1316,

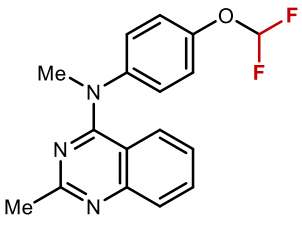
1290, 1255, 1192, 1169, 1126, 1087, 1031, 1017, 983, 942, 921, 908, 866, 810; **MP**: 155 – 157 °C.

4-(1-(difluoromethyl)-1*H*-benzo[*d*]imidazol-2-yl)thiazole (5.31g)



GP2 was followed (1.0 mmol scale) to yield compound **5.31g** (246 mg, 0.98 mmol, 98%) as a light-yellow oil. **^{1}H NMR** (400 MHz, $CDCl_3$) δ 9.15 – 8.77 (m, 2H), 8.43 (d, J = 2.17 Hz, 1H), 7.85 – 7.76 (m, 2H), 7.44 – 7.35 (m, 2H); **^{13}C NMR** (101 MHz, $CDCl_3$) δ 153.8, 146.1, 144.6, 142.5, 131.8, 125.1, 124.6, 123.1, 120.0, 113.4 (t, J = 3.2 Hz), 110.5 (t, J = 249.5 Hz); **^{19}F NMR** (377 MHz, $CDCl_3$) δ -96.3 (d, J = 59.1 Hz); **HRMS** (ESI-TOF): calculated for $C_{11}H_8N_3F_2S$ ($[M+H]^+$): 252.0402; found: 252.0401; **IR** (neat): 2922, 1636, 1456, 1039, 906, 728, 2922, 1039, 906, 728; **MP**: 166 – 167 °C.

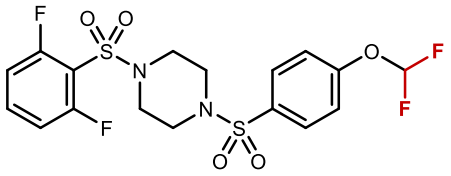
***N*-(5-(difluoromethoxy)-2-phenoxyphenyl)-*N*-(2,5-dimethoxybenzyl)acetamide (DF-MPC-6827)**



This reaction was performed by Dr. Jeroen Sap. GP1 was followed (0.5 mmol scale) to yield **DF-MPC-6827** (92 mg, 0.59 mmol, 59%) as a white solid. **^{1}H NMR** (400 MHz, $CDCl_3$) δ 7.80 (dt, J = 8.3, 1.0 Hz, 1H), 7.57 (ddd, J = 8.4, 5.1, 3.1 Hz, 1H),

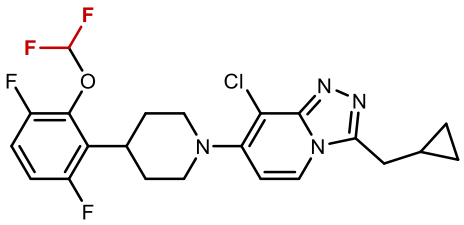
7.20 – 7.09 (m, 4H), 7.06 – 6.99 (m, 2H), 6.54 (t, *J* = 73.5 Hz, 1H), 3.62 (s, 3H), 2.75 (s, 3H). **^{13}C NMR** (101 MHz, $CDCl_3$) *δ* 163.37, 161.85, 151.87, 148.73, 145.98, 132.08, 127.68, 126.96, 125.94, 124.39, 121.12, 115.70 (t, *J* = 261.50 Hz), 114.61, 42.40, 26.35.**^{19}F NMR** (377 MHz, $CDCl_3$) *δ* -81.11 (d, *J* = 73.7 Hz); **HRMS** (ESI-TOF): calculated for $C_{17}H_{15}F_2N_3O$ ($[M+H]^+$): 316.1256; found: 316.1256. Spectroscopic data is in accordance with literature.[13]

1-((4-(difluoromethoxy)phenyl)sulfonyl)-4-((2,6-difluorophenyl)sulfonyl) piperazine (DF-DASA23)



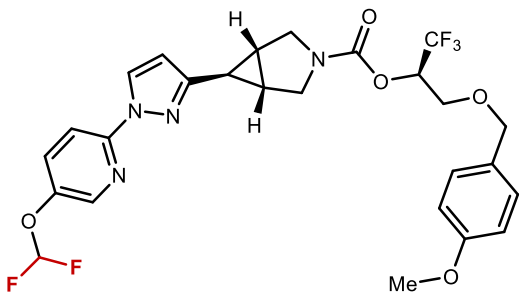
GP1 was followed (1.0 mmol scale) to yield **DF-DASA23** (341 mg, 0.73 mmol, 73%) as a white solid. **^{1}H NMR** (400 MHz, $CDCl_3$) *δ* 7.66 – 7.53 (m, 2H), 7.39 (tt, *J* = 8.4, 5.9 Hz, 1H), 7.22 – 7.01 (m, 3H), 6.97 – 6.76 (m, 2H), 6.47 (t, *J* = 72.4 Hz, 1H), 3.23 (t, *J* = 5.1 Hz, 6H), 3.00 (t, *J* = 5.0 Hz, 5H); **^{13}C NMR** (101 MHz, DMSO-d_6) *δ* 158.8 (dd, *J* = 256.9, 4.1 Hz), 154.6 (t, *J* = 3.3 Hz), 136.4 (t, *J* = 11.3 Hz), 131.2, 130.0, 118.8, 118.6 – 113.0 (m), 45.3, 44.5; **^{19}F NMR** (377 MHz, $CDCl_3$) *δ* -82.2 (d, *J* = 72.5 Hz), -105.2 (dd, *J* = 9.5, 6.0 Hz); **HRMS** (ESI-TOF): calculated for $C_{17}H_{16}F_4N_2O_5S_2$ ($[M+H]^+$): 469.0510; found: 469.0510; **IR** (neat): 3031, 2922, 1668, 1612, 1469, 1386, 1364, 1343, 1296, 1235, 1171, 1127, 1107, 1081, 1044, 1003, 941; **MP**: >200 °C.

8-chloro-3-(cyclopropylmethyl)-7-(4-(2-(difluoromethoxy)-3,6-difluorophenyl)piperidin-1-yl)-[1,2,4]triazolo[4,3-*a*]pyridine (DF-JNJ-42491293)



GP1 was followed (0.05 mmol scale) to afford crude **DF-JNJ-42491293**. Note: the product was unstable on silica and only limited amounts of the phenol was available. The purity of the crude product was 90%. **^{1}H NMR** (400 MHz, $CDCl_3$) δ 7.80 (d, *J* = 7.4 Hz, 1H), 6.97 (td, *J* = 9.4, 4.8 Hz, 1H), 6.88 (ddd, *J* = 10.2, 9.2, 4.2 Hz, 1H), 6.74 – 6.28 (m, 2H), 3.69 – 3.62 (m, 2H), 3.23 (tt, *J* = 12.5, 3.7 Hz, 1H), 3.01 – 2.90 (m, 4H), 2.40 – 2.25 (m, 2H), 1.77 – 1.70 (m, 2H), 1.16 – 1.03 (m, 1H), 0.58 – 0.50 (m, 2H), 0.31 – 0.22 (m, 2H); **^{19}F NMR** (377 MHz, $CDCl_3$) δ -81.8 (dd, *J* = 74.7, 6.6 Hz), -115.9 – -116.0 (m), -132.7 – -133.1 (m); **MS** (ESI) 469.2 [$(M+H)^+$].

(*R*)-1,1,1-trifluoro-3-((4-methoxybenzyl)oxy)propan-2-yl(1*R*,5*S*,6*R*)-6-(1-(5-(difluoromethoxy)pyridin-2-yl)-1*H*-pyrazol-3-yl)-3-azabicyclo[3.1.0]hexane-3-carboxylate (5.20w)



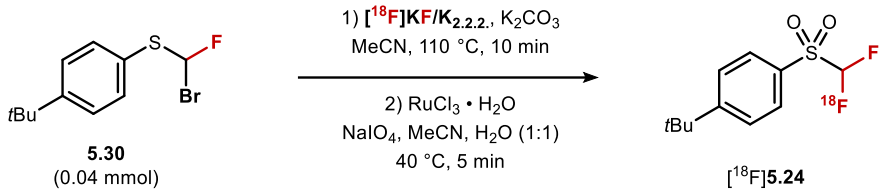
This reaction was performed by Dr. Jeroen Sap. GP1 was followed (1.0 mmol scale) to yield compound **5.20w** (306 mg, 0.54 mmol, 54%) as a colourless oil. **^{1}H NMR** (400 MHz, $CDCl_3$) δ 8.40 (d, *J* = 2.6 Hz, 1H), 8.25 (d, *J* = 2.7 Hz, 1H), 7.92 (dd, *J* = 9.0, 1.5 Hz, 1H), 7.60 (dd, *J* = 8.9, 2.8 Hz, 1H), 7.35 – 7.21 (m, 2H), 6.99 – 6.85 (m, 2H), 6.55 (t, *J* = 72.7 Hz, 1H), 6.19 (dd, *J* = 9.9, 2.6 Hz, 1H), 5.45 – 5.35 (m, 1H), 4.58 (dd, *J* = 11.7, 4.6 Hz, 1H), 4.50 (d, *J* = 11.7 Hz, 1H), 3.88 (td, *J* = 11.1, 4.2 Hz, 2H), 3.82 (s, 3H), 3.80 – 3.53 (m, 5H), 2.04 (dd, *J* = 5.7, 1.7 Hz, 2H), 1.87 (dt, *J* = 8.6, 3.5 Hz, 1H); **^{13}C NMR** (101 MHz, $CDCl_3$) δ 159.4, 154.8, 153.2 (d, *J* = 4.0 Hz), 148.8, 144.9, 140.3, 131.7 – 127.7 (m), 124.8, 122.0, 115.4 (t, *J* = 265.3 Hz), 113.9 (d, *J* = 4.3 Hz), 112.7, 105.7 (d, *J* = 3.3 Hz), 72.9 (d, *J* = 2.0 Hz), 69.7 (q, *J* = 31.3 Hz), 66.1, 55.3 (d, *J* = 1.9 Hz), 49.2, 48.5 (d, *J* = 6.7 Hz), 26.1 (d, *J* = 3.3 Hz), 25.3, 21.2 (d, *J* = 4.7 Hz); **^{19}F NMR** (376 MHz, $CDCl_3$) δ -75.4 – -75.5 (m), -81.3 – -81.6 (m); **HRMS** (ESI-TOF): calculated for $C_{26}H_{25}F_5N_4O_5$ ($[M+H]^+$): 569.1818; found: 569.1808; **IR** (neat): 2882, 1720, 1612, 1532, 1514, 1480, 1416, 1369, 1230, 1181, 1149, 1101, 1081, 1040, 983, 953, 909, 833, 761, 730.

6.4.5 Radiochemistry:

General Information

[^{18}F]Fluoride was produced by Alliance Medical (UK) via the $^{18}O(p,n)^{18}F$ reaction and delivered as [^{18}F]fluoride in O-18-enriched-water. Radiosynthesis and azeotropic drying was performed on a NanoTek microfluidic device (Advion).

Synthesis of [^{18}F]*t*BuPhSO$_2$CF$_2$H ([^{18}F]5.24)



5.30
(0.04 mmol)

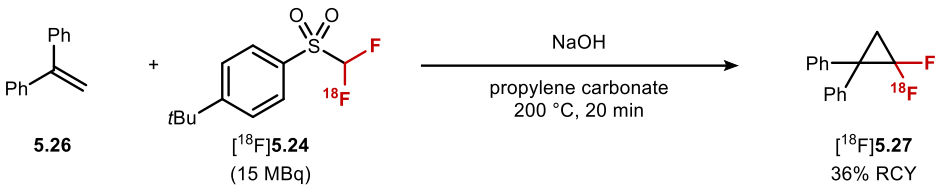
[^{18}F]**5.24**

[^{18}F]KF/K$_{222}$ capture: [^{18}F]fluoride was separated from ^{18}O-enriched-water using an anion exchange cartridge (Waters Sep-Pak AccellPlus QMA Carbonate Plus Light Cartridge, activated with H_2O (10.0 mL) prior to use) and released with a solution of Kryptofix222 (7.5 mg) and K_2CO_3 (1.5 mg) in MeCN/H_2O (0.75 mL, 4:1, v/v). The solution was dried by azeotropic drying using dry MeCN (200 µL) under a flow of N2 at 105 °C (CE1-Temp: 105 °C).

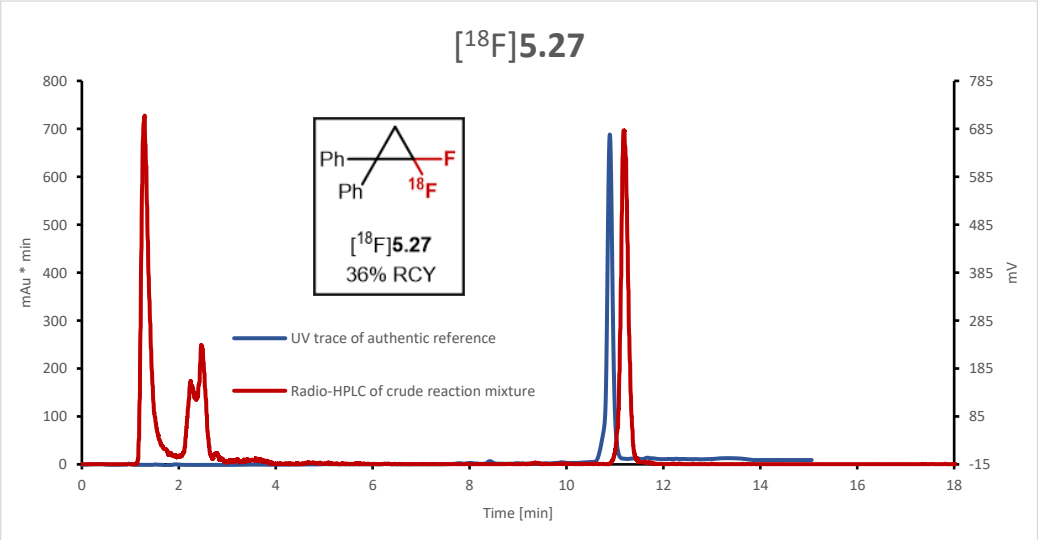
Synthesis of [^{18}F]*t*BuPhSO$_2$CF$_2$H ([^{18}F]5.24): Upon cooling of the v-vial, a solution of (4-(*tert*-butyl)phenyl)(bromofluoromethyl)sulfane **5.30** (11.2 mg, 0.04 mmol) in MeCN (dry, 300 µL) was added. The resulting solution was stirred at 110 °C (CE1-Temp: 110 °C) for 10 minutes, after which time it was allowed to cool to 40 °C. To the mixture was added $RuCl_3$ x H_2O (2 mg, 20 mol%) and $NaIO_4$ (52 mg, 0.16 mmol) in MeCN/H_2O (1:1, v/v, 0.5 mL). This mixture was stirred at 35 °C (CE2 - Temp: 36 °C) for 10 minutes. The mixture was diluted with a mixture of water (3.2 mL) and EtOH (0.8 mL) and trapped on a C18 plus cartridge (conditioned 10 mL MeOH, then 10 mL H_2O). The mixture was eluted with MeCN (1.5 mL) and loaded onto the HPLC sample-loop for preparative HPLC purification (using isocratic 65% MeCN in 25 mM ammonium formate buffer, Q = 4 mL/min, t_R([^{18}F]**5.24**) = ca. 11-14 minutes). [^{18}F]**5.24** was collected in a vial containing H_2O (20 mL), which was shaken and eluted over a C18 Plus cartridge (pre-conditioned with 10 mL MeOH

and 10 mL of H_2O). The ^{18}F-product was released from the C18 Plus cartridge with MeCN (2.0 mL) into a V-vail.

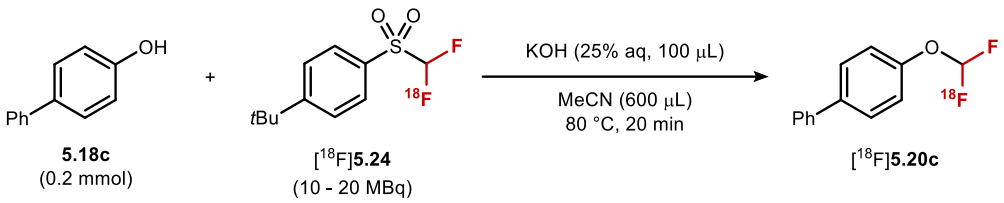
^{18}F-Difluorocyclopropanation of 1,1-diphenylethylene



To a mixture of alkene (0.1 mmol) and NaOH (0.05 mmol) in propylene carbonate (300 µL) in a V-vial was added [^{18}F]**5.24** (15 MBq) in propylene carbonate (20 µL). The mixture was stirred at 200 °C for 20 min. The mixture was cooled to room temperature and quenched by addition of an ethanol solution in water (1:1, 500 µL). An aliquot of this mixture was analysed by radioHPLC.



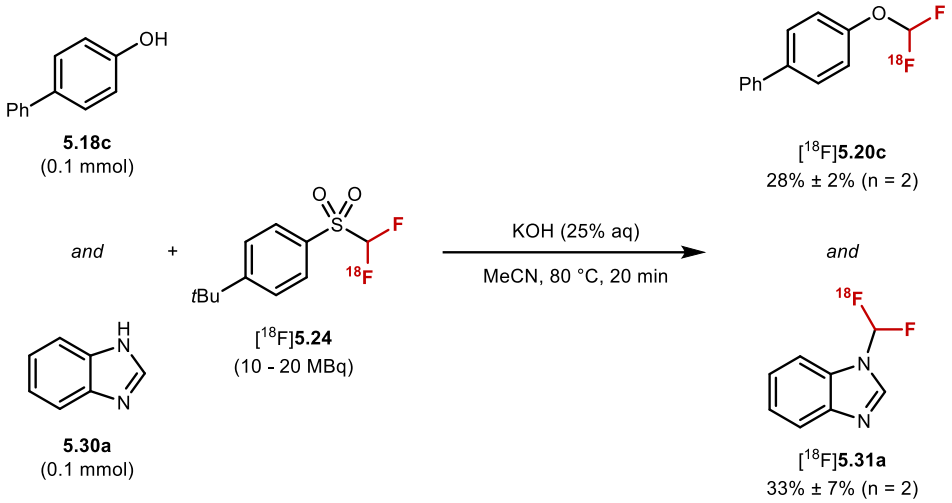
^{18}F-Difluoromethylation Optimisation



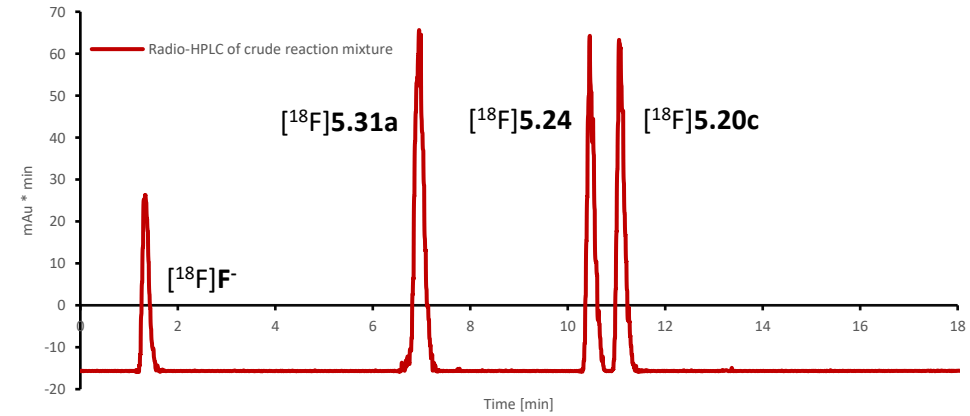
To a V-vial containing phenol **5.18c** (0.2 mmol) was added [^{18}F]**5.24** in MeCN (20-50 µL). Then a mixture of MeCN (600 µL) and KOH (25% aq., 100 µL) was added, and the mixture was stirred at 80 °C for 20 min. The mixture was cooled to room temperature and quenched by addition of an ethanol solution in water (1:1, 500 µL). An aliquot of this mixture was further analysed by radioHPLC.

Competition experiments

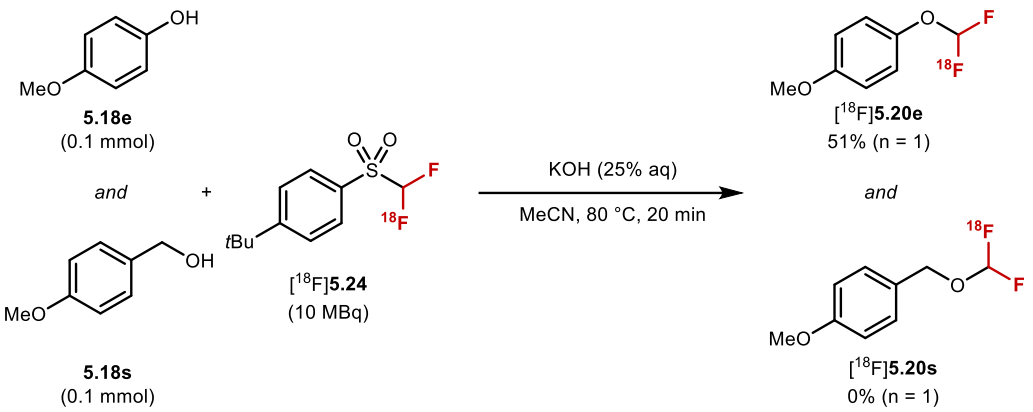
Benzimidazole vs Phenol



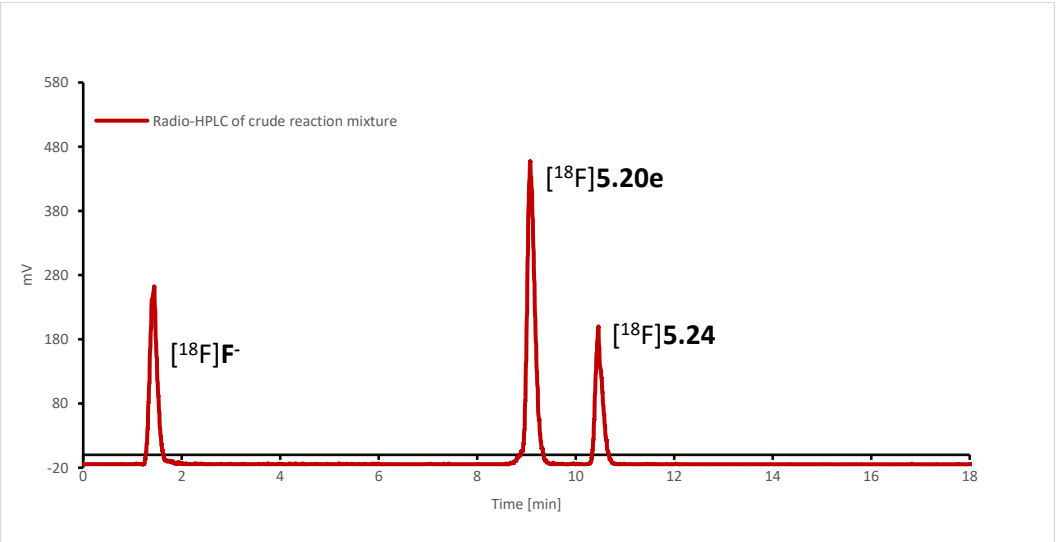
To a V-vial containing phenol **5.18c** (0.1 mmol) and benzimidazole **5.30a** (0.1 mmol) was added [^{18}F]**5.24** in MeCN (20-50 µL). Then a mixture of MeCN (600 µL) and KOH (25% aq., 100 µL) was added, and the mixture was stirred at 80 °C for 20 min. The mixture was cooled to room temperature and quenched by addition of an ethanol solution in water (1:1, 500 µL). An aliquot of this mixture was further analysed by radioHPLC.



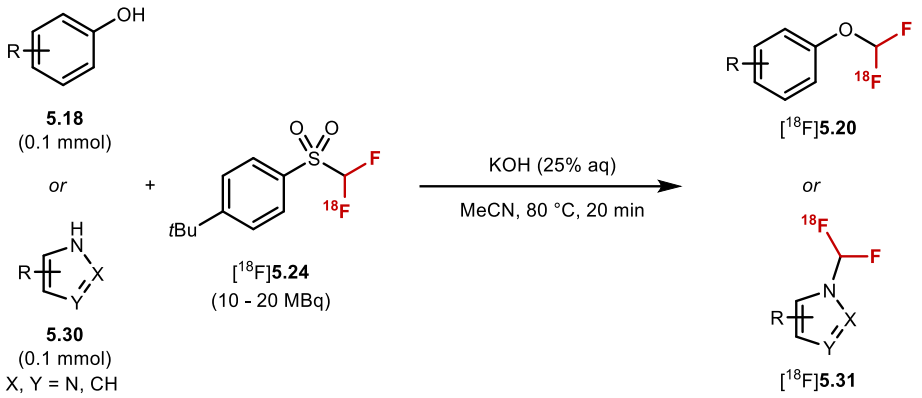
Phenol vs Benzylic alcohol



To a V-vial containing phenol **5.18e** (0.1 mmol) and benzimidazole **5.18s** (0.1 mmol) was added [^{18}F]**5.24** in MeCN (20-50 µL). Then a mixture of MeCN (600 µL) and KOH (25% aq., 100 µL) was added, and the mixture was stirred at 80 °C for 20 min. The mixture was cooled to room temperature and quenched by addition of an ethanol solution in water (1:1, 500 µL). An aliquot of this mixture was further analysed by radioHPLC.

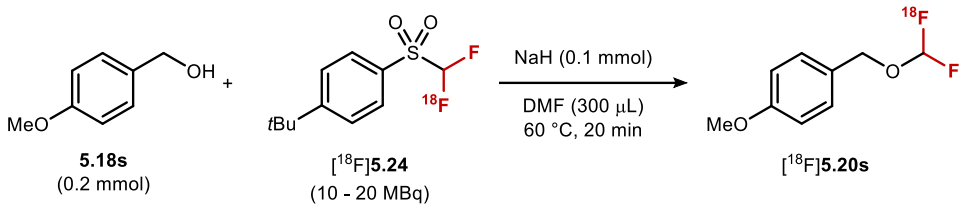


General procedure 3 (GP3): ^{18}F-difluoromethylation of (thio)phenols and *N*-heterocycles



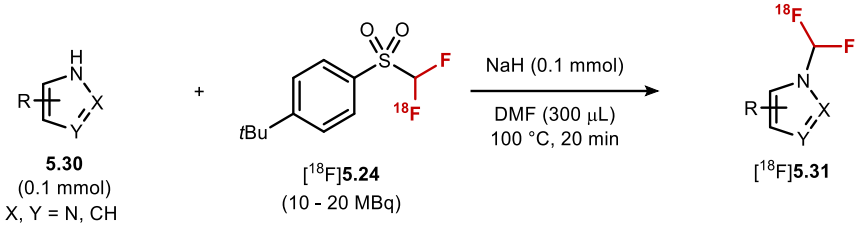
To a V-vial containing (thio)phenol or *N*-heterocycle (0.2 mmol) was added [^{18}F]**5.24** in MeCN (20 - 50 µL). Then a mixture of MeCN (600 µL) and KOH (25% aqueous, 100 µL) was added, and the mixture was stirred at 80 to 100 °C for 20 min. The mixture was cooled to room temperature and quenched by addition of an ethanol solution in water (1:1, 500 µL). An aliquot of this mixture was further analysed by radioHPLC.

General procedure 4 (GP4): ^{18}F-difluoromethylation of 5.18s



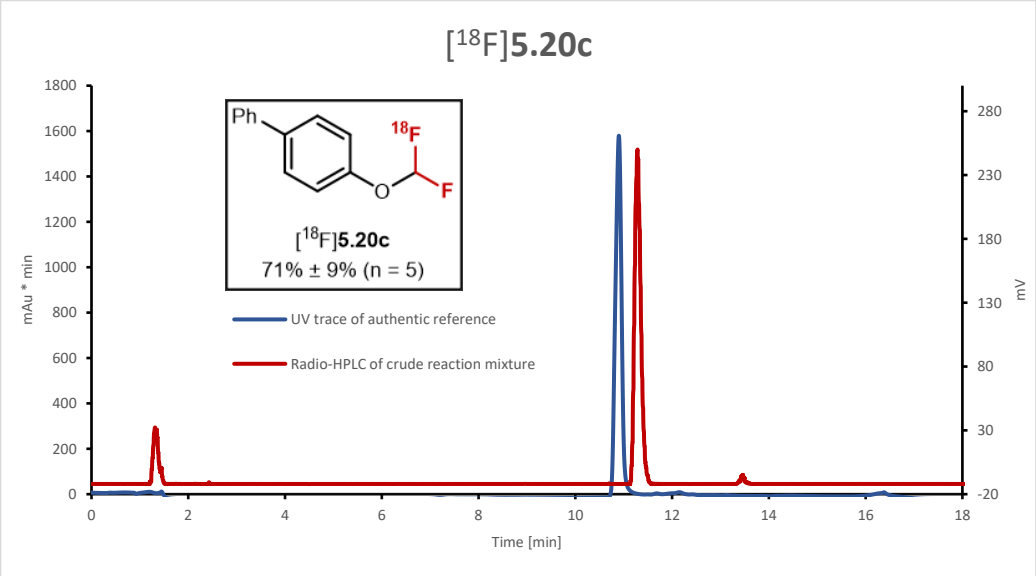
To a V-vial containing **5.18s** (0.2 mmol) in DMF (300 µL) was added NaH (0.1 mmol) at 0 °C. Then a solution of [^{18}F]**5.24** in DMF (20 - 50 µL) was added, and the mixture was stirred at 60 °C for 20 min. The mixture was cooled to room temperature and quenched by addition of an ethanol solution in water (1:1, 500 µL). An aliquot of this mixture was further analysed by radioHPLC.

General procedure 5 (GP5): ^{18}F-difluoromethylation *N*-heterocycles under anhydrous conditions



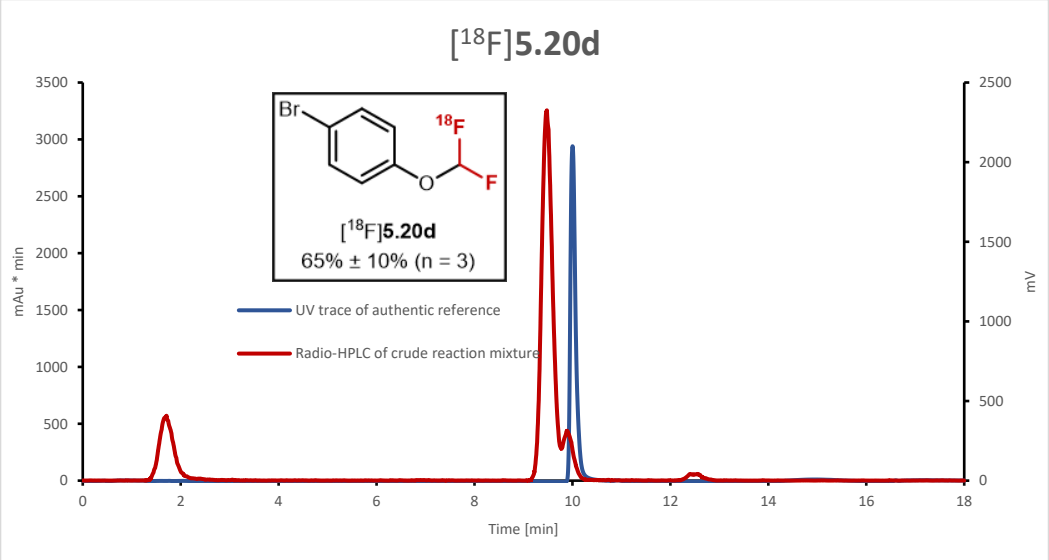
To a V-vial containing *N*-heterocycle (0.2 mmol) in DMF (300 µL) was added NaH (0.1 mmol) at 0 °C. Then a solution of [^{18}F]**5.24** in DMF (20 - 50 µL) was added, and the mixture was stirred at 100 °C for 20 min. The mixture was cooled to room temperature and quenched by addition of an ethanol solution in water (1:1, 500 µL). An aliquot of this mixture was further analysed by radioHPLC.

6.4.6 Overlays of radiotraces



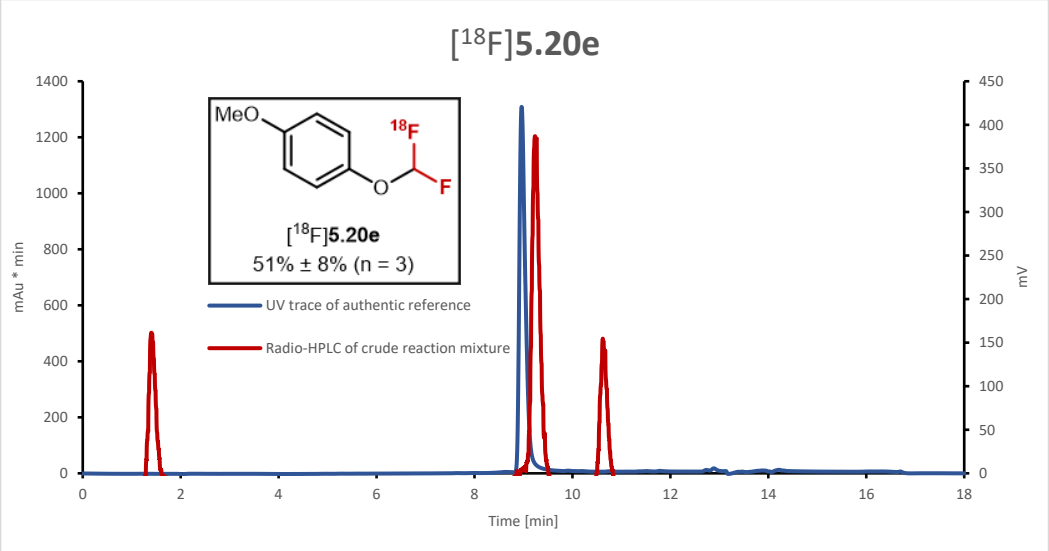
GP3 was followed to afford [^{18}F]**5.20c**. The crude mixture was analysed by radioHPLC.

Reaction	Radiochemical Yield
1	86%
2	71%
3	71%
4	65%
5	67%



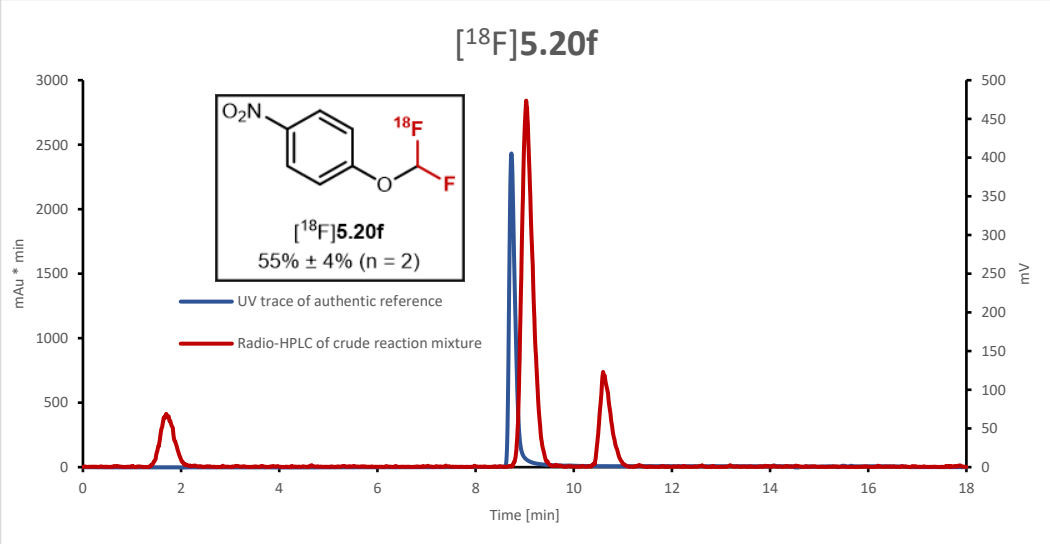
GP3 was followed to afford [^{18}F]**5.20d**. The crude mixture was analysed by radioHPLC.

Reaction	Radiochemical Yield
1	73%
2	70%
3	51%



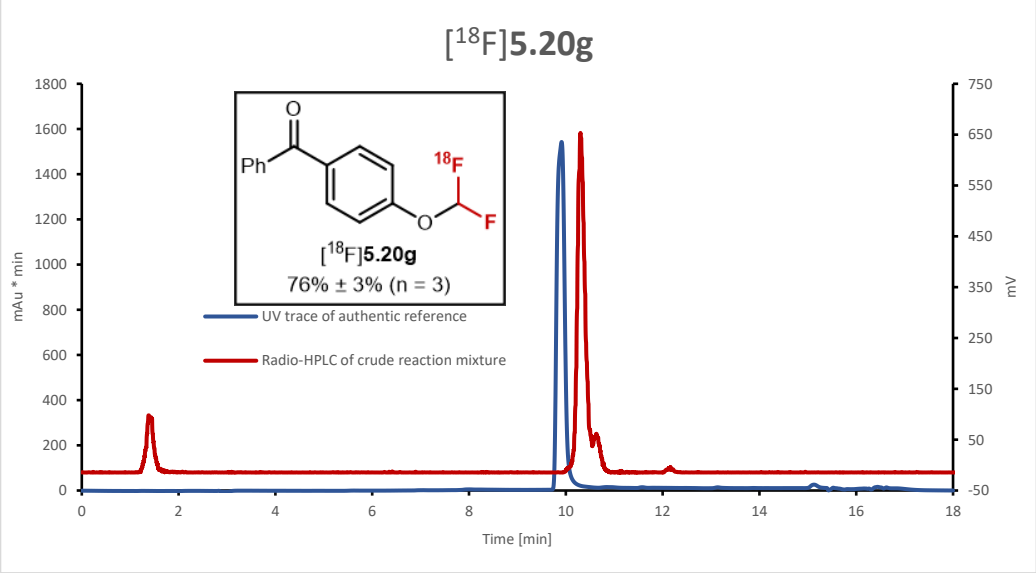
GP3 was followed to afford [^{18}F]**5.20e**. The crude mixture was analysed by radioHPLC.

Reaction	Radiochemical Yield
1	40%
2	58%
3	55%



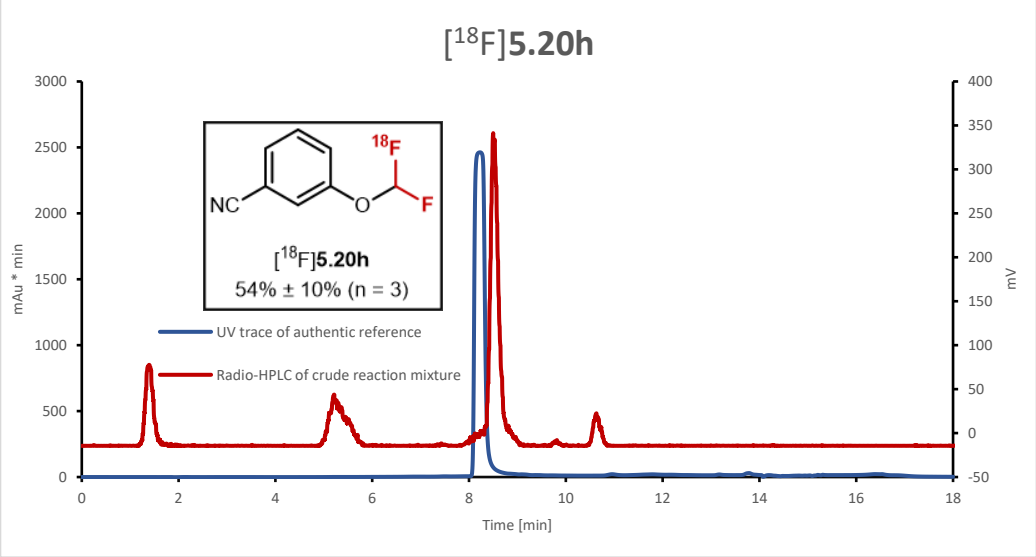
GP3 was followed to afford [^{18}F]**5.20f**. The crude mixture was analysed by radioHPLC.

Reaction	Radiochemical Yield
1	51%
2	58%
3	70%



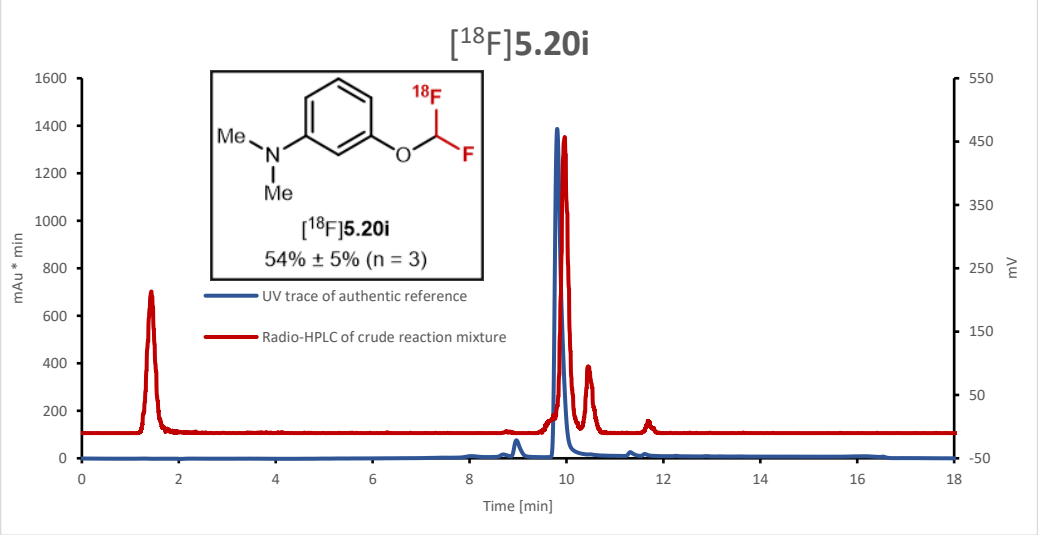
GP3 was followed to afford [^{18}F]**5.20g**. The crude mixture was analysed by radioHPLC.

Reaction	Radiochemical Yield
1	72%
2	79%
3	61%



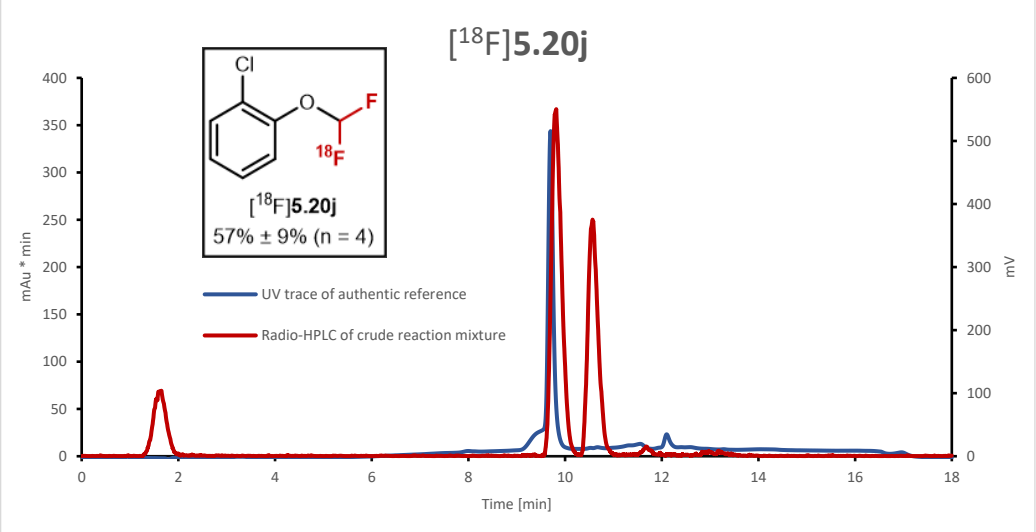
GP3 was followed to afford [^{18}F]**5.20h**. The crude mixture was analysed by radioHPLC.

Reaction	Radiochemical Yield
1	61%
2	61%
3	40%



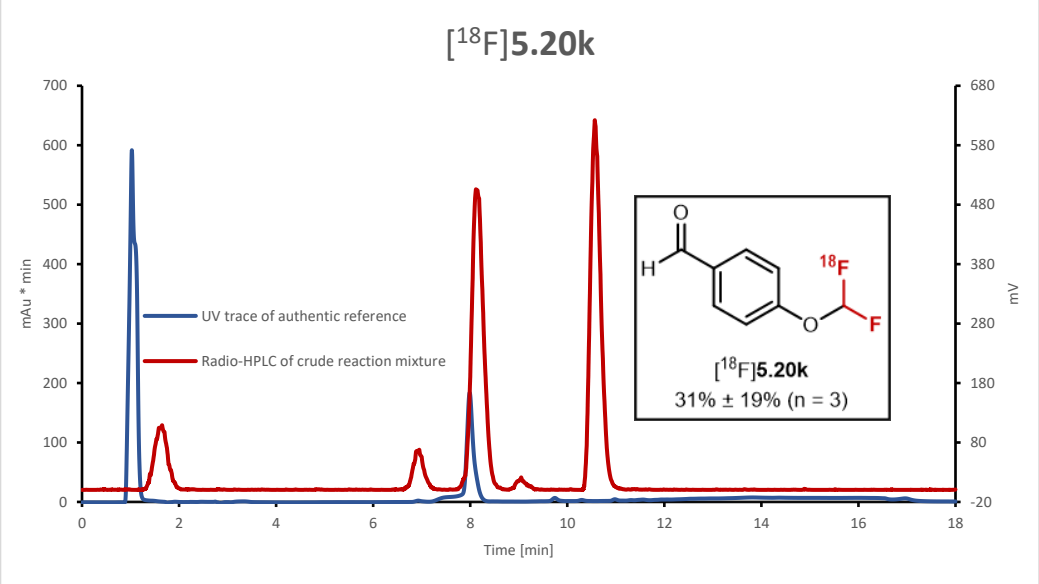
GP3 was followed to afford [^{18}F]**5.20i**. The crude mixture was analysed by radioHPLC.

Reaction	Radiochemical Yield
1	58%
2	56%
3	47%



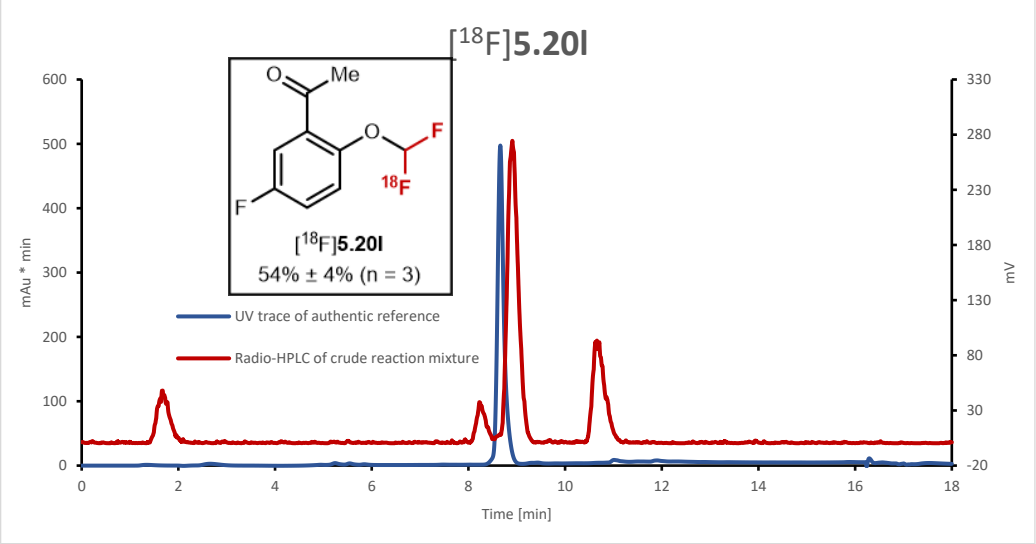
GP3 was followed to afford [^{18}F]**5.20j**. The crude mixture was analysed by radioHPLC.

Reaction	Radiochemical Yield
1	68%
2	62%
3	44%
4	52%



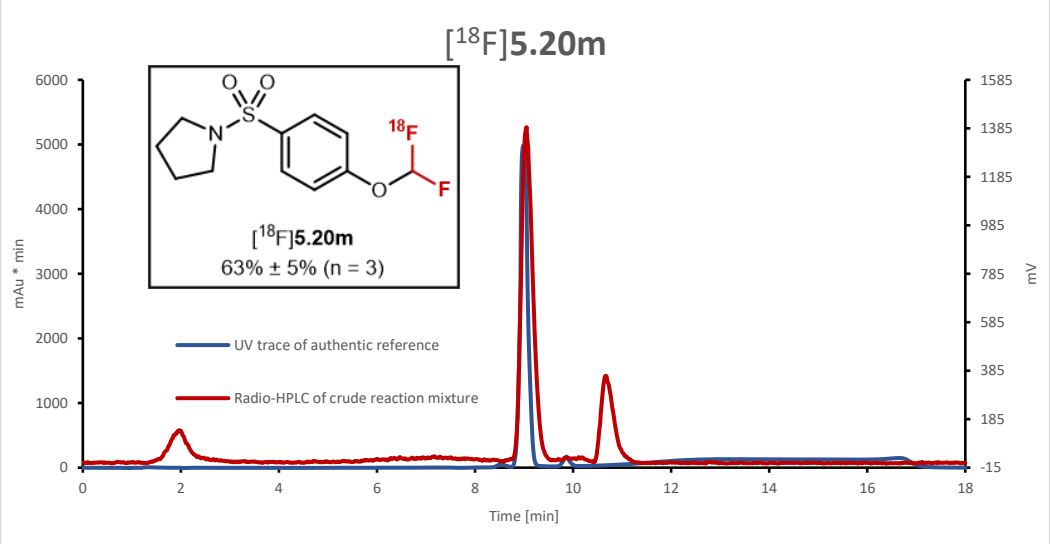
GP3 was followed to afford [^{18}F]**5.20k**. The crude mixture was analysed by radioHPLC.

Reaction	Radiochemical Yield
1	48%
2	0%
3	42%



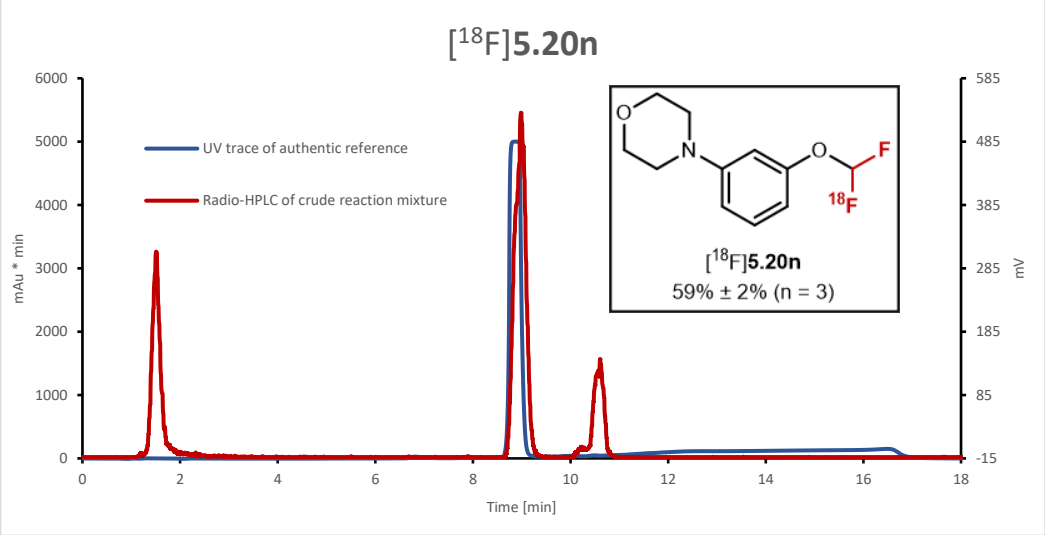
GP3 was followed to afford [^{18}F]**5.20l**. The crude mixture was analysed by radioHPLC.

Reaction	Radiochemical Yield
1	60%
2	51%
3	51%



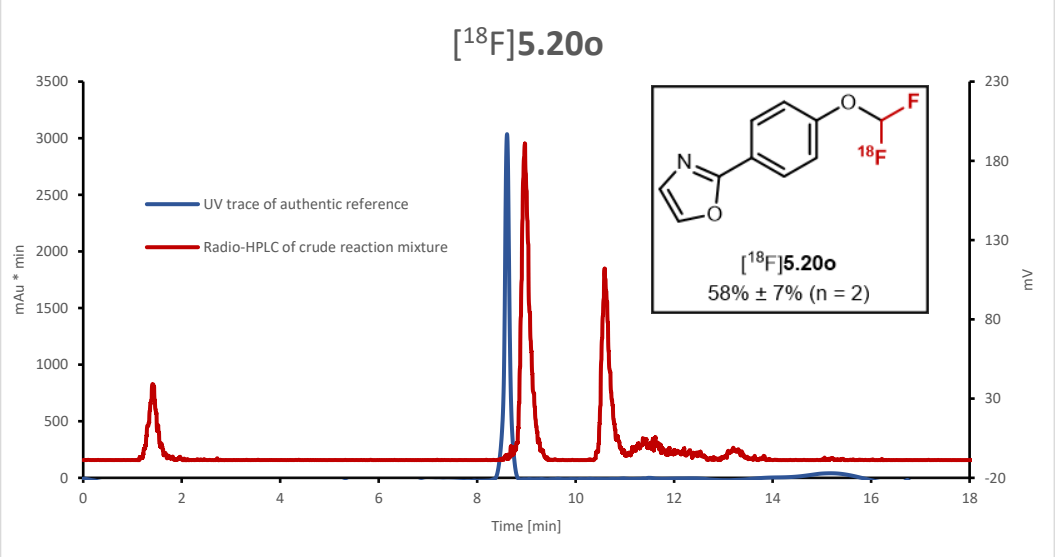
GP3 was followed with the following exception: the reaction was performed at 100 °C to afford [^{18}F]**5.20m**. The crude mixture was analysed by radioHPLC.

Reaction	Radiochemical Yield
1	56%
2	66%
3	66%



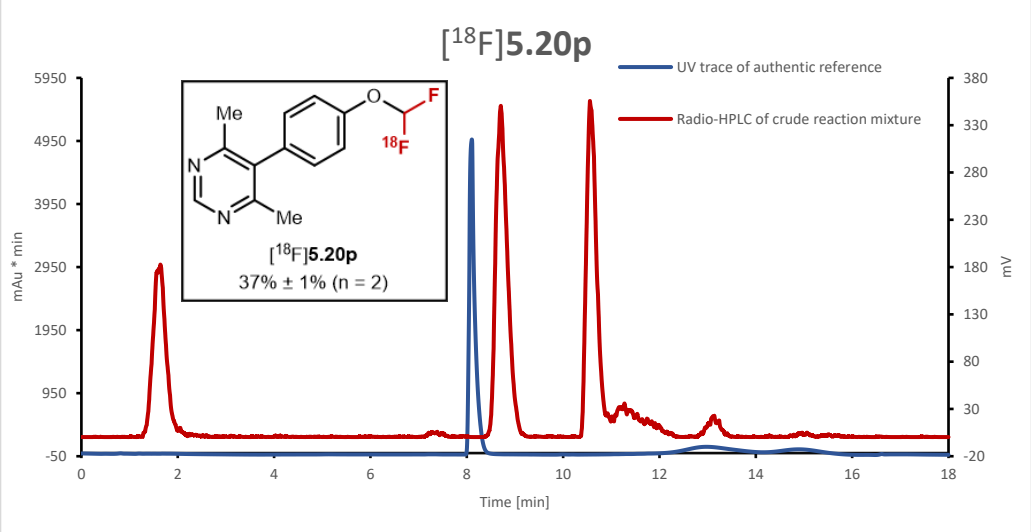
GP3 was followed to afford [^{18}F]**5.20n**. The crude mixture was analysed by radioHPLC.

Reaction	Radiochemical Yield
1	61% (at 80 ˚C)
2	60% (at 80 ˚C)
3	57% (at 80 ˚C)



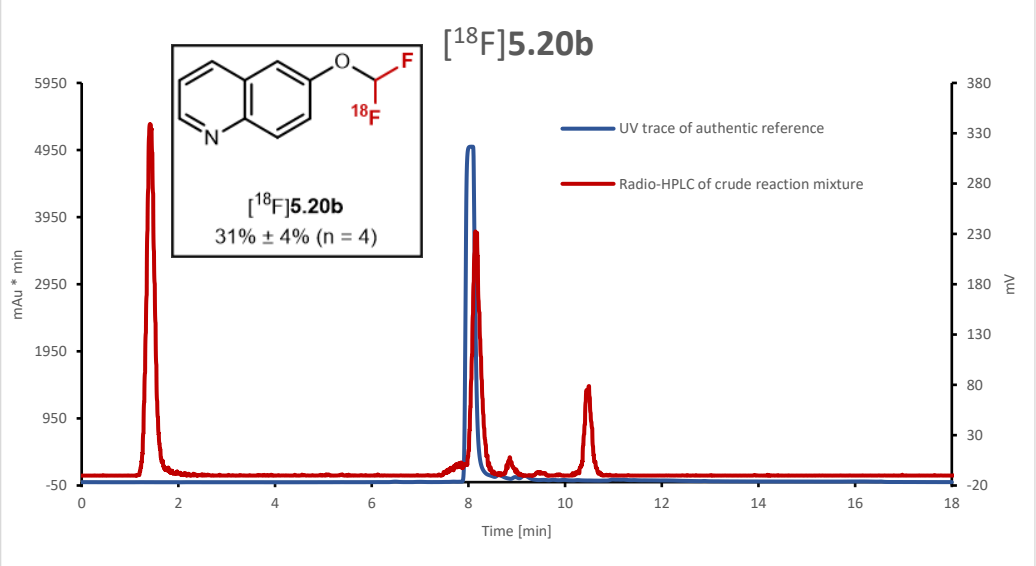
GP3 was followed to afford [^{18}F]**5.20o**. The crude mixture was analysed by radioHPLC.

Reaction	Radiochemical Yield
1	65%
2	51%



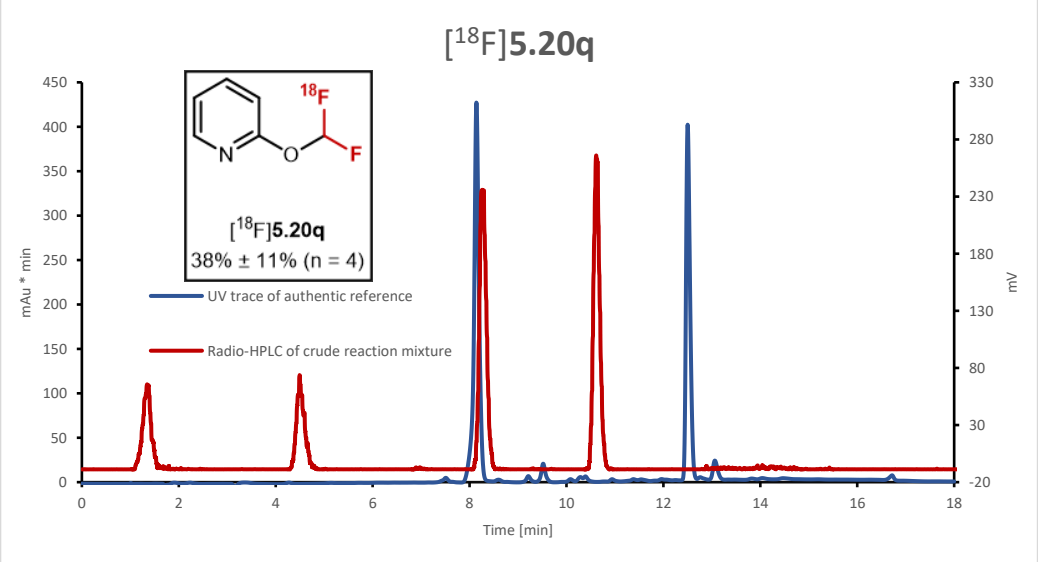
GP3 was followed to afford [^{18}F]**5.20p**. The crude mixture was analysed by radioHPLC.

Reaction	Radiochemical Yield
1	38%
2	36%



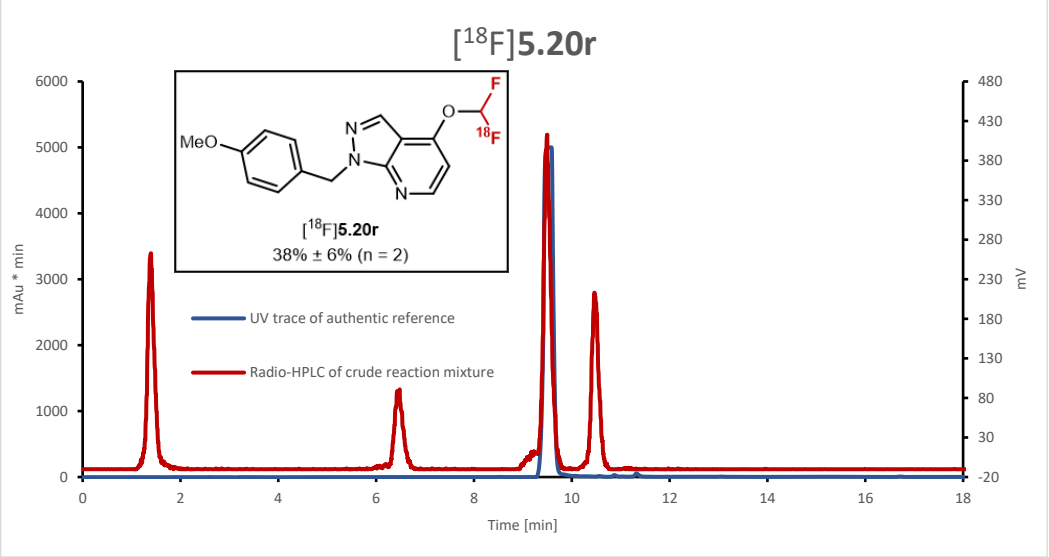
GP3 was followed to afford [^{18}F]**5.20b**. The crude mixture was analysed by radioHPLC.

Reaction	Radiochemical Yield
1	29%
2	37%
3	32%
4	25%



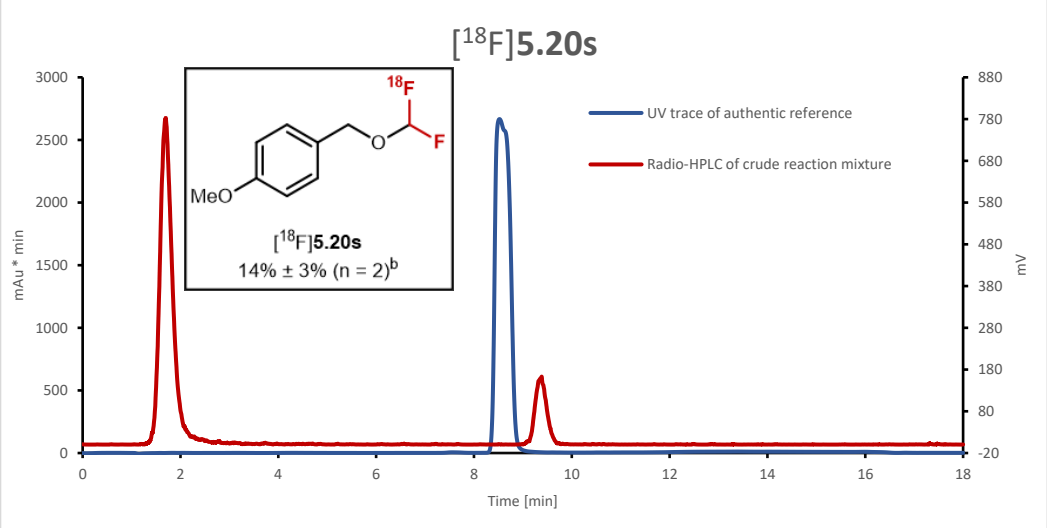
GP3 was followed to afford [^{18}F]**5.20q**. The crude mixture was analysed by radioHPLC.

Reaction	Radiochemical Yield
1	52%
2	22%
3	38%
4	38%



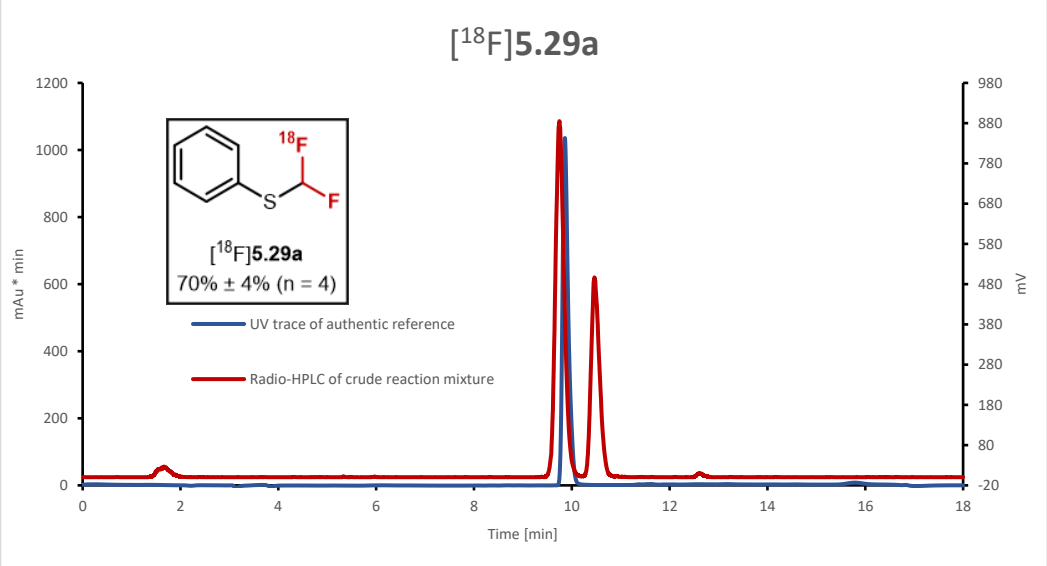
GP3 was followed to afford [^{18}F]**5.20r**. The crude mixture was analysed by radioHPLC.

Reaction	Radiochemical Yield
1	32%
2	44%



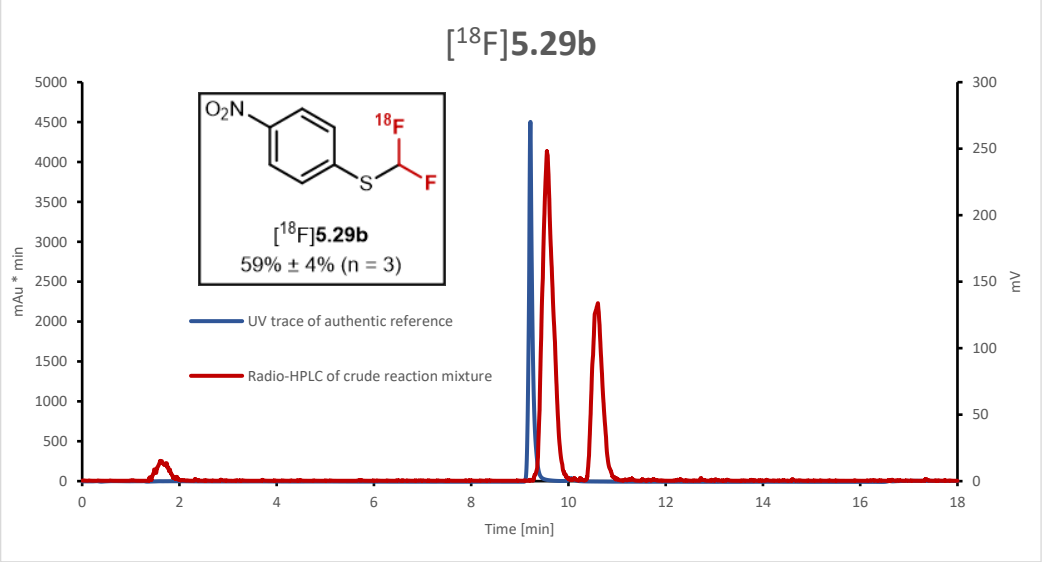
GP4 was followed to afford [^{18}F]**5.20s**. The crude mixture was analysed by radioHPLC.

Reaction	Radiochemical Yield
1	16%
2	11%



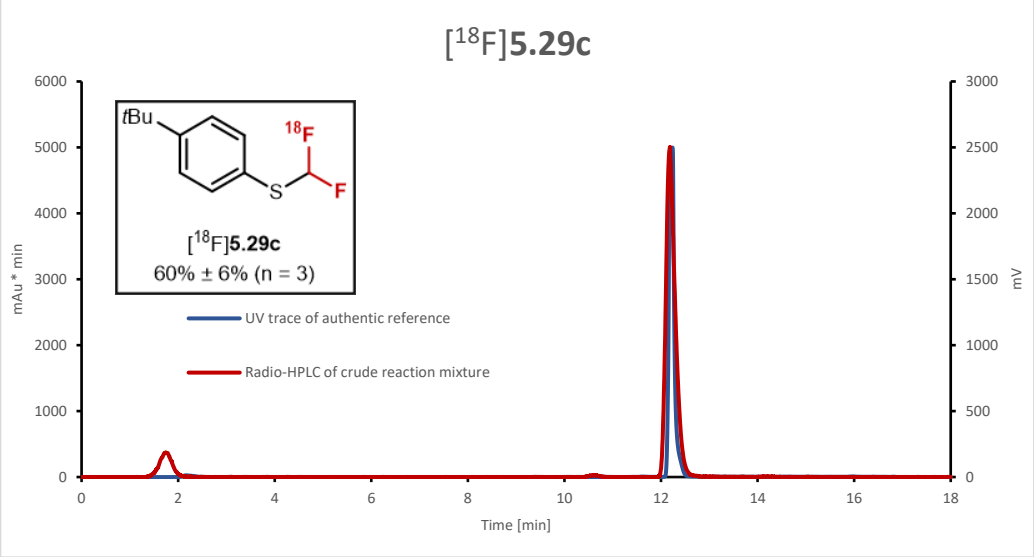
GP3 was followed to afford [^{18}F]**5.29a**. The crude mixture was analysed by radioHPLC.

Reaction	Radiochemical Yield
1	65%
2	67%
3	74%
4	75%



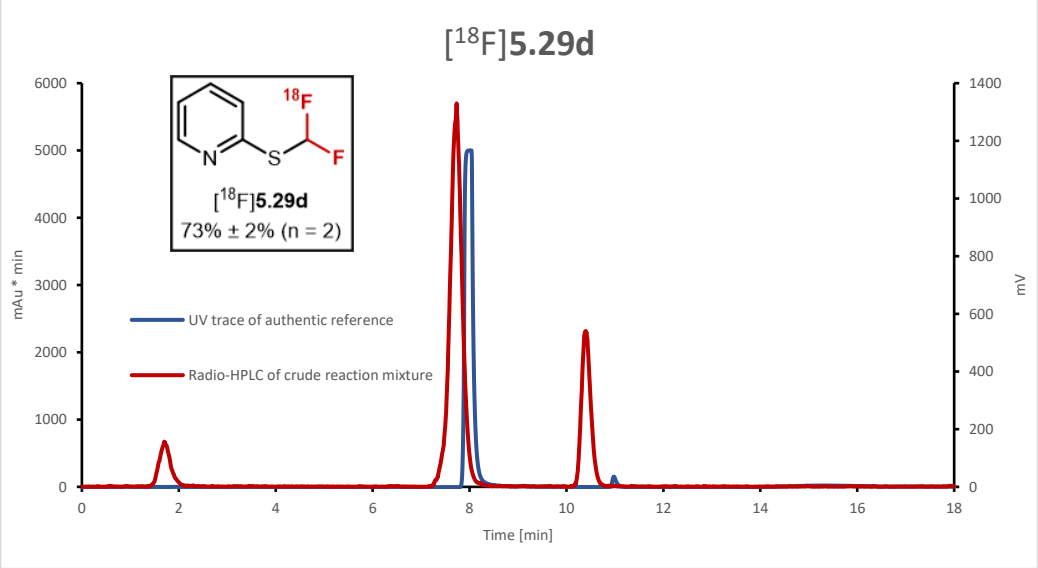
GP3 was followed to afford [^{18}F]**5.29b**. The crude mixture was analysed by radioHPLC.

Reaction	Radiochemical Yield
1	53%
2	61%
3	63%



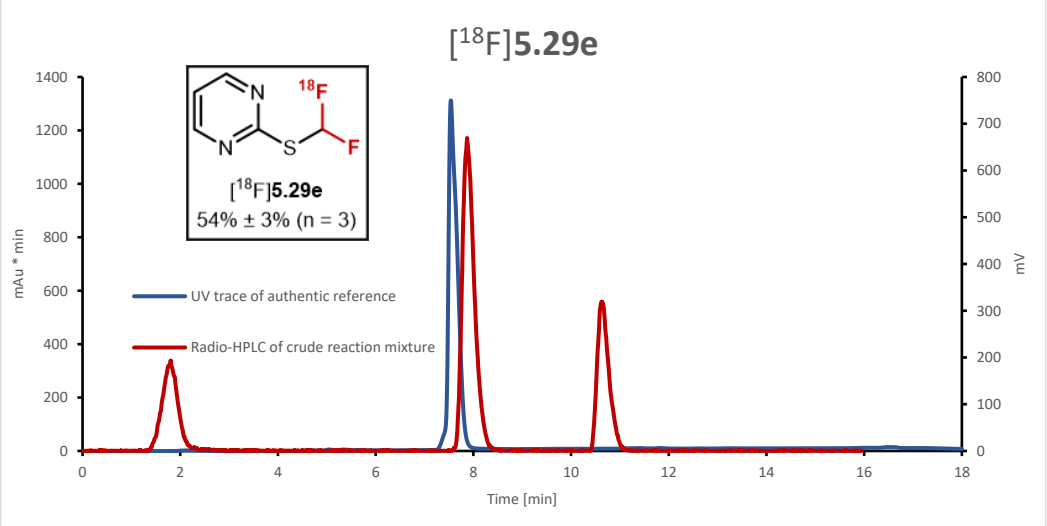
GP3 was followed to afford [^{18}F]**5.29c**. The crude mixture was analysed by radioHPLC.

Reaction	Radiochemical Yield
1	53%
2	67%
3	60%
4	90% (reaction performed at 100°C)



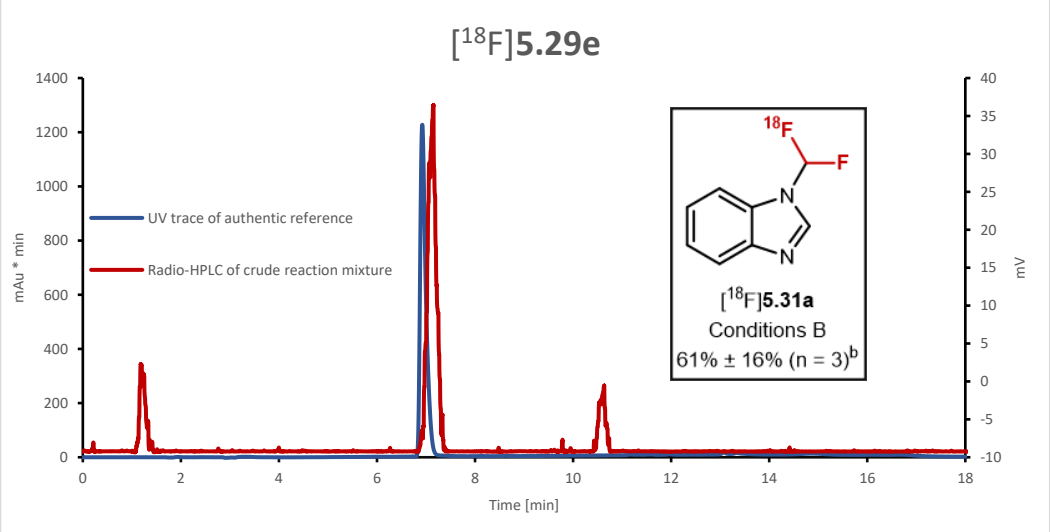
GP3 was followed to afford [^{18}F]**5.29d**. The crude mixture was analysed by radioHPLC.

Reaction	Radiochemical Yield
1	71%
2	74%



GP3 was followed to afford [^{18}F]**5.29e**. The crude mixture was analysed by radioHPLC.

Reaction	Radiochemical Yield
1	50%
2	55%
3	57%

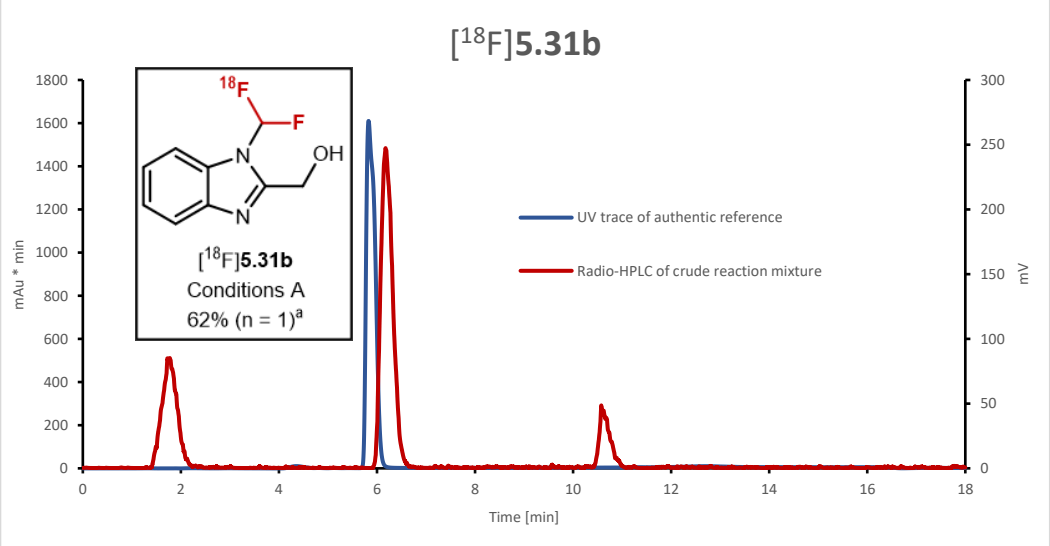


GP3 was followed to afford [^{18}F]**5.31a**. The crude mixture was analysed by radioHPLC.

Reaction	Radiochemical Yield
1	53%
2	43%
3	48%
4	53%

GP5 was followed to afford [^{18}F]**5.31a**. The crude mixture was analysed by radioHPLC.

Reaction	Radiochemical Yield
1	69%
2	76%
3	39%

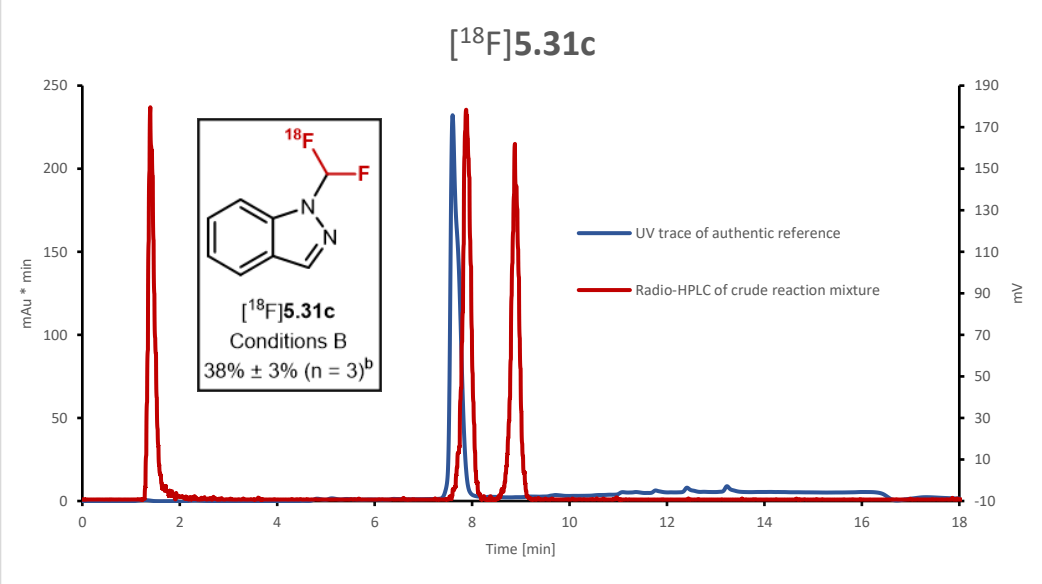


GP3 was followed to afford [^{18}F]**5.31b**. The crude mixture was analysed by radioHPLC.

Reaction	Radiochemical Yield
1	62%

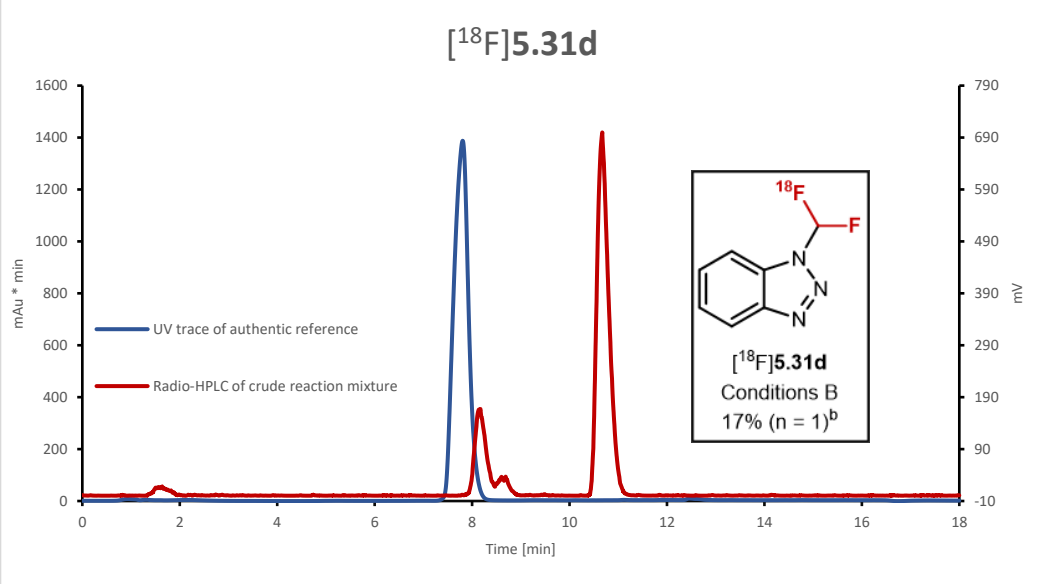
GP5 was followed to afford [^{18}F]**5.31b**. The crude mixture was analysed by radioHPLC.

Reaction	Radiochemical Yield
1	14%
2	21%
3	50%



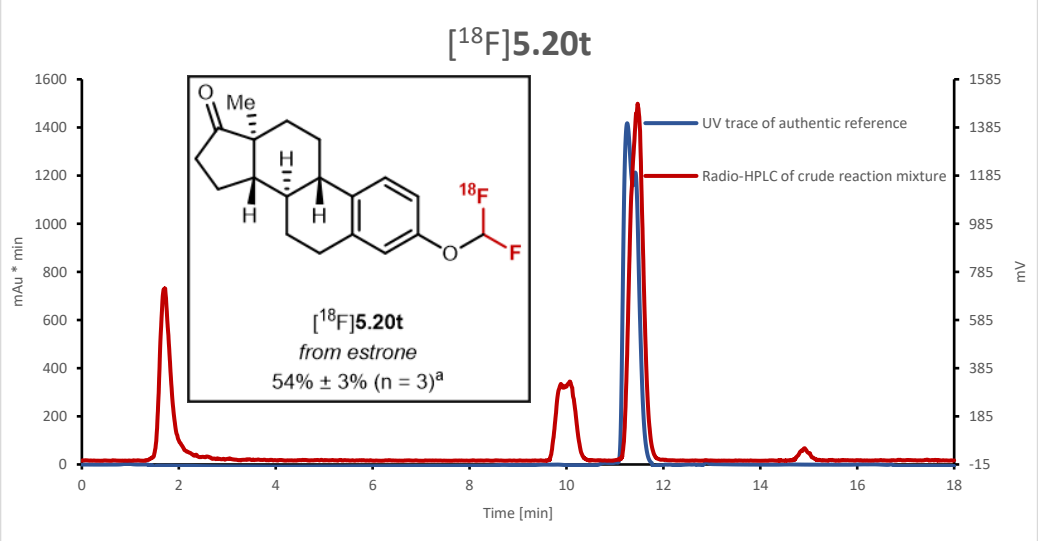
GP5 was followed to afford [^{18}F]**5.31c**. The crude mixture was analysed by radioHPLC.

Reaction	Radiochemical Yield
1	38%
2	34%
3	42%



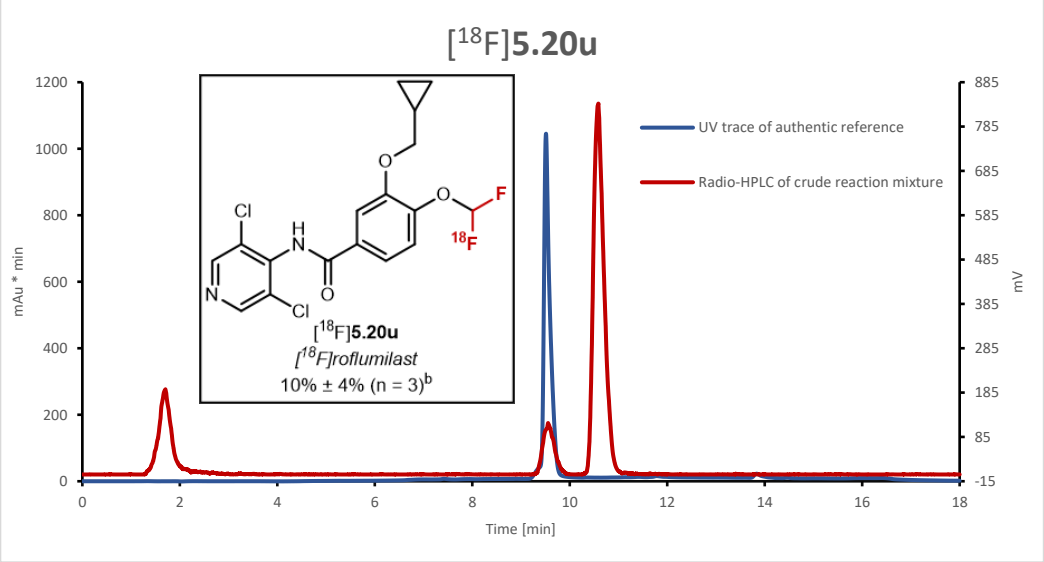
GP5 was followed to afford [^{18}F]**5.31d**. The crude mixture was analysed by radioHPLC.

Reaction	Radiochemical Yield
1	17%



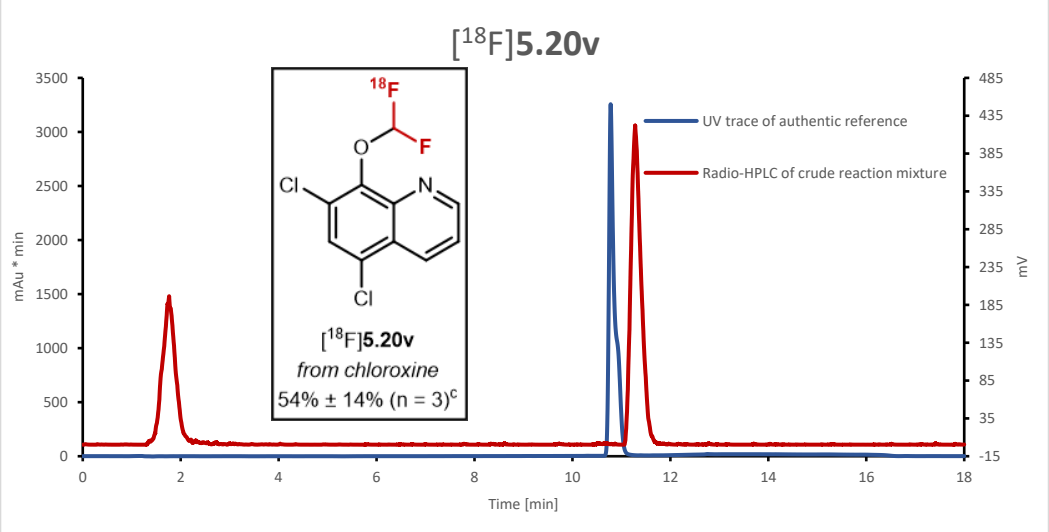
GP3 was followed to afford [^{18}F]**5.20t**. The crude mixture was analysed by radioHPLC.

Reaction	Radiochemical Yield
1	55%
2	58%
3	50%



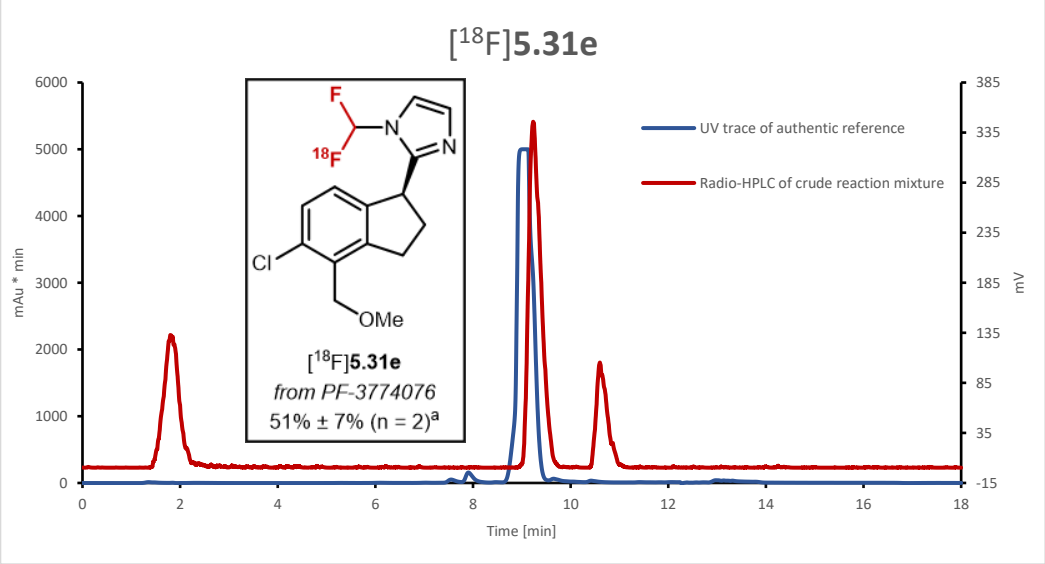
GP3 was followed with the following exceptions: the reaction was performed on 0.1 mmol scale at 100 °C to afford [^{18}F]**5.20u**. The crude mixture was analysed by radioHPLC.

Reaction	Radiochemical Yield
1	11%
2	14%
3	4%



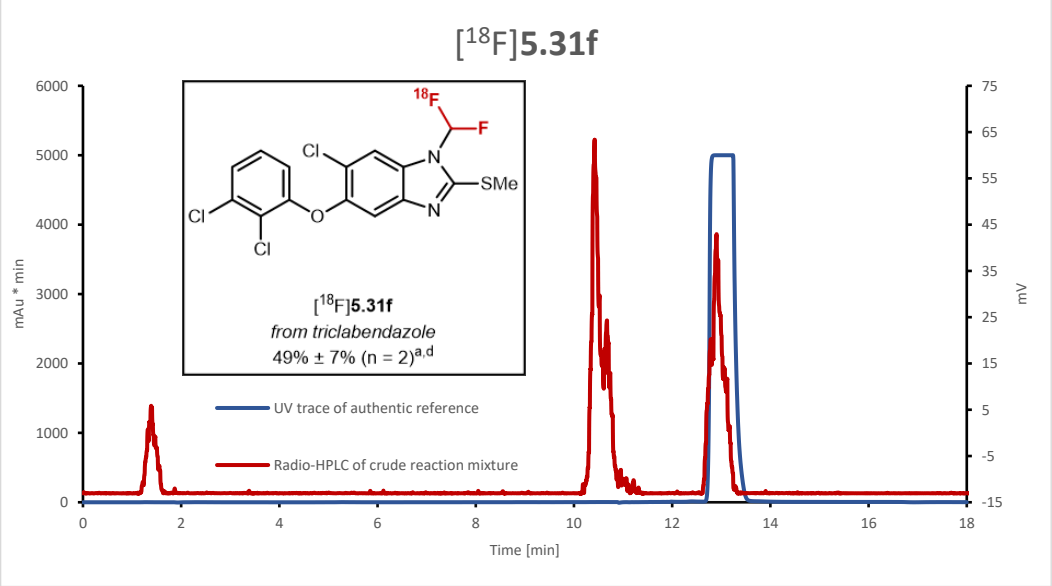
GP3 was followed with the following exception: the reaction was performed at 100 °C to afford [^{18}F]**5.20v**. The crude mixture was analysed by radioHPLC.

Reaction	Radiochemical Yield
1	63%
2	64%
3	35%



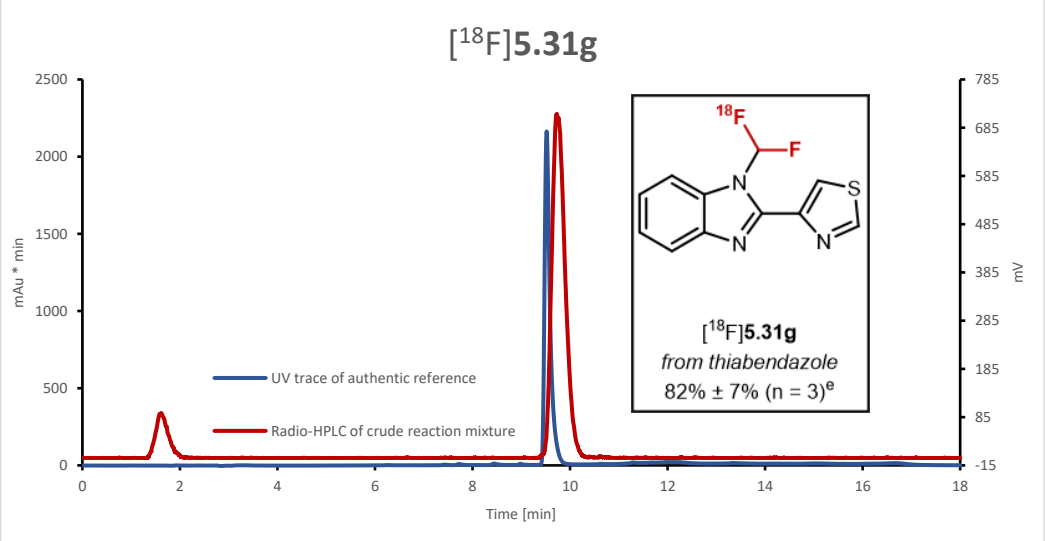
GP3 was followed to afford [^{18}F]**5.31e**. The crude mixture was analysed by radioHPLC.

Reaction	Radiochemical Yield
1	58%
2	44%



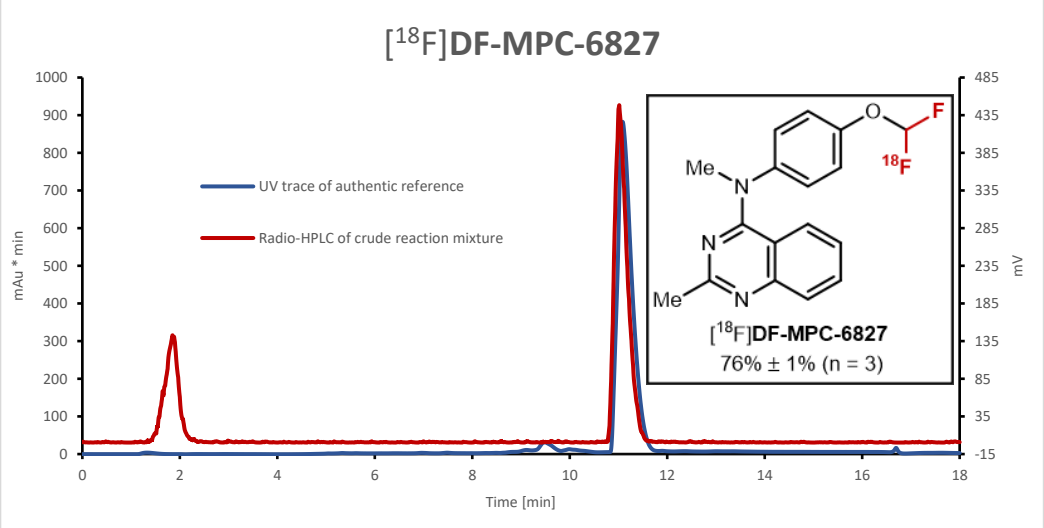
GP3 was followed to afford [^{18}F]**5.31f**. The crude mixture was analysed by radioHPLC. Note: The regioselectivity could not be assessed from the crude radioHPLC. Likely the reaction affords two regioisomers.

Reaction	Radiochemical Yield
1	55%
2	42%



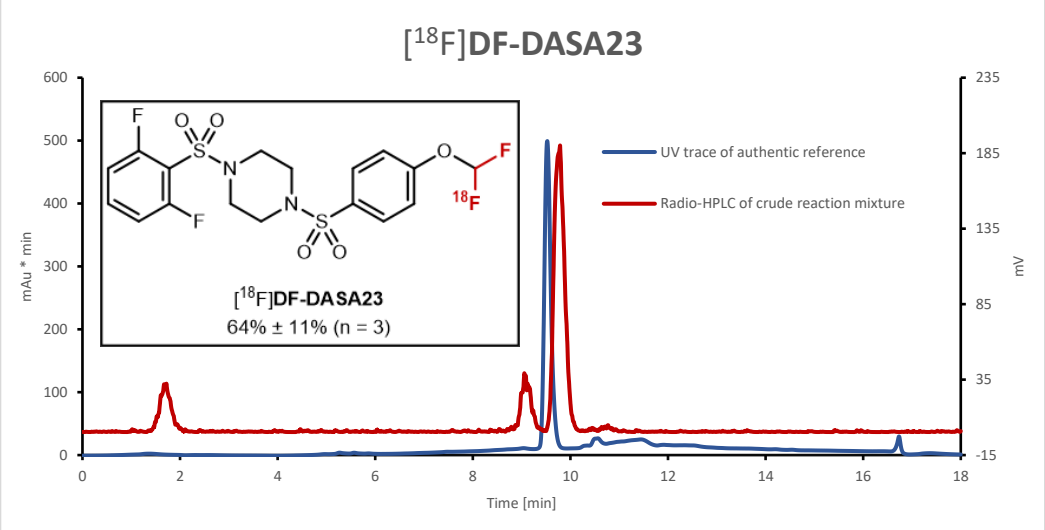
GP5 was followed with the following exception: the reaction was performed at 140 °C to afford [^{18}F]**5.31g**. The crude mixture was analysed by radioHPLC.

Reaction	Radiochemical Yield
1	73%
2	89%
3	85%



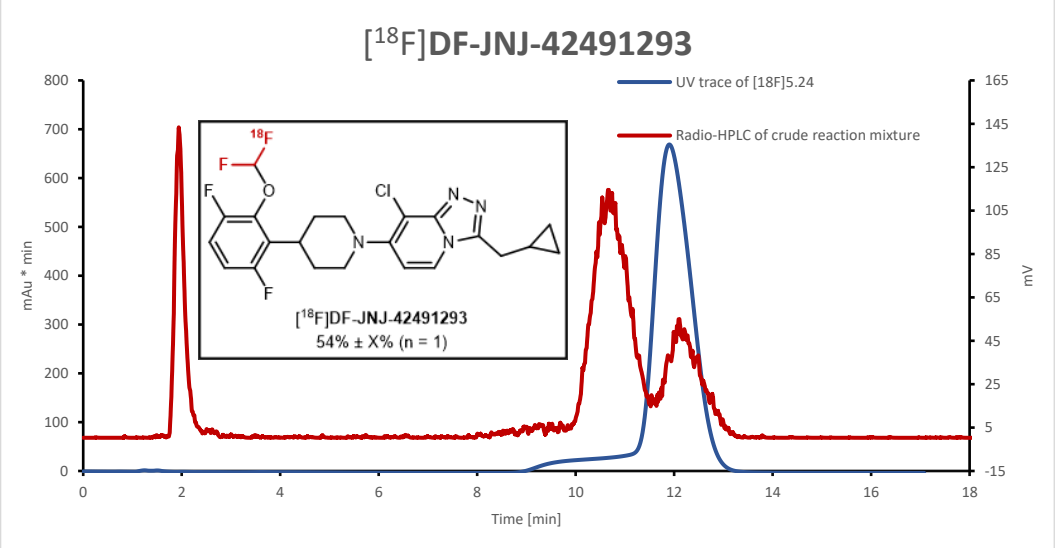
GP3 was followed with the following exception: the reaction was performed at 100 °C to afford [^{18}F]**DF-MPC-6827**. The crude mixture was analysed by radioHPLC.

Reaction	Radiochemical Yield
1	75%
2	76%
3	78%



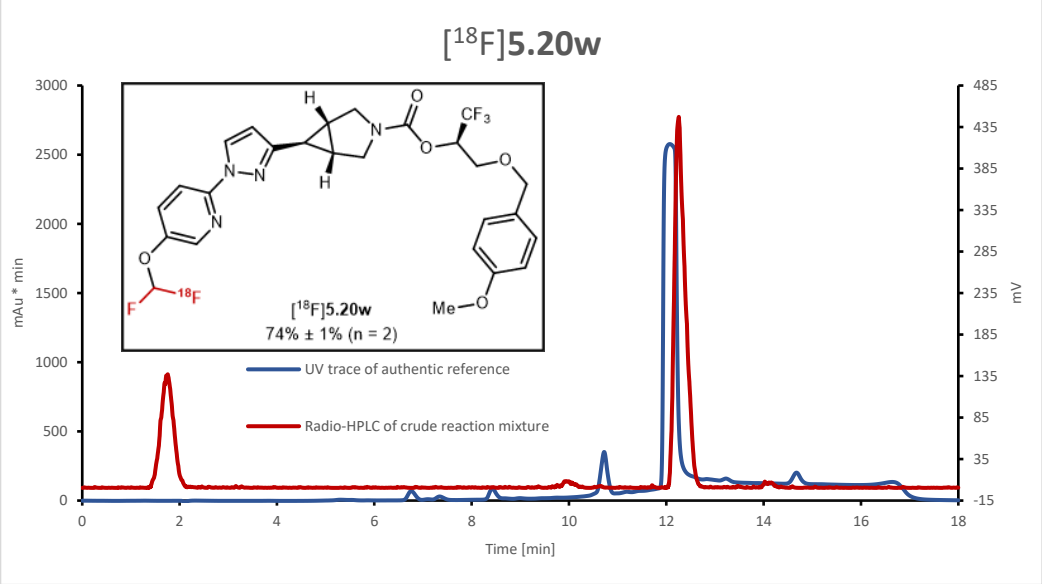
GP3 was followed with the following exception: the reaction was performed at 100 °C to afford [^{18}F]**DF-DASA23**. The crude mixture was analysed by radioHPLC.

Reaction	Radiochemical Yield
1	73%
2	70%
3	49%



GP3 was followed with the following exceptions: the reaction was performed on 0.05 mmol to afford [^{18}F]**DF-JNJ-42491293**. The crude mixture was analysed by radioHPLC.

Reaction	Radiochemical Yield
1	54%



GP3 was followed with the following exception: the reaction was performed at 100 °C to afford [^{18}F]**5.20c**. The crude mixture was analysed by radioHPLC.

Reaction	Radiochemical Yield
1	75%
2	73%

6.5 References

[1] Q. Y. Lin, X. H. Xu, K. Zhang, F. L. Qing, *Angew. Chem. Int. Ed.* **2016**, *55*, 1479-1483.
[2] B. Yang, X. H. Hu, F. L. Qing, *Org. Lett.* **2016**, *18*, 5956-5959.
[3] G. Q. Liu, C. H. Yang, Y. M. Li, *J. Org. Chem.*, **2015**, *80* (22), 11339–11350.
[4] N. W. Mszar, F. Haeffner, A. H. Hoveyda, *J. Am. Chem. Soc.*, **2014**, *136*(9), 3362–3365.
[5] H. K. Hun, F. T. Luo, *J. Ch. Chem. Soc.,* **2012**, *59*(3), 394-498.
[6] P. J. Bhuyan, H. N. Borah, J. S. Sandhu, *J. Chem. Soc., Perkin Trans. 1*, **1999**, 3083-3084.